DEPARTAMENT OF CHEMISTRY

Managing of Chronic Myeloid Leukemia via Au-nanoconjugates In TKIs Sensitive/Resistance CML Cells

BILAL RABAH QASIM ABDULMAWJOOD

Master in Medical Laboratory Science

DOCTORATE IN BIOCHEMISTRY

NOVA University Lisbon

March, 2025

NOVA SCHOOL OF SCIENCE & TECHNOLOGY

DEPARTAMENT OF CHEMISTRY

Managing of Chronic Myeloid Leukemia via Au-nanoconjugates In TKIs Sensitive/Resistance CML Cells

BILAL RABAH QASIM ABDULMAWJOOD

Master in Medical Laboratory Science

Adviser: Maria Alexandra Núncio de Carvalho Ramos Fernandes
Full Professor, NOVA School of Science and Technology, NOVA University Lisbon

Co-adviser: Pedro Miguel Ribeiro Viana Baptista
Full Professor, *NOVA School of Science and Technology, NOVA University Lisbon*

Examination Committee:

Chair: Ana Cecília Afonso Roque
Full Professor, *NOVA School of Science and Technology,* NOVA University Lisbon

Rapporteurs: Jorge Manuel Moreira Gonçalves
Full Professor, Faculty of Pharmacy, University of Porto

Maria Luísa Teixeira de Azevedo Rodrigues Corvo
Principal Investigator with Habilitation, Faculty of Pharmacy, University of Porto

Adviser: Maria Alexandra Núncio de Carvalho Ramos Fernandes
Full Professor, *NOVA School of Science and Technology,* NOVA University Lisbon

Members: Ana Cecília Afonso Roque
Full Professor, *NOVA School of Science and Technology,* NOVA University Lisbon

Maria Joana Pinto Desterro
Coordinator of the Hemato-Oncology Laboratory, Instituto Português de Oncologia de Lisboa Francisco Genti

DOCTORATE IN BIOCHEMISTRY

NOVA University Lisbon
March, 2025

Managing of Chronic Myeloid Leukemia via Au-nanoconjugates In TKIs Sensitive/Resistance CML Cells

To my beloved parents, whose love and support made this journey possible

ACKNOWLEDGMENTS

I would like to express my deepest gratitude to everyone who has supported me throughout this PhD journey. This thesis would not have been possible without the guidance, encouragement, and unwavering support of many individuals.

First and foremost, I extend my heartfelt appreciation to my advisors, Prof. Pedro Baptista and Prof. Alexandra Fernandes, for their invaluable mentorship, insightful guidance, and constant encouragement. Their expertise, patience, and dedication have been instrumental in shaping my research and academic growth. I am truly grateful for their trust in my abilities and their unwavering support throughout this process.

A special thanks to my colleagues and friends at FCT Nova, particularly my lab members and collaborators (Catarina, Luis, Pedro P, Margarida S, Beartriz O, Daniella F, Ruben, Sandra, Andre, Beatriz C, Cynthia and Patricia) for their camaraderie, stimulating discussions, and invaluable assistance in the lab. The encouragement and shared experiences have made this journey more enriching and enjoyable.

I am profoundly grateful to my family; above all, my deepest gratitude goes to my father who supported me unconditionally, even while bravely fighting his battle with cancer. His strength, resilience, and love have been my greatest source of inspiration. Despite his struggles, he remained my pillar of encouragement, always believing in my dreams. This PhD is as much his achievement as it is mine. I am also profoundly grateful to my mother and my sister (Sarah), for their unwavering love, patience, and encouragement. Their belief in me has been my greatest source of strength during the most challenging times of this journey.

A heartfelt thank you to my uncle (Assil) and my cousins (David and Nadia), for their generosity and hospitality in hosting me in their home during this journey. Their kindness, support, and warm companionship made my stay much more comfortable and enjoyable, and I am truly grateful for their help.

I am also deeply grateful to Portugal for warmly hosting me during my PhD. The country's rich culture, welcoming people, and inspiring academic environment have made my experience truly memorable. I feel privileged to have had the opportunity to conduct my research in such a vibrant and supportive setting.

I acknowledge the Department of Life Sciences of NOVA School of Science and Technology, UCIBIO, from NOVA University Lisbon, for hosting the Biochemistry PhD program and providing all the necessary means for this academic effort.

Lastly, this work was financed by national funds from FCT– NOVA School of Science and Technology, I.P., in the scope of the project UIDP/0 4378/2020 and UIDB/0 4378/2020 of the Research Unit on Applied Molecular Biosciences– UCIBIO and the project LA/P/0140/2020 of the Associate Laboratory Institute for Health and Bioe conomy– i4HB and project NANOHEAT (2022.04315.PTDC).

This PhD has been a long and challenging endeavor, but it has also been an incredibly rewarding journey. To everyone who has played a part in it, thank you.

"To exist is to change, to change is to mature, to mature is to go on creating oneself endlessly. " (Henri Bergson)

ABSTRACT

Chronic myeloid leukemia (CML) is a rare disease caused by the presence of Philadelphia chromosome as a result of the fusion between the Breakpoint Cluster Region (*BCR*) gene in chromosome 22 and the Abelson tyrosine-protein kinase1 (*ABL1*) gene in chromosome 9. This fusion encodes a tyrosine kinase (TK) constitutively expressed in CML cells. Imatinib (IM) is the first line TK inhibitor used in CML treatment. Molecular detection of *BCR-ABL1* transcription is crucial for diagnosis and treatment strategies. Point mutations in the ABL1 gene contribute to resistance against TKIs, suggesting a need for modification in treatment protocols. In a high percentage of CML patients, poor response with relapses and disease progression is associated with resistance through various mechanisms, including dysregulation of the c-MYC proto-oncogene.

Gold nanoconjugates (Au-nanoconjugates) have shown improved efficacy in gene silencing approaches towards cancer therapy. Herein, we evaluated the silencing potential of AuNPs functionalized with antisense oligonucleotides targeting e14a2*BCR-ABL1* or the *c-MYC* alone and combination, demonstrating efficient silencing of gene expression and downregulation of protein levels in IM-senstive and IM-resistant cell lines. Combining TK inhibitor (IM) with other kinase inhibitors showed synergistic activity in IM-sensitive cell line. Moreover, the effect of the Au-nanoconjugates with danusertib (Danu), volasertib (Vola) and adavosertib (Adavo) on IM-resistant cells was also analyzed and showed a synergistic effect.

These Au-nanoconjugates may be useful to tackle IM-resistance mechanisms and provide an additional tool for future combinatory schemes to fight CML with imatinib resistance.

Key Words: Anti-sense oligonucleotides, *BCR-ABL1*, chronic myeloid leukemia, *c-MYC*, gold nanoparticles

RESUMO

A leucemia mieloide crónica (LMC) é uma doença rara causada pela presença do cromossoma filadélfia derivado da fusão entre o gene Breakpoint Cluster Region (*BCR*) no cromossoma 22 com o gene Abelson Tyrosine-Protein Kinase 1 (*ABL1*) no chormossoma 9. Este gene de fusão codifica para uma tirosina quinase (TK) constitutivamente activa nas células de doentes com LMC. O Imatinib (IM) é um inibidor específico da oncoproteína BCR-ABL1 usado como primeira linha no tratamento da LMC. A detecção molecular do transcrito *BCR-ABL1* é crucial para o diagnóstico e para as estratégias de tratamento da LMC. Mutaçoes pontuais no gene *ABL1* contribuem para a resistência aos TKIs, levando à necessidade de modificação nos protocolos de tratamento. Numa elevada percentagem de doentes com LMC, observa-se uma falha na resposta terapêutica com progressão da doença, associada a vários mecanismos moleculares de resistência, incluindo a desregulação do proto-oncogene c-MYC.

Os nanoconjugados de ouro (Au-nanoconjugados) demonstraram uma eficácia melhorada em abordagens de silenciamento de genes para terapia do cancro. Neste estudo, avaliámos o potencial de silenciamento de AuNPs funcionalizadas com oligonucleótidos anti-sentido dirigidos a e14a2*BCR-ABL1* ou *c-MYC* isoladamente ou em combinação, demonstrando um silenciamento eficiente da expressão génica e a regulação negativa dos níveis proteicos em linhagens celulares sensíveis e resistentes ao IM. A combinação do inibidor da TK (IM) com outros inibidores da quinase mostrou atividade sinérgica na linhagem celular sensível à IM. Para além disso, o efeito da conjugação dos Au-nanoconjugados com os inibidores danusertib (Danu), volasertib (Vola) e adavosertib (Adavo) mostrou um efeito sinérgico em células resistentes ao IM.

Este trabalho demonstra a utilidade dos Au-nanoconjugados para contornar os mecanismos de resistência ao IM, fornecendo uma ferramenta adicional para futuros esquemas combinatórios no combate à LMC resistente ao IM.

Palavras-chave: Oligonucleotídeos anti-sense, *BCR-ABL1*, leucemia mieloide crónica, *c-MYC*, nanopartículas de ouro

CONTENTS

LIST OF FIGURES

LIST OF TABLES

ACRONYMS

ABL1	Abelson Murine Leukemia Virus homolog1
aCML	Atypical chronic myeloid leukemia
Adavo	Adavosertib
ADO	Antisense double-stranded DNA oligonucleotide
ALL	Acute lymphocytic leukemia
AML	Acute myeloid leukemia
AP	Accelerated phase
ASOs	Antisense oligonucleotides
AuNPs	Gold nanoparticles
AURK	Aurora kinase
AURK-Is	Aurora kinase inhibitors
B-ALL	B-cell precursor
BAX	BCL-2–associated X
BBB	Blood-Brain Barrier
BCL-2	B-cell lymphoma/leukemia 2 protein
BCR	Breakpoint Cluster Region
BP	Blast phase
BSA	Bovine serum albumin
CHK	Checkpoint kinase
CLANs	Cationic lipid-assisted polymeric nanoparticles
CLL	Chronic lymphocytic leukemia
CML	Chronic meyloid leukemia
CML-N	Neutrophilic chronic myeloid leukemia
c-MYC	Cellular myelocytomatosis

CP	Chronic phase
CRISPR/Cas9	Clustered regularly interspaced short palindromic repeats/CRISPR-associated protein
CT	Computed tomography
CTCF	Corrected total cells fluorescence
Danu	Danusertib
DDR	DNA damage repair
DLS	Dynamic light scattering
DMEM	Dulbecco's modified eagle medium
DMR	Deep molecular response
DNMTs	DNA methyltransferases
DSBs	DNA double-strand breaks
DTT	Dichloro-diphenyl-trichloroethane
EDTA	Ethylenediaminetetraacetic acid
EGFP	Enhanced green fluorescent protein
EPR	Enhanced permeability and retention
FBS	Fetal bovine serum
FDA	Food and Drug Administration
FISH	Fluorescent in situ hybridisation
gRNA	Guide RNA
HDOs	Heteroduplex oligonucleotides
ICC	International Consensus Classification
IM	Imatinib
KD	Kinase domain
K562-IM	Imatinib-resistant derived cell line K562
lncRNAs	Long noncoding RNAs
LSCs	Leukemia stem cells
LPCs	Leukemia progenitor cells
MDRI	Multidrug resistance 1
MDS	Myelodysplastic syndrome
miRISCs	miRNA-induced silencing complexes
miRNAs	Micro RNAs
MRI	Magnetic resonance imaging
M-BCR	Main breakpoint cluster region
μ-BCR	Micro breakpoint cluster region

m-BCR	Minor breakpoint cluster region
NaDoc	Sodium-deoxycholate
ncRNAs	non-coding RNAs
NGS	Next generation sequencing
NIR	Near-infrared
NSB	Nano Swarna Bhasma
$O_2^- \cdot$	Superoxide anions
PB	Peripheral blood
PBS	Phosphate buffer saline
PDT	Photodynamic therapy
PDXs	Patient-derived xenografts
PEG	Polyethylene glycol
PET	Positron emission tomography
P-gp	P-glycoprotein
Ph	Philadelphia
PI	Polydispersity index
PLK	Polo-like kinase
PMSF	Phenylmethylsulfonyl fluoride
PSs	Photosensitizers
PTT	Photothermal therapy
QDs	Quantum dots
rhTNF	Tumor necrosis factor alpha
ROS	Reactive oxygen species
RPMI	Roswell park memorial institute
RT-nested PCR	Reverse transcription nested polymerase chain reaction
RT-qPCR	Reverse transcription quantitative polymerase chain reaction
SDS	Sodium dodecyl sulphate
SgRNA	Single guide RNA
SLC	Solute carrier
SLL	Small lymphocytic lymphoma
SPECT	Single photon emission computed tomography
SPIO	Superparamagnetic iron oxide
SPR	Surface plasmon resonance
SS	Sanger sequencing
T-ALL	T-cell linage

TBST	Tris-buffered saline with tween 20
TEM	Transmission electron microscopy
TFR	Treatment-free remission
TKIs	Tyrosine kinase inhibitors
UCNPs	Upconversion nanoparticles
VEGF	Vascular endothelial growth factor
VNB	Vapor nanobubble
Vola	Volasertib
WBCs	White blood cells
WHO	World health organization
ZNFs	Zinc finger nucleases

1

INTRODUCTION

Part of the literature review presented in this chapter has been published, whole or in part, elsewhere. The author of this thesis reviewed and critically discussed the references cited in the text.

Abdulmawjood B, Costa B, Roma-Rodrigues C, Baptista PV, Fernandes AR. Genetic Biomarkers in Chronic Myeloid Leukemia: What Have We Learned So Far? Int J Mol Sci. 2021 Nov 19;22(22):12516. doi: 10.3390/ijms222212516. PMID: 34830398; PMCID: PMC8626020.

1.1 Leukemias

Hematologic malignancies are defined as those affecting bone marrow, blood cells, and lymphatic system [1]. Leukemia, lymphoma, and myeloma are the most commonly noted types of hematological malignancies [2]. These forms of cancer are the most prevalent affecting children and adolescents [2]. Various disruptive biomolecular abnormalities, including chromosomal aberrations and/or genetic mutations, may emerge throughout distinct phases of hematopoietic development, leading to diverse cancer subtypes and clinical manifestations [3]. Leukemia is a kind of cancer characterized by the abnormal multiplication of white blood cells (WBCs) present in the bone marrow, which can be either a primary or secondary process [4].

Leukemia is markedly different from other cancer forms and can affect people of any age, owing to the considerable variety of WBCs in the body. Moreover, demographic factors, including race, age, and lifestyle, do not reduce the risk, in contrast to most malignancies. Annually, there are more than 50,000 new leukemias diagnoses [2].

1.1.1 Classifications

Throughout the twentieth century, the taxonomy of leukemia gradually evolved to encompass more precisely defined entities characterized by phenotypic, genetic traits, morphological and unique clinical presentations. The World Health Organization (WHO) endorsed this integrated approach in their 2008 categorization of hematopoietic neoplasms and more recently, in the 2016 revision. The diagnosis and classification of acute myeloid leukemia (AML) underwent major changes in 2022 with the introduction of the WHO 5th edition and the International Consensus Classification (ICC) of hematopoietic neoplasms [5]

Leukemia is categorized as chronic or acute according to the rate of growth and as myeloid or lymphoid depending on the cell of origin. The primary subtypes are acute myeloid leukemia (AML) and chronic myeloid leukemia (CML), which affect the myeloid lineage; and acute lymphoblastic leukemia (ALL); and chronic lymphocytic leukemia (CLL), which affect the lymphoid lineage [6]. The most common characteristics of the different types of leukemia are described in Table 1.1.

Table 1.1 – Most common characteristic of different types of leukemia in what concerns the type of cells involved, cytology information, common genetic alterations, symptoms, affected age, prevalence and respective references.

Types	**Cell involved**	**Cytology**	**Common genetic alterations**	**Symptoms**	**Afected age**	**Ref**
AML	Immature myeloid lineage cells (marrow)	Oncogene mutations, single myeloblast mutation, Cytogenetic abnormalities	t(15;17)(q22,q21) *PML-RARA*, inv16(p13;q22)or t(16;16)(p13;q22) *CBFB-MYH11*, t(8;21)(q22;q22) *RUNX1-RUNX1T1* , t(9;11)(p22;q23) *KMT2A-MLLT3*	Anemia, spontaneous bleeding	Adults	[7] [8]
CML	Myeloid stem cells (marrow)	Chromosomal translocation, granulocytes	t(9;22)(q34;q1) *BCR-ABL1*	Anemia, low platelet count, enlarged spleen	In adults and rare in children	[7] [6]
ALL	Immature B or T cell (lymph nodes)	Chromosomal aberration	t(12;21)*ETV6-RUNX1*, t(1;19)*TCF3-PBX1* t(9;22)*BCR-ABL1*	Disturb marrow function	Children	[7] [9]
CLL	Peripheral lymphoid B or T cell (lymph nodes)	Chromosomal abnormalities	del(13q), del(17p)*P53*, del(11q)*ATM* Trisomy 12	Swelling of lymph nodes, spleen increase	Commonly affects people over 60 of age	[7] [10]

ALL is the predominant form of this leukemia, representing over 80% of all acute leukemia occurrences. It can be categorized into B-cell precursor (BCP-ALL/B-ALL) or T-cell linage (T-ALL) type, with the former comprising around 85% of ALL cases [11]. BCP-ALL and T-ALL immunophenotypes encompass several subgroups characterized by several chromosomal abnormalities, which are suggested to represent leukemia-initiating lesions [12]. In pediatric

patients diagnosed with B-ALL, prevalent chromosomal translocations comprise t(12;21) ETS variant transcription factor 6 (*ETV6)*- runt-related transcription factor 1 *(RUNX1)* (25%), t(1;9) Transcription Factor class C (*TFC3)*- pre-B-cell leukemia transcription factor 1 *(PBX1)* (5%), t(9;22) breakpoint cluster region (*BCR)*-abelson murine Leukemia virus homolog1 *(ABL1)* (3%), and translocations including the mixed-lineage leukemia 1 (*MLL)* gene with distinct partner fusion genes (5%) [9].

CLL is distinguished by the expansion of monoclonal lymphoid cells. It predominantly impacts adults aged 60 to 70. CLL is often regarded as an indolent disease, indicating that not all diagnosed individuals necessitate immediate treatment; therapy usually starts after the emergence of symptoms [6]. CLL and small lymphocytic lymphoma (SLL) exhibit distinct clinical symptoms of the same underlying illness, frequently categorized together as CLL [10]. About 80% of CLL patients display at least 1 of 4 prevalent chromosomal abnormalities: a deletion of 13q14.3 (del[13q]), deletion of 11q ataxia-telangiectasia mutated gene (*ATM)* (del[11q]), deletion of 17p tumor protein p53 (*TP53)* (del[17p]), or trisomy 12 [13]. The predominant mutation is (del[13q]), observed in roughly 55% of cases [13]. *TP53* mutations occur in 4-37% of CLL patients and correlate with a significantly adverse outcome in multiple studies [13].

AML is a hematological illness marked by the clonal proliferation of genetically modified hematopoietic stem cells and progenitor cells inside the bone marrow. These genetic alterations confer a proliferative advantage and impair normal hematopoiesis [14]. AML constitutes 15-20% of pediatric acute leukemia cases and around 80% of adult leukemia cases. Although it is the predominant type of leukemia in neonates and adults, it constitutes a minor proportion of leukemia cases in infancy and adolescents [14]. The principal cytogenetic subgroups with favorable karyotypes encompass AML, characterized by the translocation between chromosomes 15 and 17 [t(15;17)(q22,q21)]. Promyelocytic leukemia (*PML)*- retinoic acid aeceptor-alpha *(RARA)* and core-binding factor beta subunit (*CBFB)*-myosin heavy chain 11 *(MYH11)* encompass the cytogenetic and molecular subgroups of inversion 16 [inv16(p13;q22)] or t(16;16)(p13;q22) and t(8;21)(q22;q22) [8]. Intermediate karyotypes, predominantly including diploid karyotypes, are observed in roughly 40-50% of patients [8]. Unfavorable karyotypes including complicated karyotypes (characterized by three or more chromosomal abnormalities), the majority of *MLL* translocations (involving 11q23), and various other particular karyotypes [8]. Furthermore, patients exhibiting translocations that affect chromosome 3q26.2, the locus of the *MECOM* (myelodysplastic syndrome 1 (*MDS1*) and etopic viral integration site 1 (*EVI1*) complex locus) gene demonstrate a markedly unfavorable prognosis [15].

CML generally arises from the reciprocal translocation and fusion of the *BCR* gene on chromosome 22 and the *ABL1* gene on chromosome 9, resulting in the dysregulated tyrosine kinase located on chromosome 22, known as the Philadelphia (Ph) chromosome [16]. As a result, it induces a monoclonal population of defective granulocytes, primarily neutrophils, basophils, and eosinophils [6].

1.1.2 Chronic myeloid leukemia

CML is a malignant myeloproliferative disease marked by the clonal expansion of hematopoietic stem cells. CML was the first tumor associated with a chromosomal anomaly [1], and its pathophysiology has been extensively investigated [17]. Moreover, CML was the first leukemia identified, attributed to Rudolph Virchow, David Craigie and John Hughes Bennet who conducted autopsies on patients exhibiting analogous symptoms, including fever, leukocytosis, hepatosplenomegaly [18], and an atypical morphology of blood and viscosity, characterized by Alfred Velpeau in the 19th century as "thick blood"[19]. Peter Nowell and David Hungerford in 1960, reported the discovery of an aberrant "minute chromosome" in individuals with chronic granulocytic leukemia, following the refinement of a method for detecting chromosomes in mitotic cells (karyotyping) [20]. This discovery was the first description of the correlation between chromosomes abnormalities and cancer. Subsequently, this chromosome was named as the Ph chromosome [21]. In 1973, Janet Rowley, using chromosomal staining methods, identified the Ph chromosome as originating from a reciprocal translocation between chromosomes 9 and 22 (t(9;22)) [22].

1.1.2.1 Disease characterization

CML advances through three distinct phases. The process initiates with a chronic phase (CP), associated with leukemia stem cells (LSCs) [16]. During this phase, unregulated clonal proliferation of leukemia progenitor cells (LPCs), results in characteristic symptoms, including splenomegaly, malaise, loss of weight, anemia, pain in the upper left quadrant and lethargy [16]. Nevertheless, 15% of patients are asymptomatic, being detected accidentally, via normal laboratory examinations [16]. Furthermore, if the immune system of the patient remains functional, they may remain asymptomatic for a prolonged period [16]. Untreated (CP-CML) will typically advance to accelerated phase (AP-CML) or blast phase (BP-CML) within an average of 3 to 5 years. The transition to AP-CML and BP-CML encompasses a spectrum of clinical manifestations (e.g., fever, bone pain, splenomegaly), additional chromosomal alterations, and blast cell counts [23].

Age, geographic, and racial disparities may contribute to the diversity in incidence between different registries, and the predisposing factors for the disease remain poorly understood [24].

According to global cancer statistics from the American Institute for Cancer Research, the global incidence of CML varies between 0.7 and 1.5 per 100,000 individuals [25]. Extensive population-based research on CML has been conducted in the USA and Europe, notably in the United Kingdom, the Netherlands, Sweden, and France [24]. Asian countries show lower incidence rates of CML, which predominantly affects a younger demographic, with a greater proportion of patients classified in the high and moderate Sokal risk categories [24]. An elevated prevalence of CML has been noted among Japanese atomic bomb survivors [24]. A correlation between the incidence of CML and lifestyle, dietary variables, as well as an elevated risk of disease progression associated with tobacco smoking has been documented [26]. Occupational pesticide exposure is regarded as a possible risk factor; yet a robust link with CML has not been proven [27]. The median age for the diagnosis of CML is between 57 and 60 years, with a male-to-female ratio of 1.2 to 1.7 [28,29].

1.1.2.2 Molecular biology

As stated, the Ph chromosome is the principal molecular hallmark of CML. The fusion of the *ABL1* gene on chromosome 9 with the *BCR* gene on chromosome 22 gives rise to this condition (Figure 1.1) [16]. This fusion results in the production of an oncoprotein known as BCR-ABL1, with constitutive tyrosine kinase activity. This constitutive activity results in insufficient cell differentiation, unregulated replication, and resistance to apoptosis [16]. The (t(9;22)) chromosomal breakpoints are extensively distributed, especially at the *ABL1* locus [22], however splicing of the main transcript results in a *BCR-ABL1* mRNA isoforms. The two predominant fusions are referred to as e13a2 (*BCR* exon 13 fused with *ABL1* exon 2) and e14a2 (*BCR* exon 14 fused with *ABL1* exon 2) [30]. These two chimeric mRNAs have been also identified as b2a2 and b3a2, with b2 (*BCR* exon 13) and b3 (*BCR* exon 14) representing the second and third exons inside the traditionally characterized major breakpoint cluster region (M-BCR) [31]. e13a2 and e14a2 encode a 210 kDa BCR-ABL1 protein (p210); however, e14a2 *BCR-ABL1* is 25 amino acids bigger than e13a2, attributable to the supplementary amino acids encoded by *BCR* exon 14. The e13a2 and e14a2 *BCR-ABL1* variants collectively represent 98% of CML patients, and mostly predominantly express e14a2. In 10% of the CML cases, expression of both isoforms (e13a2 and e14a2) is observed [30].

In 2% of CML cases, atypical *BCR-ABL1* fusions arising from *BCR* breakpoints outside the M-BCR region (Figure 1.1) may be found (e.g. e1a2, e6a2, e8a2, e19a2, e13a3, and e14a3)

[16]. Among these atypical fusions, the e19a2 transcript encodes a p230 BCR-ABL1 fusion protein, arising from the micro breakpoint cluster region (µ-BCR) located between exons 19 and 20 of *BCR* gene. This fusion is frequently associated with neutrophilic chronic myeloid leukemia (CML-N) [16]. The e1a2 transcript encodes a small p190 BCR-ABL1 isoform, arising from the minor breakpoint cluster region (m-BCR) located between exon 1 and exon 2 of *BCR* gene (the predominant isoform in *BCR-ABL1* positive ALL) is detected in 1% of CML cases and is associated with a poor prognosis [30]

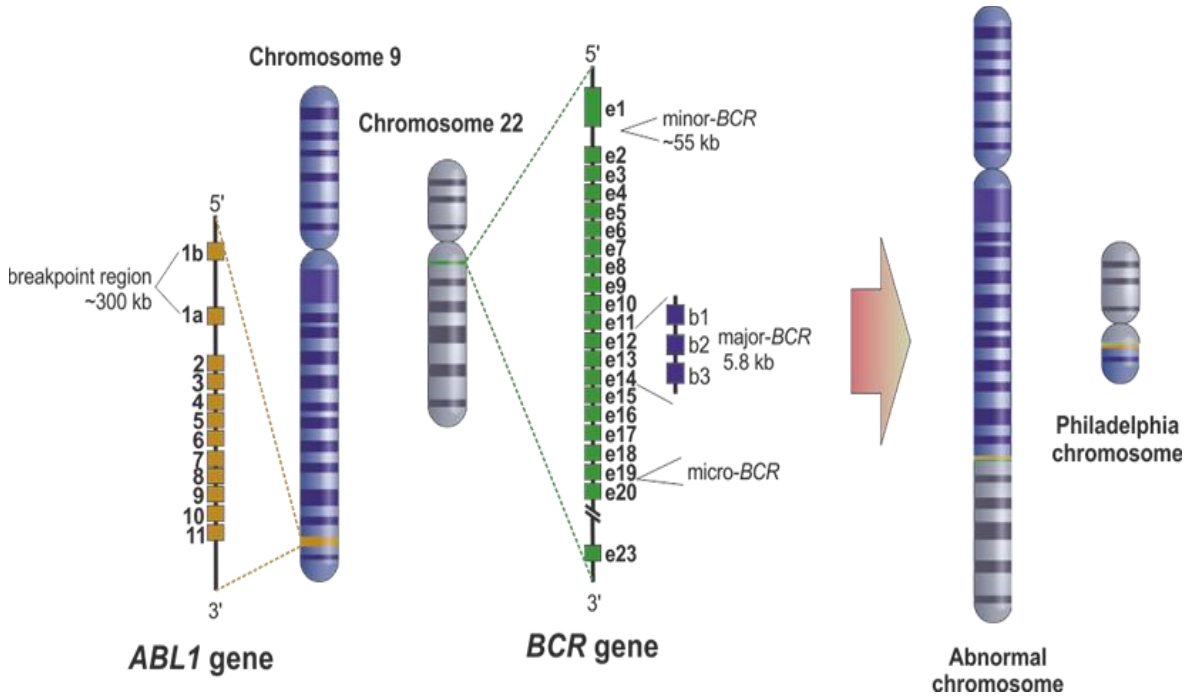

Figure 1.1 — The formation of the Philadelphia chromosome. The Philadelphia (Ph) chromosome arises from the translocation of the Abelson murine leukemia (*ABL1*) gene on chromosome 9 and the breakpoint cluster region (*BCR*) gene on chromosome 22. Three breakpoint sites may be implicated in this translocation: i) intron 13 or 14 of *BCR*, referred to as the major breakpoint (M-*BCR*), ii) intron 1 of *BCR*, identified as the minor breakpoint (m-*BCR)*, and iii) exon 19 of *BCR*, termed the micro breakpoint (µ-*BCR*). The *ABL1* breakpoint often occurs in the region between exons 1b and 2. Retrieved from *Abdulmawjood* et al., (2021) [16].

1.1.2.3 Variations of the Philadelphia Chromosome

While 90% of CML patients present with Ph positive chromosome (Ph^+), about 5 to 10 % lack it and may present other abnormalities [32]. It may be in a single form (including 22q11 and a single breakpoint) or in a more complex form (including 9q34, 22q11, and multiple additional breakpoints) [33]. Variations arise from breakpoints in genomic hotspots, frequently located in CG-rich areas that are susceptible to chromosomal breaks and repair mechanisms

[16]. Cytogenetics, particularly karyotyping, is the definitive method for identifying Ph^+ chromosomes and assessing cytogenetic response [16]. Identifying further chromosomal abnormalities is essential, particularly in Ph^+/negative clones throughout treatment, as they may indicate clonal development towards more complex and serious disorders such as myelodysplastic syndrome or AML [16]. Most of studies demonstrate no differences in prognosis between standard and variant translocations [32,34-38]; however, some suggest inferior outcomes associated with Ph^+ variants [39-42].

Indeed, in a study including 250 Mexican Ph^+ CML patients, in 90.4% a single p210 *BCR-ABL1* isoform was present, whereas in around 7% of Ph^+ CML patients, both b3a2 and b2a2 isoforms were detected [43]. Only 5% of the patients exhibited the co-expression of p190/p210 *BCR-ABL1* fusions, and those with co-expression of at least 2 or all p190/p210/p230 *BCR-ABL1* fusions demonstrated a worse prognosis [43]. In a study published by *Vinhas* et al., [42] a CML patient, resistant to IM treatment, no *ABL1* mutations were detected but *BCR-ABL1* expression and *ABL1* phosphorylation were observed due to the presence of double Ph^+ cells with 2 protein isoforms, the common p210 and the uncommon p195 isoform. The patient started bosutinib and later exhibited a favorable response. This work underscores the importance of discovering numerous transcripts to enhance treatment [42].

1.1.2.4 Genetic Biomarkers in CML

Genomic instability leads to modifications in DNA, characterized by increased mutation rates, microsatellite instability, and further chromosomal abnormalities [44]. The *BCR-ABL1* fusion gene is the primary driver of gene deregulation in CML and the primary therapeutic target using tyrosine kinase inhibitors (TKIs) in this disease. *BCR-ABL1* gene deregulation and other chromosomal abnormalities drive genomic instability, crucial for the progression from CML-CP to the more aggressive CML-BP [45]. Evaluation of *BCR-ABL1* gene expression levels can enhance diagnosis and prognosis of CML [16].

Indeed, CML progression typically occurs by an initial evasion of cellular differentiation and resistance to programmed cell death, involving increased expression of genes stimulating different proliferation signaling pathways, modifications of cell adhesion markers and secondly, modifications in gene expression during treatment may lead to relapse, suggesting that progression continues in a subset of CML cells [16]. Other genes, such as transforming growth factor beta (*TGF-β*), tumor necrosis factor (*TNF*), *TP53* and vascular endothelial growth factor A (*VEGFA*), may act as possible biomarkers for prognosis and therapeutic responsiveness or resistance [46-52]. Epigenetic modifications, including DNA methylation

and histone modification, together with the expression of long noncoding RNAs (lncRNAs) and microRNAs (miRNAs), may also play a role in CML transformation/progression [51,53,54].

Epigenetic dysregulation collaborates with genetic abnormalities to creat an environment that promotes formation, maintenance and progression of tumor [51]. Alterations or reprograming in epigeneteic pathways resulting in changes in histon modifications, DNA methylation and transcriptional dysregulation throughout the progression of CML [55]. Abnormal epigenetic regulation in the expression of some genes associated with CML may significantly influence its pathogenesis and the mechanisms affecting therapeutic responsiveness [54].

1.1.2.4.1 Genomic instability in CML

Transitioning from CML-CP to CML-BP involves increased genomic instability of LSCs, leading to microsatellite variations, telomerase activity, and cytogenetic instability [56-59]. LSCs heterogeneity, where TKI-resistant quiescent LSCs present in the bone marrow microenvironment [59,60] interacts with adjacent stromal cells promoting genomic instability and facilitating BP-CML development [59, 61] (see Figure 1.2).

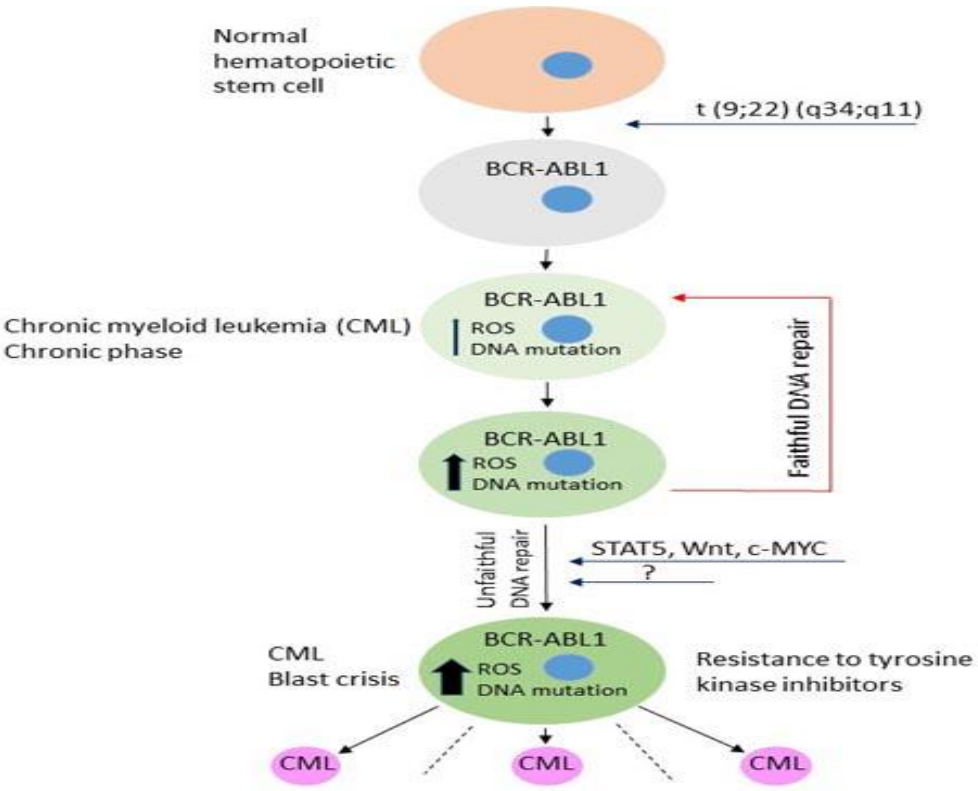

Figure 1.2 — BCR-ABL1 protein activity in CML. The persistent of BCR-ABL1 protein kinase activity promotes excessive proliferation of leukemia stem cells (LSCs), leading to chronic phase (CP). The development of resistance to tyrosine kinase inhibitors (TKI), along with a distinct bone marrow microenvironment and the buildup of reactive oxygen species (ROS), induces genomic instability in quiescent leukemia stem cells (LSCs), leading to an accelerated phase (AC) that culminates in a blast crisis with worsened symptoms. Retrieved from *Pawlowska et al.,* (2015) [62].

Compared to normal cells that effectively repair DNA damage, LSCs possess impaired DNA repair mechanisms due to mitochondrial alterations induced by Rac2-MRC-cIII GTPase activity in BCR-ABL1-positive cells [63], leading to elevated levels of reactive oxygen species (ROS), namely superoxide anions ($O_2^{-}\cdot$) associated with single- and double-strand DNA damage [64,65], leading to further increase genomic instability of LSCs cells (Figure 1.2). Moreover, elevated levels of telomerase activity and enhanced proliferation due to defective checkpoint regulatory proteins may also contribute to this genomic instability of CML [66,67]. Prevalent genetic alterations have been observed in CML cells at both the chromosomal (e.g., monosomy 7, trisomy 8, duplication of Ph, duplication of chromosomes 19, 21 or 17, isochromosome 17 or loss of chromosome Y) [68,69] and gene levels (see Table 1.2). Indeed, the use of bioinformatic tools and molecular data from patients databases allows us to retrieve information incorporated into multiple studies, to identify the genes and molecular pathways most frequently altered in CML [49]. For a more detailed description about the altered genes and their molecular pathways in CML please see *Abdulmawjood* et al., (2022) [16], *Ochi* et al., (2023) [70] and *Alkhatabi* et al., (2024) [71].

Table 1.2 — Genes whose expression is altered in CML.

Gene (Protein)	Description	NCBI Gene ID	Protein function	CML analysis	Reference
ABL1 (ABL1)	ABL proto-oncogene 1, non-receptor tyrosine	25	Cell division, adhesion, differentiation, and response to stress	Chronic phase Blast crisis	[49]
AKT1 (AKT1)	AKT serine/threonine kinase 1	207	Regulation of cell proliferation, survival, metabolism, and angiogenesis	Chronic phase Blast crisis	[49]
ATM (ATM)	ataxia-telangiectasia mutated serine/threonine kinase	472	Cell cycle checkpoint	Blast crisis	[46]
BCL2 (BCL2)	BCL2 apoptosis regulator	596	Regulation of apoptosis	Chronic phase Blast crisis	[49]
BTK (BTK)	Bruton tyrosine kinase	695	B-cell development	TKIs[1] resistance	[72]
CDKN2A	Cyclin dependent kinase inhibitor 2A	1029	Regulation of cell cycle progression	Blast crisis	[46]
c-MYC (c-MYC)	MYC proto-oncogene, bHLH transcription factor	4609	Regulation of cell cycle progression, apoptosis, and cellular transformation	Good response to TKIs[1]	[46]
CTNNB1 (CTNNB1)	Catenin beta 1	1499	Cell adhesion	Chronic phase Blast crisis TKIs[1] resistance	[46,49]
E2F (E2F)	E2F transcription factor 1	1869	Cell cycle regulation	Good response to TKIs[1]	[40]
EGFR (EGFR)	Epidermal growth factor receptor	1956	Cell proliferation	Chronic phase Blast crisis	[49]
FYN (Fyn)	FYN proto-oncogene, Src family tyrosine	2534	Regulation of cell growth	sChronic phase Blast crisis	[49]
IL1B (ILB1)	Interleukin 1 beta	3553	Cytokine involved in inflammatory response, cell proliferation, differentiation, and apoptosis	Chronic phase Blast crisis	[49]

JAK2 (JAK2)	Janus kinase 2	3717	Regulation of cell growth, development, and differentiation	Chronic phase Blast crisis	[49]
MAPK1 (MAPK1)	Mitogen-activated protein kinase 1	5594	Regulation of proliferation, differentiation, transcription, and development	Chronic phase Blast crisis	[49]
MAPK3 (MAPK3)	Mitogen-activated protein kinase 3	5595	Regulation of proliferation, differentiation, and cell cycle progression	Chronic phase Blast crisis	[49]
PDGFR-β (PDGFRB)	platelet-derived growth factor receptor, beta polypeptide	100487523	Regulation of cell proliferation, survival, differentiation, chemotaxis, and migration	Chronic phase Blast crisis	[49]
PTKB2 (PTKB2)	Protein tyrosine kinase 2 beta	2185	Calcium-induced regulation of ion channels	Chronic phase Blast crisis	[49]
SRC (SRC)	SRC proto-oncogene, non-receptor tyrosine kinase	6714	Regulation of cell growth	Chronic phase Blast crisis	[49]
TGFB1 (TGFB1)	Transforming growth factor beta 1	7040	Regulation of cell proliferation, differentiation, and growth	Chronic phase Blast crisis	[49]
TGFB2 (TGFB2)	Transforming growth factor beta 2	7042	Regulation of cell proliferation, differentiation, and growth	Chronic phase Blast crisis	[49]
TNFA (TNF)	Tumor necrosis factor	7124	Cytokine is involved in inflammatory response.	Chronic phase Blast crisis	[49]
TP53 (p53)	Tumor protein p53	7157	Regulation of cell-cycle, apoptosis, and autophagy	Chronic phase Blast crisis Mutations correlated to poor prognosis	[49-52,73]
VEGFA (VEGFA)	Vascular endothelial growth factor A	7422	Proliferation and migration of vascular endothelial cells	Chronic phase Blast crisis	[49]

Moreover, next generation sequencing (NGS) and fluorescent in situ hybridisation (FISH) technologies allowed to analyse the relationship among the copy number, expression, and activity of *BCR-ABL1* with the copy number, mutational status, and expression of telomere maintenance genes in 5 *BCR-ABL1* positive cell lines (K562, MEG-A2, MOLM-1, KU-812, and LAMA-84) [48]. Despite no pathological alterations were detected in telomere-associated genes, mutations and/or copy number variations in tumor suppressor genes, namely *TP53* (loss and mutations), ataxia telangiectasia mutated (*ATM*) (mutations), and cyclin-dependent kinase inhibitor 2A (*CDKN2A*) (deletion) were observed [48]. Nevertheless, a connection between *BCR-ABL1* expression and telomere length was identified, consistent with another research [66]. The significance of *TP53* mutations or function loss, particularly at (codon 72), has been previously demonstrated to be critical for CML progression and resistance to therapy [50-52,74-77]. Analysis of NGS data indicated that the deletion of *CDKN2* and mutations in the *ATM* and in the homologous ataxia telangiectasia and rad3-related protein (*ATR*) gene contributed to the progression of CML and enhanced genomic instability [78-80].

Moreover, some studies performed in cell lines demonstrated the involvement of DNA damage repair (DDR) in TKI resistance. The increase of alternative nonhomologous DNA end joining (NHEJ) factors poly(ADP-ribose) polymerase 1 (PARP1), werner Syndrome ATP-dependent helicase (WRN), and DNA ligase IIIa, together with the downregulation of canonical NHEJ proteins artemis and DNA ligase IV, illustrates the involvement of the inefficient and error-prone alternative NHEJ pathway in TKI-resistance [81,82]. Moreover, other *in vitro* models of TKI-resistance demonstrated the activation of the base excision repair genes methyl-CpG binding domain protein 4 (*MBD4*) and Nth endonuclease III-like 1 (*NTHL1*) in TKI-resistance [83,84].

The evidence indicates that the impairment of DNA damage repair in CML is directly implicated in resistance to TKIs and the progression of CML. The dysregulation of these processes can indirectly contribute to resistance by causing genomic instability, leading to the accumulation of point mutations and chromosomal abnormalities [85]. Point mutations in the *ABL1* kinase domain can inhibit the binding of TKIs. Additionally, point mutations and chromosomal abnormalities may activate alternate cellular signaling pathways that contribute to TKI-resistance, including the phosphatidylinositol 3-kinase (*P13K*)/ AKT serine/threonine kinase 1 (*AKT*), Janus kinase (*JAK*)/ signal transducer and activator of transcription (*STAT*), rat sarcoma virus *RAS*/ mitogen-activated protein kinase (*MAPK*), and SRC proto-oncogene, non-receptor tyrosine kinase (*SRC*) pathways [86].

1.1.2.4.2 Epigenetic Regulation in CML

The epigenetic status of a cell can be modulated through histone modification, DNA methylation, and post-transcriptional regulation by non-coding RNAs. These mechanisms can influence the cell at several levels: by modifying DNA conformation and its suitability for transcription, damage, or repair; by influencing RNA expression levels and stability; and by governing protein translation or post-translational changes (Figure 1.3) [53].

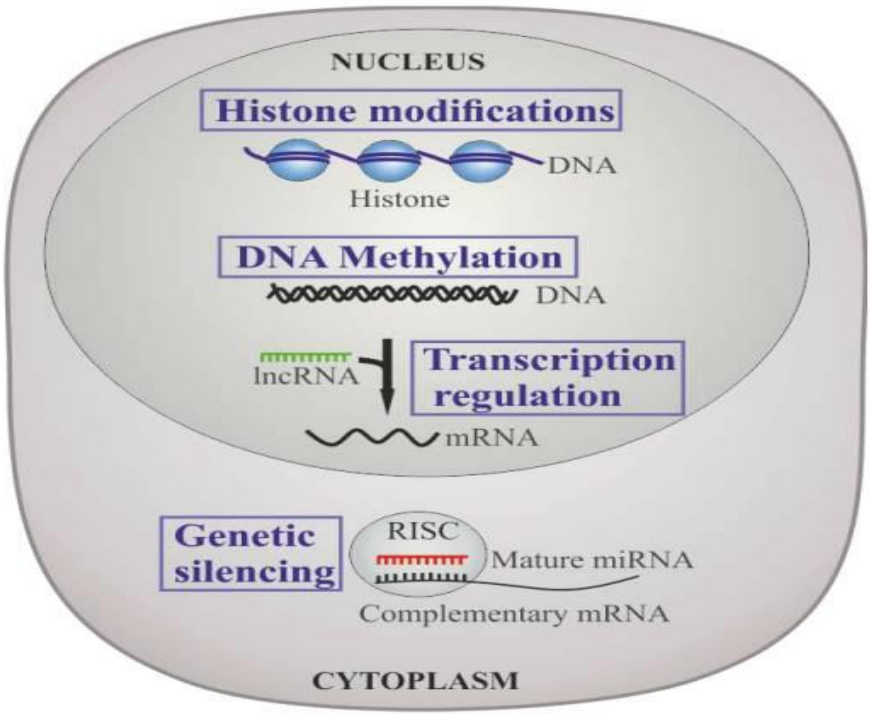

Figure 1.3 — Epigenetic regulation in CML. Histone modification is essential in gene regulation. DNA methylation typically inhibits gene transcription via DNA methyltransferases (DNMTs) and methyl-cytosine dioxygenases at cytosine residue inside CpG dinucleotides. Non-coding RNAs are essential in modulating gene expression, either through miRNA-induced silencing complexes (miRISCs) that target mRNA for degradation, or through lncRNAs that participate in the regulation of gene transcription, post-transcriptional processing, and epigenetic modifications. Retrieved from *Abdulmawjood* et al., (2021) [16].

Histone modifications have a critical function in the regulation of gene transcription [16]. These modifications mostly encompass methylation, phosphorylation, acetylation [16], and other post-translational alterations [16]. Numerous data indicate that the activation of oncogenes and the inactivation of tumor suppressor genes correlate with the progression of CML [87]. Dynamic alterations in histone modifications are associated with loss-of-function mutations in genes implicated to CML [88-90]. Histone hypoacetylation in promoter areas leads to the silencing of pyruvate dehydrogenase complex, E1-alpha polypeptide 1 (*PDH1*) [91],

hence reducing the levels of mRNA and protein of BCR-ABL1 in CML and LAMA-84 cells [92]. Conversely, histone hyperacetylation enhances the expression of genes such as *p21* and *p27* [54].

DNA methylation is a critical epigenetic process that plays a significant role in chromatin architecture and the regulation of gene expression [16]. Dysregulation of DNA methylation has a crucial role in solid tumors and leukemias, including CML [16]. Research indicates that the tumor suppressor metastasis suppressor protein 1 (*MTSS1*) is frequently downregulated in both leukemic stem cells and progenitor cells in CML, although its expression normalizes during TKI therapy, leading to decreased cell proliferation and motility [93]. Moreover, hypermethylation of the hypermethylated in cancer 1 (*HIC1*) gene, a repressor that modulates sirtuin 1 (*SIRT1*) expression, leads to *SIRT1* overexpression in CML, particularly as CML advances [94-96]. Finally, the CD70/CD27 axis has been demonstrated to induce non-canonical Wnt signaling in the presence of TKI, contributing to the survival of leukemic stem cells [97].

Non-coding RNAs (ncRNAs) are important in modulating gene expression throughout several stages, including transcription, RNA processing, and translation [16]. In CML, deregulated miRNAs function as both oncogenes and tumor suppressors genes [16]. lncRNAs have been identified as significant regulators of gene expression [98], comprising approximately 200 nucleotides in length [99]. These lncRNAs have diverse roles in gene regulation, encompassing transcription, epigenetic modifications, and post-transcriptional processes such as mRNA splicing and stability [100-104]. Certain lncRNAs have been recognized as critical biomarkers for many cancer types [105-108]. In CML, a new lncRNA known as lncRNA-BGL3 has been identified as a crucial regulator of BCR-ABL1-mediated cellular transformation [109,110]. For a more detailed review of lncRNAs in CML please see *Dutta* et al., (2024) and *Rudich* et al., (2022) [111, 112].

1.1.2.4.3 miRNAs Dysregulation in CML

miRNAs are short, conserved non-coding RNA sequences, generally measuring approximately 20 to 23 nucleotides in length, that modulate gene translation. They are essential in various biological processes by preferentially binding to mRNA transcripts, slowing translation, and decreasing protein production (Figure 1.4) [16]. It is believed that miRNAs govern around 60% of the transcriptome, influencing essential cellular processes such as proliferation, development, differentiation, cell fate determination, and death [113]. Moreover, miRNAs have demonstrated their significance as crucial biomarkers for tumor detection and monitoring, as they can be identified in body fluids (e.g. peripheral blood, urine, etc) [99].

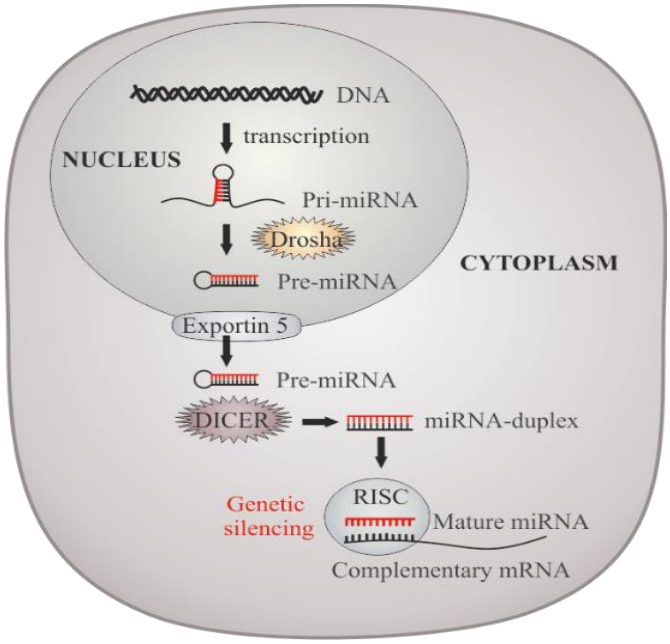

Figure 1.4 — Biogenesis and molecular processing/action of miRNAs. Pri-miRNAs are generated in the nucleus and then identified and cleaved by Drosha into a smaller stem-loop structure known as pre-miRNA. Pre-miRNAs are subsequently transported to the cytoplasm for further processing by Dicer, resulting in the formation of mature miRNAs, which will incorporate into the miRISC. The efficacy of genetic silence or translation inhibition is dependent upon the degree of homology between miRNAs and their corresponding target regions, predominantly located inside the 3′-UTRs of mRNAs. Retrieved from *Abdulmawjood* et al., (2021) [16].

The regulation of carcinogenesis in CML is a complex process involving multiple variables, including several dysregulated miRNAs (Table 1.3) [114]. Specific miRNAs have been associated with patient responses to TKIs, including imatinib (IM), the first TKI used in CML treatment (see Table 1.3) [115]. Patients that respond to TKI exhibit elevated levels of miRNA-26a, miRNA29c, miRNA-130b and miRNA-146a relative to non-responders [115]. This variance may result from the downregulation of their targets, such as cellular inhibitor of apoptosis protein-1 (cIAP1) and myeloid cell leukemia sequence 1 (MCL1), which are essential for tumor cell survival following TKI therapy [16]. The overexpression of miRNA-23a, miRNA-30a, miRNA-30e, miRNA-203, miRNA-320, and miRNA-424, which target *BCR-ABL1*, is advantageous for TKI-responsive patients [115]. Specifically, miRNA-451 levels can act as an effective biomarker for predicting TKI response and are associated with a positive prognosis [116], as it directly targets *ABL1* and *BCR-ABL1* [115]. For a more detailed review in miRNAs in CML please see *Rudich* et al., (2022) [112].

Table 1.3 — miRNAs involved in CML phenotype.

miRNA	Expression in CML	Process involved/Biological relevance	References
miRNA-21	Upregulated	One of the most highly expressed miRNAs in various cancers, associated with drug resistance. Lower levels at diagnosis indicate a better response to TKI treatment. Serves as a marker for disease progression, with higher expression from CP to BP. Its inhibition causes G1-phase arrest, reduced growth, and apoptosis.	[114,117- 119]
miRNA-29b	Downregulated	Expression is inversely related to *MCL-1* and *BCL-2* levels. Its reduced expression contributes to the avoidance of apoptosis.	[120]
miRNA-30a	Downregulated	Plays a role in suppressing autophagy, thereby enhancing IM-induced cytotoxic effects. Higher expression is observed in IM responders. Its levels are inversely correlated with the Sokal score and *BCR-ABL1* after treatment.	[121,122]
miRNA-138	Downregulated	Linked to reduced *BCR-ABL1* expression, inhibition of cell proliferation, and increased apoptosis induced by IM treatment.	[123]
miRNA-203	Downregulated	Frequently silenced in CML due to monoallelic loss and promoter hypermethylation. IM treatment reverses promoter methylation, leading to increased miRNA-203 expression, which reduces *BCR-ABL1* levels and inhibits CML cell proliferation.	[124,125]
miRNA-451	Downregulated	Serves as a biomarker for disease progression, with expression decreasing from CP to BP. A reciprocal regulatory relationship exists between miRNA-451 and *BCR-ABL1*. Its levels at diagnosis predict TKI treatment outcomes, and it is involved in IM resistance.	[114,126-129]
miRNA-144/451	Downregulated	Involves a regulatory pathway miRNA-144/451 with *c-MYC*. Expression is lower in IM-resistant patients (where *c-MYC* is overexpressed). Restoring miRNA-144/451 levels sensitizes CML cells to IM treatment.	[130]
miRNA-486-5p	Downregulated	Acts as a prognostic biomarker, with higher expression at diagnosis linked to better overall outcomes and quicker achievement of complete hematologic response to IM.	[131]

1.1.2.5 Diagnosis

CML diagnosis depends on physical examination, medical history, and laboratory results, including cytogenetic and molecular analyses. By integrating this information, healthcare providers can determine the illness stage and suggest appropriate monitoring and treatment strategies [17]. CML is frequently identified during normal medical examinations or via blood testing in asymptomatic patients [132]. The diagnosis of typical chronic CML is simple and requires confirming the presence of the Ph chromosome abnormality t(9;22), in instances of continuous unexplained thrombocytosis or leukocytosis [133]. This can be accomplished through standard cytogenetics (Karyotype) or molecular cytogenetics (e.g. FISH) or by molecular analyses that detect *BCR-ABL1* transcripts such as qualitative (e.g. reverse transcription nested polymerase chain reaction (RT- nested PCR) or reverse transcription quantitative polymerase chain reaction (RT-qPCR) testing that allows to measure the levels of *BCR-ABL1* transcripts [133]. FISH analysis depends on the co-localization of extensive genomic probes targeting the *BCR* and *ABL1* genes [133].

Atypical chronic myeloid leukemia (aCML) is defined by the absence of the Ph chromosome and the absence of *BCR-ABL1* rearrangement [17]. It affects around 5% of CML patients, presenting with leukocytosis accompanied by a left shift, splenomegaly, and significant myeloid dysplasia [17]. These individuals typically exhibit a bad prognosis and a reduced response to the treatment [17]. Given that most patients are presented without symptoms and required differential diagnosis with other systemic and hematological disorders, various laboratory tests are crucial for the CML diagnosis such as blood count, bone marrow aspiration, karyotyping, cytogenetics and both qualitative and quantitative PCR [134].

1.1.2.6 Therapies

TKIs constitute the gold standard treatment for Ph^+ CML-CP, recognized for achieving exceptional rate of hematological, molecular and cytogenetic responses [135]. IM was the first TKI licensed by the U.S. Food and Drug Administration (FDA) for the treatment of CML [136]. IM interacts with the *BCR-ABL1* kinase domain (KD) that adopts an inactive conformation within a pocket designated for the binding of ATP, hence inhibiting the phosphorylation of tyrosine on the protein substrate and the consequent activation of the phosphorylated protein [136]. Its efficacy encompasses all stages of CML, and clinical trials have shown that most of patients treated in the CML-CP reach a normal life expectancy [137-141]. Deep molecular response (DMR) is characterized by ≤0.01% IS of *BCR-ABL1* levels, with distinct thresholds for MR4 (≤0.01% IS), MR4.5 (≤0.0032% IS), and MR5 (<0.001% IS) [2]. DMR has been identified in > 80% of patients, with over 70% maintaining remission post-treatment

cessation. This achievement has led to the idea of treatment-free remission (TFR), which reduces low-grade adverse effects such as muscle cramps and exhaustion [2].

As a result of decreased efficacy of IM in patients with mutations in the KD of BCR-ABL1 protein, that induces resistance to IM, second generation TKI such as dasatinib, bosutinib, and nilotinib were developed [142]. Mutations in the kinase domain associated with resistance to IM occurred in 4.6% of 1551 CP-CML patients over a decade [2]. These second generation TKIs induce more rapid responses than IM when used as a second-line treatment [16]. Third generation (TKIs), including ponatinib and asciminib (ABL001), are designed to target specifically the *BCR-ABL1*-T315I and compound mutations [16]. ABL001 functions as an allosteric inhibitor of *ABL1* kinase via binding to the myristoyl pocket in place of the catalytic pocket of *BCR-ABL1* [16].

1.1.2.6.1 Therapies other than TKIs

In the last twenty years, targeted therapy with TKIs such as IM, nilotinib, dasatinib, bosutinib, and ponatinib has shown significant outcomes. Nevertheless, the heterogeneity of the disease and development of resistance continues to pose considerable difficulty in the management of CML [143,144]. Both primary and secondary resistance to TKIs can be induced by BCR-ABL1-independent signals, thereby enhancing the self-sustenance of the LSC clone [145].

Aurora kinase inhibitors (AURK-Is) block the serine/threonine kinase activity of the Aurora kinase (AURK) family, which controls cell division. Dysregulation of AURK activity can lead to chromosomal abnormalities and DNA changes that promote cell transformation [144]. In hematological malignancies like CML, AURK is typically overexpressed, rendering AURK inhibitors an attractive therapeutic strategy for treatment [146]. AURKs are regarded as promising therapeutic targets for the development of anticancer pharmaceuticals. The relationship between *BCR-ABL1* and AURK in the pathogenesis of CML remains incompletely defined; however, the efficacy of AURK inhibitors in the therapy of CML has been extensively researched [147,148].

Danusertib (Danu), a dual inhibitor of AURK and *ABL1* (including both wild-type and mutant variants, including T315I), has demonstrated encouraging efficacy in leukemia and solid malignancies [144]. Danu specifically reduces the proliferation of immortalized BCR-ABL1-positive cells and CML CD34-positive progenitors from patients who exhibit either sensitivity or resistance to TKIs [149,150]. Danu has demonstrated acceptable dose-dependent toxicities and encouraging efficacy in advanced and resistant ALL, and CML patients during phase II clinical trial [151]. In this clinical trial, 4 of 29 patients with accelerated

or blast phase CML exhibited a response, all of whom have the T315I *BCR-ABL1* mutation [151]. These findings facilitate additional preclinical and clinical progress [151].

The polo-like kinase (PLK) family, which includes PLK1, PLK2, PLK3, PLK4, and PLK5, comprises serine/threonine protein kinases [152]. PLK1 predominantly expressed in the late G2 and M phases, controls mitosis and exhibits elevated expression in numerous malignancies, which is associated with unfavorable prognosis [153]. In CML, PLK1 is present in its phosphorylated state in both K562 cells line and primary CML cells [154]. Inhibition of *BCR-ABL1* by IM or nilotinib diminishes PLK1 expression, suggesting that *BCR-ABL1* facilitates PLK1 production [154]. Inhibition of PLK1 in CML cells leads to cell cycle arrest and apoptosis [154]. The PLK1-targeting agent BI 2536 inhibits the proliferation of both imatinib-sensitive and IM-resistant CML cells, including those harboring the T315 mutation of *BCR-ABL1* [154].

Volasertib (Vola), a low molecular weight molecule, is one of the most prominent PLK inhibitors, demonstrating significant anti-leukemic efficacy [152]. The combination of Danu and Vola in both sensitive and resistant CML cell lines has been shown to inhibit proliferation and trigger considerable caspase-dependent death. Notably, in contrast to IM, these two TKIs function by targeting different pathways. Both Danu and Vola induce a significant elevation in the number of cells in the G2/M phase [145].

Wee1 G2 checkpoint kinase (Wee1), a serine/threonine protein kinase, is crucial for the G2/M phase checkpoint and DDR [155,156]. In response to DNA double-strand breaks (DSBs), the ATR and ATM pathways are activated, with ATM activating Checkpoint kinase 2 (CHK2) and ATR activating CHK1, which collectively activate Wee1 [157]. Upon activation, Wee1 phosphorylates the Tyr15 site of CDK1, thereby inhibiting its activity, postponing cell progression into the M phase, and facilitating DNA replication [158-160]. The upregulation of Wee1 is correlated with several cancers, like lung cancer, breast cancer, hepatocellular carcinoma, and leukemia, and is associated with tumor development and worse prognosis [161-168]. Wee1 is extensively engaged in DNA damage response signaling and the repair of double-strand breaks. Inhibiting the overexpression of Wee1 has demonstrated therapeutic advantages in CML, particularly in CML-sensitive cases [157]. Wee1 facilitates cell proliferation and IM resistance in CML by modulating DNA damage response via the ATM- gamma histone variant H2AX (γH2AX) - mediator of DNA damage checkpoint 1 (MDC1) pathway, rendering it a potential therapeutic target [157,169]. Adavosertib (Adavo) is a selective small inhibitor molecule of the Wee1 TK, an essential regulator of the intra-S and G2/M phase cell cycle checkpoints. Wee1 can regulate DNA replication and mitosis by phosphorylating and inhibiting CDK 1 and 2 [170]. Furthermore, Adavo enhances the efficacy of chemotherapeutic drugs by impairing the DNA damage response, leading to buildup of DNA damage [171].

The effectiveness of Adavo in conjunction with other anticancer treatments has been examined in preliminary clinical trials [172-174]. The combination of Adavo and bortezomib markedly enhanced apoptosis in multiple myeloma cell lines compared to the administration of either agent individually [175]. Furthermore, Adavo enhanced the sensitivity of myeloid leukemia cells (AML, CML, and myelodysplastic syndrome (MDS)) to the inhibitory effects of cytarabine, resulting in higher apoptosis in these neoplastic cells [176].

1.1.2.7 Drugs resistance mechanisms

Despite the significant success of TKI therapy, approximately 50% of patients who discontinue medication develop a recurrence due to their failure to eradicate persisting CML cells [177]. Furthermore, around 20% of CML patients have inadequate responses to initial therapy, with 5-10% advancing to blast crisis [178]. This process is associated with the emergence of resistance, which constitutes a "bottleneck to cure" [179]. TKI resistance may be influenced by both dependent and independent BCR-ABL1 pathways, contingent upon their relationship with the *ABL1* KD [180]. Although considerable advancements have been achieved in knowing the BCR-ABL1-dependent mechanisms of resistance, which depend on the reactivation of *BCR-ABL1*, the mechanisms of BCR-ABL1-independent resistance remain more obscure [181].

1.1.2.7.1 BCR-ABL1-dependent resistance

In CML, BCR-ABL1-dependent pathways represent well-defined forms of TKI resistant treatment [182]. BCR-ABL1-dependent processes encompass *BCR-ABL1* mutations, gene amplification, and upregulation [180]. The T315I mutation in BCR-ABL1 protein was the first mutation identified in in CML patients with IM resistant and is the most challenging one [182]. The T315I mutant variant of *BCR-ABL1* is lacking threonine residue at position 315, which functions as a gatekeeper [16]. Mutation of this residue to isoleucine blocks TKI entry into the hydrophobic pocket while permitting ATP access [16]. Despite the encouraging effectiveness of asciminib, especially against the T315I mutation, certain CML patients develop mutations in the myristoyl-binding pocket [183]. Some mutations such as V468F, I502L, P465S, C464W, and A337V have been demonstrated to confer resistance to asciminib while maintaining the sensitivity to ATP-competitive kinase inhibitors [184,185]. Mutant clones possessing mutations in the KD and myristoyl-binding site exhibited asciminib or ponatinib resistant; however, this resistance was significantly decreased when combing these two therapies [177].

Genomic instability leads to the accumulation of mutations in the *ABL1* KD and other molecular or chromosomal abnormalities [180]. Conversely, the increase of BCR-ABL1 fusion proteins may induce genomic instability in CML cells [186]. Partial deletions of PR-domain zinc finger protein 16 (*PMRD16*) and runt-related transcription factor 1 (*RUNX1*), the expression of the *PMRD16/RUNX1* fusion, and mutations that activate GATA-binding protein 2 (*GATA2*) have been linked with the progression of CML, also may be recognized in the disease [180]. The extent of *BCR-ABL1* transcript overexpression associated with IM resistance has been investigated in both cell lines and patients, with estimates varying from several-fold increases to over one log. This has been investigated in cell lines, revealing a two- to ten-fold elevation in BCR-ABL1 target protein expression [187-190].

1.1.2.7.2 BCR-ABL1-independet resistance

Approximately 50% of CML patients exhibiting inadequate responses or disease progression had KD mutations, whereas the remainder exhibits other resistance mechanisms [191]. Tumor growth happens when critical cellular pathways, including the MAPK/ extracellular signal-regulated kinase (ERK) pathway JAK2/STAT, PI3K/AKT/ mammalian target of rapamycin (mTOR) and (RAS/ rapidly accelerated fibrosarcoma (RAF)/MEK/ERK), are invaded by oncogenes or when direct stimulation of the elements or upstream activators of these cascades [182]. These modifications can modify sensitivity to small inhibitors molecules employed in treatment of cancer [182].

The MAPK/ERK pathway, a critical downstream signaling pathway of BCR-ABL1, facilitates cell proliferation and survival in BCR-ABL1-positive cells [192]. TKIs can inhibit this mechanism through inhibition of *BCR-ABL1* and triggering apoptosis of CML cells. Nonetheless, independent stimulation of the RAS pathway may result in resistance to TKIs [193,194]. The JAK/STAT signaling pathway is a significant downstream route of BCR-ABL1 that influences survival, proliferation and treatment of the resistance in CML. This pathway encompasses critical effectors including STAT3 and STAT5 [177]. Deininger et al. conducted a study indicating that the phosphorylation of STAT3 at Y705 confers resistance to TKIs in CML CD34+ cells [195]. mTORC1 is a downstream effector of AKT and can be stimulated by phosphorylated AKT [196]. A study by Burchert et al. demonstrates that PI3K/AKT/ mTOR signaling is elevated when responded to IM, hence facilitating resistance to IM [197]. A study by Mancini et al. indicated that the AURK A/ PLK1/ forkhead box M1 (FOXM1) axis is another mechanism involved in BCR-ABL1 independent resistance [198]. The amplification and hyperactivation of this axis, found in primary patient cells and resistant cell lines, induces IM resistance by activating many pathways that increase the proliferation and survival of leukemic hematopoiesis [198]. The JAK/STAT, RAS/MAPK, and PI3K/AKT pathways can reg-

ulate Cellular myelocytomatosis (*c-MYC*) mRNA expression and increase c-MYC stability [199]. c-MYC is an inherently disordered protein that is part of the basic helix-loop-helix-leucine zipper (BHLHZip) family found in the cell nucleus [200]. The carcinogenicity of c-MYC can increase the transcription levels of high-affinity target genes or induce saturation; furthermore, it can upregulate or downregulate low-affinity target genes, converting normal cells into tumor cells [201]. The aberrant kinase activity of BCR-ABL1 enhances c-MYC transcription and translation, a critical phase in the disease's progression to blast crisis [202]. The inhibition of BCR-ABL1 tyrosine kinase activity by IM markedly reduces c-MYC expression and hematological tumor features in CML cells [203]. The downregulation of c-MYC is an essential process in imatinib-induced apoptosis in chronic myeloid leukemia [201]. c-MYC suppressed erythroid differentiation and apoptosis induced by IM or dasatinib, demonstrating its essential role in drug sensitivity [201]. c-MYC overexpression has been linked to worse IM responses in untreated CML patients and non-responders, perhaps because of its role in promoting chromosomal instability [202].

Moreover, BCR-ABL1 independent resistance is associated with the expression levels and functioning of solute carrier (SLC) transporters, categorized into influx and efflux types depending on their transport mechanisms [180]. The impact of efflux transporters on IM pharmacokinetics has been extensively studied, and their elevated expression is typically associated with variation in IM response [204,205[. The most extensively researched transporter protein is P-glycoprotein (P-gp), which can eject IM from leukemic cells [206]. This protein is encoded by the ATP binding cassette subfamily B bember 1 (*ABCB1*) gene, part of the ATP-binding cassette subfamily B, often known as *MDR1* (multidrug resistance 1) [207]. A study by *Ammar* et al. showed that the overexpression of P-gp on lymphocytes is substantially connected with the poor molecular response to IM in patients with CML [208].

1.1.2.8 Gene therapy in CML

Gene therapy use genetic material that can change the respective encoding protein or alter the biological properties of tissues in several ways, including the replacement or inactivation of malfunctioning genes, and the introduction of novel genes. The increasing knowledge of tumor cells and their surroundings has encouraged the application of gene therapy through novel delivery mechanisms and advanced gene expression systems to get effective cancer treatment. These systems include Antisense oligonucleotides (ASOs), zinc finger nucleases (ZFNs), clustered regularly interspaced short palindromic repeats/CRISPR-associated protein 9 (CRISPR/Cas9), and small interfering RNA (siRNA) [209]. For a more detailed review of nucleic acid therapeutics for myeloid leukemias please see *Kovecses* et al. (2024) [210].

1.1.2.8.1 ASOs

Antisense technology is a useful tool for modulating gene expression and addressing human disorders. ASOs are synthetic single-stranded DNA analogues, often 15–30 base pairs in length that are complementary to a specific mRNA sequence [211]. ASOs target RNA by binding specifically to sequences, hence altering oncogene expression. ASOs operate by activating RNase H, which cleaves DNA/RNA hybrids, inhibiting translation, or altering alternative splicing, which leads to the destruction of cells possessing the specified gene marker [201].

A study by Rowely et al., [212] found that circular ASOs targeting the BCR-ABL1 junction efficiently suppressed the proliferation of CML cells. In a separate study, *Ashizawa* et al., [213] examined BP1001, an ASO targeting the *Grb2* gene, an essential partner of the BCR-ABL1 protein in CML evolution. BP1001 demonstrated preclinical efficacy in reducing CML burden and is undergoing further development as a therapeutic option [213]. A recent study by *Hoshiki* et al., [214] employing DNA/RNA heteroduplex oligonucleotides (HDOs) demonstrated that the naked BCR-ABL1-targeting antisense double-stranded DNA oligonucleotide (ADO) was markedly more effective than siRNA in decreasing of *BCR-ABL1* mRNA expression in CML cell lines [214]. Furthermore, ADO reduced the BCR-ABL1 protein levels in a dose-dependent strategy that impaired cell proliferation and enhanced the effect of IM [214].

1.1.2.8.2 ZFNs

ZFNs are synthetically engineered by combining a site-specific zinc finger protein with the non-specific cleavage domain of the FokI restriction endonuclease. The DNA-binding component has 3–6 zinc finger repeats, each able to recognize 9-18 base pairs. A ZFN typically comprises three zinc fingers, each specific to a three-base pair DNA sequence, creating a three-finger array that binds to a 9-base pair target site with the non-specific cleavage domain [216,217]. Gene disruption via ZFN was first demonstrated in 1994 when a three-finger protein was engineered to precisely inhibit the production of the *BCR-ABL1* human oncogene in a murine cell line [218]. In 2018, Wenli Feng's team demonstrated that alternative genome-editing nucleases, like ZFNs, might likewise destroy the *BCR-ABL1* oncogene. By targeting exon 1 of *BCR* with a pair of ZFNs, they generated a premature stop codon, leading to a shortened oncoprotein. This leads to increased apoptotic rates and less proliferative potential in the modified cells [219].

1.1.2.8.3 CRISPR/Cas9

CRISPR/Cas9 gene editing technology, a promising cancer gene-suppression therapy, possesses the potential to permanently eliminate genes responsible for tumor survival, thereby

addressing the limitations of repeated dosing inherent with conventional cancer treatments and enhancing therapeutic efficacy [220]. The CRISPR/Cas9 system comprises two components: Cas9, a nuclease that cleaves DNA at a designated spot, and a single guide RNA (sgRNA) that directs Cas9 to the precise DNA locus. Due to the necessity of manipulating the nuclear genome, the components of this complex must be translocated into the nucleus [221,222]. In recent years, gene editing methodologies, primarily CRISPR/Cas9, have garnered considerable attention in leukemia research. The CRISPR/Cas9 system has been documented to effectively suppress the *BCR-ABL1* oncogene, counteracting its tumor-promoting activity [223]. In a CML xenograft model, subcutaneous injection of altered single-cell-derived clones did not result in tumor development. The findings indicate that CRISPR/Cas9 technology may serve as a promising therapeutic option for CML patients exhibiting TKI resistance [223].

In 2017, *Garcia-Tunon* et al., employed CRISPR/Cas9 technology to target BCR-ABL1-positive CML and demonstrated the effective inhibition of the p210 variant of the *BCR-ABL1* fusion gene in both a Boff-p210 leukemia cell line and a murine disease model [224]. Recently, *Vuelta* et al., developed an innovative CRISPR/Cas9 short-deletion strategy that effectively targets the *BCR-ABL1* oncogene in both murine and human cell lines, and for the first time, in primary leukemic stem cells (CD34+ from CML patients and Sca1+ from a CML mice model) [225]. They reported that CRISPR/Cas9-modified LSCs reduced the tumorigenic activity and restored multipotency [225]. The administration of these modified LSCs demonstrated considerable therapeutic advantages in orthotopic patient-derived xenografts (PDXs) and CML mice models [225].

For a more detailed review of the role of CRISPR technology in CML please see *Kaur* et al. (2024) [226].

1.1.2.8.4 siRNA

siRNAs act by selectively silencing genes associated with the disease through sequence-specific binding [227]. Synthetic siRNAs possess a unique structure characterized by a short double-stranded RNA sequence including sense (non-guide) and anti-sense (guide) strands, approximately 21 bp in length, with phosphorylated 5′ ends and hydroxylated 3′ ends, with two nucleotides overhanging at the 3′ end of each strand [228]. Moreover, the design of siRNA sequences facilitates the targeting of previously deemed undruggable genetic regions, thereby addressing a significant obstacle in tailored medicine [227].

SiRNA has been investigated over the past 15 years as an alternative therapeutic strategy for leukemia in both in vitro and in vivo models [229]. In the context of CML therapy, siRNA targeting the *BCR-ABL* gene was administered in K562 cells utilizing various lipopol-

ymers: palmitic acid, α-linolenic acid, and cholesterol served as lipid modifications on PEI (PEI-PA, PEI-αLA, and PEI-Chol, respectively) [230-232], which resulted in reduced cell viability, enhanced apoptosis, and increased drug sensitivity in IM-resistant cells. Finally, the administration of BCR-ABL1 siRNA/PEI-αLA lipopolymer was investigated in solid K562 tumors, which inhibited the growth of subcutaneous tumors in a CML mouse model [233].

For a more detailed review of siRNA role in CML targeting please see *Vysochinskaya* et al. (2024) [234].

1.2 Nanomedicine

Nanomedicine can be defined as the use of nanotechnology for medical applications [235-237]. Nanotechnology, which deals with technology at the nanoscale (size between 1 to 100 nanometers (nm)), exhibit unique physical and chemical features that can be precisely adjusted to enhance interactions with the various biological systems toward enhanced delivery and specific targeting of therapeutics, optimized imaging modalities and diagnostic [238].

Nanoscaled particles have transformed drug delivery by enabling the selective targeting of therapeutic agents at the organ, tissue, and cell-specific levels, hence reducing the exposure of healthy tissues to pharmaceuticals [239]. Nanomedicines have markedly enhanced drug delivery systems, tackling issues such as inadequate pharmacokinetics, restricted bioavailability, and increased toxicity linked to traditional pharmaceuticals [240]. Nanoparticles and liposomes have significantly improved the therapeutic indices of drugs through targeted delivery, controlled release, and enhanced solubility and stability [241]. These innovations have resulted in more efficacious treatments with diminished side effects, e.g. reduced toxicity and enhanced pharmacokinetic parameters, including distribution, prolonged circulation time, targeted controlled release, elevated intracellular concentration, and improved solubility and stability of drugs within the organism [242].

Nanomedicines have already made their way to the clinics, particularly through liposome-mediated drug delivery systems and the encapsulation of medications like Doxorubicin [243]. Lipid nanoparticles have encouraging efficacy in facilitating the delivery of synthetic chemicals - nanodrugs [244].

Incorporating mRNA and therapeutic proteins has strongly beneficted from nanomedicine concepts (e.g. SARS-CoV-2 vaccines) [245]. Lately, the utilization of nanomedicine and immunotherapy has arisen in the treatment of diverse cancers, suggesting that the combination of these two therapeutic approaches may establish novel paradigms in cancer treatment [246].

Still, safety issues still need to be addressed with the use of nanomedicines, highlighting the need for a comprehensive understanding of the essential properties that affect the interaction of nanomaterials with tissues and organs [247]

1.2.1 Nanomedicine for diagnostics and therapeutics

Nanomedicines provide unique physicochemical features not only as drug-delivery nanocarriers but also as synthetic scaffolding for imaging probes used in cancer diagnosis [248]. The efficacy and application of these systems are determined by their chemical composition (such as metallic, lipidic, polymeric, and inorganic types), structural attributes, including surface properties (such as charge and hydrophobicity), physical characteristics (such as size, shape, and stiffness), and surface functionalization with targeted ligands and functional groups [249].

1.2.1.1 Specific targeting and EPR

Tumor tissue targeting is primarily dependent on the impaired tumor vasculature and inadequate tumor lymphatic system, allowing nanoscale particles to passively diffuse towards and accumulate in fast growing solid tumors via the enhanced permeability and retention (EPR) effect [250]. The EPR effect has been fundamental to the advancement of cancer nanomedicine, e.g. the first FDA-approved nanomedicine, Doxil® (PEGylated liposomal doxorubicin), and Apealea® (paclitaxel micellar), both rely on the EPR effect to induce clinical outcome [250]. Also, standard clinical practice has incorporated at least fifteen cancer nanomedicines, all of which utilize EPR-mediated passive tumor targeting [250].

1.2.1.1.1 Passive targeting

The EPR effect underpins passive targeting, a crucial mechanism for the accumulation of potential nanocarriers in tumors [251]. Passive targeting effect depends on tumor biology, involving aspects like the extent of vascular and lymphatic vessels synthesis, perivascular tumor infiltration, and intra-tumoral pressure. These factors, in conjunction with the physical and chemical features of nanoparticles, dictate the efficacy of passive nanomedicine targeting [238]. The efficacy of targeting is significantly dependent on blood circulation time. Particle sizes ranging from 5 to 250 nm can diffuse through compromised vasculature and accumulate over time, due to the lack of functional lymphatic drainage [238].

Nanoparticle sizes must be selected considering the interactions between nanoparticles and biological tissues and organ physiology [252]. Surface characteristics, including hydro-

phobicity and charge, are crucial in affecting cellular absorption rates and protein photochemical alterations [253]. Hydrophilic and negatively or neutral particles have reduced nonspecific internalization rate and reduced *in vivo* circulation half-lives in contrast to hydrophobic and positively charged particles [253]. Stability, a crucial factor influencing the circulation time of nanoparticles, is also essential for effective tumor acccumulation. Research indicates that drug leakage from stable nanoparticles frequently occurs prior to reaching their intended target, making premature drug release a critical factor affecting efficacy [238].

1.2.1.1.2 Active targeting

Active targeting refers to a specific ligand-receptor interaction that transpires following blood circulation and extravasation. It mostly depends on the biological interaction between target cells and the ligands on nanoparticles [254], i.e. particular ligands are used to identify and attach to receptors exclusive to the target cell [255]. An essential element of this strategy is the ligand-mediated identification of the target substrate receptor [256]. Ligand and target interaction can induce intramembrane folding, resulting in nanoparticle uptake by receptor-mediated endocytosis. After internalization, endogenous particles are conveyed to the nuclear endosome, where additional particle processing and drug release transpire [238]. This targeted delivery enables the nanoparticle to infiltrate the cell and discharge its therapeutic cargo. Active targeting focuses on specific cells, thereby reducing the effects on healthy tissues and improving the treatment's therapeutic efficacy [257]. Multiple studies emphasize the efficacy of cell targeting, demonstrating a substantial increase in cellular nanoparticle uptake in vitro [258].

1.2.1.2 Phototherapy

Photodynamic therapy (PDT) and photothermal therapy (PTT) are novel light-mediated approaches in cancer treatment. PDT uses light-activated photosensitizers (PSs) to generate dangerous ROS inside neoplastic cells, resulting in their annihilation [259]. Nonetheless, PDT encounters difficulties caused by tumor hypoxia, restricted tissue penetration of short wavelength light, aggregation-stimulated quenching of PSs, and the possible phototoxicity arising from systemic distribution of PSs [260]. These challenges can be overcome by nanophotosensitizers, which offer improved photophysical characteristics and enable regulated administration of PSs [238]. For instance, *Liang* et al. created a TME-responsive AuNC@MnO2 (AM) nanoplatform for oxygen-enhanced PDT, which successfully inhibits the growth and metastasis in breast cancer metastatic cells [261].

Additionally, *Li* et al. synthesized thiolated heparin-pheophorbide A (PhA) linked hybrid nanoparticles of iron oxide and gold (Fe3O4/AuNP) to efficient monitoring of PDT [262]. Magnetic nanoparticles, including magnetite (Fe3O4), can be transported to the targeted area using an external magnetic field [263]. PS-conjugated magnetic nanoparticles have been utilized for PDT [264]. Conversely, PTT operates by exploiting the heightened thermal sensitivity of malignant cells and transforming light energy into heat, resulting in intratumoral damage [238]. This methodology employs several near-infrared (NIR) nanomaterials, including carbon nanotubes and gold nanorods, among others [265,266].

Chen et al., designed a nanocomplex system for simultaneous fluorescence optical imaging and magnetic resonance imaging [267]. This system is called a gold nanoshell-based system which is utilized for targeting cancer and PTT for HER2 overexpressing and drug-resistant ovarian cancer cells (OVCAR3) [267]. This nanocomplex system afterward treated with NIR laser which selectively eliminates OVCAR3 cells [267]. *McGrath* et al. have proven the production and efficacy of palladium gold nanostructures for improved PTT applications [268]. The efficacy of photothermal applications was further validated by the eradication of HeLa cells in vitro and the elimination of cervical cancer cells of male B9 mice in HeLa tumor xenografts, utilizing a combination treatment with 808 nm diode laser radiation [268]. To achieve combined PDT/PTT with photodecomposable, photothermal, and photodynamic characteristics, SP3NPs were synthesized from self-assembled PEGylated cypate, which comprises PEG and an Indocyanine green (ICG) derivative [269]. It can produce singlet oxygen for PDT and induce photothermal effects for PTTand exhibits significant accumulation in tumors because of the presence of PEG on its surface and its small size (~60 nm) [269]. These attributes render it a viable option for application in image-guided PDT/PTT [269].

1.2.1.3 Imaging

Conventional non-invasive imaging modalities, including computed tomography (CT), magnetic resonance imaging (MRI), *p*ositron emission tomography (PET), and single photon emission computed tomography (SPECT), are essential, however having difficulties with sensitivity and specificity, hindering thorough disease assessment [270]. Nevertheless, these techniques can only assess alterations on the tissue surface at a relatively advanced stage of disease progression; however, enhancements can be achieved through the application of contrast and targeting agents utilizing nanotechnology to augment resolution and specificity by pinpointing the diseased area at the tissue level [271]. Medical imaging contrast agents currently used are predominantly tiny compounds characterized by rapid metabolism and non-

specific distribution, which may consequently lead to adverse toxic side effects [272]. The dimensions of the nanoparticles markedly affect their biodistribution, blood circulation half-life, cellular absorption, tissue penetration, and targeting efficacy (see above the EPR effect), which will improve the signal to noise ratio of these imaging strategies [272].

For instance, superparamagnetic iron oxide (SPIO) and ultrasmall SPIO are utilized in MR, AuNPs in CT, quantum dots (QDs) and upconversion nanoparticles (UCNPs) in OI, and carbon nanotubes and gold nanorods in photoacoustic contrast [273]. Moreover, nanoparticles coated iodine (CT contrast agent) enhanced imaging results while reducing cytotoxicity of iodine [238]. Nanoparticles-enhanced CT imaging and SPECT/CT demonstrated significant potential for cancer diagnosis at early stages, as evidenced by promising outcomes in breast cancer and melanoma models [274,275]. AuNPs possess significant potential in SPECT imaging and may serve as a contrast agent [269]. An investigation demonstrated another approach for functionalizing AuNPs with mannose. Technetium (99mTc)-radiolabeled AuNPs functionalized with mannose can monitor and accumulate in lymph nodes. It may serve as a SPECT contrast agent for lymphatic mapping [269]. *Giovinazzo* et al. examined an indirect method for visualizing liposomal drug delivery, utilizing Tc-99m sulfur colloid (TSC, Technecoll®) to elucidate the distribution of PEGylated liposomal doxorubicin (Doxil®) [276]. TSC and other Tc-99m-labeled colloids are clinically authorized and routinely employed for lymphoscintigraphy and cancer staging [277].

1.2.1.4 Theranostics

Theranostics is the combination of therapeutics and diagnostics in one system/device, which has gained momentum through the development of nanomedicine [278]. Nanotheranostics involves the application and advancement of nanomedicine techniques for enhanced theranostics, specifically through the utilization of nanosystems (e.g. polymer conjugates, dendrimers, micelles, liposomes, metal and inorganic nanoparticles, carbon nanotubes, and biodegradable polymer nanoparticles) to attain sustained, controlled, and targeted delivery of diagnostic and therapeutic agents [279]. Nanotheranostics hold potential for severe diseases such as cancer, cardiovascular disorders, and AIDS, offering the possibility of less burdensome treatments and improved prognoses, thereby conserving resources and boosting patients' quality of life [279].

For instance, iron oxide nanoparticles (IONPs) coated with human serum albumin provides a biocompatible material for a chemotherapeutic drug, PSs, and imaging [280]. Extensive investigations were conducted on polymeric conjugates concerning drug transport, biodistribution, and pharmacological efficacy [281]. Polymeric micelles, and nano-core/shell

structures formed by amphiphilic co-polymers, were extensively evaluated as theranostic carriers and imaging probes [282-285]. The amphiphilic block co-polymers encapsulated SPIO or Mn-SPIO nanoparticles and are utilized for MRI [286]. β-cyclodextrin (β-CD) has effectively encapsulated SPIONs and small molecule anticancer agents [287].

Guo et al. introduced a new multifunctional nanoenzyme-driven theranostic molecule—PPy@MnO2-BSA(Ce6)—engineered for MRI-controlled PDT and PTT in oncology [288]. The nanoparticles were using the polymerization of pyrrole followed by oxidation with high-valent manganese salts, specifically potassium permanganate (KMnO4). The compound was subsequently stabilized using bovine serum albumin (BSA). The primary focus of the synthesis was the functionalization with chlorine 6 (Ce6), which gives the entire nanoparticle with distinctive and critical activities, including the generation of oxygen and ROS, as well as the conversion of photons to heat PPy@MnO2-BSA(Ce6) has the potential for monitoring and precisely targeting the cancer microenvironment [288].

1.2.2 Gold nanoparticles

Gold has maintained a dynamic emphasis within the innovation community, dating back to ancient times when it was primarily utilized for coloring glass and ceramic decorations [289]. The application of molecular structures of gold in the clinicals has been used to mitigate rheumatoid arthritis [290].

AuNPs are easy to synthesize in aqueous media and offer adjustable physicochemical characteristics dependent on size [291]. For example, AuNPs can be easily functionalized with various biomolecules, such as ligands, DNA, proteins, and polymers [292-295]. Moreover, AuNPs possess a distinctive local surface plasmon resonance (SPR) suitable for optical imaging and and sensing applications [291]. The AuNP SPR depends on the particle size, morphology, and aggregation state. Furthermore, AuNPs exhibit good chemical stability and biocompatibility [291].

Due to their properties and apparent lack of acute toxicity when used in low dosages, AuNPs have been used in several nanotheranostics applications mainly via intravenous administration. Upon entering the bloodstream, nanoparticles encounter an environment abundant with cells and proteins. Small particles with sizes lower than 3 nm can pass through the endothelium of lung and muscle capillaries; however, nanoparticles with size lower than 60 nm can enter the endothelium of kidney, liver, and spleen because of their wider interstices which facilitate the entrance of nanoparticles [296]. Smaller nanoparticles have the possibility to infiltrate cells and can be identified in cell nuclei, resulting in further DNA damage [297]. Subcutaneous, intramuscular, or topical delivery of colloidal drug carri-

ers typically prolongs the retention of the drug carrier compared to the free drug, with the carriers predominantly maintained by local lymph node. The distribution in vivo is significantly influenced by the nanoparticle's size, shape, surface charge, and surface hydrophobicity [298].

AuNPs can also be combined with other nanomaterials. For example, Fe3O4, which is approved by the FDA as negative contrast agent, resulting in Fe3O4@AuNPs with unique magnetic properties and a gold coating, providing photothermal, photodynamic, or SERS capabilities and targeting antibody action [299]. *Iancu* et al examined the physical and biological characteristics of these nanoparticles and achieved stable nanoparticles that induced a negative T2 signal in vivo upon injection into rats, indicating their potential as negative contrast agents in MRI. A decrease in cytotoxicity was also noted [300].

1.2.2.1 AuNPs for gene therapy/gene silencing delivery

Nanoparticles have been proven to be suitable vehicles for gene therapy, being easy to produce and bind nucleic acids, with minimal immunogenicity and toxicity [301]. AuNPs for gene therapy in vitro and preclinical animal models show high payload capacity, low toxicity, effective cellular uptake, rapid endosomal escape, prolonged half-life, effective and selective gene silencing and transfection, as well as the ability to broadly activate the innate immune response [302].

The modification of AuNPs surface is crucial for their cellular absorption [302]. AuNPs can effectively bind to amine and thiol groups, enabling their functionalization with diverse biological molecules for therapeutic purposes [303]. AuNPs can incorporate therapeutic agents, like siRNA, therapeutic oligonucleotides and drugs [304]. Chemical functionalization of AuNPs with polymeric stabilizers like polyethylene glycol (PEG), imparts a neutral charge to the surface, which is crucial for enhancing biocompatibility, circulation duration and solubility in biological systems [304]. Furthermore, the neutralization of charged nanoparticles ensures minimal adhesion to circulating plasma proteins, hence preventing the clearance of AuNPs from circulation by phagocytosis [305]. Moreover, AuNPs can be functionalized with targeting-specific elements, such antibodies and peptides, to enhance their effectiveness in targeted drug delivery [306].

Gene silence includes the intracellular administration of siRNA or ASOs to modulate gene expression [305]. Most of gene silencing strategies target related oncogenes such as *BCR-ABL1*, *c-MYC*, *KRAS*, and *EGFR*, which induce aberrant cell proliferation through heightened gene expression or enhanced activity of the resultant oncoproteins; they can also

suppress tumor suppressor genes that typically inhibit cell proliferation and tumorigenesis; or affect other genes associated with tumor survival [307].

DNA and RNA are characterized by their pronounced negatively charge, which can associate with cationic AuNPs by ionic interactions [308,309]. AuNPs can be functionalized using thiolated oligonucleotides, alkythiol-terminated oligonucleotides, cysteamine-terminated miRNAs, or amine-terminated siRNAs [305].

For instance, AuNP-based dendrimers (Au DENPs) have effectively facilitated the delivery of vascular endothelial growth factors (VEGF) or B-cell lymphoma/leukemia 2 protein (BCL-2) siRNA to a human glioma cell line [310]. Additionally, it has been employed to administer a BCL-2 siRNA to a human cervical cancer cell line [311].A distinct investigation indicated that the AuNP-folic acid combination was employed to transport functional siRNA to silence RELA expression in prostate cancer cells [312]. Furthermore, the AuNP-folic acid combination effectively inhibited the proliferation of MDA-MB-231 breast cancer cells in vitro [312]. The effectiveness of RNAi AuNP-based nanocarriers against the c-MYC proto-oncogene has been established [312].

Moreover, Anti-VEGF siRNAs were administered to U87MG cells utilizing AuNPs conjugated with cell-penetrating peptides, resulting in gene silencing that decreased tumor growth in mice after 3 days [313].

In addition to gene silencing therapy and gene construct delivery, AuNPs may be utilized for the distribution of genome editing products [313]. A notable instance of genome editing via AuNPs was a proof-of-concept work by *Raes* et al. [314], in which nanosphere AuNPs were employed indirectly to facilitate pore formation for the transport of CRISPR-based tools. SPR was utilized for photoporation to generate vapor bubble cavitation in several adherent and suspension cells, facilitating the entry of Cas9 and sgRNA complexes into the cells [314]. The genetic product complexes significantly diminished EGFP expression levels by over 80% in H1299-EGFP lung cancer cells while exhibiting low cytotoxicity [314].

1.2.3 Nanomedicine in CML

At present, organic nanomaterials provide the foundation of FDA-approved or clinically investigated nanomedicine for hematological malignancies [315]. Conventional treatment for CML includes chemotherapy, radiation, immunotherapy and phototherapy. Chemotherapy agents such as cisplatin and carboplatin exhibit adverse effects due to their neurotoxic and nephrotoxic properties [316]. Although various treatments for CML exist, nanomedicine offers a distinct advantage due to the dimensions of nanoparticles and their capacity to exclusively target cancer cells [316].

For example, *Lui* et al. [317] aimed to utilize a CRISPR/Cas9 system for CML treatment by encapsulating a CRISPR/Cas9 plasmid (pCas9) that expresses Guide RNA (gRNA) to target the *BCR-ABL1* (pCas9/g*BCR-ABL1*) within PEG-b-poly (lactic acid-co-glycolic acid) (PEG–PLGA)- based cationic lipid-assisted polymeric nanoparticles (CLANs). The synthesized nanoparticles effectively targeted the CML-associated *BCR-ABL1* gene while sparing the corresponding gene in normal cells, therefore enhancing the rates of survival in CML animal model. Furthermore, an antisense oligonucleotide developed by *Vinhas* et al. [318]. Specifically targeted the expression of e14a2 *BCR-ABL1* in K562 cells. The AuNPs effectively silenced the genes, resulting in a substantial rise in cell mortality. The alteration in BCL-2 and BAX protein expressions, the increase in caspase-3 activity, and the detection of apoptotic bodies in cells treated with the Au-nanoconjugate signify the compound's ability to induce apoptosis in K562 cells. Moreover, *Fan* et al. [319] synthesis a double oligopeptide-conjugated nanoparticles to target the osteoblastic and vascular niches in bone marrow. The synthesized nanoparticles improved the stability and loading effectiveness of arsenic trioxide, specifically targeting cancer lesions to eradicate primitive CML cells, while also enhancing the protective effects of arsenic trioxide on original CML cells and diminishing the size of the K562–HUVEC organoid.

Another study by *Min* et al., [320] which employed exosomes by collecting them from IM resistant CML cells and utilizing them as vectors for the delivery of miR-365. The effective absorption of exosomes by CML cells was accomplished, together with the successful targeting of receptors on recipient cells, resulting in the accumulation of miRNA in the target tissues. *Liu* et al. [321] encapsulated homoharringtonine, a therapeutic agent for patients resistant to TKIs, within PEGylated liposomes, demonstrating comparable safety and reduced toxicity relative to unencapsulated medication. Furthermore, *Elderdery* at al., [322] used CuO-TiO_2 –Chitosan-Berbamine nanocomposites against K56 cell line in a dose-dependent way using IC_{50} of 113.54 g/ mL which results in the death of CML cells through targeting of BCL-2 and BAX and increasing the p35 levels which results in mitochondrial apoptosis.

Additionally, *Jiang* et al., [323] synthesized a poly(d,lactide-co-glycolide) nanopartciles loaded with Anti-BCR-ABL1 antibodies and labeled with transferrin on the nanopartciles surface (Ab@Tf-Cou6-PLGA NPs) to target CML cells. The results demonstrate that Ab@Tf-Cou6-PLGA NPs was effectively able to degrade the BCR-ABL1 oncoprotien in CML cells. Moreover, *Amerigos* at el., [324] utilized solid lipid nanoparticles (MTO/βE-SLNs) to overcome MDR1 in CML cells by co-encapsulation a chemotherapeutic drug of mitoxantrone and P-gp inhibitor of β-elemene inside the MTO/βE-SLNs. The results show that the MDR1 was overcome by blocking the intracellular ATP and p-glycoprotien by β-elemene.

The discovery of several indicators and molecular actors in the pathogenesis of CML is anticipated to facilitate the development of a nanomedicine-based therapy to enhance treatment strategies.

1.2.3.1 AuNPs - From research lab to clinics

The first clinical trial evaluating the application of AuNPs s as a drug delivery system was carried out by *Libutti* et al. (NCT00356980) in 2010 [325]. This work formulated recombinant human tumor necrosis factor alpha (rhTNF) for administration as a therapeutic agent. PEG and rhTNF were conjugated to a colloidal gold nanoparticle (27 nm), a system designated as CYT-6091. This solution was provided within a vein to individuals aged eighteen years and older with advanced and/or metastatic solid organ malignancies. The results demonstrated safe, systemic administration of 1.2 mg of rhTNF without the dose-limiting toxicities, which included hypotension and hepatotoxicity, formerly seen with native rhTNF [325]. The prevalent negative effects associated with CYT-6091 treatment comprised hypokalemia, hypophosphatemia, hypoalbuminemia, elevated aminotransferases and lymphopenia. AuNPs and the drugs encapsulated within them may induce systemic toxicities and unfavorable occurrences; however, these issues were mitigated through appropriate protocol management, and none were deemed dose-limiting toxicities. The data indicate that although adverse implications were noted, they were manageable and should not undermine confidence in the safety of AuNPs. Furthermore, CYT-6091exhibited non-antigenicity and was infrequently detected in healthy tissue [325].

In 2020, a pilot clinical trial was conducted by *Khoobchandani* et al., [326] which examined an oral nano-mediated medication, Nano Swarna Bhasma (NSB), which consists of AuNPs functionalized with phytochemicals derived from mango peel for treatment of breast cancer [326]. NSB offers a reproducible and scientifically verifiable formulation of 'Swarna Bhasma', an ancient Indian Ayurvedic medicine recognized for its anti-cancer properties, although hindered in development due to the scarcity of reproducible Ayurvedic formulations. In the trial, 6 patients with invasive breast cancer were allocated into two groups, receiving either "Standard of care treatment" comprising doxorubicin and cyclophosphamide, or "Standard of care treatment" with NSB. The study outcomes revealed that hyperacidity and widespread weakness were observed in 1 patient from each therapy group. A single instance of severe anemia was documented only in the NSB medication adjuvant cohort, although it was deemed unrelated to NSB [326]. The authors believe that NSB has shown satisfactory safety as an adjuvant therapeutic drug in the treatment of breast cancer of human [326].

AuNPs were also utilized to facilitate gene silencing by RNAi. In 2021, *Kumthekar* et al., [327] conducted a clinical trial (NCT03020017) evaluating the efficacy and safety of an RNAi-based nanoparticle formulation, NU-0129, for glioblastoma therapy. The research sought to inhibit the BCL-2-like protein 12 (*BCL2L12*) oncogene to enhance the prognosis of glioblastoma by reducing tumorigenic *BCL2L12* derivatives. NU-0129 consists of a spherical gold nanoparticle core covalently linked to *BCLl2L12*-targeting siRNA, together with an oligoethylene glycol backfill. 8 patients with recurrent glioblastoma, aged between 32-66 years, received an intravenous administration of 0.4 mg/kg of NU-0129 and were evaluated every week over a 21-day period for adverse effects [327]. Throughout the follow-up time, 7 adverse events were recorded; yet only 2 were deemed severe: lymphopenia and hypophosphatemia. These symptoms were potentially associated with the NU-0129 formulation and showed improvement by the conclusion of the follow-up period. As an AuNPs-based drug delivery system, the NU-0129 therapy shows well tolerated without linked to long-term toxicity [327].

1.3 Scope of The Thesis

The treatment of chronic hematological malignancies is advancing rapidly, with newer targeted therapies increasingly being used in place of conventional chemotherapy. Nanomedicine, particularly AuNP-based technology, may provide additional tools for the development of molecularly targeted therapeutic strategies for CML management.
In CML, the molecular hallmark of disease is BCR-ABL1 fusion transcript provides an optimal molecular target for the demonstration of gene silencing approaches based on AuNP vectorization. Since this oncogene triggers the downstream overexpression of c-MYC it can also be used as a molecular target for combinatory approaches towards improvement of the silencing capability of the regulatory pathway.

Despite the enormous success of TKIs therapy, several challenges remain. For instance, resistance to IM has been related to BCR-ABL1- dependent or -independent mechanisms, and induction of c-MYC might be triggered via BCR-ABL1 leading to high levels of c-MYC that correlate with poor response to IM and, at molecular level, to genomic instability. Additionally, combination of Au-nanoconjugates with TKIs and/or other kinase inhibitors such as Danu, Vola and Adavo could provide an effective treatment option for CML patients.

The main objective of this thesis was to develop new combinational targeted strategies to tackle imatinib resistance in CML. The work has been broadly divided into three stages:

1. Characterization of BCR-ABL1 fusion transcripts in patient samples to support the identified molecular target sequences and optimize the recognition of point-mismatches in ABL1 domain associated with TKI resistance in CML.
2. Individual and combinational strategies for specific and selective gene silencing via Au-nanoconjugates to downregulate BCR-ABL1 and c-MYC and demonstrate the capability to counteract imatinib resistance.
3. Combining of Au-nanoconjugates with TKIs (IM) and other kinase inhibitors (Danu, Vola and Adavo) targeting CML sensitive and resistance cell lines.

2

CLINICAL SAMPLE CHARACTERIZATION

2.1 Introduction

The Ph chromosome is the hallmark of CML. In most CML Ph+ cases, *BCR-ABL1* fusion transcripts, such as e13a2 or e14a2, both encoding the p210 fusion protein (with a molecular weight of 210 kDa) are present [328]; nevertheless, in a minority of cases other oncogenic isoforms, such e1a2 or e19a2, associated to p190 or p230, respectively, may be present (alone or in combination with p210) due to the varying BCR breakpoint regions [329]. The use of sensitive molecular diagnostics techniques, that allow a precise identification of the *BCR-ABL1* transcript in each individual patient, is critical, for diagnosis and also for selecting the most precise targeted therapy [330]. Moreover, the transcript type is believed to have a significant prognostic value [330].

For 15-30% of CP-CML patients, that initiated a first-line TKI therapy, no optimal response is achieved, which indicates that some TKI resistance mechanism is present. In 25-50% of those patients experiencing treatment failure, *BCR-ABL1* KD mutations are present [331]. In this regard, screening for mutation status is crucial, as these mutations are involved in the mechanisms contributing to TKI resistance, either from pre-existing mutations (primary resistance affects one-third of patients) or mutations that develop because of TKI treatment pressure (acquired resistance). Patients who do not respond to IM, dasatinib, nilotinib, bosutinib, and ponatinib should be treated based on the outcomes of the mutational analysis [332].

This chapter reports the screening of *BCR-ABL1* transcripts in samples from patients to identify *BCR-ABL1* KD mutations in CML patients that might be associated to resistance to

TKIs. For those patients where mutations are not found, other resistance mechanisms might be considered such as overexpression of P-gp. In this regard, the outcome of this chapter was considered as a molecular basis for determining the subsequent work strategies by providing information on which cell models should be used to better mimic the most common *BCR-ABL1* transcript in the studied populations and the eventual molecular alterations associated with TKI resistance.

2.2 Materials and methods

2.2.1 Identification of *BCR-ABL1* transcripts in patients' samples

2.2.1.1 Patients samples

A total of 10 patients sent for the hematology department of Hospital dos Capuchos (Lisbon, Portugal) for leukemia diagnosis were included in this study. Written informed consents were obtained from each individual patient, and the study was previously approved by Hospital dos Capuchos Ethics Committee. All approved ethical requirements for sample collection at diagnostics (peripheral blood (PB) in ethylenediaminetetraacetic acid (EDTA)-treated tubes), assortment, processing, and analysis required by the Ethics Committee have been strictly followed. Patient's physical, hematological (WBC counts) were consistent with CML. Fluorescence in situ hybridization (FISH) for *BCR-ABL1* was positive for all patients.

2.2.1.2 Extraction of RNA from peripheral blood and cDNA synthesis

Briefly, 5 mL of PB from each patient were mixed with 10 mL of red blood cells lysis solution (5 mM $MgCl_2$, 10 mM NaCl, 10 mM Tris-HCl pH 7) and centrifuged (400 x g, 5 min). The procedure was repeated 1x to lyse any residual red blood cells. Total RNA extraction from white blood cells pellet was performed using SV Total RNA Isolation System (Promega, Madison, WI, USA), according to the manufacturer's instructions. For that, cell pellets were lysed (solution containing 4 M guanidine thiocyanate, 0.1 M Tris-HCl pH 7.5, and 1 % (v/v) β-mercaptoethanol) and subsequently centrifuged (13000 x g, 10 min) to clear all the precipitated proteins and cellular debris. Nucleic acids were precipitated with 30 % (v/v) ethanol; bound to the silica surface of glass fibers; and washed (60 mM potassium acetate, 10 mM Tris-HCl pH 7.5, and 60 % (v/v) ethanol). DNase I treatment on-column lasted for 15 min at room temperature to remove any genomic DNA from lysates. After two washing steps, RNA was resuspended in nuclease-free water and stored at −80 °C until use. As a control, total

RNA was also extracted from p210 BCR-ABL1 expressing cell lines: K562 (e14a2) and BV173 (e13a2). RNA concentration and purity were determined by UV-Vis spectroscopy. Total RNA extracted (100 ng) was reverse transcribed into cDNA, using the NZY M-MuLV First-Strand cDNA Synthesis kit (Nzytech, Lisbon, Portugal).

2.2.1.3 Nested PCR

Nested- PCR amplification of *BCR-ABL1* was performed in two setups: one that identifies the p210 isoforms of *BCR-ABL1* (e14a2 or e13a2) and another that identifies rarer isoforms, such as the p195 (e6a2) – see primers in Table 2.1. The PCR mixture components included 1x NH_4 reaction buffer (Bioline, Taunton, MA, USA), 2.5 mM $MgCl_2$, 0.15x Hi-Specific additive (Bioline), 200 μM dNTPs, 400 nM primers, and 0.02 U/μL BIOTAQ DNA polymerase (Bioline). Outer PCR was performed using 3 μL of cDNA in a 50 μL-reaction, under the following conditions: initial denaturation at 95 °C for 5 min; 30 cycles of 94 °C for 30 sec, 55 °C for 30 sec, 72 °C for 1 min; and a final extension step at 72 °C for 10 min.

Inner PCR was performed using 1 μL of outer PCR product in a 50 μL-reaction, under the following conditions: initial denaturation at 95 °C for 5 min; 30 cycles of 94 °C for 15 sec, 55 °C for 30 sec, 72 °C for 1 min; and a final extension step at 72 °C for 10 min. A control PCR, for the amplification of *ABL1*, was performed using primers (Table 2.1) and the same conditions described for the outer PCR.

All PCR products were analyzed in a 2 % (w/v) agarose gel electrophoresis and subsequently investigated by Sanger sequencing (SS) at STABVIDA (Setúbal, Portugal). The presence of mutations in the *ABL1* kinase domain was also investigated by nested PCR using primers (Table 2.2) followed by SS.

Table 2.1 — Nested-PCR primers for *ABL1* and *BCR-ABL1* molecular analysis of p210 and rare isoforms (p190, p195, and p200) in CML [333].

	ABL1 – Control	**p210**	**p190, p195 or p200**
Outer PCR	For 5’GGCCAGTAGCATCTGACTTTG (ABL1 exon 2) Rev 5’ATGGTACCAGGAGTGTTTCTCC (ABL1 exon 3)	For 5'GAAGTGTTTCAGAAGCTTCTCC (BCR exon 12) Rev 5’GTTTGGGCTTCACACCATTCC (ABL1 exon 3)	For 5'GACTGCAGCTCCAATGAGAAC (BCR exon 1) Rev 5’GTTTGGGCTTCACACCATTC (ABL1 exon 3)
Inner PCR	N/A	For 5’CAGATGCTGACCAACTCGTGT (BCR exon 13) Rev 5’TTCCCCATTGTGATTATAGCCTA (ABL1 exon 3)	For 5’CAGAACTCGCAACAGTCCTTC (BCR exon 1) Rev 5’TTCCCCATTGTGATTATAGCCTA (ABL1 exon 3)
Final PCR prod-uct size	296 bp	e14a2 - 360 bp e13a2 - 284 bp	e1a2 - 381 bp e6a2 - 1023 bp e8a2 - 1284 bp

For, forward; Rev, reverse; N/A, not applicable

Table 2.2 — Nested PCR primers for *BCR-ABL1* amplification and subsequent analysis of *ABL1* mutational status in CML. Modified from van Dongen et al., 1999 [333].

	p210 (e14a2)
Outer PCR *BCR-ABL1* fusion	For 5′ TGCTGACCAACTCGTGTGTGA (BCR exon 13) Rev 5′ CTTCGTCTGAGATACTGGATTCCT (ABL1 exon 9)
Inner PCR *ABL1* exons 4-7	For 5′ GCAACAAGCCCACTGTCTAT (ABL1 exon 4) Rev 5′ TGTTGTAGGCCAGGCTCTC (ABL1 exon 7)
Inner PCR *ABL1* exons 7-9	For 5′ TGAGCAGGTTGATGACAGG (ABL1 exon 7) Rev 5′ TGAGATACTGGATTCCTGGAAC (ABL1 exon 9)

For, forward; Rev, reverse

2.3 Results

2.3.1 *BCR-ABL1* transcripts in clinical samples

Nested-PCR has numerous advantages, with the enhancement of DNA amplification specificity being essential, as it employs two sets of primers in two consecutive PCRs. Molecular analyses are essential for diagnostic assessment and allow tracking treatment response in individuals with CML [334].

Of the 10 patients, 8 harbored the e14a2 (80%) variant and the remaining expressed e1a2 (20%) Table (2.2) and Figure (2.1 and 2.2). Subsequently, the resulting amplicons were subjected to direct SS for the identification of possible mutations.

Table 2.2 — *BCR-ABL1* transcripts in clinical samples.

Ref no	**Sample type**	***BCR-ABL1* Transcript fusion**
1	PB	p190; e1a2
2	PB	p190; e1a2
3	PB	p210; e14a2
4	PB	p210; e14a2
5	PB	p210; e14a2
6	PB	p210; e14a2
7	PB	p210; e14a2
8	PB	p210; e14a2
9	PB	p210; e14a2
10	PB	p210; e14a2

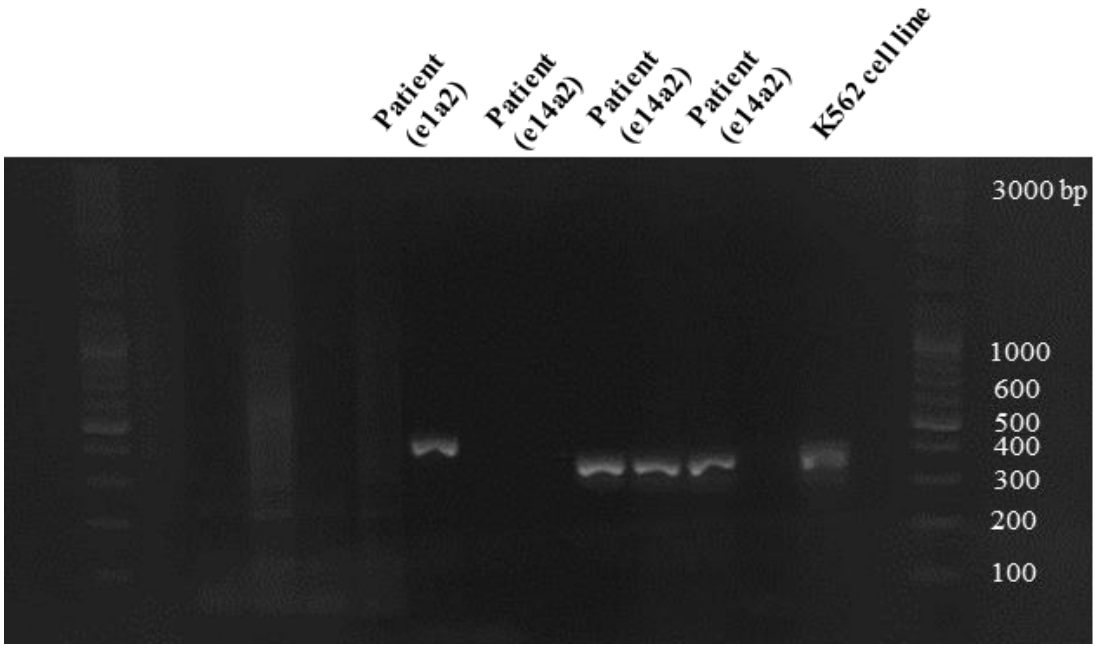

Figure 2.1 — Example of the different *BCR-ABL1* transcripts in clinical samples. Nested-PCR amplification of *BCR-ABL1* transcripts from CML patients. PCR products (1 µl) were resolved via a 2 % (w/v) agarose gel electrophoresis; Ladder - GeneRuler DNA Ladder Mix SM0331 (Thermo Scientific, Waltham, MA, USA)

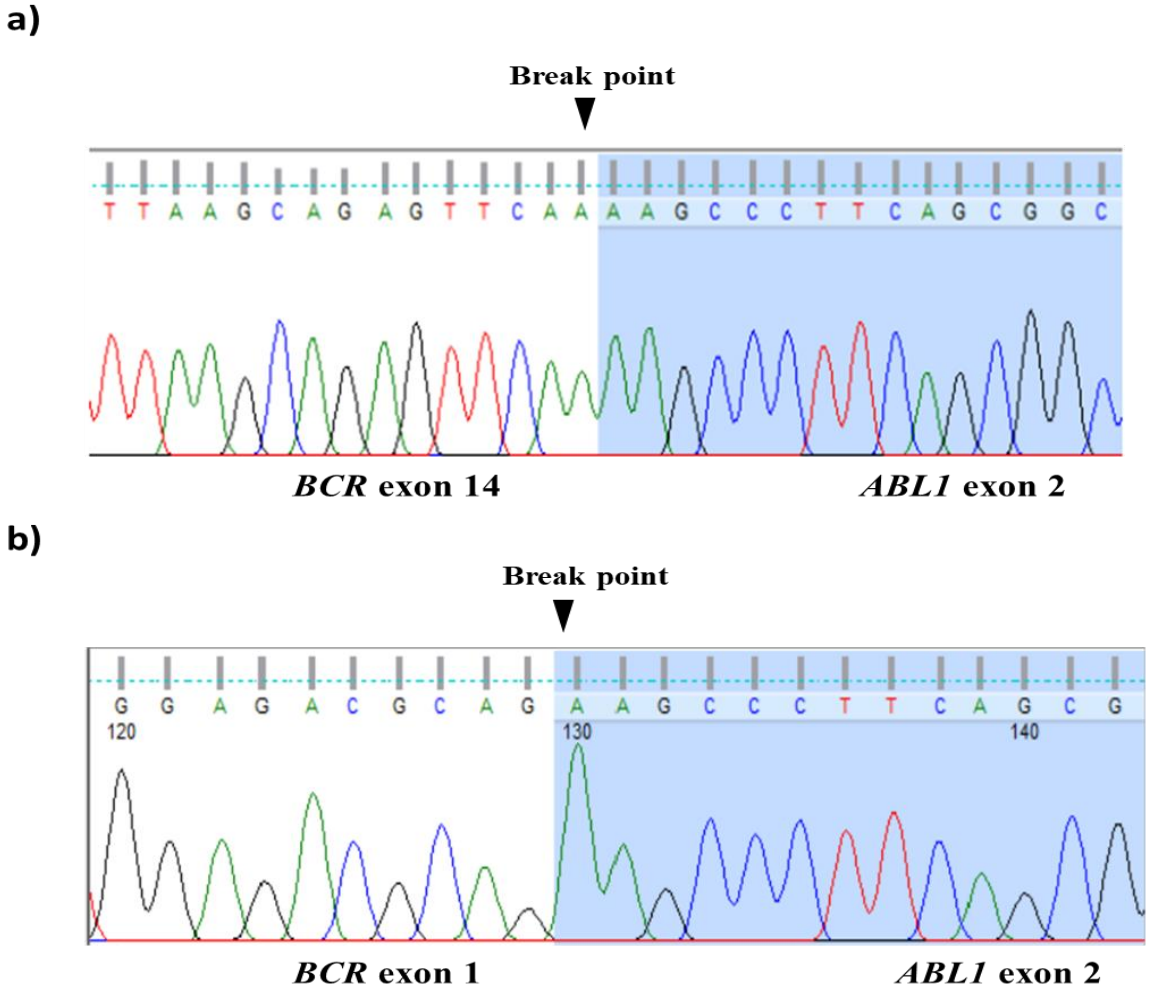

Figure 2.2 — Sequence analysis of *BCR-ABL1* from patient samples. a) Sanger sequencing of PCR product represented the e14a2 transcript in CML patient. b) Sanger sequencing of PCR product represented the e1a2 transcript in CML patient.

Our nested-PCR results indicated that the majority of CML patients exhibit the e14a2 *BCR-ABL1* transcript (80%), whereas the remaining others exhibited the e1a2 *BCR-ABL1* transcript (20%). The resultant PCR products were further evaluated using Sanger sequencing, the gold standard for confirmation of the fusion sequence.

These data align with several studies documenting the prevalence of *BCR-ABL1* transcripts across various populations. Numerous studies indicate that over fifty percent of CML patients exhibit the e14a2 variant, with over ninety-five percent of cases linked to the e14a2 and/or e13a2 *BCR-ABL1* variants [335-339].

2.3.2 Mutational status of *ABL1* kinase domain in CML patients

Amplification of the target sequences of *ABL*1 kinase domain of CML patients was also performed via PCR (Figure 2.3). Afterward, the PCR products were sequenced to analysis *ABL1* mutational region of transcript fusions. The results have not shown any associated mutations in regions (exons 4-7) or (exons 7-9) in *ABL*1 KD of the patient samples.

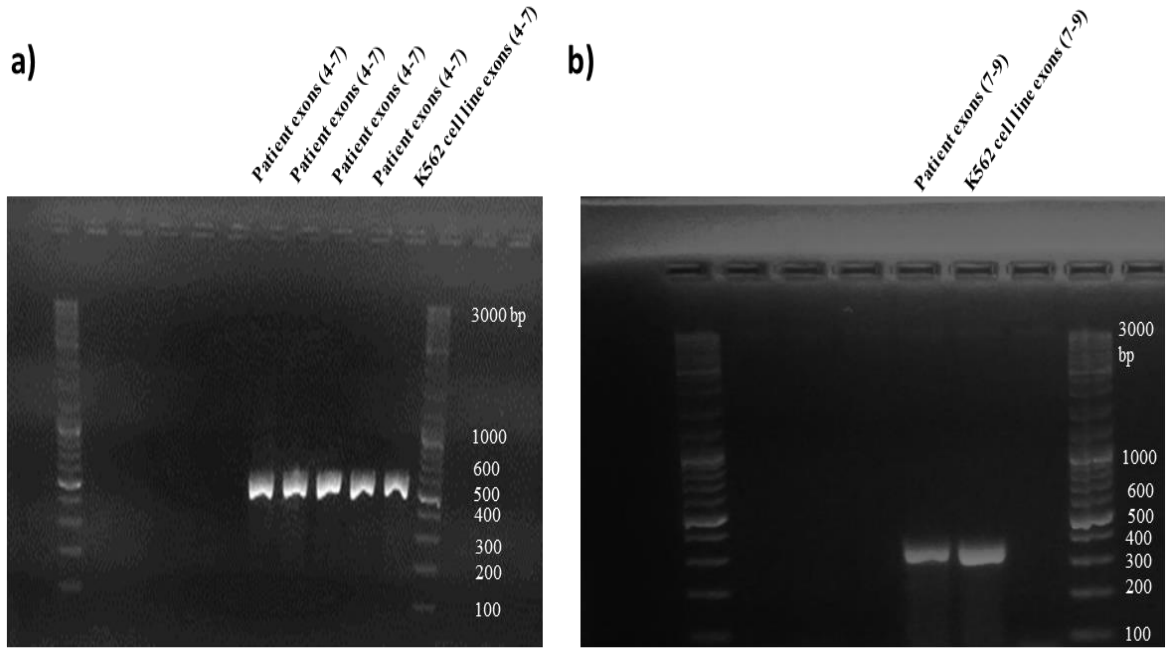

Figure 2.3 — *ABL1* kinase domain amplification. a) represent nested-PCR amplification of *ABL1*mutational region exons (4-7) from CML patients. b) represent nested-PCR amplification of *ABL1*mutational region exons (7-9) from CML patients. PCR products (1 µl) were resolved via a 2 % (w/v) agarose gel electrophoresis; Ladder - GeneRuler DNA Ladder Mix SM0331 (Thermo Scientific, Waltham, MA, USA

Advanced molecular approaches are designed to identify *BCR-ABL1* transcript levels for monitoring treatment response (molecular responses) associated with these transcript levels [330]. Transcript typing is essential for identifying minimal residual disease and achieving a molecular response by facilitating targeted therapy [330]. Despite the significant success of TKI therapy, 20–30% of patients exhibited either primary or secondary resistance to treatment during the progression of the disease [340]. The predominant mechanism linked to resistance is the emergence of point mutations in the *BCR-ABL1* gene [341]. Sanger sequencing is the preferred technique for identifying *BCR-ABL1* KD mutations due to its higher efficiency and precision [341].

The resultant PCR products were further evaluated using SS, the gold standard for identifying gene variants and quantifying mutational burden, which is crucial in the charac-

terization of clonal disorders such as CML. The sequencing examination of clinical samples revealed no mutations linked with the ABL1 KD. Considering the attained nested-PCR results on the samples retrieved from patients, it becomes clear that the best-matching cell model for subsequent studies is the K562 cell line (ATCC® CCL-243™) [243].

The imatinib-resistant derived cell line (K562-IM) has been generated from K562 cell line by increasing the concentration of IM for more than 50 passages [344]. In order to better characterize the mechanism responsible for the resistance of this cell line, we have: i) assessed BCR-ABL1 mutational status using nested-PCR amplification and ii) assessed of MDR1 expression on K562-IM cells via RT-qPCR and western blot.

Figure 2.4 shows the nested-PCR amplification of p210 *BCR-ABL1* (e14a2) transcript and the mutational regions of ABL1 KD in K562-IM cell line. Sequencing results of the nested-PCR products did not show any associated mutations in the *ABL1* KD regions (exons 4-7 and exons 7-9; Figure 2.5).

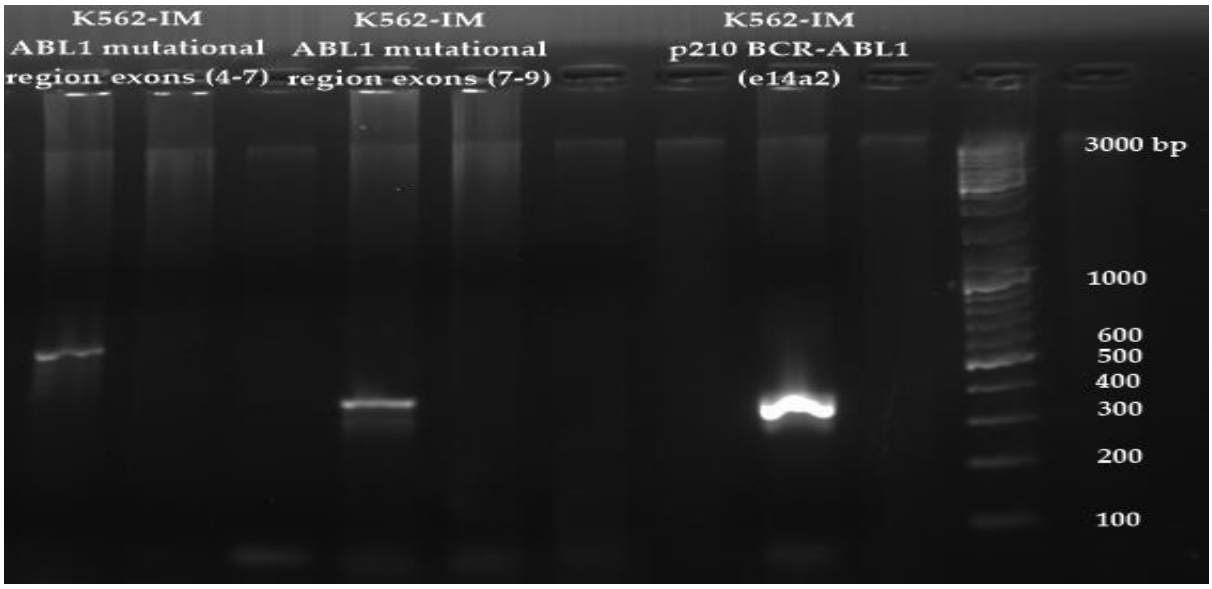

Figure 2.4 – *ABL1* and *BCR-ABL1* amplification. Nested-PCR amplification of *BCR-ABL1* e14a2 isoform and *ABL1* from K562-IM cells. PCR products (1 µl) were resolved via a 2 % (w/v) agarose gel electrophoresis; Ladder - GeneRuler DNA Ladder Mix SM0331 (Thermo Scientific, Waltham, MA, USA).

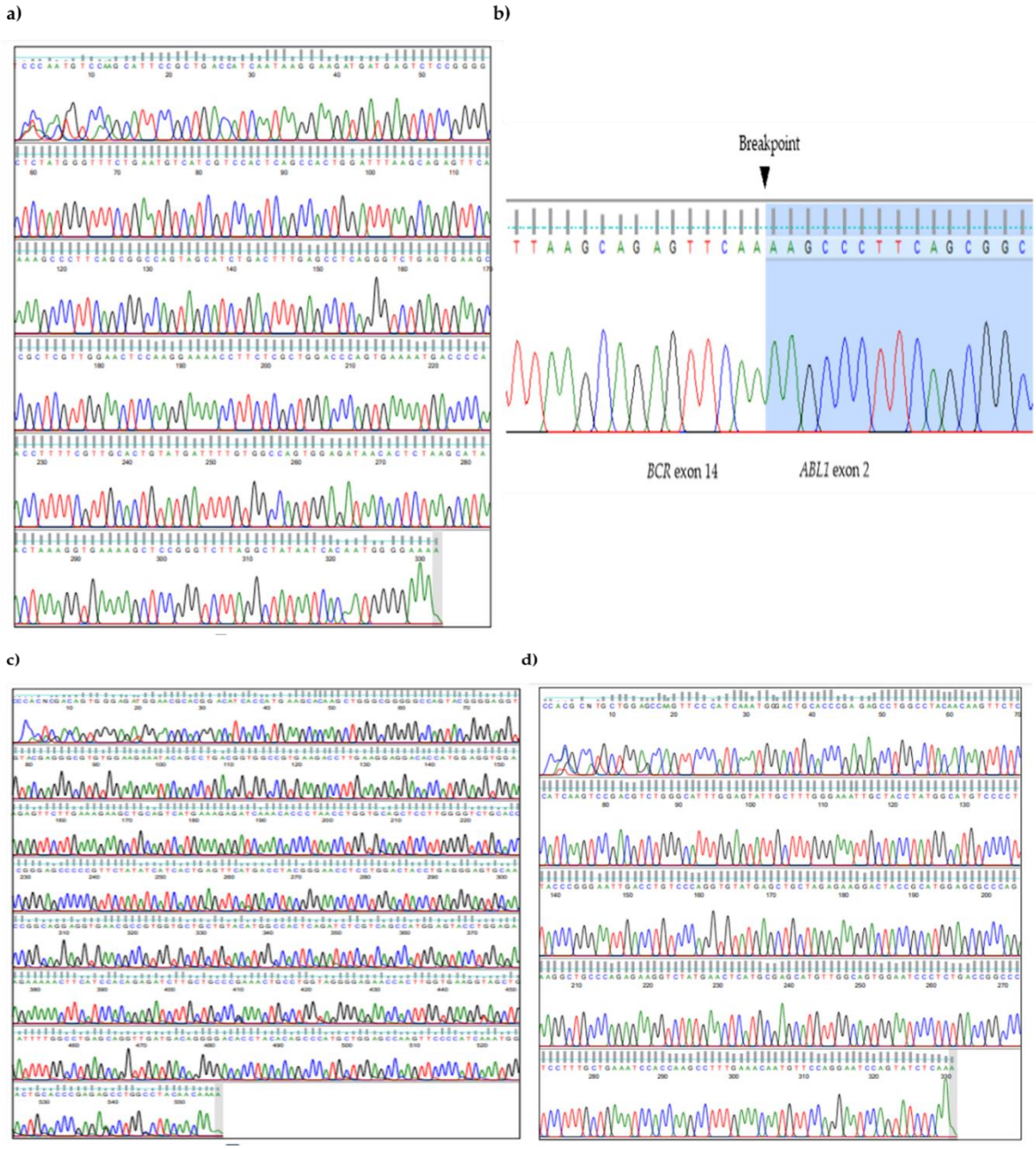

Figure 2.5 – Sequence analysis of *BCR-ABL1* and *ABL1* in K562-IM cell line. (a) *BCR-ABL1* fusion (e14a2 isoform); (b) *BCR-ABL1* fusion (e14a2 isoform) break point; (c) *ABL1* mutational region (exons 4-7); (d) *ABL1* mutational region (exons 7-9).

Afterward, the expression of MDR1 was also analyzed in K562 and K562-IM to further understand the mechanism of resistance in K562-IM cell line. The results of RT-qPCR and western blot demonstrated that the resistance mechanism in K562-IM was associated with the overexpression of MDR1 compared to K562 cell line Figure 2.6.

Considering that no *ABL1* KD mutations were identified in the patients' samples, additional resistance mechanisms might be considered, such as overexpression of MDR1, similarly to K562-IM cell line Figure 2.6.

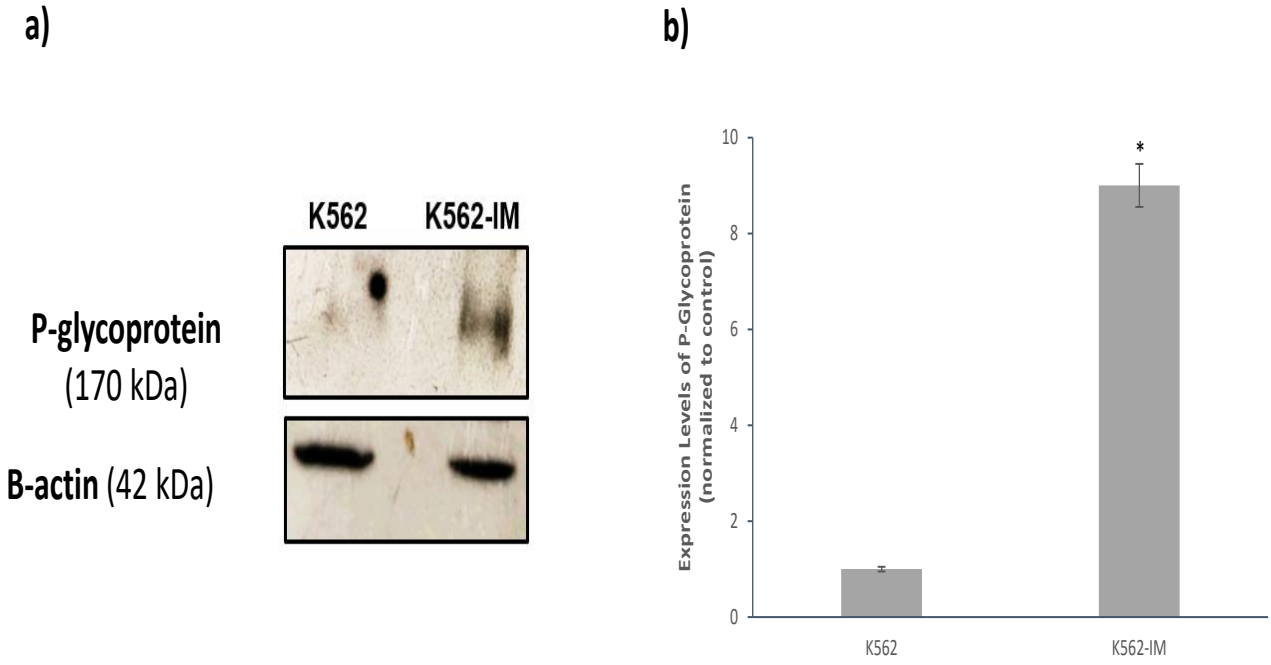

Figure 2.6 — Overexpression of MDR1 (P-glycoprotein) in K562-IM when compared with K562 parental cells line. (a) Western blot images of P-Glycoprotein and β- actin in K562 and K562-IM cells (b) Expression levels of P-glycoprotein in K562-IM normalized to K562. Band quantification was first normalized against ß-actin (loading control) and, subsequently, to the control condition (K562 cells). Error bars represent the standard error of the mean of three independent experiments. *$p<0.05$ relative to respective controls, Tukey's test statistical significance.

Data indicate that both cell lines exhibit the e14a2 *BCR-ABL1* isoform and lack any mutations in the *ABL1* KD. In CML, *BCR-ABL1* mutations and variations in multidrug resistance transporters are likely the most common TKIs-resistance mechanisms [345]. The overexpression of *MDR1* has been identified as a mechanism of resistance to IM [346]. Our data indicates that the K562-IM cell line exhibits a BCR-ABL1 independent mechanism due to the overexpression of *MDR1* (when compared to K562 cell line).

2.4 Conclusion

Molecular detection of *BCR-ABL1* transcription is essential for the diagnosis of CML, and its molecular quantification is crucial for evaluating treatment strategies and clinical interventions. Recent advancements in the treatment of CML via molecular monitoring have successfully lowered morbidity and mortality rates. Advanced molecular techniques are designed to detect *BCR-ABL1* transcript levels for monitoring molecular responses associated with these transcript levels. In the context of CML, point mutations in the *ABL1* gene pose a challenge for clinical guidelines, as various mutations contribute to resistance against TKIs, suggesting a potential need for modification in the treatment protocol.

Herein, the objective was not to provide for a broad assessment of transcript and/or mutation profiles for patients, but rather to characterize the molecular starting point of the hypotheses put forward in the core of the Thesis, i.e. the relevance of the cell models used in the next chapters, their transcript signatures and the absence of mutations in the *ABL1 KD* in patients as well in both cell lines (sensitive and resistant to IM) that could be a target for gene silencing.

3

GENE SILENCING

A large extent of this chapter has been published in Bilal Abdulmawjood, Catarina Roma-Rodrigues, Pedro V. Baptista and Alexandra R. Fernandes. Tackling Imatinib Resistance via Au-nanoconjugates using a CML resistant cell line. Part. Part. Syst. Charact. (2023). doi: 10.1002/ppsc.202300090. Bilal Abdulmawjood was responsible for the laboratory work and preparing the manuscript.

3.1 Introduction

CML is a rare malignant proliferative hematopoietic cell disorder with a global incidence of 1 to 2 cases per 100,000 adults [29]. The Ph chromosome is the main molecular hallmark of CML, which results from the translocation t(9;22)(q34;q11.2) yielding the *BCR-ABL1* fusion gene [138], encoding a fusion oncoprotein (BCR-ABL1) with constitutively active tyrosine kinase activity. BCR-ABL1 persistently activates several signaling pathways causing uncontrolled cell differentiation, unrestricted replication, and resistance to apoptosis [138,346].

TKIs are the mainstay of CML treatment [347] and were specifically designed to selectively hinder the kinase activity of the fusion oncoprotein, weakening the interaction between BCR-ABL1 and ATP, blocking cell signaling and, consequently, reducing cell proliferation and inducing death of CML clones [85]. The first line TKI for CML is IM, which has been associated with the development of resistance in some patients with advanced-stage CML [208]. About 40% of CML patients fail TKI therapy in the presence of sustained BCR-ABL1 inhibition and resistance is attributed to kinase independent mechanisms [348], where increased activity in RAS, RAF, MEK, ERK-MAPK signaling pathway might be the trigger for BCR-ABL1-independent IM resistance [349].

c-MYC is an intrinsically disordered protein that belongs to the BHLHZip family presented in the cell nucleus [200]. c-MYC regulates as many as 15% of all human genes [200], with particular significance for genes involved in the control of normal cellular functions including growth, proliferation, differentiation, progression of cell cycle, maintenance of cell size, genomic integrity, angiogenesis, and apoptosis [350]. Expression of c-MYC is tightly controlled in normal cells (protooncogene) but becomes dysregulated and overexpressed in most human cancers [351], making it one of the most important human oncogenes. Alteration of c-MYC levels can help or prevent oncogenic transformation and tumor progression [352].

The oncogenic potential of c-MYC stems from its function as a transcriptional regulator that binds DNA on heterodimerization with MAX. Once dimerized, the c-MYC/MAX complex acts as a master transcriptional regulator by binding via its basic region to a specific DNA consensus called E-box [200]. Many signaling pathways, including the PI3K /AKT and RAS, RAF, MEK and ERK, can regulate c-MYC mRNA expression and promote c-MYC stability [199]. The carcinogenicity of c-MYC can raise the transcription level of high-affinity target genes or push them to saturation; furthermore, it can up or down regulate low-affinity target genes, transforming normal cells into tumor cells [353]. In CML, BCR-ABL1 aberrant kinase activity induces c-MYC transcription and translation, which is a critical step of disease progress into blast crisis Figure (3.1) [202].

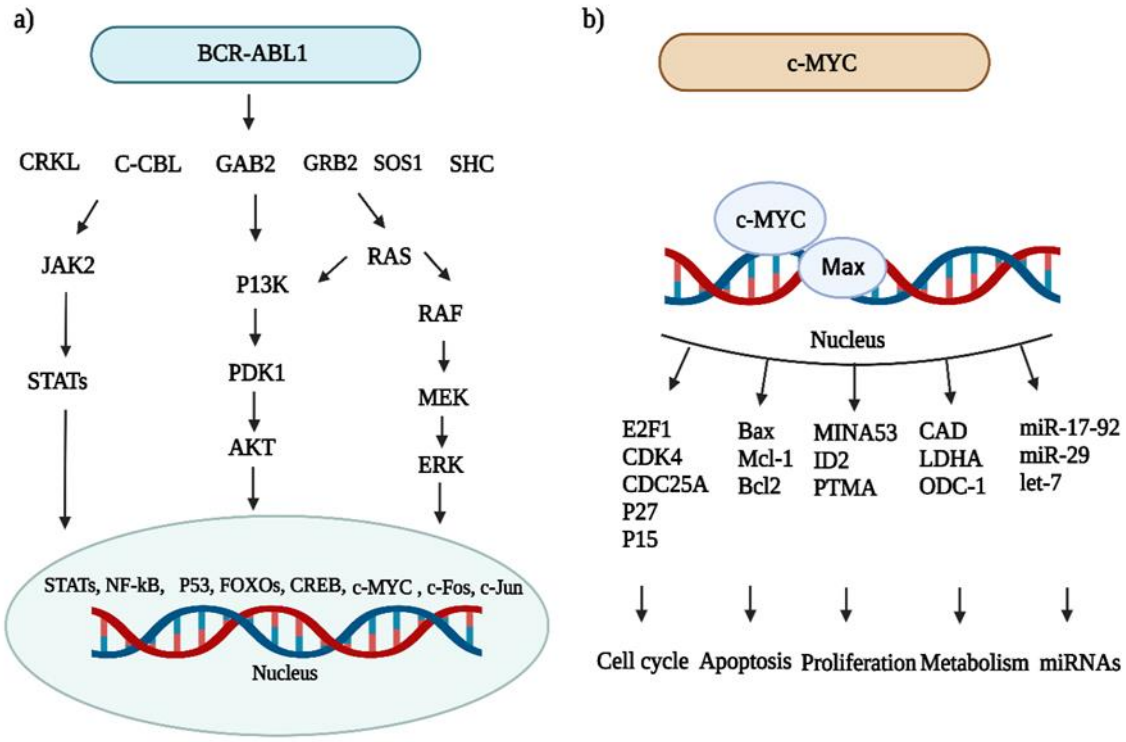

Figure 3.1 — Signaling pathways mediated c-MYC levels through BCR-ABL1 in CML. (a) the induction of c-MYC by BCR-ABL1 occurs mainly via JAK2 activation, which positively regulates c-MYC levels. Furthermore, BCR-ABL1 indirectly activated c-MYC via PI3K/AKT, Ras-Raf-MEK-ERK MAPK; (b) c-MYC controls the expression of many genes that are involved in the regulation of cell cycle progression, apoptosis, proliferation or metabolism. Retrieved from *Abdulmawjood* et al., [201].

The inhibition of BCR-ABL1 tyrosine kinase activity by IM strongly reduces c-MYC expression and hematopoietic tumoral features of CML cells [203]. Importantly, c-MYC downregulation represents a key step for IM-induced cell death in CML [203]. c-MYC antagonized IM or dasatinib induced erythroid differentiation and apoptosis [354], suggesting its vital roles in drug sensitivity. Nevertheless, overexpression of c-MYC has been correlated to poor IM-responses in untreated CML patients and non-responding patients, possibly through promotion of genomic instability [202].

Antisense technology is a great tool to manipulate gene expression within cells and to treat human diseases [355]. ASOs are synthetic single-stranded DNA analogues, usually in the range of 15-30 base pairs in length and complementary to a target mRNA sequence [356]. In cancer, ASOs have been used to target oncogenic RNAs via sequence-specific binding to modify the expression of oncogenes [318]. The use of ASOs for gene silencing has re-emerged due to its combination with nanotechnology-based vectorization strategies, pivotal for the development of optimized nanomedicines against cancer. AuNPs have demonstrated great efficiency in gene silencing approaches towards cancer therapy [357-35], particularly as

vehicles for antisense DNA and siRNA therapy, which are easily internalized by cells and effective in silencing gene expression. Our group has already reported the efficient silencing of e14a2 BCR-ABL1 fusion transcript on K562 cells line at different time points by using Au-nanoconjugates [357].

Herein, we used AuNPs functionalized with ASOs targeting each individual mRNA in an IM-resistant K562 cell line model, to efficiently silence the e14a2 BCR-ABL1, c-MYC or both simultaneously. Gene silencing leads to a reduced expression at the protein level, which results in increased death of IM resistant cells. These findings may hint at the possibility to develop combined regiments, using Au-nanoconjugates for specific gene silencing as an adjuvant treatment to overcome toxicity and resistance mechanisms related to TKIs in CML.

3.2 Materials and Methods

3.2.1 Extraction and purification of RNA

RNA extraction from cell lines was performed using TRIsure (Bioline, Taunton, USA) following the manufacturer's instructions. Briefly, a 2 x 105 cells per well (24-well plates) were centrifuged at 300 x g for 5 min at room temperature, and the supernatant discarded. The pellets were then rinsed with 1 mL PBS and centrifuged at 300x g for about 5 min at room temperature and the supernatant discarded. Afterward, 300 µL of TRIsure was added to pellet and incubated for 5 min at the room temperature. Then added 100 µL of chloroform, carefully stirred, and centrifuged for 5 min at 12,000 x g. The result of the aqueous phase was then transferred to a new tube (1.5 mL), with 200 µL of isopropanol. This mixture was kept at room temperature for about 10 min and then centrifuged at 12,000 x g for 10 min at 4°C and the supernatant discarded. The pellet was washed with 500 µL of 75% ethanol and then allowed to dry. RNA was resuspended in DECP-treated water and kept at -80°C.
RNA purity and quantification was assessed using a Nanodrop 1000 spectrophotometer.

3.2.2 cDNA synthesis

For cDNA synthesis, 100 ng of total RNA was reversely transcribed to cDNA by using the NZY-M-MuLV First-strands cDNA synthesis kit (Nzytech, Lisbon, Portugal) following the manufacturer's instructions. The 100 mg of RNA was mixed with ZYRTEC 2x Master Mix and NZYM-MuLV RT Enzyme Mix., along with DEPC-treated water and incubated for 10 min at 25˚C followed by 50 min at 37˚C. Reaction was cooled on ice and the enzyme heat-

inactivated for 5 min at 85˚C. After adding NZY RNase H, the mixture was incubated for 20 min at 37˚C. The resulting cDNA was kept at 4ºC until use.

3.2.3 Synthesis and characterizations of AuNPs

Citrated capped AuNPs (citrate-AuNPs) were synthesized using Lee and Meisel's citrate reduction protocol with slight modifications [318,344,360]. A diluted solution of tetrachloroauric acid (100 mL, 1 mM) in water was continuously heated till boiling and then rapidly mixed with a hot solution of trisodium citrate (5 mL, 2% w/v). When a deep red color starts to be observed, it indicates the formation of AuNPs. The solution was continuously stirred for 15 min and then allowed cool and equalized the room temperature. The sterile-filtered method was performed for AuNP@citrate by using 0.2 µm filter syringe Supor™ Membrane, REF 4645, United States) and then stored at 4°C until used. The AuNPs were characterized by UV-Vis spectroscopy, transmission electron microscopy (TEM), and dynamic light scattering (DLS).

For the UV-Vis spectroscopy, spectra were taken in the range between 400 and 800 nm at room temperature using Suprasil® cuvettes with 1 cm path quartz. For the DLS, the hydrodynamic and Z-potential were determined by a Nanoparticles Analyzer-100 using a 90º scattering angle at 25ºC. The AuNP solutions were diluted with milliQ water to reach 4 nM as a final concentration before the analysis.

For TEM analysis, 10 µL of citrate-AuNP were uploaded on a carbon copper grid and washing with milliQ water 2 times and let it dry. TEM was performed as a service at Instituto Superior Técnico, Universidade de Lisboa (Portugal).

3.2.4 Synthesis and characterizations of Au-nanoconjugates (PEG and ASO binding)

AuNPs were subsequently functionalized with thiol-modified polyethylene glycol (PEG) to attain 30% of coverage. Briefly, 14 nM of citrate-capped AuNPs were incubated with 0.028% (w/v) SDS (Sodium dodecyl sulphate) (CAS: 151-21-3, Sigma-Aldrich), and 0.003 mg/mL of PEG (O-(2-Mercaptoethyl)-O′-methyl-hexa(ethylene glycol) (MW= 356.48 g/mol) (Ref 672572, Sigma-Aldrich), for 16 h under agitation [344]. Afterwards, the solution was centrifuged for 45 min at 14,000x g at 4ºC to remove the unbound PEG.

To infer the amount of PEG conjugated to the AuNPs, the amount of free thiol in the supernatants was assessed via Ellman's assay. (5,5-dithio-bis-(2-nitrobenzoic acid, Cat. No.

22582, Thermo Scientific™, United States) [237]. The last PEG concentration that had no detectable thiols in the supernatant was defined as 100% coverage.

Conjugation of ASO with AuNP@PEG was performed according to Pedrosa at el. [344], and using the sequences; 5′TTTCGGCGCTGAAGGGCT TTTGAACTCCGAAA-3′ targeting the e14a2 BCR-ABL1 and 5′GCGCCCA TTTCTTCCAGATATCCTCGCTGGGCGC-3′ targeting the c-MYC. The AuNP@PEG solution was mixed with purified thiol-modified oligonucleo-tide with a ratio of 1 to 100 (AuNP:oligos). Afterwards, a solution of 10 mM phosphate buffer pH = 8, 2% SDS (AGEI) was added to a final concentration of 10 mM phosphate buffer (pH = 8) and 0.01% (w/v) SDS. Subsequently, the ionic capacity of the solution was consistently elevated in increments of 50 mM by adding 10 mM phosphate buffer pH = 8, 1.5 M NaCl, 0.01% SDS (AGE II) in appropriate volumes to a final concentration of 10 mM phosphate buffer (pH = 8), 0.05 M NaCl and 0.01% (w/v) SDS solution. Serial additions of AGE II were performed to attain final concentrations of 0.1, 0.2 and 0.3 M of NaCl. The mixture was then allowed to equilibrate overnight at room temperature. Then, the functionalized AuNP@PEG with ASO were distributed in 2 mL tubes and centrifuged for 40 mins at 14,000 x g. After removing the supernatant, the oily pellet was subjected to two washes with 10 mM phosphate buffer at pH 8, followed by a single wash with 10 mM phosphate buffer at pH 8 containing NaCl. The pallets then mixed, and the functionalized AuNP@PEG with ASO concentration was subsequently measured by the Lambert-Beer law assuming a calculated molar absorbance of surface plasmon resonance (SPR) peak (at 522 nm) of 2.33 x 108 M -1 cm -1 [361].

Afterward, UV-vis spectroscopy was used to measure supernatant to quantifying the oligonucleotides number using Nanodrop 1000 Spectrophotometer (Fisher scientific, Portugal). The quantity of oligonucleotides conjugated to the surface of AuNP was determined by subtracting amount of oligonucleotides in the supernatant from initial total amount of oligonucleotides. Moreover, the oligonucleotides number that bound to the surface of AuNPs was further assured by utilizing Quant-iT ssDNA Reagent (USA).

The Au-nanoconjugates were stored in the dark at 4°C. The characterizations of AuNP func-tionalized with PEG (AuNP@PEG) and PEG with oligonucleotides (AuNP@PEG@e14a2 and AuNP@PEG@c-MYC) were performed using UV-vis and DLS as described above.

3.2.5 Maintaining and culturing cells

K562 is an immortalized cell line distinguished by the presences of e14a2 BCR-ABL1 fusion gene (CLL-243, ATCC) that derived from CML patients in BC phase. The THP1 cell line characterized by the lack of BCR-ABL1. These cells lines serve as positive and negative controls for the detection of BCR-ABL1 mRNA. K562-IM is an IM resistant cell line which was

established by our lab group by incubating K562 sensitive cell along with increasing IM (IM from Selleck Chemicals) concentrations, beginning with 0.01 µM and ends with 1 µM with over than fifty passages, while preserving culture conditions to verify the resistance phenotype caused by increasing MDR1 expression [344] (results in chapter 2, Figure 2.6).

Both k562 and k562-IM cell lines were cultured in Dulbecco's modified Eagle (DMEM) medium, while THP1 was cultured in Roswell Park Memorial Institute (RPMI) medium. DMEM and RPMI were supplemented with 5% CO2, 10% FBS at 37°C as well as 99% of the ratio of moisture in the air. However, DMEM medium was additionally supplemented with 1 µM of IM in K562-IM to sustain the selective pressure of IM along with the overexpression of MDR1 [344].

3.2.6 Cell challenge with Au-nanoconjugates

Cells were cultured in a density of $2x10^5$ cells/well (24 well plate) or $0.1x10^5$ cells/well (96 well plate). Both cell lines underwent treatment with Au-nanoconjugates for duration of 24 h in vitro studies. The time point was chosen according to Vinhas et al. [318] which showed that challenging cells with Au-nanoconjugates for 24 h resulted in significantly decreased expression of the e14a2 BCR-ABL1 fusion transcript in k562 cell line.

The K562 and K562-IM cell lines were used for the studies of e14a2 BCR-ABL1 targeting. Both cell lines were challenged with AuNP@PEG @14a2 (0.35 nm), which corresponds to 30 nM oligonucleotide with a ratio of Au:oligonucleotide = 1:84, for 24 h. The same cell lines were also used for targeting c-MYC by challenged the cells for 24 h with AuNP@PEG@c-MYC (0.6 nm) which corresponding to 45 nM oligonucleotide with ratio of (Au:oligonucleotide = 1:75).

In the combination strategy, both cell lines were also used for the synchronous targeting of BCR_ABL1 and c-MYC (AuNP@PEG@e14a2 and AuNP@PEG@c-MYC, respectively).
The concentrations of AuNP@PEG@e14a2 and AuNP@PEG@c-MYC were determined based on previous studies [318].

For comprehensive analysis, the concentrations of oligonucleotide were maintained as the same concentrations of the individual experiments. Additionally, AuNP@PEG was used as a standard for all silencing experiment findings. For the K562-IM cell line, cells treated with 1 µM of IM served as a control for the normalization of AuNP@PEG.

3.2.7 Analysis of gene expression by RT-qPCR

Total RNA purification and cDNA synthesis were performed as described in sections (3.2.1 and 3.2.2). qPCR on the cDNA was performed on a Corbett Rotor-Gene 6000 thermal cycler (Qiagen, Hilden, Germany). Mixture of the reaction for RT-qPCR was prepared in a final volume of 20 µL by mixing the following primers (100 nM each) with 2 µL of cDNA as well as the NZYSupreme qPCR Green Master Mix (2x) (NZYTech): For 18S, forward (5'-GTAACCCGTTGAACCCCATT) and reverse (5'- CCATCCAATCGGTAGTAGCG). For BCR-ABL1, BCR forward (5'- GAAGTGTTTCAGAAGCTTCTCC) and ABL1 reverse (5' GTTTGGGCTTCACACCATTCC). For c-MYC, forward (5'GCTCATTTCTGAAGAGGACTTGT) and reverse (5'AGGCAGTTTACATTATGGCTAAATC).

The conditions of qPCR start with denaturation for 2 min at 95°C and 40 cycles at 95°C for a duration of 20 sec each, 55°C (18S, BCR-ABL1 as well as c-MYC) for duration of 20 sec, finally at 72°C for 30 sec. Afterwards, CT method (2-ΔΔCt) was used to analyze the qPCR results [362], which gives the determination for the desired genes, (BCR-ABL1 and c-MYC) which are related to internal control (18S), where is relative to gene expression and then normalized to control (AuNP@PEG) as the formula 1 & 2 below:

(1) Δ CT= CT (*BCR-ABL1* or *c-MYC*) – CT (*18S*).

(2) ΔΔ CT= ΔCT (Au-nanoconjugate) – ΔCT (AuNP@PEG).

3.2.8 Cell Viability

3.2.8.1 MTS assay

To evaluate the cell viability, we performed standard 3 (4,5 dimethylthiazol-2-yl)-5-(3-carboxymethoxyphenyl)-2-(4-sulfophenyl)-2H tetrazolium (MTS) assay . For this assay, the 96-Cell Titer® liquid-Non-Radioactive was utilized. This assay is a colorimetric method to estimate the number of viable cells. It is based on the dehydrogenation by metabolically active cells of MTS tetrazolium compound into formazan, a soluble coloured product. In brief, K562 and K562-IM cells was cultured to 96-well plates for 24 h after being challenged with AuNP@PEG, AuNP@PEG@e14a2, and AuNP@PEG@c-MYC either alone or with in a combination. Furthermore, Au-nanoconjugates and IM were administered to K562-IM cells concur-

rently for duration of 24 h. The intensity of absorption was determined using a Tecan-Infinite-M200 microplate reader at 490 nm.

3.2.8.2 Trypan Blue assay

After plating of K562 and K562-IM cells onto 24-well plates, these cells were subjected to a 24 h exposure to AuNP@PEG, AuNP@PEG@e14a2, and AuNP@PEG@c-MYC, either individually or in various combinations. Utilizing the trypan blue (0.2%) exclusion test (ThermoFisher), which shows that dead cells have no cell membranes and appear blue, while living cells have intact membranes that exclude dye, the viability was determined manually by counting of the number of living cells.

3.2.9 Apoptosis

Au-nanoconjugates were applied to cells placed onto 24-well plates; these were centrifuged at 400 × g for duration of 5 min at temperature of 4 °C, then washed with a cold Phosphate buffer solution. Following the manufacturer's instructions, cells were then doubly stained using the "Dead Cell Apoptosis Kit with Annexin V AlexaFluor (AF488)" (ThermoFisher). Green vs red fluorescence density plots and SSC-A measurements of Ten thousand events each reading were performed on the samples using an Attune Acoustic Focusing Cytometer (ThermoFisher). Cytometer's software v2.1 was used to quantify the proportion of necrotic cell (stained with PI), cells exhibiting early apoptosis (indicated by staining with AlexaFluor 488), cells demonstrating late apoptosis (characterized by double staining), and cells that remain viable (unstained).

3.2.10 Cell cycle analysis

Through the application of double-blocking with 2 mm thymidine, the cycles of each cell line were synchronized during the S-phase. After the second obstruction, cells were allocated to 24-well plates and exposed to the Au-nanoconjugates. Cells were extracted using 500 x g centrifuged for duration of 5 min at temperature of 4 °C, after 12, or 24 h of treatment. They were then treated with 50 μg/mL-1 RNAse A (NZYTech), fixed then permeabilized along with eighty percent (v/v) ethanol, then stained using 25 μg mL-1 PI (ThermoFisher). Using an Attune acoustic focusing cytometer as well as the appropriate software (ThermoFisher), the percentage of cells in each step was examined.

3.2.11 Cell differentiation analysis

The erythrocytic differentiation markers Glycophorin A, CD235a, and tetraspanin CD71 were assessed. As outlined in the foregoing processes, imatinib–resistant K562 cells was challenged using nano-formulations for 24 h before being harvested utilizing centrifuge at 500 x g for 5 min. Following a 30 min blocking period, the cells were rinsed with Phosphate buffer solution and incubate with either anti-CD71 conjugated with FITC or anti-CD235a conjugated by FITC for 30 min on ice, rinsed with PBS, and then resuspended in PBS. A BD accuri C6 was used to measure fluorescence, and Flow-Jo -software (version-X- 10.0.7r2, BD) was used to analyze the data. For control purposes, K562 sensitive cells and THP-1 cell culture from human monocytes which are isolated from the patient having acute-monocytic-leukemia were also examined for control reasons.

3.2.12 Protein expression analysis by Western Blot

After challenging with Au nanoconjugates for 24 h, cells were washed with Phosphate Buffer Saline (PBS) and resuspended in lysis buffer 150 mM NaCl, 50 mM Tris (pH 8.0), 5 mM EDTA, 2 % (v/v) NP-40, 1x phosphatase inhibitor (PhosStop, Roche, Basel, Switzerland), 1x protease inhibitor (cOmplete Mini, Roche), 1 mM phenylmethylsulfonyl fluo ride (PMSF), and 0.1 % (w/v) dichloro-diphenyl-trichloroethane (DTT). Nevertheless, using of this lysis buffer results in some unspecific protein bands and black dots (original blots in appendices, Figures A.1 and A.2), the lysis buffer was then replaced with new lysis buffer containg 150 mm NaCl, 50 mm Tris (pH 8.0), 5 mm EDTA, 1% (v/v) Triton, 1x phosphatase inhibitor (PhosStop, Roche, Basel, Switzerland), 1x protease inhibitor (cOmplete Mini, Roche), 1 mm (PMSF), 0.5% (w/v) sodium deoxycholate (NaDoc), and 0.1% (w/v) sodium dodecyl-sulfate (SDS).

Following three sonication, whole-cell extracts were subjected to centrifugation for 15 min at 16,000 x g. In accordance with the manufacturer's guidelines, the Pierce (660 nm) Protein Assay Reagent (ThermoFisher) was used to extract the supernatant and quantify the protein content. Hyperfilm ECL to complete the revelation process. The Image J program was used to quantify the protein bands. Then, 20 µg total protein extracts were separated by SDS polyacrylamide gel electrophoresis (SDS-PAGE in a 7% (37.5:1) acrylamide-bisacrylamide gel (Merck Millipore, Billerica, MA USA), following semidry transfer onto a 0.45µm polyvinylidene (PVDF) membrane (GE Healthcare, Little Chal font, UK), and blocking with 5% (w/v) of bovine serum albumin (BSA) was performed. Membranes were incubated overnight at 4 °C with primary antibodies against c-Abl for BCR-ABL1 detection (reference no. 2862S, Cell Signaling Technology, Danvers, MA, USA) or c-MYC (reference no. ab

cam AB32072) in tris-buffered saline with 0.1% (v/v) tween 20 (TBST) and 5% (w/v) milk solution or incubated 1 h at room temperature with ß actin (reference no. A5441, Sigma-Aldrich) in TBST. Afterward, membranes were washed with TBST and incubated with the appropriate secondary antibody conjugated with horseradish peroxidase (reference no. 7076, Cell Signaling Technology).

WesternBright ECL (Advansta, Menlo Park, CA, USA) was applied to themembrane, and ther evealing step was performed by exposing the membrane with the AmershamHyperfilm ECL (Reference no. 28-9068-36, GE Healthcare). Quantification of protein bands (original blots in appendices, Figures A.3 and A.4) was performed using Image J software.

3.2.13 Darkfield and Fluorescence Microscopy

K562-IM cells were subjected to AuNPs nanoconjugates onto 24-well plates for duration of 24 h, as previously stated. Following pelleting by centrifuge at 500 x g for 5 min at 4 °C, the cells were fixed then permeabilized using 80% (v/v) ethanol. The samples underwent incubation for 1 h using anti-c-MYC antibody after 30 min of block by 1% (w/v) BSA (NZYtech-Portugal). Cells underwent centrifugation to duration of 5 min at 1500 x g and 4 °C after three washes with PBST (PBS supplemented with 0.05% (v/v) Tween-20 (Sigma Aldrich). Samples then incubate for 30 min with the appropriate secondary antibody-antirabbit TRITC (ab6718; Abcam). After the 3 washes with PBST, those cells were incubated with 1% (w/v) BSA for blocking, followed by the addition of anti-BCRABL1 primary overnight at 4 °C. Subsequently, three PBST washes were conducted, followed by a 1 h incubation with the appropriate secondary antibody conjugated along with FITC, specifically anti-mouse-FITC (F0257, Sigma), as well as concluded along with an additional PBST wash. Prolong Glass from ThermoFisher Scientific was used to fix the pelleted cells after their suspension in 10 µL of PBST.

We employed a Ti-U Eclipse inverted microscope (Nikon, Japan), equipped with DAPI (excitation at 360/40 nm alongside emission on 460/50 nm), FITC (excitation with 480/30 nm alongside emission at 535/40 nm), and G2A (excitation at 535/50 nm and emission > 590 nm) fluorescence filters. A 100x objective was used to observe the cells, and images were captured to evaluate a minimum of 30 cells each sample. The measure of the intensity of fluorescence that exists in each image was determined using Image J software, along with the corrected total cells fluorescence (CTCF) for each cell was calculated as follows: integrated density - (cell area × mean fluorescence of background).

3.2.14 Statistical analysis

Errors bars illustrating the mean ± standard error from a minimum of the three distinct investigations are included to depict all findings. Tukey's multiple comparison test was used to evaluate statistical significance after the completion of one-way ANOVA and two-way ANOVA using GraphPad Prism 8.

3.3 Results and discussion

3.3.1 Au-nanoconjugates synthesis and characterization

Citrate-caped AuNPs (citrate-AuNPs) were synthesized with an average diameter of 14 nm (Figure 3.2) and further functionalized with thiolated-PEG (AuNP@PEG) for biocompatibility according to previously published protocols [318,363,364,365]. PEG functionalization is crucial to increase biocompatibility and stability in biological media.[364] AuNP@PEG were then used as a starting point to graft thiolated ssDNA-oligonucleotides targeting each of the selected mRNAs or scramble control (not targeting any sequence in human cells), obtaining AuNP@PEG@e14a2, targeting e14a2 mRNA, AuNP@PEG@c-MYC targeting c-MYC mRNA (see (Figure 3.3)) or AuNP@PEG@scramble, respectively.

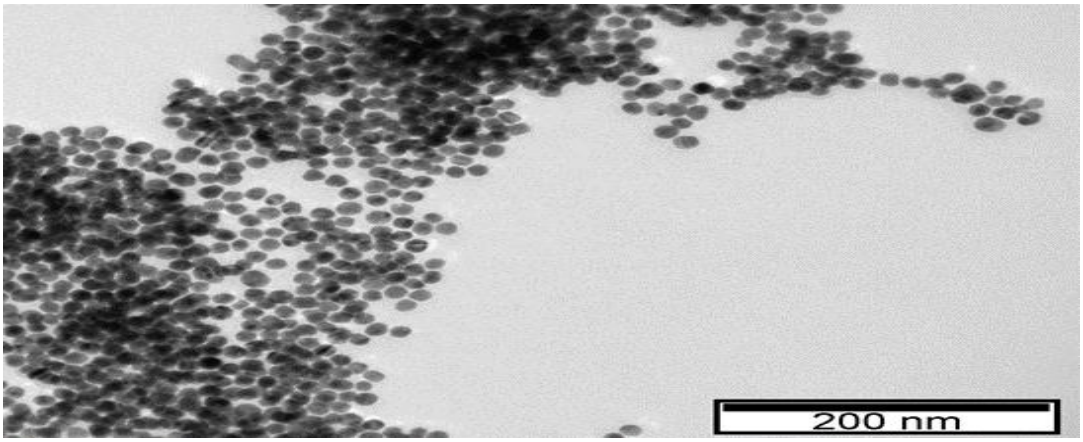

Figure 3.2 — Transmission electron microscopy (TEM) image of the synthesized citrate-AuNPs with an average diameter of 14 nm.

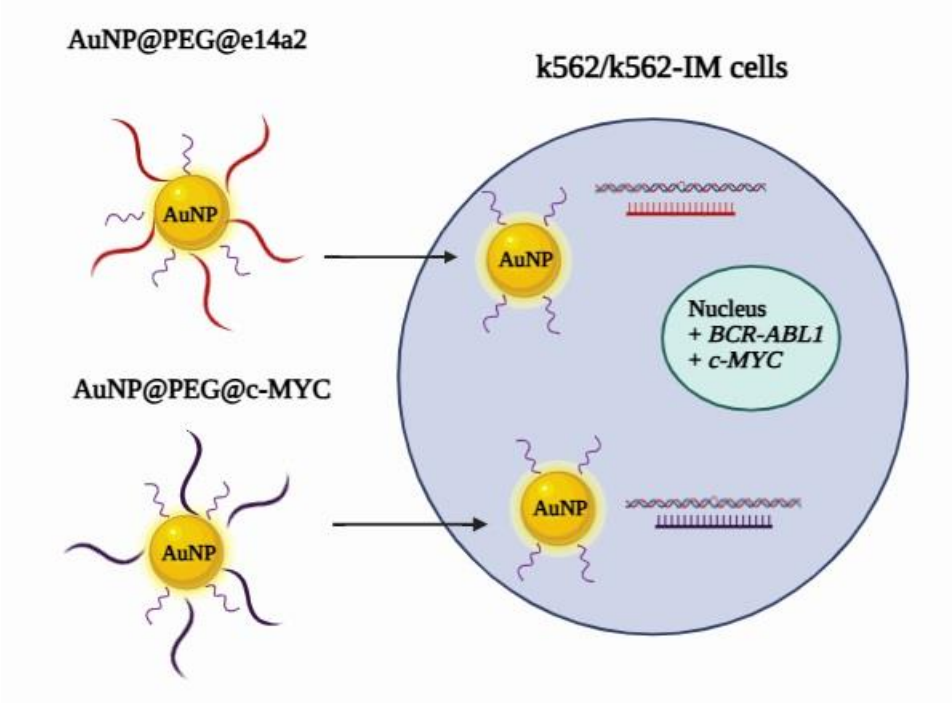

Figure- 3.3 — Schematic representation of PEGylated AuNPs functionalized with ASOs targeting e14a2 *BCR-ABL1* and *c-MYC* mRNA.

All conjugates were characterized after each functionalization step (Table 3.1), where the increase to the DLS and variation of the Z-average, together with the red shift of the SPR peak indicate successful functionalization with the relevant moieties [318,366]. Indeed, data related to Z-average and SPR peak shift show an increased size upon PEG functionalization and, even more, after oligonucleotide (e14a2, c-MYC or scramble) loading onto the AuNPs. The polydispersity index (PI) is relatively constant (between 0.16-0.22) and indicative of monodisperse populations [364], supported by the Z-potential data showing the magnitude of the electrostatic and/or charge repulsion/attraction between particles, leading to increased stability and dispersion in aqueous media [368]. The binding of PEG to the surface of AuNPs induces a shift from more negative (−71.4 mV) to more neutral values (−40.7 mV), whereas functionalization with ssDNA induced more negative values (from −40.7 mV (AuNP@PEG) to −65.6 mV (AuNP@PEG@c MYC) or −64.9 mV (AuNP@PEG@e14a2)), due to the negative charge of ssDNA molecules (Table 3.1).

Table 3.1 – Citrate-AuNPs, AuNP@PEG, AuNP@PEG@scramble, AuNP@PEG@e14a2 and AuNP@PEG@c-MYC characterization through, the size, inferred by the Z-average, and polydispersion index obtained by Dynamic Light Scattering (DLS) analysis, and the surface plasmon resonance (SPR) peak obtained by ultraviolet-visible (UV-Vis) spectroscopy.

	Z-average (nm)	**Zeta Potential (ζ)**	**Polydispersion index**	**SPR peak (nm)**
Citrate-AuNPs	16	-51	0.20	519
AuNP@PEG	20	-67	0.21	520
AuNP@PEG@scramble	34	-60	0.16	522
AuNP@PEG@e14a2	37	-64	0.22	522
AuNP@PEG@c-MYC	33	-65	0.16	522

3.3.2 Gene silencing of BCR-ABL1 and c-MYC

To understand if the prepared Au-nanoconjugates were able to silence the respective mRNAs in K562-IM cultures, cells were challenged with AuNP@PEG@e14a2 and AuNP@PEG@c-MYC for 24 h, and then the total RNA was purified and used for quantification of each targeted genes by RT-qPCR (as comparison purposes K562 cells were also used). As controls, both cell lines (sensitive and resistant) were also challenged with AuNP@PEG and AuNP@PEG@scramble (Figure 3.4). It was observed that, as previously described for K562 [318], *BCR-ABL* mRNA expression levels after exposure of AuNP@PEG and AuNP@PEG@scramble nanoconjugates to K562-IM cells are identical (Figure 3.4), so from now on, AuNP@PEG will be used as the sole control in experiments.

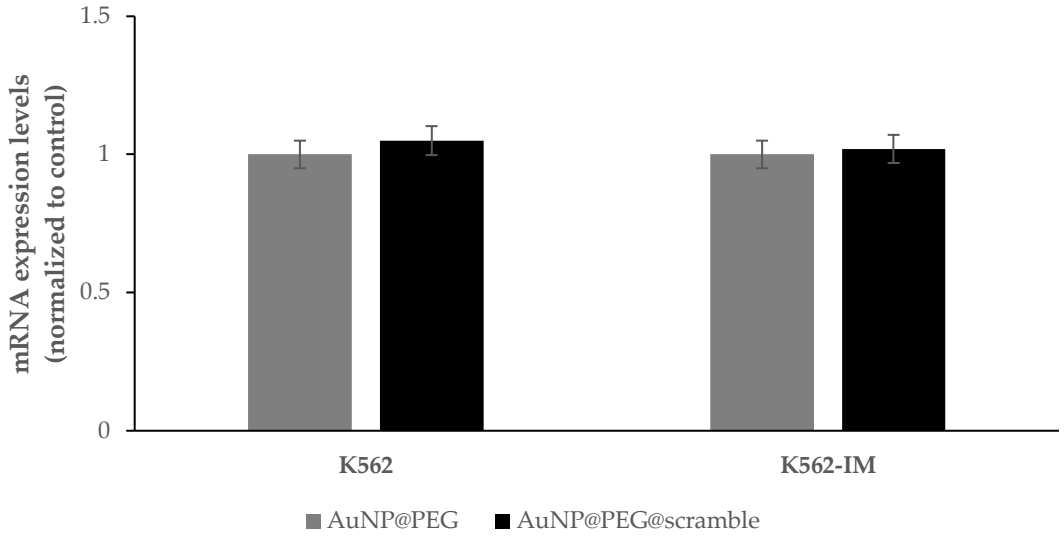

Figure 3.4 — mRNA expression levels of BCR-ABL1 in K562 and K562-IM cell lines after the challenge for 24 h with AuNP@PEG (grey) or AuNP@PEG@scramble (black). Error bars represent the standard error of the mean of three independent experiments. Expression results were normalized to AuNP@PEG (control).

Data show that, after 24 h exposure of K562-IM and K562 cells to AuNP@PEG@e14a2, the expression levels of the *BCR-ABL1* fusion transcript decreased in both cell lines (Figure 3.5a and Figure 3.6a, respectively). Interestingly, the silencing efficacy of *BCR-ABL1* gene was higher for K562-IM cells (Figure 3.5a) compared to K562 parental sensitive cell line (Figure 3.6a) – with a decrease of 86.3% or 44% of *BCR-ABL1* expression (compared to control), respectively. Concerning *c-MYC* expressions there is also a reduction in both cell lines compared to the control, as expected, but in this case with a strong reduction for K562 (54%) (Figure 3.6b) compared to K562-IM (15%) (Figure 3.5b).

We then added both Au-nanoconjugates simultaneously to each cell line and assessed expression variation –Figure 3.6c and Figure 3.5c. The most effective gene silencing was obtained for *BCR-ABL1* in K562 cells line (reduction of 61.3%, Figure 3.6c), which was higher compared to AuNP@PEG@e14a2 alone (reduction of 44%, Figure 3.6a). In the resistant K562-IM cell line, there was also a reduction in *BCR-ABL1* levels, but a more noticeable reduction was observed when the AuNP@PEG@e14a2 was added alone (86.3%) compared to the combined approach (26.3%) - Figures 3.5a and 3.5c.

When we look at *c-MYC* expression, the more effective silencing was observed for K562 challenged with AuNP@PEG@c-MYC alone (54%), compared to the simultaneous addition of both Au-nanoconjugates (3.6b and 3.6c). In K562-IM, a more profound reduction was observed when both Au-nanoconjugates were added simultaneously (40.6%) compared to AuNP@PEG@c-MYC alone (15%) (Figure 3.5b and 3.5c). As explained before, due to the dif-

ferent properties of the nanoconjugates (size, charge, polydispersion index) their internalization rate might vary, and one type may be internalized faster and/or more efficiently compared to the other, leading to different silencing efficacies at mRNA level (as we are targeting mRNA) compared to the protein levels (as observed in this study) [369-372].

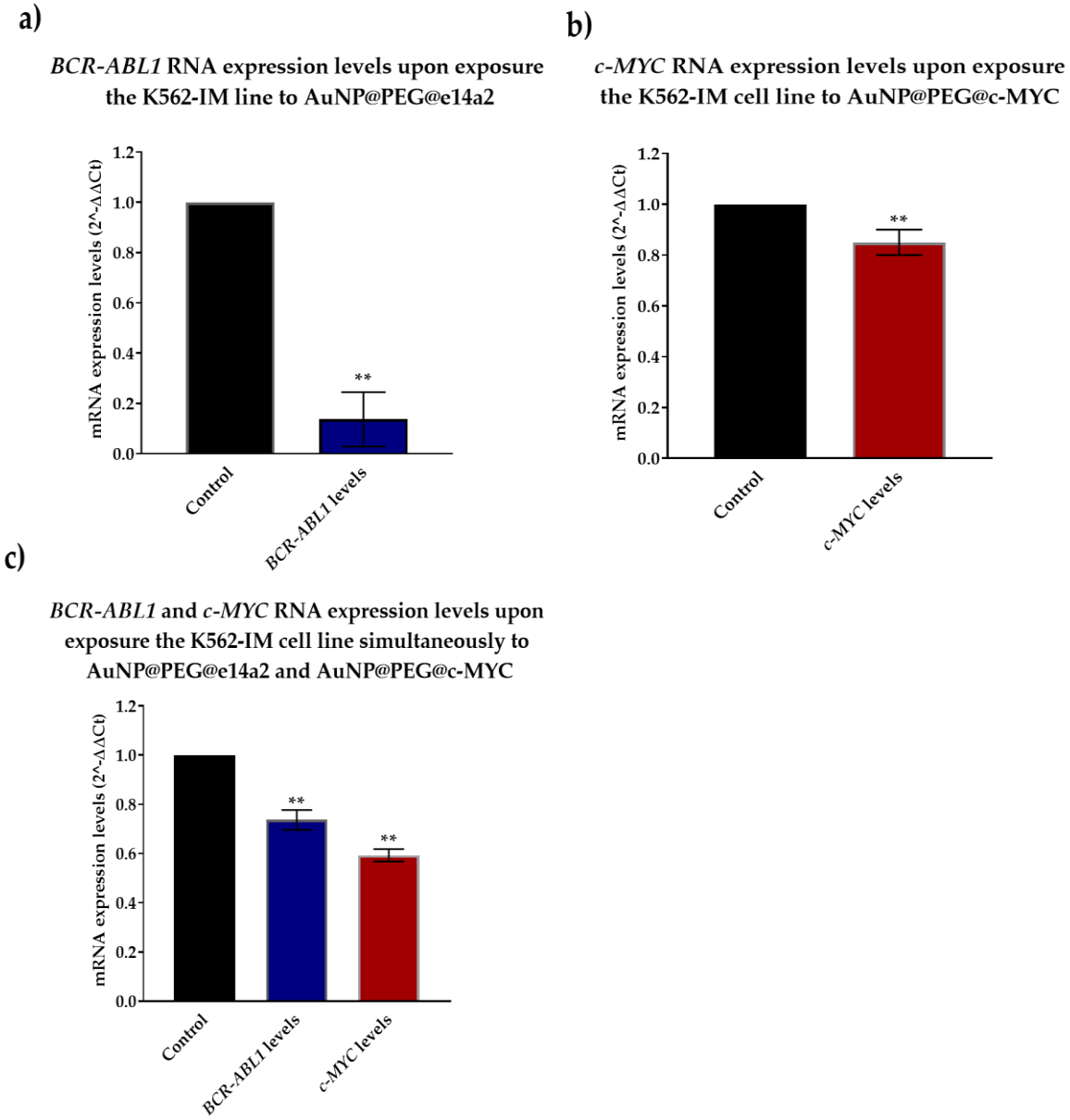

Figure 3.5 — mRNA expression levels of *BCR-ABL1* and *c-MYC* genes in K562-IM cell line. (a) mRNA relative expression levels of *BCR-ABL1* after the challenge for 24 h with AuNP@PEG@e14a2; (b) mRNA relative expression levels of *c-MYC* after the challenge for 24 h with AuNP@PEG@c-MYC; (c) mRNA relative expression levels of *BCR-ABL1* and *c-MYC* after the challenge for 24 h with AuNP@PEG@e14a2 and AuNP@PEG@c-MYC. Data were normalized to the *18S* gene and then to cells exposed to control (AuNP@PEG). Ct, threshold cycle. Error bars represent the standard error of the mean of three inde-

pendent experiments. * p<0.05, ** p<0.01, relative to respective control, using Tukey's test statistical significance.

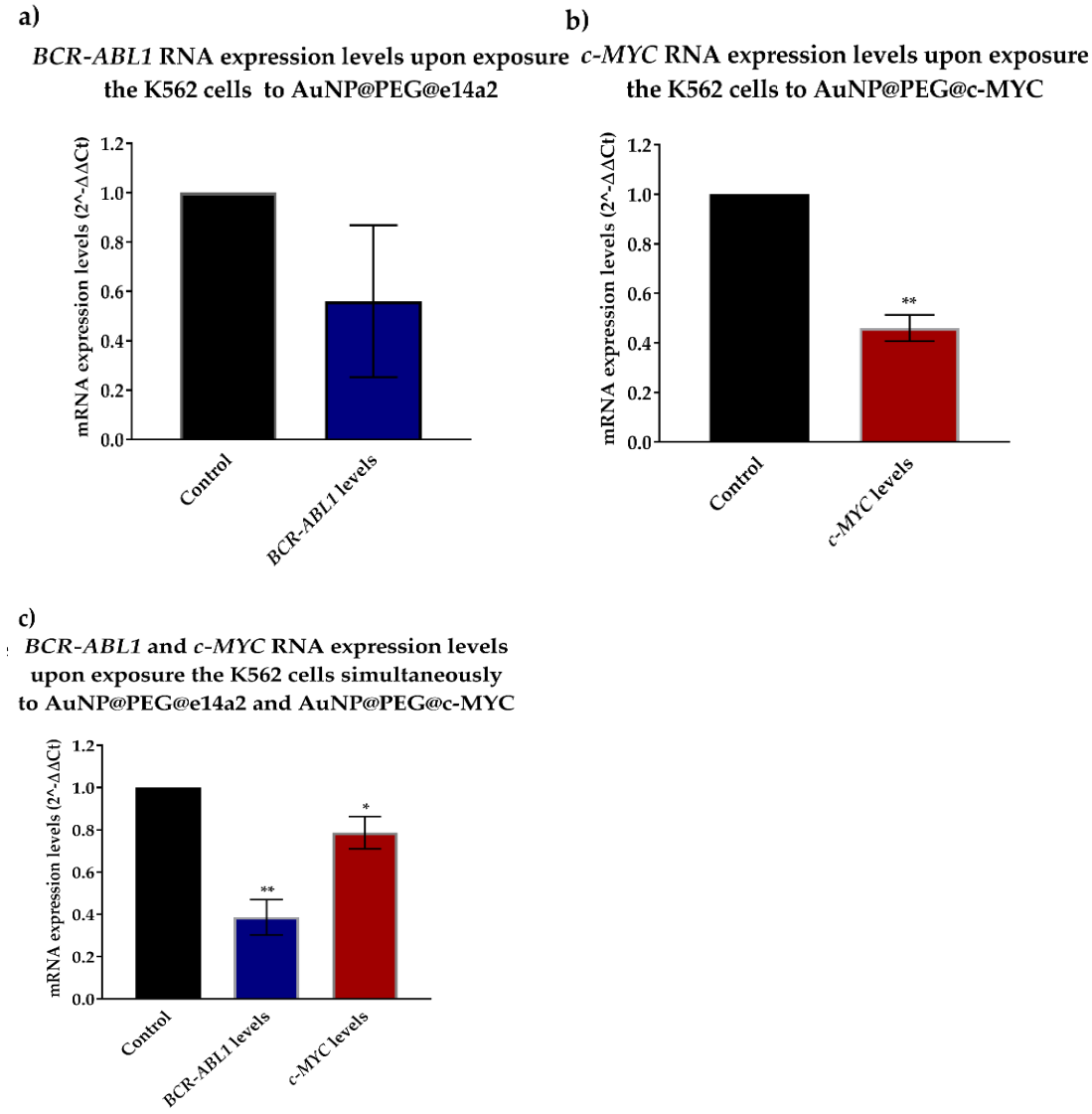

Figure 3.6 — mRNA expression levels of *BCR-ABL1* and *c-MYC* genes in K562 cells. mRNA relative expression levels of *BCR-ABL1* after the challenge for 24 h with AuNP@PEG@e14a2; (b) mRNA relative expression levels of *c-MYC* after the challenge for 24 h with AuNP@PEG@c-MYC; (c) mRNA relative expression levels of *BCR-ABL1* and *c-MYC* after the challenge for 24 h with AuNP@PEG@e14a2 and AuNP@PEG@c-MYC. Data were normalized to the *18S* gene and then to cells exposed to control (AuNP@PEG). Ct, threshold cycle. Error bars represent the standard error of the mean of three independent experiments. *p<0.05, ** p<0.01 relative to respective control, using Tukey's test statistical significance.

AuNP@PEG@c-MYC alone leads to a lower gene silencing effect compared to AuNP@PEG@e14a2 alone, while when both are added together a silencing of both genes simultaneously is observed with a higher reduction of *c-MYC* expression. This more marked

reduction to *c-MYC* expression might be due to the simultaneous targeting of *c-MYC* and *BCR-ABL1* mRNAs with an end-point impact in *c-MYC* gene expression (see schematic in Figure 3.1). Our data show efficient silencing for both cell lines, higher for K562-IM than for the parental cell line (K562) particularly for AuNP@PEG@e14a2 alone – Figure 3.5a and Figure 3.6a. c-MYC can lead to an up-regulation of *BCR-ABL1* mRNA levels [373], which is critical for CML progression from chronic phase to blast crisis [374]. A study by *Albajar* et al. (2011) demonstrated that c-MYC expression levels are higher in CML patients not responding to IM treatment, meaning that high levels of c-MYC might be an indication for a therapy failure [375].

3.3.3 Cellular effects

The effect of the Au-nanoconjugates on cell viability was assessed via the MTS assay after exposure the K562 and K562-IM cells to nanoconjugates for 24 h. K562-IM cells exposed to AuNP@PEG@e14a2, AuNP@PEG@c-MYC and both nanoconjugates showed a significant reduction of viability: 17.2%, 21.5% and 15.6%, respectively (Figure 3.7). Interestingly, a similar behavior was observed when K562-IM cells were exposed to the Au-nanoconjugates but in the presence of 1μM of IM, which can trigger a significant reduction in K562 cell viability but not in K562-IM (Figures 3.7, 3.8 and 3.9). No significant differences of viability were observed after incubation of K562-IM cells with the Au-nanoconjugates in the presence or absence of IM (Figure 3.8). We may infer that, despite reducing cells' viability, the Au-nanoconjugates do not resensitize K562-IM cells to this concentration of IM. Incubation of K562 cells with AuNP@PEG@c-MYC induced a reduction of 15.83% in cell viability compared to the control AuNP@PEG, while no significant reduction was observed when cells were exposed to AuNP@PEG@e14a2 or both nanoconjugates: 4.5% and 5.2%, respectively (Figure 3.9).

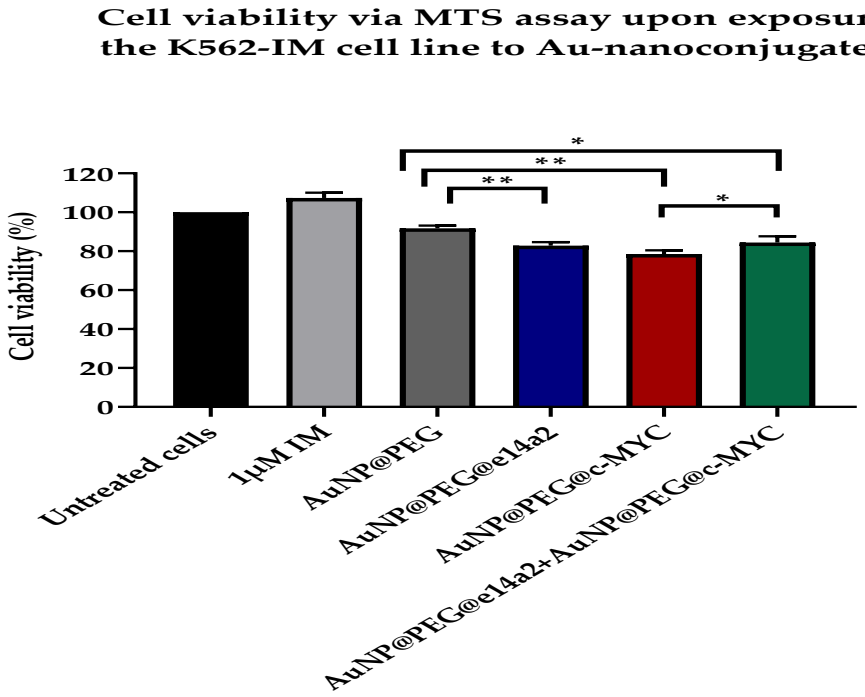

Figure 3.7 — Cell viability in K562-IM Cells. cell viability via MTS assay upon exposure of K562-IM cells to 1μM IM, AuNP@PEG, AuNP@PEG@e14a2, AuNP@PEG@c-MYC, and both Au-nanoconjugates simultaneously for 24 h.** $p<0.01$, * $p<0.05$ relative to respective control, using Tukey's test statistical significance.

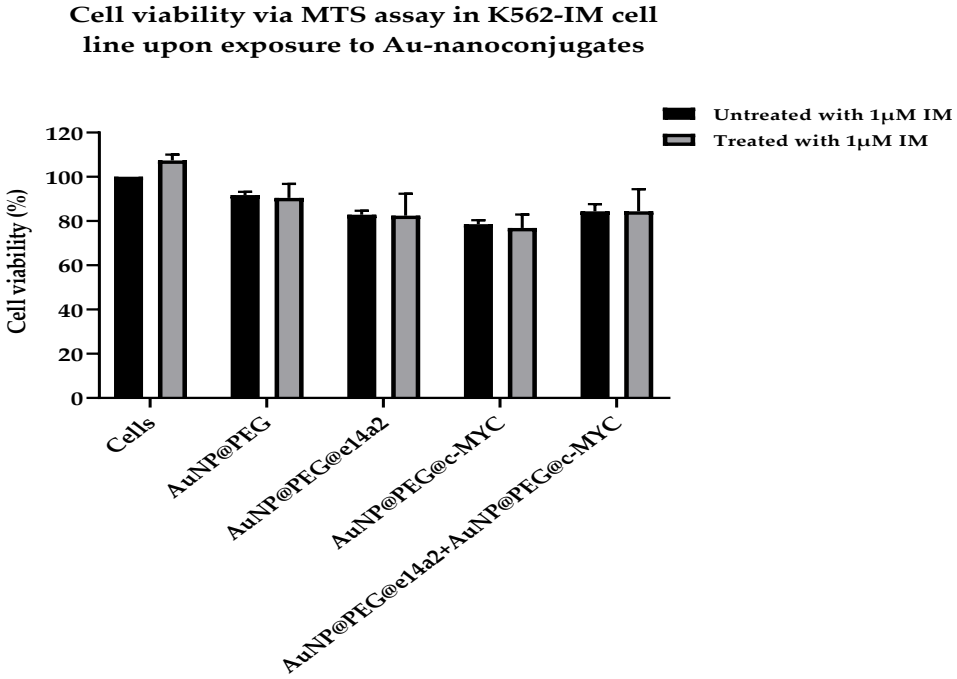

Figure 3.8 — Cell viability via MTS assay upon exposure of K562-IM cells to AuNP@PEG, AuNP@PEG@e14a2, AuNP@PEG@c-MYC, and both Au-nanoconjugates simultaneously in combination

with 1μM IM (grey bars) or without 1μM IM (black bars) for 24 h. Error bars represent the standard error of the mean of three independent experiments.

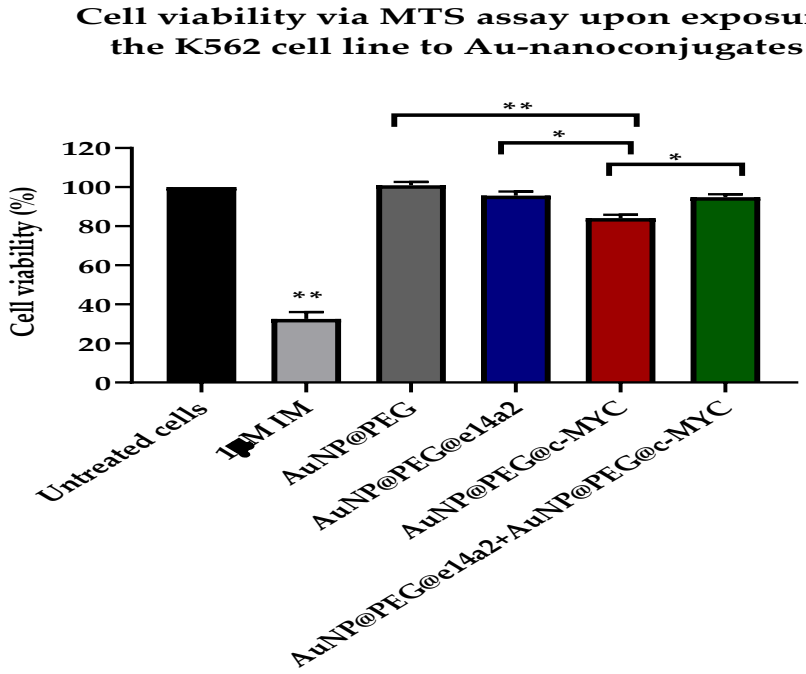

Figure 3.9 — Cell viability via MTS assay upon exposure of K562 cells to 1μM IM, AuNP@PEG, AuNP@PEG@e14a2, AuNP@PEG@c-MYC, and both Au-nanoconjugates simultaneously for 24 h. Error bars represent the standard error of the mean of three independent experiments. ** $p<0.01$, * $p<0.05$ relative to respective control using Tukey's test statistical significance.

We have further assessed the number of viable cells by the Trypan blue exclusion assay 24 h after exposition of K562 and K562-IM cells to Au-nanoconjugates. This assay allows differentiating between live cells (unstained) and cells with compromised membrane (blue stained). Results show that exposure to control AuNP@PEG resulted in only a slight reduction of cell viability (Figures 3.10 and 3.11). When K562 and K562-IM cells were exposed to AuNP@PEG@e14a2, a significant reduction of the % of viable cells was observed (38.7% and 36.4%, respectively) (Figures 3.10 and 3.11). A similar behavior was observed when K562 and K562-IM cells were exposed to AuNP@PEG@c-MYC, with a significant reduction of the % of viable cells (22.1% and 28.5%, respectively) –Figures 3.10 and 3.11. When cells were exposed to both Au-nanoconjugates simultaneously, the highest reduction in the % of viable cells was observed for K562-IM cells (40.9%) (Figure 3.11). Indeed, this reduction was much higher not

only compared to the simultaneous exposition of both Au-nanoconjugates to K562 (18.3%), but also to the individual exposition (Figure 3.11).

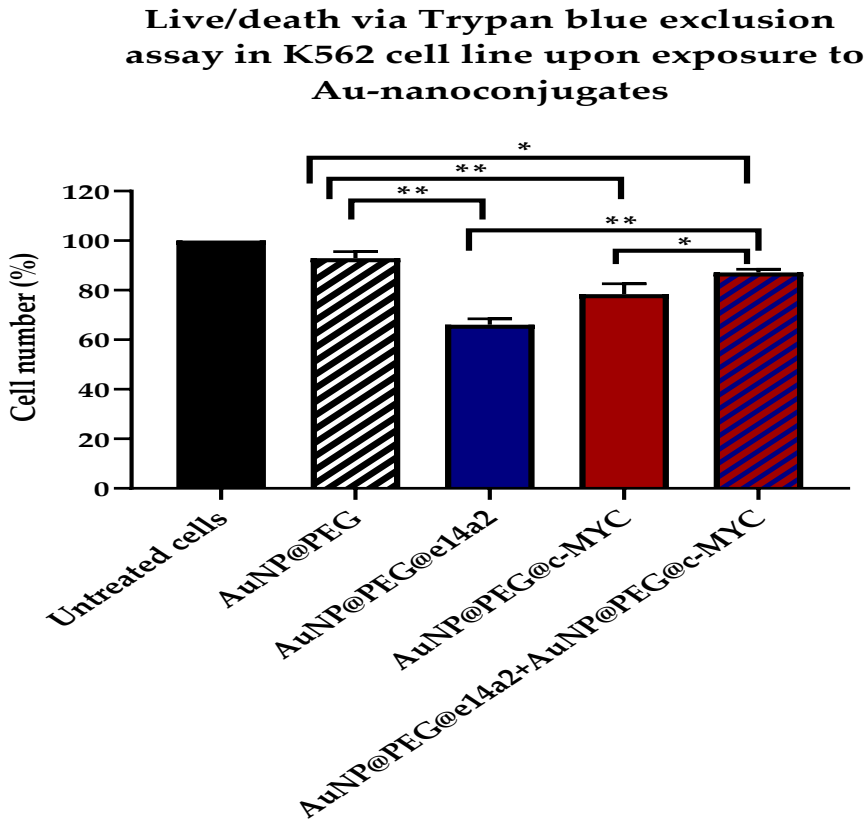

Figure 3.10 – Cell number (%) via Trypan blue exclusion assay upon exposure of K562 cells to AuNP@PEG, AuNP@PEG@e14a2, AuNP@PEG@c-MYC, and both Au-nanoconjugates simultaneously for 24 h. Error bars represent the standard error of the mean of three independent experiments. ** $p<0.01$, * $p<0.05$ relative to respective control, using Tukey's test statistical significance.

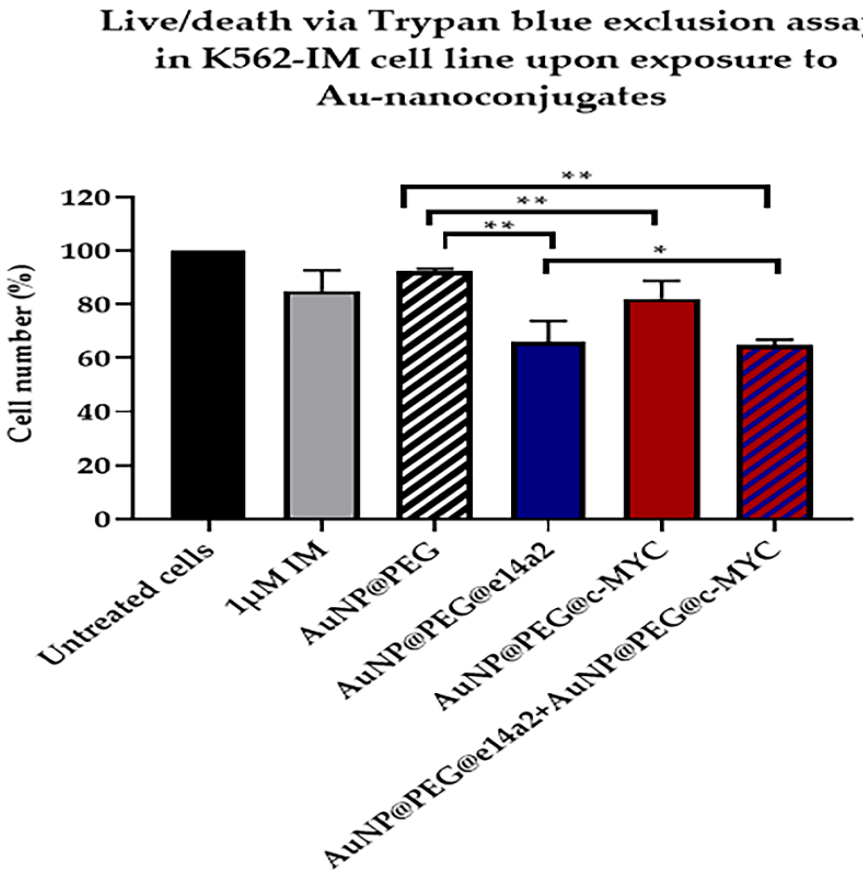

Figure 3.11 — Cell number (%) via Trypan blue exclusion assay upon exposure of K562-IM cells to AuNP@PEG, AuNP@PEG@e14a2, AuNP@PEG@c-MYC, and both Au-nanoconjugates simultaneously for 24 h. Error bars represent the standard error of the mean of three independent experiments. ** $p<0.01$, * $p<0.05$ relative to respective control, using Tukey's test statistical significance.

To further understand the effect of the Au-nanoconjugates on cell death, their cytotoxic potential was analyzed by double staining with Annexin V conjugated with AlexaFluor 488 and propidium iodide (PI). This procedure takes advantage of the translocation of phosphatidylserine (PS) to the outer leaflet of the cell membrane in the onset of apoptosis, and of the high affinity of Annexin V to PS [377]. Since PI only stains nucleic acids of cells with compromised membrane, it is possible to distinguish between live cells (unstained), cells in initial apoptosis (stained only with Annexin V – AlexaFluor 488), cells in late apoptosis (double stained with Annexin V – AlexaFluor 488 and PI) or necrotic cells (only stained with PI) [377]. Results showed that while no significant differences are observed in K562 cell line (Figure 3.12), exposure of K562-IM cells to Au-nanoconjugates resulted in a small yet statistically significant increase of cells in late apoptosis, increasing from 1.1% in AuNP@PEG treated samples to 1.8% in AuNP@PEG@c-MYC, 1.5% in AuNP@PEG@e14a2, and 1.7% in cells incubated with both Au-nanoconjugates (Figure 3.13).

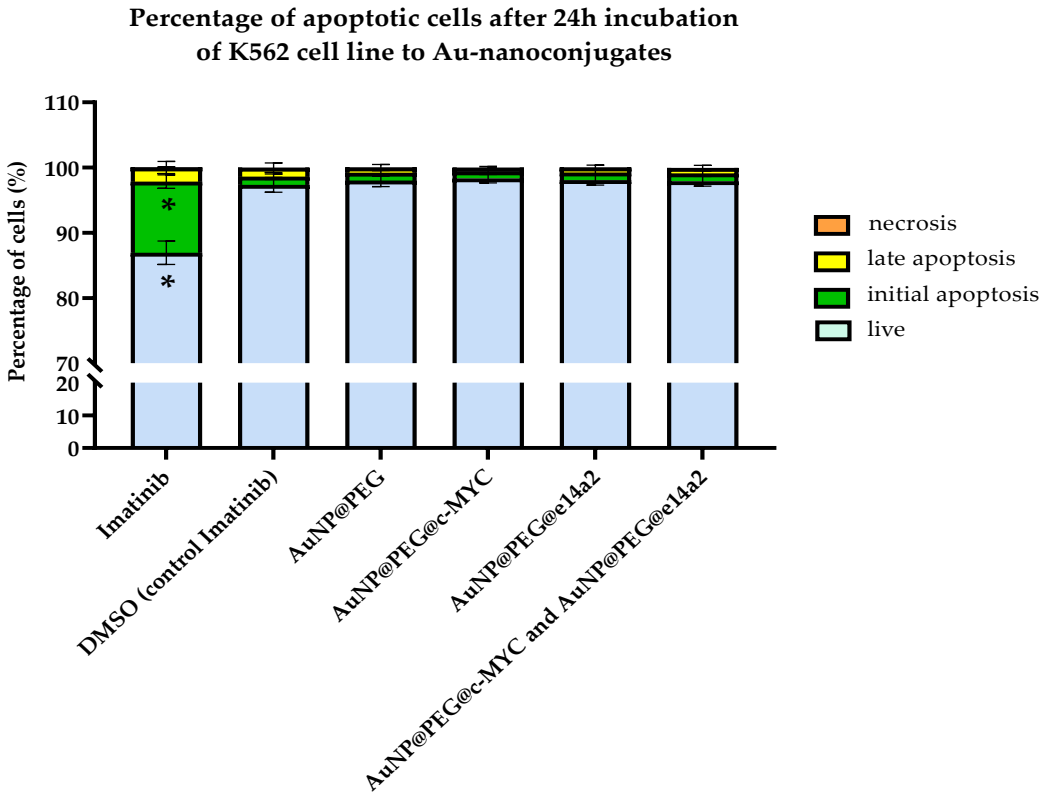

Figure 3.12 — Percentage of apoptotic cells upon exposure of K562 cells to imatinib (positive control), DMSO (vector control for imatinib), AuNP@PEG, AuNP@PEG@e14a2, AuNP@PEG@c-MYC, and both Au-nanoconjugates simultaneously. After 24 h, cells were double stained with AnnexinV conjugated with AlexaFluor488 and propidium iodide and the apoptotic events were quantified in an Attune acoustic flow cytometer (ThermoFisher Scientific). Error bars represent the standard error of the mean of three independent experiments. * $p<0.05$ relative to respective control, Tukey's test statistical significance.

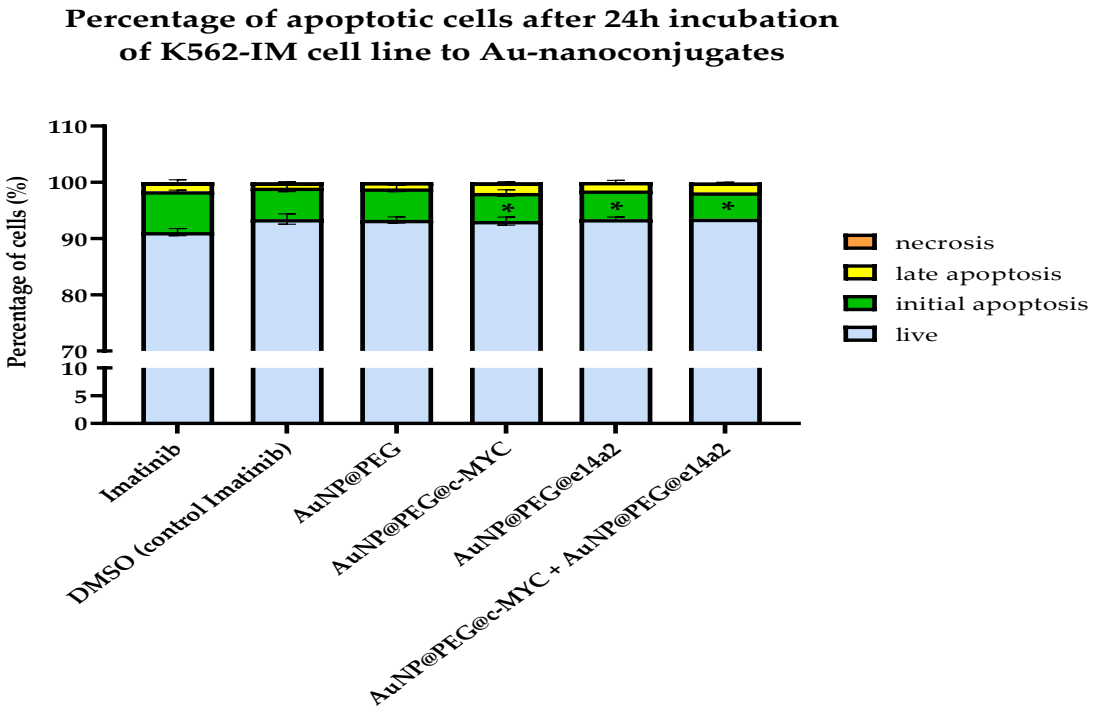

Figure 3.13 – Percentage of apoptotic cells upon exposure of K562-IM cells to imatinib (positive control), DMSO (vector control for imatinib), AuNP@PEG, AuNP@PEG@e14a2, AuNP@PEG@c-MYC, and both Au-nanoconjugates simultaneously. After 24 h, cells were double stained with AnnexinV conjugated with AlexaFluor488 and propidium iodide and the apoptotic events were quantified in an Attune acoustic flow cytometer (ThermoFisher Scientific). Error bars represent the standard error of the mean of three independent experiments. * $p<0.05$ relative to respective control, Tukey's test statistical significance.

Despite the statistically significant difference in the percentage of late apoptotic K562-IM cells after incubation with Au-nanoconjugates (Figure 3.13), this small increase does not justify the lessening cell viability determined by the MTS and Trypan blue assay (Figure 3.7; and Figure 3.11). Hence, the cytostatic potential of the Au-nanoconjugates was evaluated by analyzing cell cycle of K562 and K562-IM after double synchronization with thymidine in the S phase, and DNA staining with PI. As expected, the exposure of K562 cell line to IM resulted in cell cycle arrest in G0/G1 after 24 h (Figure 3.14a), and exposure of K562-IM to the TKI resulted in a small delay of the cell cycle observed after 12 h by an increased percentage of cells in G2/M and after 24 h in G0/G1 (Figure 3.15a). Figure 3.15b,c suggests that exposition of K562-IM cell line to AuNP@PEG@c-MYC or AuNP@PEG@e14a2 result in an increased percentage of cells in G0/G1 and decreased percentage in G2/M after 12 or 24 h, respectively, when compared to K562-IM cells exposed to AuNP@PEG.

The simultaneous exposure of K562-IM cells to both Au-nanoconjugates resulted in cell cycle delay in G0/G1 observed at 12 and 24 h (Figure 3.15d). A cell cycle arrest in K562 cells

incubated with Au-nanoconjugates was also observed, but with distinct patterns than those presented by the resistant K562-IM cells (Figure 3.14). A delay in G2/M was observed after 12 and 24 h for K562 cells exposed to AuNP@PEG@c-MYC (Figure 3.14b), and after 12 h in K562 cells exposed to AuNP@PEG@e14a2 at the same stage (Figure 3.14c). When K562 cells were exposed simultaneously to both Au-nanoconjugates showed different percentage of cells arrested in G2/M after 6 h, and lower percentage of cells in G0/G1 after 12 h (Figure 3.14d). All the referred alterations are relative to the respective control for the same cell line at the same time point.

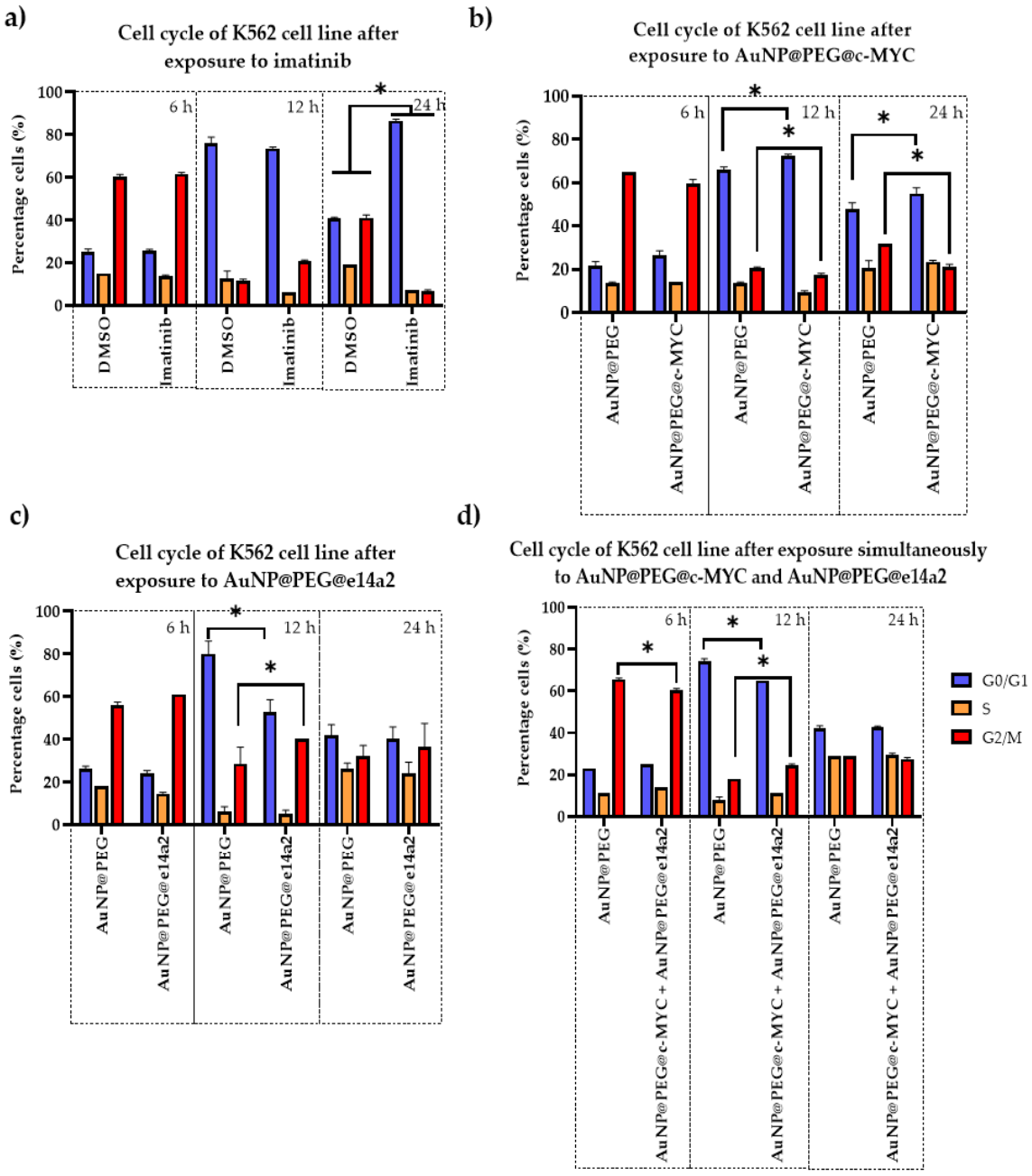

Figure 3.14 — Cell cycle analysis for 6 h, 12 h or 24 h of K562 upon exposure of (a) imatinib and respective vector control (DMSO); (b) AuNP@PEG@c-MYC alone; (c) AuNP@PEG@e14a2 alone, or (d) both Au-nanoconjugates simultaneously. Cells were stained with propidium iodide and the percentage of cells in each cell cycle stage was quantified in an Attune acoustic flow cytometer and respective software (ThermoFisher Scientific). Error bars represent the standard error of the mean of three independent experiments. * $p<0.05$ relative to respective control, Tukey's test statistical significance.

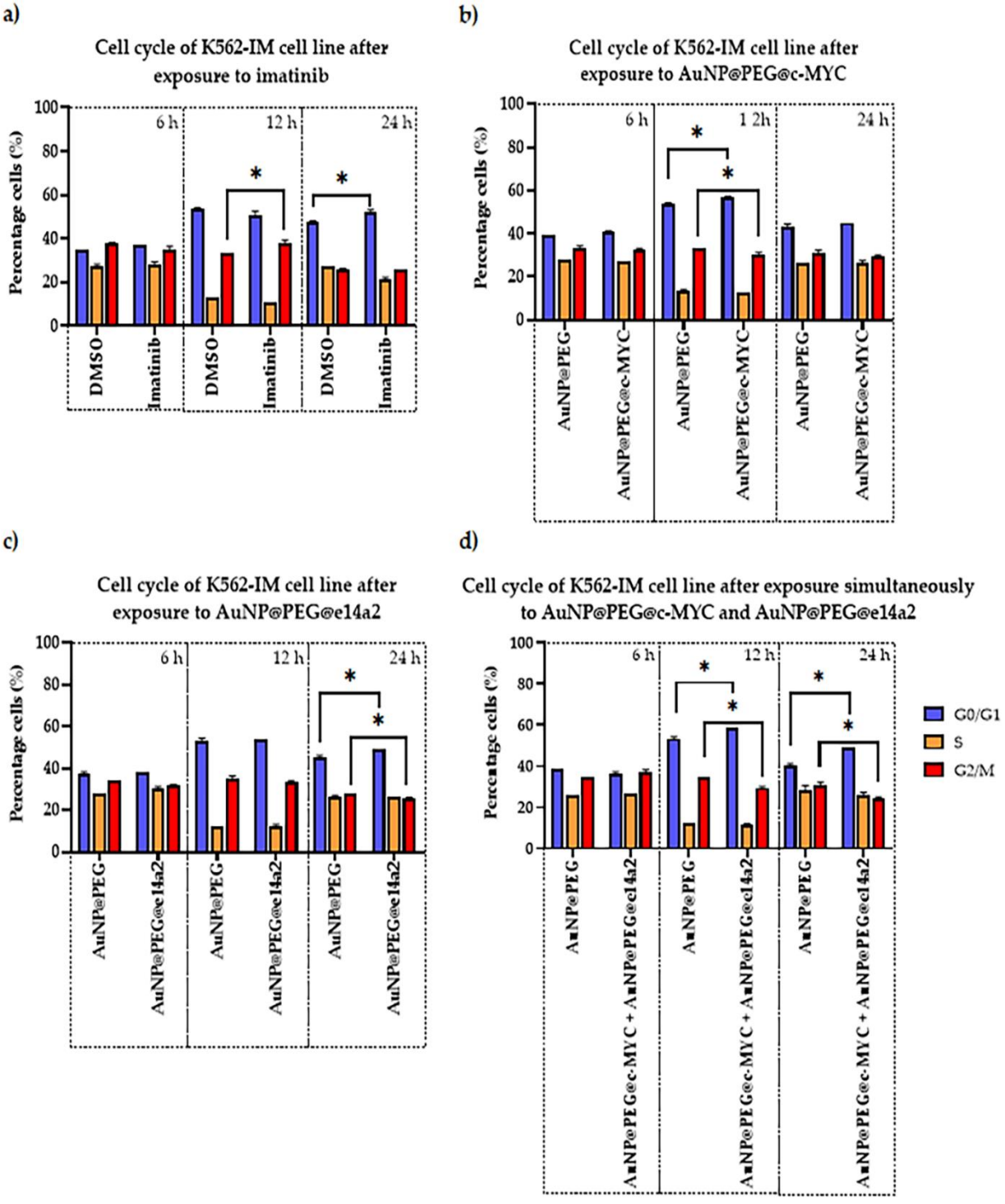

Figure 3.15 — Cell cycle analysis for 6 h, 12 h or 24 h of K562-IM upon exposure of (a) imatinib and respective vector control (DMSO), (b) AuNP@PEG@c-MYC alone, (c) AuNP@PEG@e14a2 alone, or (c) both Au-nanoconjugates simultaneously. Cells were stained with propidium iodide and the percentage of cells in each cell cycle stage was quantified in an Attune acoustic flow cytometer and respective software (ThermoFisher Scientific). Error bars represent the standard error of the mean of three independent experiments. * $p<0.05$ relative to respective control, Tukey's test statistical significance.

By targeting both genes simultaneously, and due to the crosstalk regulation of BCR-ABL1 and c-MYC proteins, the simultaneous decrease of these end effectors can induce a lower capability of cells to respond to the insult and a more effective cellular outcome on the level of reducing the number of viable cells (Figure 3.11) pointing this combination as a promising strategy toward targeting IM resistant CML cells. Silencing of c-MYC in various BCR-ABL1 positive cell lines has been shown to cause a significant downregulation of BCR-ABL1, consequently decreasing proliferation and inducting cell death [373]. Our data shows a strong reduction of K562-IM viability in the presence of the Au-nanoconjugates (Figure 3.7 and Figure 3.11), possibly due to cell cycle arrest (Figure 3.15), which is in line with ours and previous reports using the Trypan blue exclusion assay (Figure 3.11) [377].

To evaluate the effect of the induction of resistance to imatinib on K562 differentiation, the expression of the erythroid cell lineage markers tetraspanin CD71 and glycophorin A, CD235a, was evaluated by flow cytometry. While there was no statistically significant alteration in CD71 expression, it was observed that a higher percentage of CD235a positive cells in imatinib resistant K562- IM versus sensitive K562 cell line (Figure 3.16). These results are in accordance with previous studies that proposed that imatinib induce erythroid differentiation in K562 cell line [378,379]. Interestingly, when K562-IM cells were incubated with 1 μm IM, the percentage of cells presenting CD235a increased, in line with the previous observations [378,379] (Figure 3.17). Based on these results, we evaluated the effect of the incubation of K562-IM cells with the different nanoconjugates for 24 h (alone and in combination). While the incubation with AuNP@PEG did not significantly alter the percentage of CD235a positive cells (Figure 3.17), the incubation of K562-IM with both silencing Au-nanoformulations resulted in a reduced percentage of CD235a positive cells, suggesting that the silencing of BCR-ABL1 and/or c-MYC induced a reduction of the number of erythrocytic differentiated cells compared to K562-IM cells treated with the non-target Au-nanoconjugate (AuNPs@PEG).

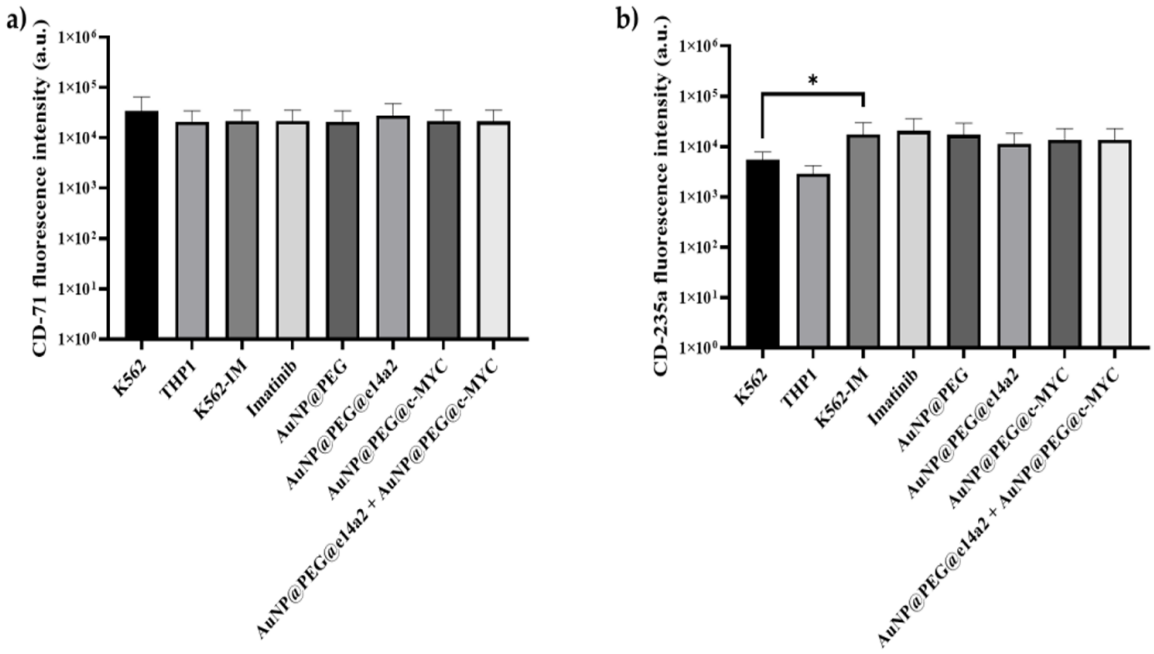

Figure 3.16 — Fluorescence intensity of the peak obtained by flow cytometry to analyze (a) CD71 and (b) CD235a expression in K562-IM cells after exposure to 1μM IM, AuNP@PEG, AuNP@PEG@e14a2, AuNP@PEG@c-MYC, and both Au-nanoconjugates simultaneously for 24 h. IM sensitive K562 cells and THP1 cells were also analyzed for control purposes.

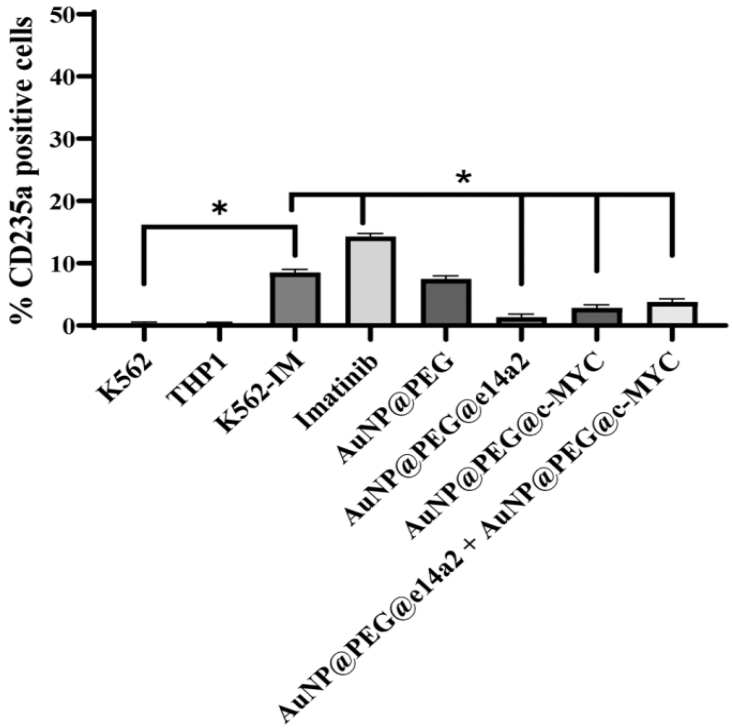

Figure 3.17 — Percentage of glycophorin A, CD235a, positive cells after 24 h incubation of K562-IM with 1 μm Imatinib (imatinib), AuNP@PEG, AuNP@PEG@c-MYC alone, AuNP@PEG@e14a2 alone, or both Au-nanoconjugates simultaneously. Imatinib sensitive K562 cells, untreated resistant K562-IM cells and

THP1 were also analyzed for control purposes. Cells were incubated with anti-CD235a conjugated with FITC and percentage of positive cells was quantified in a BD accuri flow cytometer and FlowJo software. Error bars represent the standard error of the mean of three independent experiments. * $p < 0.05$, Tukey's test statistical significance.

3.3.4 BCR-ABL1 and c-MYC Protein

Expression BCR-ABL1 and c-MYC protein expression were analyzed via Western Blot to evaluate if the silencing of both genes at the mRNA level, independently or in combination, could also impact the amount of protein present in K562-IM and K562 cells (Figures 3.18 and 3.19). Protein quantification for K562-IM cells challenged for 24 h with AuNP@PEG@e14a2 show a 25% reduction in p210 BCR-ABL1 levels, whereas c-MYC protein levels decreased by 12% (Figure 3.18b,c). When K562-IM cells were challenged with AuNP@PEG@c-MYC for 24 h, p210 BCR-ABL1 showed a reduction of 58%, while c-MYC protein expression levels showed a reduction of 35% (Figure 3.18b,c). Challenging K562-IM cells for 24 h with a combination of both Au-nanoconjugates (AuNP@PEG@e14a2 and AuNP@PEG@c-MYC) resulted in a higher decrease for both protein levels – p210 BCR-ABL1 protein levels (54% reduction) and c-MYC protein levels (36% reduction) (Figure 3.18b,c). For comparison purposes, K562 cells were also challenged with the Au-nanoconjugates alone or in combination and p210 BCR-ABL1 and c-MYC expression levels evaluated (Figure 3.19). When K562 cells were challenged with Au-nanoconjugates alone or simultaneously, the p210 BCR-ABL1 protein levels were reduced to levels compared to those in K562- IM (Figure 3.19b). In comparison, the protein levels of c-MYC in K562 cells were more reduced after incubation with AuNP@PEG@e14a2 alone and less reduced after incubation with AuNP@PEG@c-MYC alone for 24 h or both Au-nanoconjugates simultaneously (Figure 3.19c).

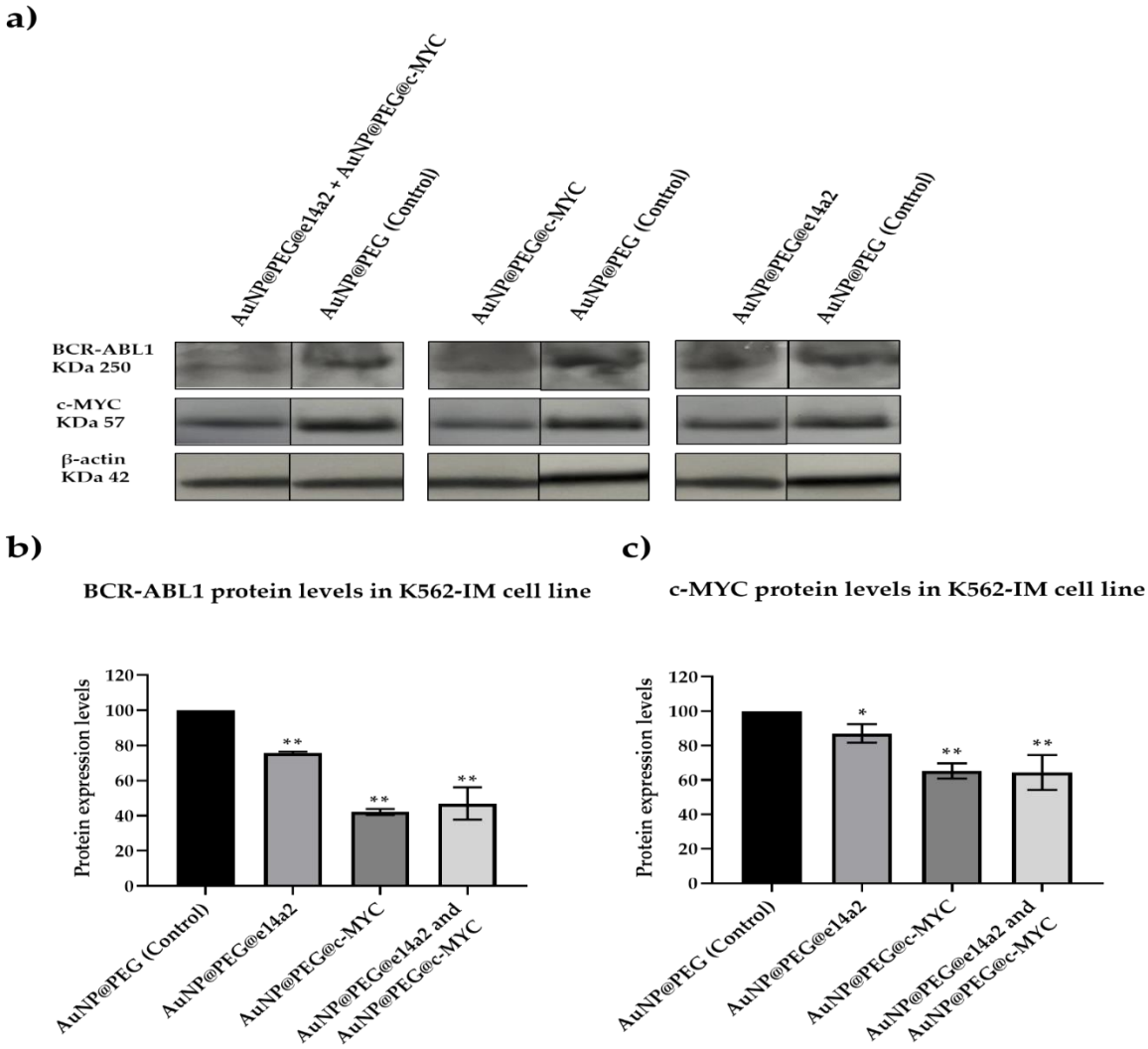

Figure 3.18 — Protein expression levels of BCR-ABL1 and c-MYC in K562-IM cell line. a) Western blot images of p210 BCR-ABL1, c-MYC, and β- actin in K562-IM cells after exposure for 24 h to Au-nanoconjugates (AuNP@PEG@e14a2 alone or AuNP@PEG@c-MYC alone or both simultaneously) or to AuNPs@PEG controls for each Au-nanoconjugate condition; b) Expression levels of p210 BCR-ABL1 after exposure to AuNP@PEG@e14a2 Au-nanoconjugate alone (intermediate grey bars), AuNP@PEG@c-MYC Au-nanoconjugate alone (dark gray bars) and to both Au-nanoconjugates (AuNP@PEG@e14a2 and AuNP@PEG@c-MYC) simultaneously (light gray bars); c) Expression levels of c-MYC after exposure to AuNP@PEG@e14a2 Au-nanoconjugate alone (intermediate gray bars), AuNP@PEG@c-MYC Au-nanoconjugate alone (dark gray bars) and to both Au-nanoconjugates (AuNP@PEG@e14a2 and AuNP@PEG@c-MYC) simultaneously (light grey bars). p210 BCR-ABL1 and c-MYC protein quantification was performed via western blotting on K562-IM cell extracts after a 24 h exposure to the Au-nanoconjugates. Band quantification was first normalized against ß-actin (loading control) and, subsequently, to the control condition (AuNP@PEG controls) (black bars in Figure 3.16b, c). Error bars represent the standard error of the mean of three independent experiments. **$p > 0.01$, *$p < 0.05$ relative to respective controls, Tukey's test statistical significance.

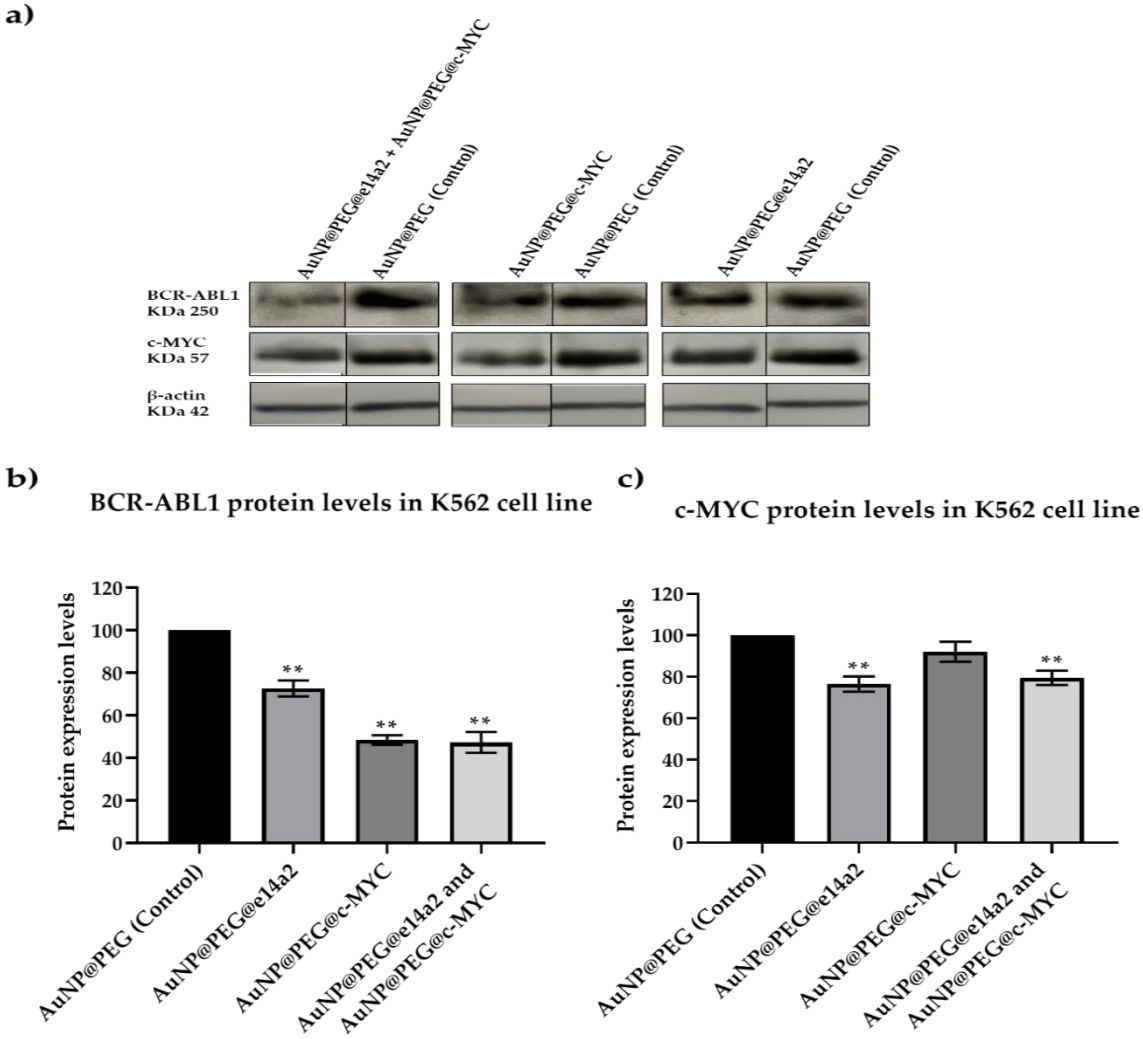

Figure 3.19 — Protein expression levels of BCR-ABL1 and c-MYC in K562 cell line. (a) Western blot images of p210 BCR-ABL1, c-MYC and β- actin in K562 cells after exposure for 24 h to Au-nanoconjugates (both simultaneously or AuNP@PEG@c-MYC alone or AuNP@PEG@BCR-ABL1 alone) or to AuNPs@PEG controls for each Au-nanoconjugate condition; (b) Expression levels of p210 BCR-ABL1 after exposure to AuNP@PEG@e14a2 Au-nanoconjugate alone (intermediate grey bars), AuNP@PEG@c-MYC Au-nanoconjugate alone (dark grey bars) and to both Au-nanoconjugates (AuNP@PEG@e14a2 and AuNP@PEG@c-MYC) simultaneously (light grey bars); (c) Expression levels of c-MYC after exposure to 13 AuNP@PEG@e14a2 Au-nanoconjugate alone (intermediate grey bars), AuNP@PEG@c-MYC Au-nanoconjugate alone (dark grey bars) and to both Au-nanoconjugates (AuNP@PEG@e14a2 and AuNP@PEG@c-MYC) simultaneously (light grey bars). p210 BCR-ABL1 and c-MYC protein quantification was performed via western blotting on K562 cell extracts after a 24 h exposure to the Au-nanoconjugates. Band quantification was first normalized against ß-actin (loading control) and, subsequently, to the control condition (AuNP@PEG controls) (black bars in Figures 3.17b, c). Error bars represent the standard error of the mean of three independent experiments. **p> 0.01 relative to respective controls, Tukey's test statistical significance.

To further corroborate these western blot results in K562-IM cells, fluorescent microscopy was used (Figure 3.20). For that c-MYC and BCR-ABL1 proteins were stained with TRITC and FITC labeled antibodies, respectively and the fluorescence intensities analyzed after challenging cells with both Au-nanoconjugates individually or simultaneously (Figure 3.20). As observed, there was a strong reduction of the fluorescence intensity of c-MYC and BCR-ABL1 after incubation with Au-nanoconjugates that seems to be more effective when K562-IM cells were exposed to AuNP@PEG@c-MYC compared to the other exposures (Figure 3.20a,b). Using brightfield microscopy we were able to observe Au-nanoparticles inside individual cells (arrows in Figure 3.20a) after exposure to each Au-nanoconjugate and simultaneously quantify the reduction on the fluorescence intensity induced by them on c-MYC and BCR-ABL1.

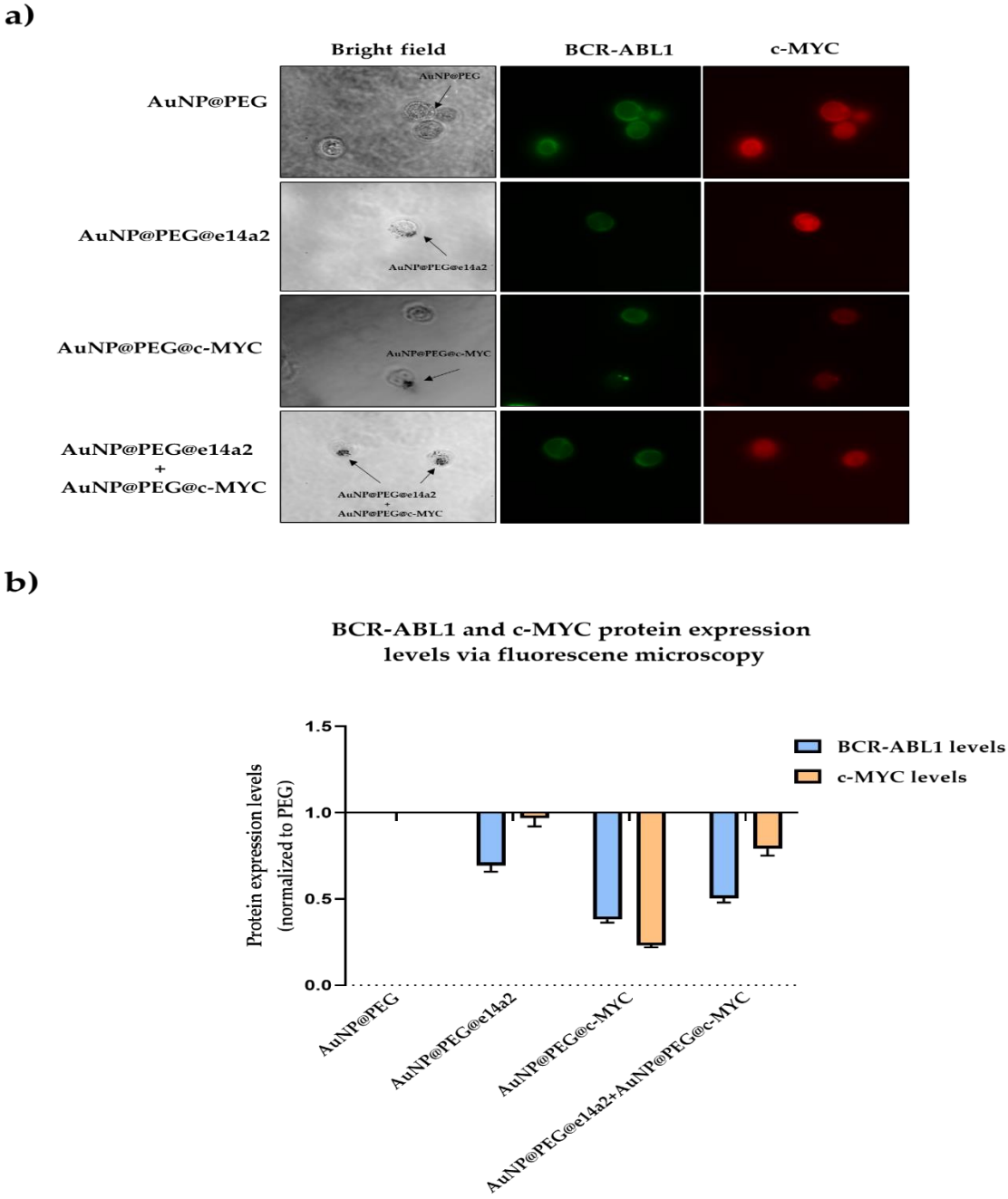

Figure 3.20 — Fluorescence microscopy analysis of c-MYC and BCR-ABL1 proteins in K562-IM cell after exposure for 24 h to Au-nanoconjugates (AuNP@PEG@e14a2 alone, AuNP@PEG@c-MYC alone or both simultaneously) and to AuNP@PEG controls. a) representative images acquired in the same frame for bright field, BCR-ABL1 antibody (FITC – green filter) and c-MYC antibody (TRITC – red filter). Arrows represent Au-nanoconjugates in cells. b) normalized BCR-ABL1 and c-MYC expression levels after exposure to AuNP@PEG@e14a2 alone, AuNP@PEG@c-MYC alone or both simultaneously for 24 h (normalization of total fluorescence intensities to the respective values of AuNP@PEG).

We demonstrate that silencing at the mRNA level translated to downregulation at the protein level, where a similar decrease in p210 BCR-ABL1 protein expression in both K562-IM and K562 cell lines exposed to AuNP@PEG@e14a2 alone was observed (Figures 3.18, 3.19 and 3.20). c-MYC expression was also downregulated after challenging K562-IM cells (and K562) with AuNP@PEG@e14a2 Au-nanoconjugates. Our data shows a reduction of c-MYC expression at the gene level that was also translated to around 35% reduction in the c-MYC protein level (Figures 3.5b and 3.18c). Protein expression decrease was more pronounced in K562-IM when compared to K562 cells (Figure 3.18c and 3.19c). Moreover, silencing of c-MYC induces a strong downregulation of p210 BCR-ABL1 protein levels in K562-IM cells (Figures 3.18b and 3.20), and even in sensitive K562 (Figure 3.19b). These observations are in line with reports highlighting that c-MYC levels are controlled by BCR-ABL1 oncoprotein via several signaling pathways [380-383] (partially summarized in Figure 3.1) and that BCR-ABL1 inhibition by IM strongly reduces c-MYC expression [375,384–386].

3.3.5 Conclusion

In CML, the molecular hallmark of disease is BCR-ABL1 fusion transcript, and c-MYC is one of the oncogenic transcription actors induced by BCR-ABL1 (Figure 3.1). Resistance to IM has been related to BCR-ABL1- dependent or -independent mechanisms [387–391], and induction of c-MYC might be triggered via BCR-ABL1 via Janus kinase 2 (JAK2) activation [392,393] or via other MAPK pathways (Figure 3.1) [380], leading to high levels of c-MYC that correlate with poor response to IM and, at molecular level, to genomic instability [375].

BCR-ABL1-dependent and/or independent resistance to IM might be tackled via the specific silencing of BCR-ABL1 and c-MYC overexpression. Herein, we demonstrate the potential of AuNPs for vectorization of ASOs capable of silencing these target genes in sensitive and IM-resistant K562 cell models. The physicochemical properties of the AuNPs, particularly their size, polydispersity index and surface charge, have been considered for improved vectorization of gene silencing strategies [394].

In the present chapter, we show the silencing capability of AuNPs and functionalized with ssDNA oligonucleotides targeting selectively the e14a2 BCR-ABL1 or the c-MYC. These Au-nanoconjugates were capable of efficiently silence both genes at the mRNA level that also led to a significant reduction of the respective protein levels in an imatinib resistant cell line – K562- IM. These reductions at gene and protein levels induced cell cycle arrest and a decrease in the number of IM resistant cells. Interestingly, the simultaneous use of both nanoconjugates also led to a reduction in the levels of both proteins (BCR-ABL1 and c-MYC) that

provided a slight reduction of the number of viable cells and an arrest of cell cycle both at 12 and 24 h. We hypothesize that when both genes are reduced at the same time, cells may be less capable to respond to the insult, with a higher impact on cell death. Still, further in vivo validation is required so support this approach as an adjuvant tool for current TKI therapy, mainly in patients that display IM resistance due to MDR1 overexpression. In CML, usually spontaneously models are used whose molecular profiles need to be carefully ascertained to provide for relevant information. Moreover, as described by *Kohnken* et al. (2017) [395], the liquid nature of these malignancies (spread all over the body) coupled to the complex micro-environment from which their arise and their multifaceted genetic basis has added to the difficulty in generating appropriate translational in vivo models to study CML, let alone models of TKI resistance.

4

COMBINATORY THERAPY – USING AU-NANOCONJUGATES FOR GENE SILENCING COMBINED WITH KINASE INHIBITORS

4.1 Introduction

Chemotherapy has been an instrumental tool in cancer treatment, supported by a wide array of chemotherapeutic agents. Integration of multiple therapeutic modalities to precisely address cancer-promoting or cell-maintaining pathways is fundamental to cancer treatment [396].

The concept of combination therapy was initially presented in 1965 when Emil Frei and colleagues initiated the first combination chemotherapy for pediatric patients suffering from acute leukemia [397]. This combination therapeutic approach has significantly transformed the field of clinical oncology since its inception [398]. As a result, significant focus in cancer research has been placed on exploring combination therapies that target various pathways that produce a beneficial anticancer response [398].

The combination of anti-cancer drugs improves efficacy relative to monotherapy by targeting essential pathways in a synergistic or additive manner [399]. This method may diminish drug resistance while offering therapeutic anti-cancer advantages, including the inhibition of tumor growth and metastasis, the arrest of mitotically active cells, the reduction of cancer stem cell populations, and the induction of apoptosis [396]. Moreover, combination therapy may mitigate the toxic effects on normal cells while simultaneously exerting cytotoxic effects on cancer cells [396]. This may happen if one drug in the combination strategy exhibits antagonistic cytotoxicity towards another drug in normal cells, thereby preserving normal cells from cytotoxic effects [400].

Mutations and genetic instability constitute the foundation for the development of cancer. Gene silencing holds significant potential for application in cancer therapy through the modulation of genes involved in cancer. The integration of chemotherapy and gene therapy would constitute an optimal strategy for cancer therapy [401]. The combined approach of chemotherapy and gene therapy has demonstrated a synergistic effect against multiple types of cancer [402-404].

Gene therapy remains an evolving field and requires additional data for determining its long-term safety and efficacy [405]. Nanomedicine is a research domain that employs nanoparticles to administer pharmaceuticals and therapies to cells [406]. Nanoparticles can facilitate gene delivery by being engineered to target specific cells or areas. Nanoparticles possess the capacity to transform gene therapy and can securely transport genetic material and accurately direct it to the required location [405]. Nanotechnology-based drug delivery systems enable the co-delivery or simultaneous administration of multiple therapeutic agents [401]. AuNPs present a distinctive opportunity to integrate multiple treatment modalities simultaneously, thereby underlining their superiority in combinatorial cancer therapy [407]. Utilizing AuNPs for the simultaneous co-delivery of multiple treatments enhances the efficacy of each therapy and may also yield additional benefits from the synergistic interactions among different modalities, leading to significantly improved therapeutic outcomes [407].

In CML, adaptative therapeutic regimens might involve the use of a novel class of targeted BCR-ABL1 inhibitors that focus on the myristoyl pocket of BCR-ABL1, in combination therapies with other kinase inhibitors, or other agents with innovative targets pertinent to CML biology [408]. AURKA is crucial for the centrosome cycle and the polar spindle assembly checkpoint, facilitating controlled advancement from G2 to M and during the M phase [145]. In CML, it is often overexpressed, resulting in genomic instability and resistance to TKIs like IM [145]. This kinase modulates the G2/M checkpoint, ensuring precise cell division [145]. Inhibition of AURKA has been shown to induce apoptosis and reduce the clonogenic potential of CML cells [145]. AURKA inhibitors have been advanced for the treatment of drug-resistant CML, including those driven by T315I BCR-ABL1 mutant, through the inhibition of BCR-ABL1 TK [409]. Danu is a dual inhibitor of AURKA and ABL1 (wild-type and mutated, including T315I), which showed promising activity both in leukemia and solid tumors [144].

PLK1 is crucial for regulating cell division, preserving genome stability during mitosis, facilitating spindle assembly, and responding to DNA damage [410]. In CML, PLK1 is overexpressed, facilitating the sustenance of leukemic stem cells and conferring resistance to TKIs. Inhibition of PLK1 can induce cell cycle arrest and apoptosis in CML cells [154]. One of

the best characterized PLK inhibitors is Vola, a low molecular weight compound that exhibits substantial anti-leukemic activity [152].

WEE1 is a tyrosine kinase that inhibits the activation of CDK1 and CDK2 to protect genomic integrity by regulating initiation of replication [411]. In CML, WEE1 participates in DDR and aids cancer cell survival by inhibiting premature mitotic entry [157]. The overexpression of WEE1 correlates with resistance to IM; thus, targeting WEE1 may augment the sensitivity of CML cells to TKIs and promote cycle arrest and apoptosis [157]. WEE1 has been considered as a distinct therapeutic target, with the agent ada now advancing through clinical trials [173,412,413]. Adavo is a first-in-class selective small-molecule inhibitor of the tyrosine kinase Wee1, a regulator of the intra-S and G2/M cell-cycle checkpoints [170]. Furthermore, ada enhances the efficacy of chemotherapeutic drugs by impairing the DNA damage response, leading to the buildup of DNA damage [171]. The effectiveness of Adavo in conjunction with other anticancer treatments has been examined in preliminary clinical trials [172-174]. Figure 4.1 summarizes the signaling pathways of Aurora A, PLK1 and WEE1 kinase and their role in CML.

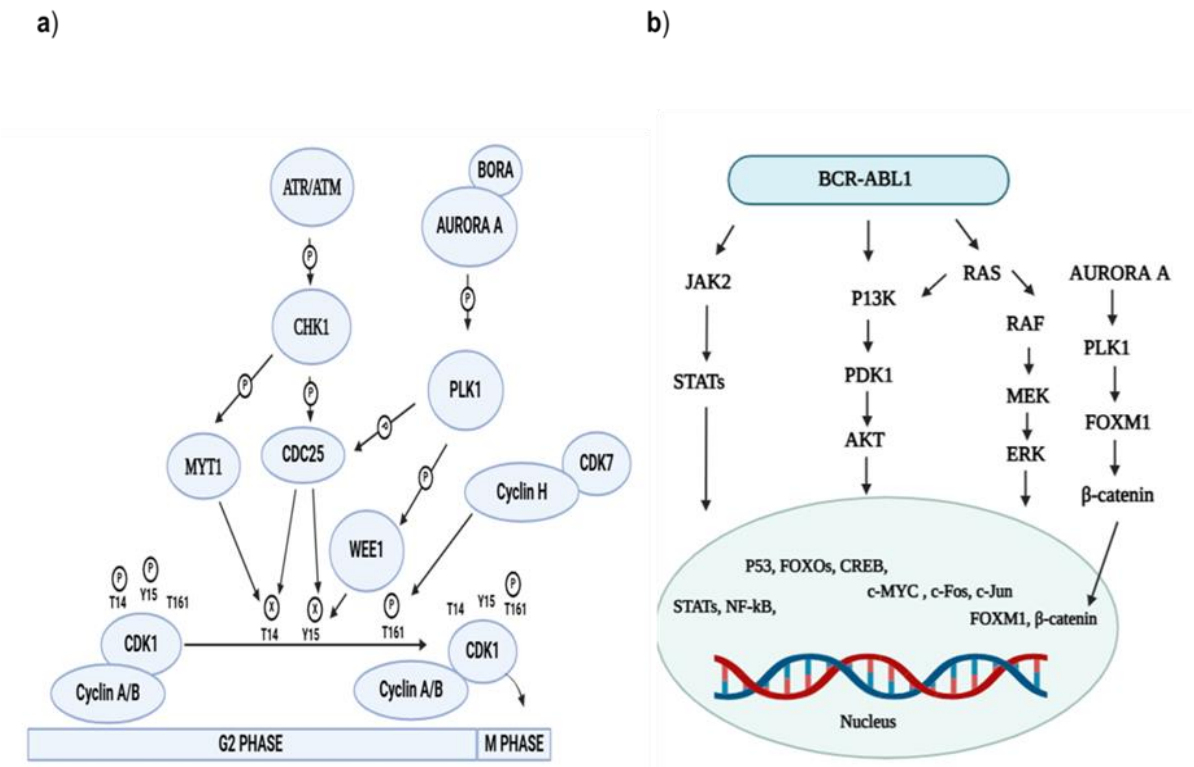

Figure 4.1 — Signaling pathways of Aurora Kinase A, Polo Kinase 1 and WEE 1 Kinase and the resistance mechanism in CML. a) AURKA modulates mitotic entry by activating the cyclin-B/CDK1 complex, AURKA phosphorylates PLK1 by the cofactor Bora. Activated PLK1 phosphorylates CDC25 phosphatases. AURKA can directly phosphorylate CDC25 to promote mitotic entry. On the other hand, activated PLK1 is able to degrade the CDK1 inhibitory kinase WEE1 to prevent the inactivation of cyclin-B/CDK1; b) Overview of the main resistance

mechanism in CML such as: activation of alternative signaling pathways (PI3K/AKT, JAK/STAT, and RAS/MAPK); activation of Aurora A-PLK1-FOXM (adapted from De Santis et al., [414] & Otto at al.,[415])

Based on the promising data from chapter 3, herein, we hypothesize that applying a combination strategy directed at different molecular targets would result in optimized efficacy in cells sensitive and resistant to IM - the first-line TKI broadly used in CML patients. Firstly, a combination of IM with other kinase inhibitors - Danu, Vola, and Adavo; and then a combination of combining Au-nanoconjugates for the direct and simultaneous silencing of BCR-ABL1 (e14a2) and c-MYC with IM and Danu, Vola, and Adavo. The effect of these combinations is assessed in terms of efficacy against the K562 cells sensitive and resistant to IM, and the potential additive/synergistic effect is analyzed in terms of counteracting resistance to IM.

4.2 Materials and Methods

4.2.1 Cell challenge with Au-nanoconjugates

K562 and K562-M Cells were cultured in a density of $0.1x10^5$ cells/well (96 well plate). Both cell lines were challenged simultaneously for 24 h with AuNP@PEG @14a2 (0.35 nm) targeting *BCR-ABL1*, which corresponds to 30 nM oligonucleotide with a ratio of (Au:oligonucleotide = 1:84) and AuNP@PEG@c-MYC (0.6 nm) targeting *c-MYC*, which corresponding to 45 nM oligonucleotide with ratio of (Au:oligonucleotide = 1:75).

4.2.2 Cell challenge with chemotherapeutics and Au-nanoconjugates

Danu, Vola, and Adavo were purchased from Selleck Chemicals. K562 and K562-IM cell lines were seeded at density of $0.1x10^5$ cells/well (96 well plate). The determination of relative IC_{50} of IM, Danu, Vola, and Adavo were performed by MTS assay by exposing k562 along with k562-IM cell lines for growing concentrations of the drugs ranging from 0.0025 to 10 µM for 48 h. The cells were firstly exposed individually or in combination to IC_{50} of IM, Danu, Vola, and Adavo for 48 h. Afterwards, the cells were subjected to challenges involving 0.35 nM AuNP@PEG@e14a2, corresponding to 30 nM oligonucleotide (with an Au: oligonucleotide ratio of 1:84), alongside 0.6 nM AuNP@PEG@c-MYC, corresponding to 45 nM oligonucleotide (maintaining the same Au: oligonucleotide ratio of 1:84), and were incubated for a duration of 24 h. As control, cells were subjected to IC_{50} of the drugs as control.

4.2.3 Cell Viability via MTS assay

The MTS examination was used to evaluate cell viability. In brief, for the combination of Au-nanoconjugates with IM and/or other kinase inhibitors (Danu, Vola, and Adavo), K562 and K562-IM cell lines were firstly subjected to the IC_{50} of the drugs and placed in 96-well plates for a total of 48 h, after 24 h of incubation with the drugs, AuNP@PEG@e14a2 and AuNP@PEG@-c-MYC simultaneously were added to cells for 24 h. For this assay, the 96-Cell Titer® liquid-Non-Radioactive was utilized. The intensity of absorption was determined using a Tecan-Infinite-M200 microplate reader at 490 nm.

4.3 Results and discussion

4.3.1 Effect of Adavosertib, Danusertib and Volasertib in K562 and K562-IM cell lines

The effect of Danu, Vola, and Adavo on K562 and K562-IM cells viability was assessed via the MTS assay after exposure of cells to increasing concentrations (ranging from 0.0025 to 10 μM) of each kinase inhibitor individually for 48 h. For IM, the relative IC_{50} was also determined via MTS assay at 48 h by exposing K562 cells to growing IM concentrations ranging from 0.01 to 10 μM in K562 cell line.

As observed in Figures 4.2 and 4.3, there is a decrease in both cells' viability with an increase of kinase inhibitor concentration.

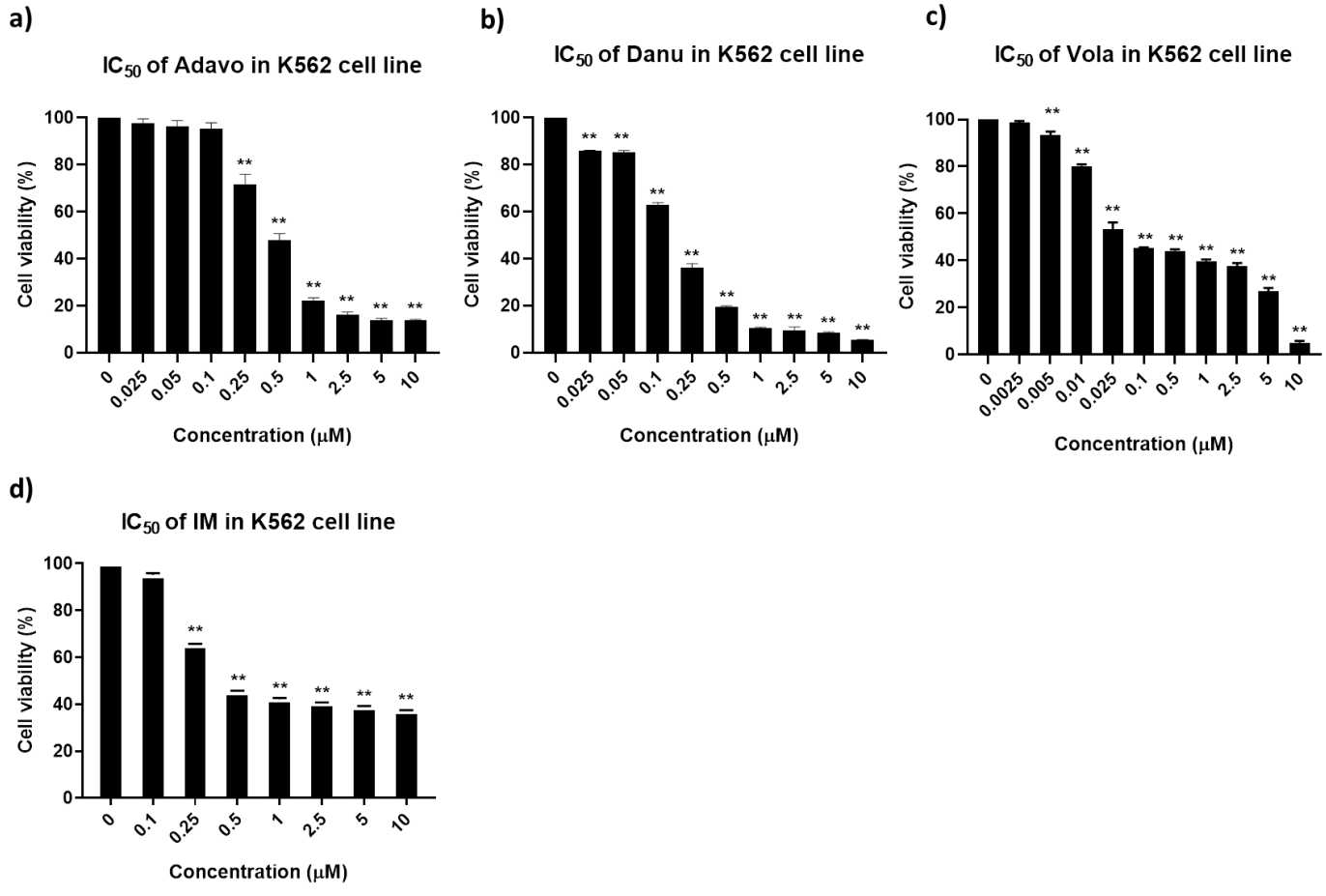

Figure 4.2— K562 Cell Viability (%) after 48h of incubation in the presence of increasing concentrations (0.0025 to 10 μM) of Adavosertib (Adavo) (a), Danusertib (Danu) (b), Volasertib (Vola) (c), and Imatinib (IM) (d).** $p<0.01$ relative to respective control, using Tukey's test statistical significance.

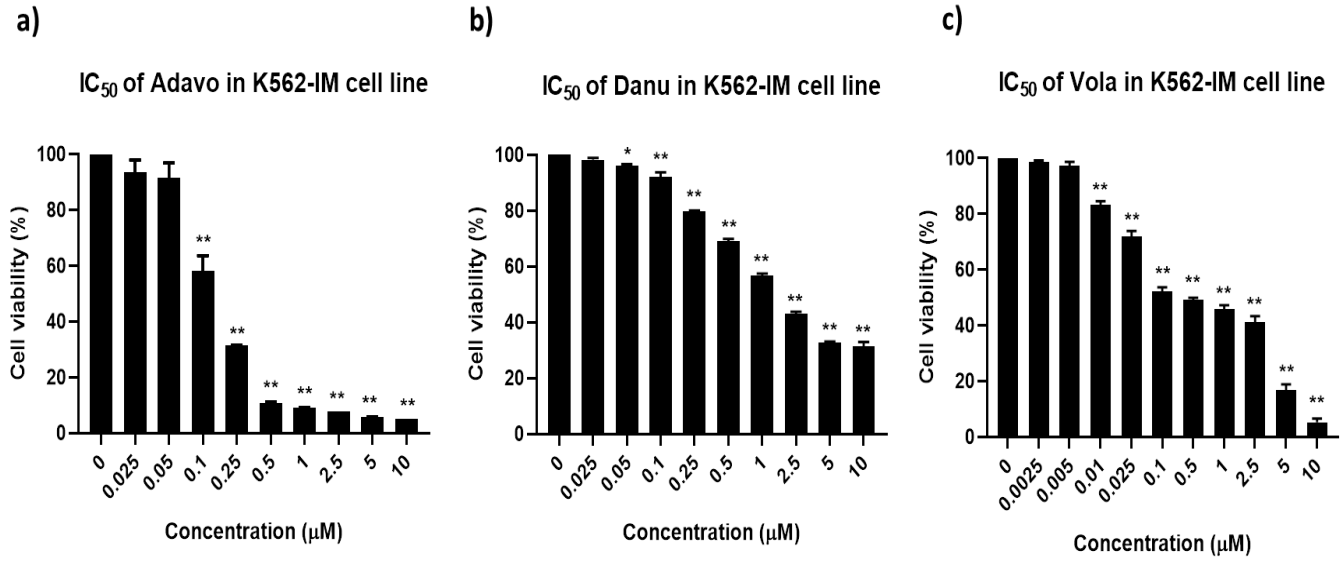

Figure 4.3 — K562-IM Cell Viability (%) after 48h of incubation in the presence of increasing concentrations (0.0025 to 10 μM) of Adavosertib (Adavo) (a), Danusertib (Danu) (b) and Volasertib (Vola) (c). * $p<0.01$, * $p<0.05$ relative to respective control, using Tukey's test statistical significance.

These cell viability as a function of concentration plots allowed calculating the relative IC_{50}, defined as the kinase inhibitor concentration resulting in 50% of reduction in cell viability (Table 4.1) [416].

Table 4.1 — Relative IC_{50} values obtained for each kinase inhibitor (Danu, Vola, Adavo and IM) in K562 or K562-IM cell lines after 48 h of exposure. IC_{50} values are expressed as the mean ± SEM of at least three biological independent assays.

	IC_{50} (μM)	
Kinase inhibitors	**K562**	**K562-IM**
Danu	0.21 ± 0.03	0.97 ± 0.02
Vola	0.025 ± 0.005	0.1 ± 0.03
Adavo	0.35 ± 0.04	0.14 ± 0.06
IM	0.18 ± 0.07	N/A

***N/A: not applicable**

In K562 the cytotoxicity order was Vola > Danu > Adavo; for K562-IM the cytotoxicity order was Vola > Adavo > Danu. (Table 4.1; Figures 4.1 and 4.2). As observed in Table 4.1 and Figures 4.1 and 4.2, among the three kinase inhibitors, Vola induced higher cytotoxicity in both cell lines (sensitive and resistant).

4.3.2 Combination of Imatinib, Adavosertib, Danusertib and Volasertib

Next, we have evaluated the effect of incubating K562 and K562-IM cells with two different TKIs simultaneously. To achieve this, both cells were exposed, for 48 h, to the IC_{50} concentrations of both kinase inhibitors (IC_{50} of IM, Danu, Vola, Adavo (see Table 4.1 above)) and the effect on cell viability determined using the MTS assay (Figures 4.4 and 4.5).

The combination of Adavo + Danu simultaneously induced a statistically significant reduction of K562 cell viability (attaining a value of 23.32%) when compared to each drug individually: Adavo (final viability of 59.24%) and Danu (final viability of 58.26%) (Figure 4.4a). A similar behavior was observed in K562-IM cell line, showing a statistically significant reduction of cells viability (with a final value of 35.77%) of the combined drugs when compared to each drug individually: Danu (viability of 66.62%) and IC_{50} Adavo (viability of 52.10%) (Figure 4.5a). Globally, the effect of this combination was more pronounced in K562 sensitive cells compared to the resistant K562 cells (Figures 4.4 and 4.5).

Concerning the combination of Vola + Adavo simultaneously in both cell lines, results show a statistically significant reduction in K562 (viability of 35.03%) compared to Vola alone (viability of 64.74%) or Adavo alone (viability of 59.24%) (Figure 4.4b). For the K562-IM cell line, a statistically significant reduction (viability of 50.78%) was observed for the combination of both drugs when compared to Vola (viability of 66.42%) alone (Figure 4.5b), but no statistically significant reduction was observed compared to Adavo alone (viability of 52.10%) (Figure 4.5b).

Additionally, the simultaneous challenge of the combination Vola + Danu in K562 cell line also showed a statistically significant decrease (viability of 38.29%) in comparison with Vola alone (viability of 64.74%) or Danu alone (viability of 58.26%) (Figure 4.4c). The same was also observed for the combination Vola + Danu in IM-resistant cell line, (viability of 53.26%) when compared to Vola alone (viability of 66.42%) or Danu alone (viability of 66.62%) (Figure 4.5c).

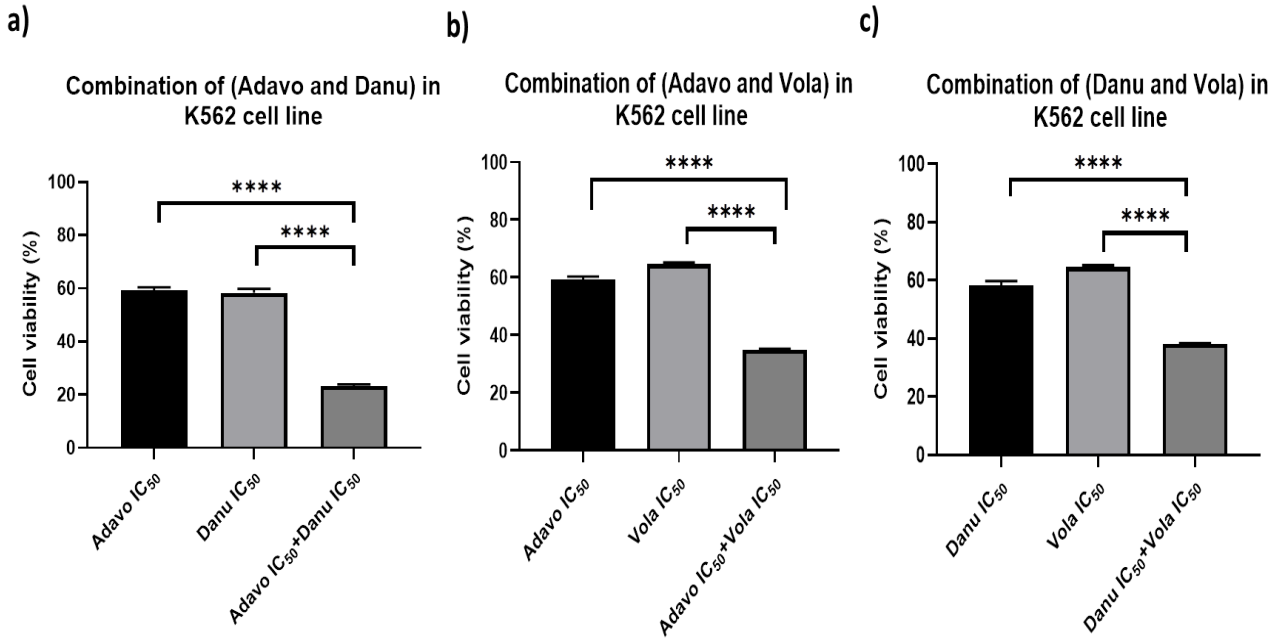

Figure 4.4 — Cell viability via MTS assay upon exposure of K562 cell line to combination of adavosertib (Adavo), danusertib (Danu), volasertib (Vola) for 48 h. (a) combination of Adavo + Danu compared to the IC_{50} of Adavo or the IC_{50} of Danu individually (b) combination of Adavo + Vola compared to the IC_{50} of Adavo or the IC_{50} of Vola individually. (c) combination of Danu + Vola compared to the IC_{50} of Vola or the IC_{50} of Danu individually. Error bars represent the standard error of the mean of three independent experiments. **** $p<0.0001$ relative to respective control using Tukey's test statistical significance.

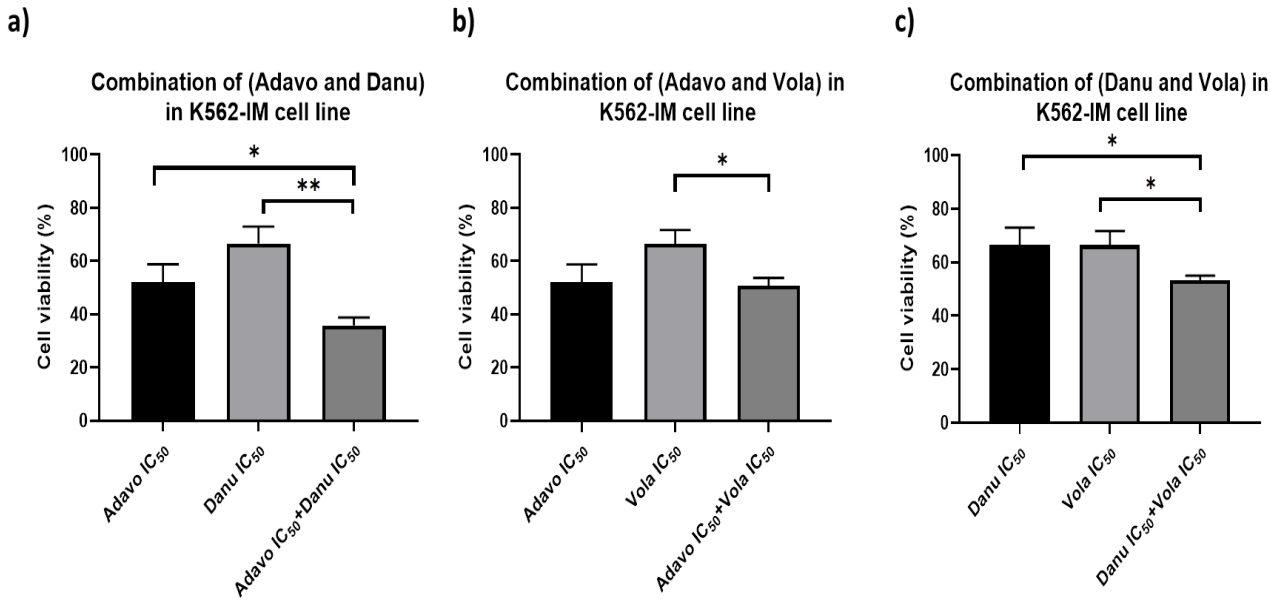

Figure 4.5 – Cell viability via MTS assay upon exposure of K562-IM cell line to combination of Adavosertib (Adavo), Danusertib (Danu), Volasertib (Vola) for 48 h. (a) combination of Adavo + Danu compared to the IC_{50} of Adavo or the IC_{50} of Danu individually (b) combination of Adavo + Vola compared to the IC_{50} of Adavo or the IC_{50} of Vola individually. (c) combination of Danu + Vola compared to the IC_{50} of Vola or the IC_{50} of Danu individually. Error bars represent the standard error of the mean of three independent experiments. ** $p<0.01$, * $p<0.05$ relative to respective control using Tukey's test statistical significance.

Considering the different combinations studied so far, the combination of Danu + Adavo induced the highest decrease in K562 and K562-IM cells viability compared to the other combinations. Moreover, the effect was higher for K562 compared to K562-IM.

We demonstrate that combining Aura kinase inhibitor (Danu) with the polo kinase inhibitor (Vola) simultaneously significantly decreases the cell viability in K562 and K562-IM (Figures 4.4c and 4.5c). Interestingly, combining tyrosine kinase Wee1 inhibitor (Adavo) with Danu or Vola simultaneously leads to much lower cell viability compared to Adavo or Danu alone in both sensitive and IM-resistant cell lines – see Figures 4.4 and 4.5. Our findings are in line with a previous report by *Mancini* et al., [145] where it is demonstrated that a combination of Wee1 inhibitor (Adavo) with Danu or Vola has a significant impact on TKI-sensitive and -resistant cell lines by enhancing the induction of apoptotic cell death when compared to Danu and Adavo alone.

We have further assessed the combination of the IC_{50} of IM with the IC_{50} of Adavo, or the IC_{50} of Danu or the IC_{50} of Vola in the K562 cell line - Figure 4.6. Similar behavior was

observed for these combinations: (IM + Adavo), (IM + Danu) and (IM + Vola), all showing a strong reduction in cell viability – resulting in viability of 10.93%, 14.73%, and 13.24%, respectively - compared to each drug alone at the respective IC_{50} (viability of 56.88%, 59.24%, 58.26%, or 64.74%, respectively) (Figure 4.6).

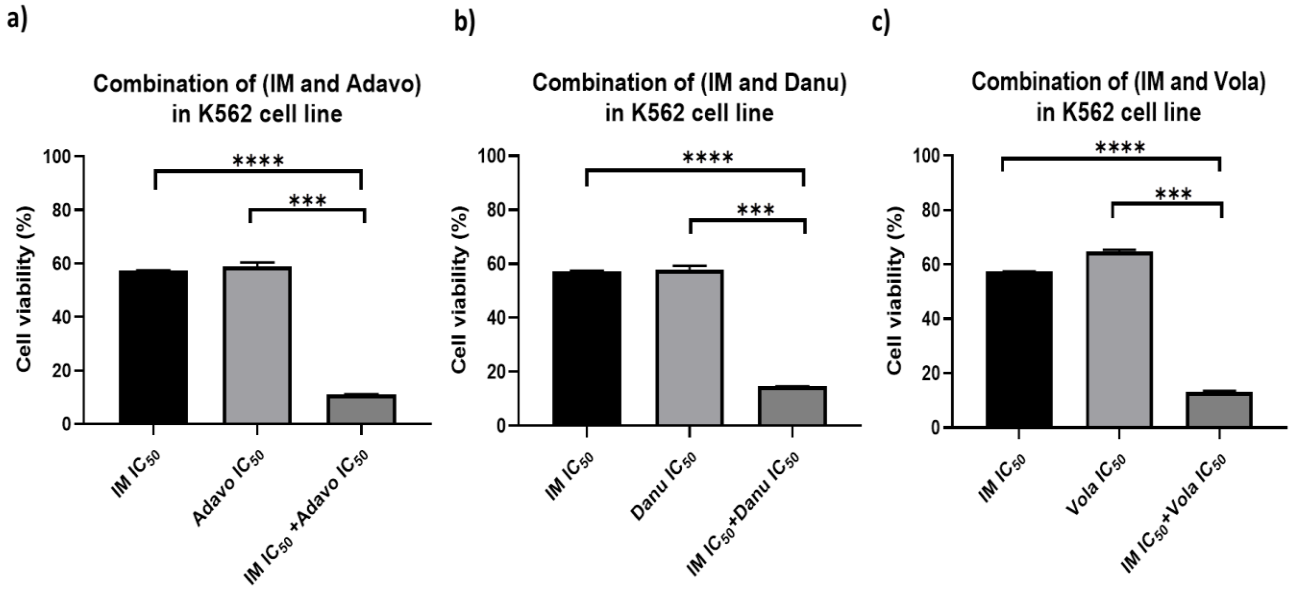

Figure 4.6 — Cell viability via MTS assay upon exposure of K562 cells to a combination of Imatinib (IM) with Adavosertib (Adavo), Danusertib (Danu) or Volasertib (Vola) for 48 h. (a) combination of IM with Adavo compared to the IC_{50} of IM or the IC_{50} of Adavo individually; (b) combination of IM + Danu compared to the IC_{50} of IM or the IC_{50} of Danu individually; (c) combination of IM + Vola compared to the IC_{50} of IM or the IC_{50} of Vola individually. Error bars represent the standard error of the mean of three independent experiments. **** $p<0.0001$, *** $p<0.001$ relative to respective control using Tukey's test statistical significance.

Overall, the combination of IM with any of the other kinase inhibitors led to the highest reduction in K562 cells (Figure 4.6). All of these combinations attained even a higher reduction compared to the combination Danu + Adavo (Figure 4.6 versus Figure 4.4a).

When evaluating the effect of combinatory challenge with TKIs and other kinase inhibitors, our data seem to point to a synergistic activity in IM-sensitive cell line. Combinations of IM with Danu, Vola, and Adavo show that the combinatory challenge strongly decreases the cell viability in the K562 cell line (Figure 4.6). A more pronounced reduction in cell viability is observed when combining IM with Danu (Figure 4.6a). These data reproduce similar observations previously reported on the combinatory effect of these drugs against CML cells. For instance, a previous study by *Balabanov* et al., [417] showed that exposure to Danu or IM

at nanomolar concentrations resulted in the inhibition of BCR-ABL1 activity. Also, simultaneous treatment with Danu and IM led to an increased rate of apoptosis in K562 cells when compared to the individual drugs [417]. A recent study by *Awad* et al., [418] screened 12 CML-LSPC samples (6 CP and 6 AP/BP) using a library of 18 IM-drug combinations that were selected based on DSRT screening of CML-LSPCs to identify synergistic TKI-drug combinations that effectively co-inhibit CML CD34+CD38 cells. The report highlights that one of the most promising IM+ drug combinations was with the kinase inhibitor Adavo, which showed a potent synergy (HSA synergy score >5) [418].

It should be noted that this study was only performed for K562 cell line and not for the K562-IM cell line due to their intrinsic resistance to IM. However, in the next section these combinations will be analysed in order to understand if these kinase inhibitors combined with Au-nanoconjugates could lead to a decrease in the IM resistance.

4.3.3 Combination of Au-nanoconjugates to silencing BCR-ABL1 and c-MYC with kinase inhibitors (Adavosertib, Danusertib, Volasertib and Imatinib)

The Au-nanoconjugates characterized for specific gene silencing described in Chapter 3 were then used in combination with these drugs, and the impact on cell viability and resistance profile was evaluated. For this, AuNP@PEG@e14a2 + AuNP@PEG@c-MYC were administered simultaneously in combination with IM (TKI) and or the other kinase inhibitors on sensitive and resistance cell lines, and cell viability was assessed via the MTS assay. Considering the previous results (chapter 3 and above), different time points were considered for the combinatory challenge: 48 h of incubation in the presence of IM or the other kinase inhibitors and 24 h of incubation for the Au-nanoconjugates (AuNP@PEG@e14a2 + AuNP@PEG@c-MYC simultaneously) (Figures 4.7 and 4.8).

The IM-sensitive K562 cell line was challenged simultaneously with the combination of (AuNP@PEG@e14a2 + AuNP@PEG@c-MYC) with the kinase inhibitors alone or combined (each of them at their relative IC_{50} values; Adavo + Danu, Adavo + Vola or Vola + Danu). For all the combinations of kinase inhibitors, the addition of the silencing Au-nanoconjugates does not induce a significant change to the observed viabilities of the drugs (alone or in combination) (Figure 4.7).

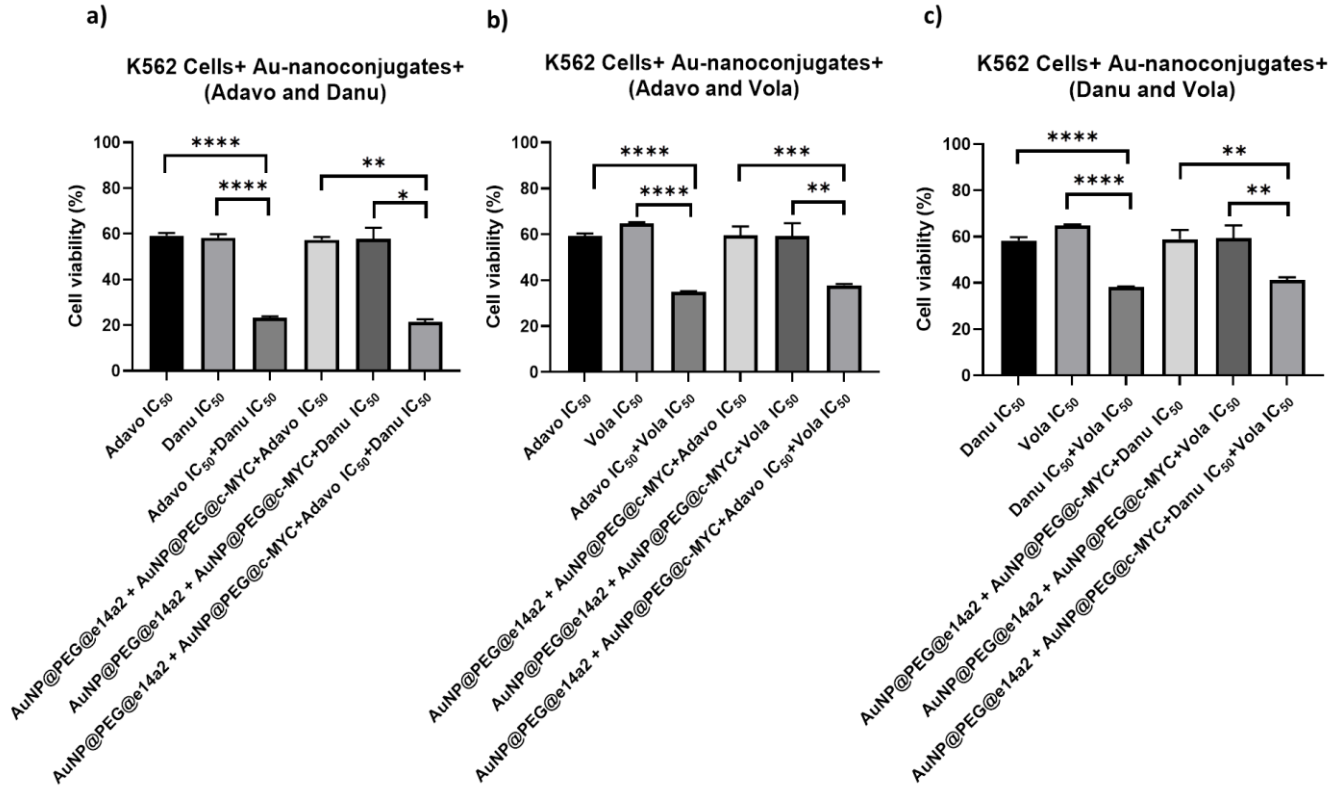

Figure 4.7 – Cell viability via MTS assay upon challenge K562 cells to a combination of Au-nanoconjugates for 24 h with the kinase inhibitors Adavosertib (Adavo), Danusertib (Danu) or Volasertib (Vola) individually or in combination for 48 h. (a) combination of AuNP@PEG@e14a2 + AuNP@PEG@c-MYC simultaneously with Adavo, Danu or Adavo + Danu. (b) combination of AuNP@PEG@e14a2 + AuNP@PEG@c-MYC simultaneously with Adavo, Vola or Adavo + Vola. (c) combination of AuNP@PEG@e14a2 + AuNP@PEG@c-MYC simultaneously with danu, Vola or Danu + Vola. Error bars represent the standard error of the mean of three independent experiments. **** $p<0.0001$, *** $p<0.001$, ** $p<0.01$, * $p<0.05$ relative to respective control using Tukey's test statistical significance.

Previously, when using IM in combination with any of the other kinase inhibitors, we observed a very strong effect in K562 cell viability (Figure 4.6). However, the combination of these kinase inhibitors with the gene silencing Au-nanoconjugates does not induce an additional loss of viability to cells (Figure 4.8 versus Figure 4.6).

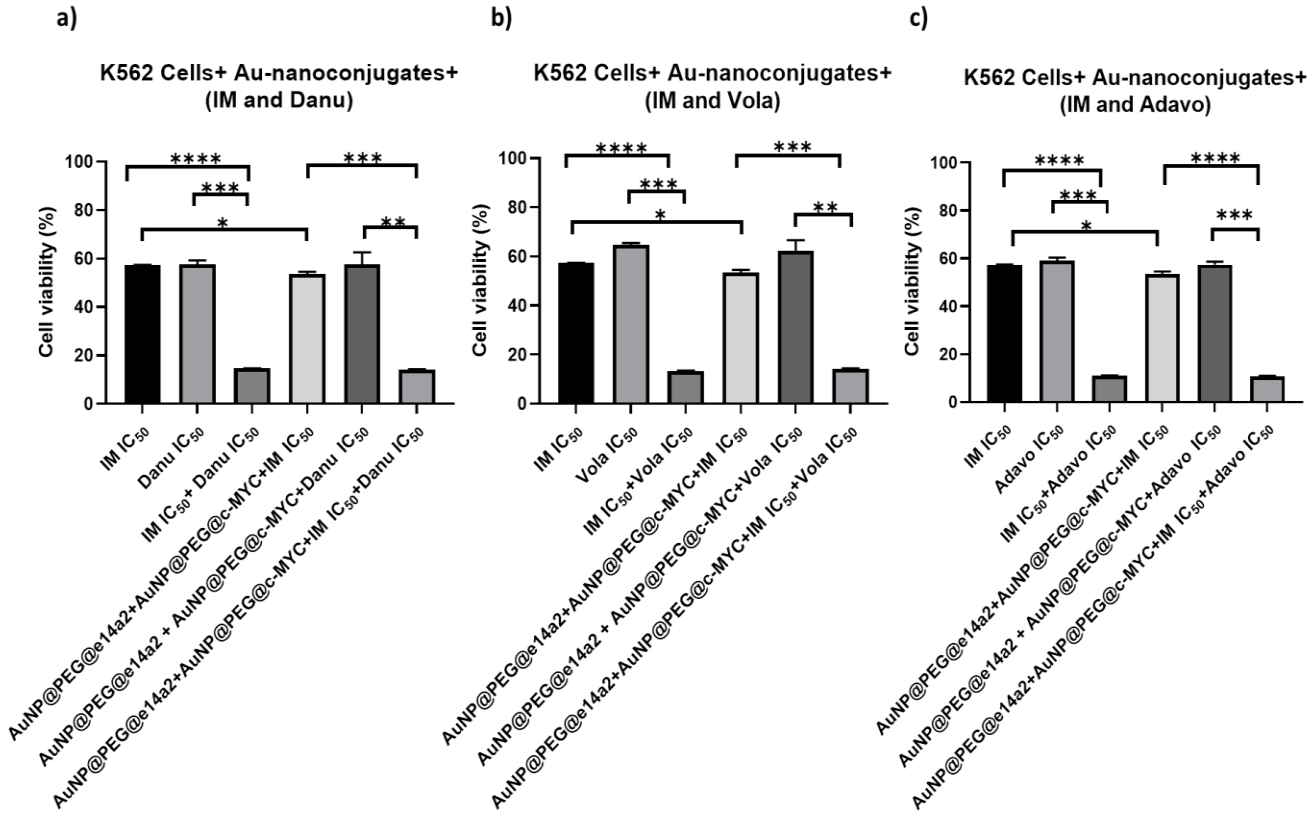

Figure 4.8 — Cell viability via MTS assay upon challenge K562 cells to a combination of Au-nanoconjugates for 24 h with Imatinib (IM), Adavosertib (Adavo), Danusertib (Danu) or Volasertib (Vola) individually or in combination for 48 h. (a) combination of AuNP@PEG@e14a2 + AuNP@PEG@c-MYC simultaneously with IM, Danu or IM + Danu. (b) combination of AuNP@PEG@e14a2 + AuNP@PEG@c-MYC simultaneously with IM, Vola or IM + Vola. (c) combination of AuNP@PEG@e14a2 + AuNP@PEG@c-MYC simultaneously with IM, Adavo or IM + Adavo. Error bars represent the standard error of the mean of three independent experiments. **** $p<0.0001$, *** $p<0.001$, ** $p<0.01$, * $p<0.05$ relative to respective control using Tukey's test statistical significance.

To understand the effect of using these combinations on the IM-resistance cell line, the same approach was then used in the K562-IM cell line (Figure 4.9). Interestingly, the addition of AuNP@PEG@e14a2 + AuNP@PEG@c-MYC simultaneously to the combined kinase inhibitors, (Danu + Vola), shows a statistically significant decrease in cell viability (cell viability of 45.95%) compared to the use of (Danu + Vola) alone (viability of 53.26 %) (Figure 4.9a).

Moreover, a statistically significant reduction in cell viability was also observed when the Au-nanoconjugates were conjugated with Vola alone at their respective IC_{50} (viability of 57.12 % versus 66.42 %) - Figure 4.9a. However, no statistically significant difference was observed for the combination of the Au-nanoconjugates with Danu alone (at IC_{50}), when compared to IC_{50} Danu alone (Figure 4.9a).

When Adavo+ Vola were used in combination with both Au-nanoconjugates, the results showed a statistically significant decrease in the cell viability (viability of 43.62 %) compared to the exposure to the kinase inhibitors alone (Adavo + Vola) (viability of 50.78 %). The combination of Au-nanoconjugates with the IC_{50} of Vola also reduced the cell viability compared to Vola alone (cell viability of 57.12% compared to 66.42 %). However, no statistically significant difference was found when the Au-nanoconjugates were combined with the IC_{50} of Adavo (cell viability of 50.18%) compared to the kinase inhibitor alone, Adavo (cell viability of 52.10%) (Figure 4.9b).

Finally, the combination of the Au-nanoconjugates with Adavo + Danu in K562-IM resulted in a statistically significant reduction of cell viability when compared to (IC_{50} Adavo + IC_{50} Danu) alone (viability of 26.45 % vs. 35.77 %) (Figure 4.9c). No significant reductions were observed for the combination of the Au-nanoconjugates with each kinase inhibitor alone (Figure 4.9c).

Take together, these last combination Au-nanoconjugates + the two kinase inhibitors, Adavo + Danu, show the strongest reduction in K562-IM cell viability (Figure 4.9c).

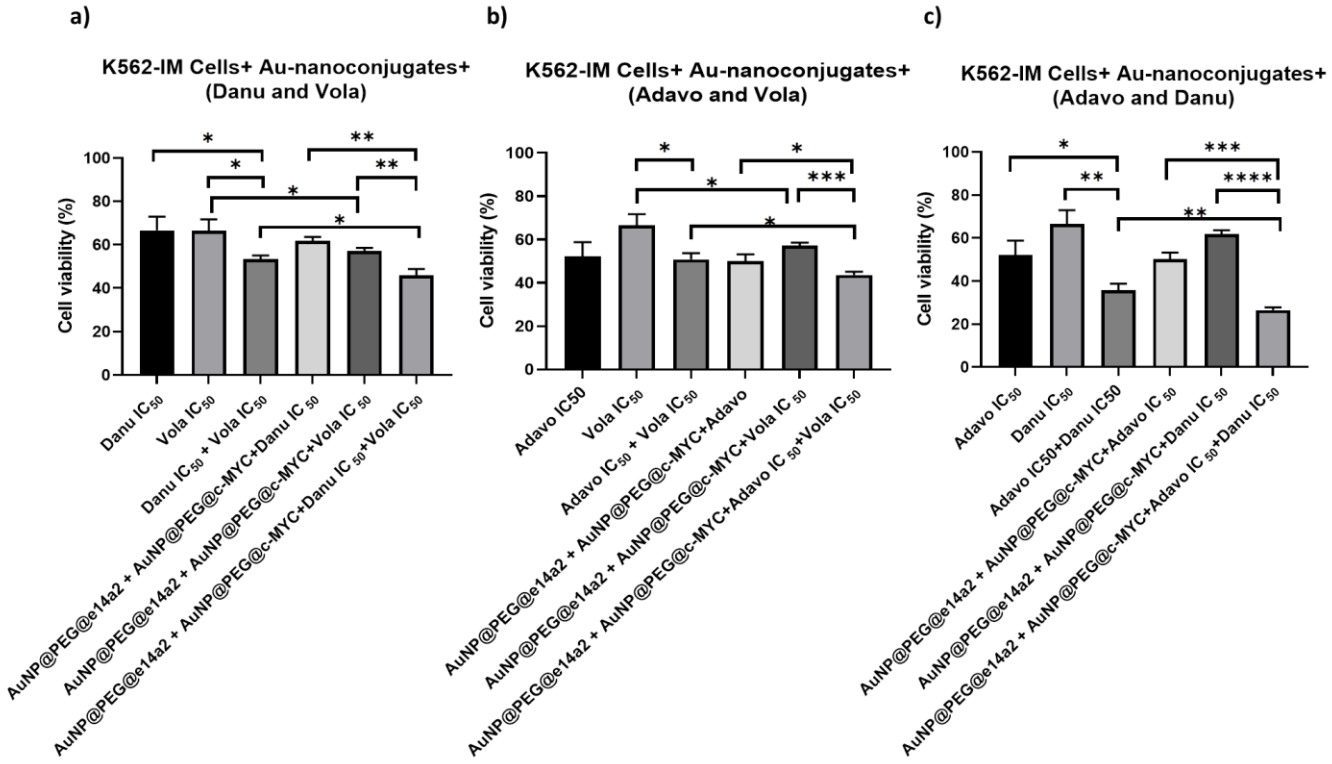

Figure 4.9 — Cell viability via MTS assay upon challenge K562-IM cell line to a combination of Au-nanoconjugates for 24 h with Adavosertib (Adavo), Danusertib (Danu) or Volasertib (Vola) individually or in combination for 48 h. (a) combination of AuNP@PEG@e14a2 + AuNP@PEG@c-MYC simultaneously with Danu, Adavo alone or with Danu + Vola. (b) combination of AuNP@PEG@e14a2 +

AuNP@PEG@c-MYC simultaneously with Adavo, Vola alone or with Adavo + Vola. (c) combination of AuNP@PEG@e14a2 + AuNP@PEG@c-MYC simultaneously with Adavo, Danu alone or with Adavo + Danu. Error bars represent the standard error of the mean of three independent experiments. **** $p<0.0001$, *** $p<0.001$, ** $p<0.01$, * $p<0.05$ relative to respective control using Tukey's test statistical significance

At the beginning of this Chapter, it was hypothesized that the combination of silencing Au-nanoconjugates with IM, Danu, Vola, and Adavo should induce an additive or synergistic effect against the CML cells. We show that combining AuNP@PEG@e14a2 + AuNP@PEG@c-MYC with IM increased the impact on CML cells when compared to IM alone (Figure 4.8). This is in line with the report by *Vinhas* et al. that demonstrated that combining AuNP@PEG@e14a2 alone with IM significantly enhances the effect of IM against cell proliferation in K562 cell line [318].

Herein, we have shown that silencing of a downstream effector (c-MYC) of BCR-ABL1 does not enhance the effect of IM, perhaps because the pathway has already been sufficiently downregulated by silencing of BCR-ABL1. On the other hand, combining AuNP@PEG@e14a2 + AuNP@PEG@c-MYC with Danu, Vola, and Adavo individually or in combination showed only a slight additive effect - Figure 4.7. The effect of the Au-nanoconjugate with Danu, Vola and Adavo on IM-resistant cell line was also analyzed and showed a synergistic effect – figure 4.9. The combination of AuNP@PEG@e14a2 + AuNP@PEG@c-MYC with Vola significantly decreases cell viability (Figure 4.9a). The highest impact on cell viability was attained via the combination of the Au-nanoconjugates with (Danu + Vola), (Adavo + Vola) and (Danu + Adavo).

4.4 Conclusion

Over the past two decades, targeted therapy against CML with TKIs such as (IM, nilotinib, dasatinib, bosutinib or ponatinib) has shown excellent results. Nonetheless, both BCR-ABL1-depenednt and -independent resistance, along with the survival of BCR-ABL1-independent LSCs, partially reduce the efficacy of TKIs. Consequently, a subset of CML patients evidently requires alternative therapeutic strategies [147]. As the understanding of CML biology expands, numerous alternatives have been investigated [408]. This may involve the utilization of a novel class of targeted BCR-ABL1 inhibitors that focus on the myristoyl pocket of BCR-ABL1, combination therapies with other established kinase inhibitors, or other pharmaceuticals with innovative targets pertinent to CML biology [408]. Nanotechnology-enabled drug

delivery systems facilitate the co-delivery or simultaneous administration of multiple therapeutic agents [401].

Combining gene silencing approaches to targeted drug and drug combinations could provide an additional tool against cancer cells. AuNPs have been shown to enable the effective transfection of gene-silencing moieties into cancer cells and effectively silence the target transcripts (see Chapter 3) [302].

Herein, we assessed the effect of combining Imatinib (TKI) and other kinase inhibitors (Danu, Vola, and Adavo), which were then further combined with the silencing Au-nanoconjugates in sensitive and IM-resistant K562 cell models.

When evaluating the effect of combinatory challenge with TKIs and other kinase inhibitors, our data seems to point to a synergistic activity in IM-sensitive CML cells.

Herein, we have shown that silencing of a downstream effector (c-MYC) of BCR-ABL1 does not enhance the effect of IM, perhaps because the pathway has already been sufficiently downregulated by silencing of BCR-ABL1. On the other hand, combining AuNP@PEG@e14a2 + AuNP@PEG@c-MYC with Danu, Vola, and Adavo individually or in combination showed only a slight additive effect in K562 cells. However, the effect of the Au-nanoconjugate with Danu, Vola, and Adavo on IM-resistant cells was also analyzed and showed a synergistic effect.

5

CONCLUSION AND FUTURE PERSPECTIVES

5.1 Conclusions

CML is a malignant myeloproliferative disease marked by the clonal expansion of hematopoietic stem cells. The Ph chromosome is the principal molecular hallmark of CML. This fusion results in the production of an oncoprotein known as BCR-ABL1, with constitutive tyrosine kinase activity. In the last twenty years, targeted therapy with TKIs such as IM, nilotinib, dasatinib, bosutinib, and ponatinib has shown significant outcomes. Nevertheless, the heterogeneity of the disease and development of resistance continues to pose considerable difficulty in the management of CML. Drug resistance by CML cells is one of the main reasons for therapeutic failure. Therefore, the developments of new therapeutic compounds or/and combined with other kinase inhibitors that can overcome this resistance are widely needed.

Nanomedicine has been pursued to address the shortcomings associated with cancer treatment using medications characterized by low specificity, fast clearance, biodegradation, and restricted targeting. Nanocarriers were suggested as a preferable alternative for targeted drug delivery to tumor tissue and controlled release of the prescribed medication. Cancer nanomedicine has been deeply focused on two main vectors: solutions for accurate molecular characterization of tumors and new approaches for improved chemotherapy. However, most of these advances are still in the pre-clinical stage of research and far from substituting or assisting traditional cancer management procedures. Moreover, the vast majority of these nanoformulations have been designed and directed at solid tumors, due to their well-studied

architecture, invasiveness and distinctive confined localization, in detriment of liquid tumors.

Molecular detection of *BCR-ABL1* transcription is essential for the diagnosis of CML, and its molecular quantification is crucial for evaluating treatment strategies and clinical interventions. Recent advancements in the treatment of CML via molecular monitoring have successfully lowered morbidity and mortality rates. Advanced molecular techniques are designed to detect *BCR-ABL1* transcript levels for monitoring molecular responses associated with these transcript levels. In the context of CML, point mutations in the *ABL1* gene pose a challenge for clinical guidelines, as various mutations contribute to resistance against TKIs, suggesting a potential need for modification in the treatment protocol.

Chapter 2 reports the screening of *BCR-ABL1* transcripts in samples from CML patients to identify *BCR-ABL1* KD mutations that might be associated to resistance to TKIs. Our nested-PCR results indicated that the majority of CML patients exhibit the e14a2 *BCR-ABL1* transcript (80%), whereas the remaining others exhibited the e1a2 *BCR-ABL1* transcript (20%). However, The Sanger sequencing results have not shown any associated mutations in regions (exons 4-7) or (exons 7-9) in *ABL*1 kinase domain of the patient samples. The results were subsequently applied to the k562 and k562-IM. Our findings indicate that both cell lines exhibit the e14a2 *BCR-ABL1* isoform and lack any mutations in the *ABL1* KD, however, k562-IM cell line exhibits a BCR-ABL1 independent mechanism due to the overexpression of *MDR1* in comparison to the k562 cell line. The objective was not to provide for a broad assessment of transcript and/or mutation profiles for patients, but rather to characterize the molecular starting point of the hypotheses put forward in the core of the Thesis, i.e. the relevance of the cell models used in the next chapters, their transcript signatures and the absence of mutations in the *ABL1 KD* in patients as well in both cell lines (sensitive and resistant to IM) that could be a target for gene silencing.

In chapter 3, we demonstrate the potential of AuNPs for vectorization of ASOs capable of silencing these target genes in sensitive and IM-resistant K562 cell models. We synthesized AuNPs and functionalized with ASOs targeting each individual mRNA in an IM-resistant K562 cell line model, to efficiently silence the e14a2 *BCR-ABL1, c-MYC* or both simultaneously. These Au-nanoconjugates were capable of efficiently silence both genes at the mRNA level that also led to a significant reduction of the respective protein levels in an IM-resistant cell line. These reductions at gene and protein levels induced cell cycle arrest and a decrease in the number of IM resistant cells. The simultaneous use of both nanoconjugates also led to a reduction in the levels of both proteins (BCR-ABL1 and c-MYC) that provided a slight reduction of the number of viable cells and an arrest of cell cycle both at 12 and 24 h. We hy-

pothesize that when both genes are reduced at the same time, cells may be less capable to respond to the insult, with a higher impact on cell death.

In the last part of this thesis, we assessed the effect of combining imatinib (TKI) and other kinase inhibitors (Danu, Vola, and Adavo), which were then further combined with the silencing Au-nanoconjugates in sensitive and IM-resistant K562 cell models (chapter 4). We show that combining Aura kinase inhibitor (Danu) with the polo kinase inhibitor (Vola) simultaneously significantly decreases the cell viability in K562 and K562-IM. Moreover, combining tyrosine kinase Wee1 inhibitor (Adavo) with Danu or Vola simultaneously leads to much lower cell viability compared to Adavo or Danu alone in both sensitive and IM-resistant cells. We then evaluating the effect of combinatory challenge with TKIs and other kinase inhibitors, our data seem to point to a synergistic activity in IM-sensitive CML cells. Combinations of IM with Danu, Vola, and Adavo show that the combinatory challenge strongly decreases the cell viability in the K562 cell line.

Moreover, we show that combining Au-nanoconjugates with IM increased the impact on CML cells when compared to IM alone. Moreover, the effect of the Au-nanoconjugate with Danu, Vola and Adavo on IM-resistant cells was also analyzed and showed a synergistic effect.

5.2 Future perspectives

In the beginning of this project, we defined 3 topics we wanted to explore to expand the knowledge in the fight against CML resistant cells. First, Identification of different *BCR-ABL1* fusion transcripts to identify target sequences and optimize the recognition of point-mismatches in *ABL1* domain associated to TKI resistance in CML clinical samples. Second, individual and combinational strategies for specific and selective gene silencing via Au-nanoconjugates to switch off *BCR-ABL1* and *c-MYC* which is responsible for drug resistance. Third, combining of Au-nanoconjugates with TKIs (IM) and other kinase inhibitors (Danu-Vola, and Adavo) targeting CML sensitive and resistance cell lines. Throughout the chapters we addressed these topics, answering some questions, and leaving some for further work.

By targeting *BCR-ABL1*, *c-MYC* and both simultaneously, our designed Au-nanoconjugates provided for an effective solution to overcome TKI resistance in CML. We demonstrate the potential of AuNPs for vectorization of ASOs capable of silencing these target genes in sensitive and IM-resistant K562 cell models. These Au-nanoconjugates were capable of efficiently silence both genes at the mRNA level that also led to a significant reduction of the respective protein levels in an imatinib resistant cell line – K562- IM. Overexpres-

sion of *MDR1*, the gene encoding for a drug efflux pump, has been identified as a mechanism of resistance to IM. Resistance to TKIs remains a significant hurdle in CML treatment. AuNPs could serve as an effective adjunct to overcome resistance by silencing genes involved in secondary mutations or alternative survival pathways. This approach could be extended to other resistance-related genes identified in future studies.

Still, it would be important to evaluate different combinations strategies (different time of addition of the Au-nanoconjugates to cells) or combining both silencing moieties in one nanoparticle (multifunctional nanoparticle). As explained before, due to the different properties of the nanoconjugates (size, charge, poly dispersion index) their internalization rate might vary, and one type may be internalized faster and/or more efficiently compared to the other, leading to different silencing efficacies at mRNA level (as we are targeting mRNA) compared to the protein levels (as observed in this study) [369–372]

AuNPs can be conjugated with seeral functionalizing moieties. For instance, functionalize AuNPs with monoclonal antibodies specific to CML-resistant cell surface markers (e.g., CD25, CD33, or CD44). This can enhance specificity by enabling targeted delivery to resistant CML cells. Furthermore, functionalize AuNPs with siRNAs or miRNAs targeting resistance-associated genes, such as *BCR-ABL1*, *c-MYC*, or other compensatory survival pathways. Addtionally, develop AuNPs as delivery vehicles for CRISPR-Cas9 components to specifically edit resistance-associated mutations in the *BCR-ABL1* gene or other oncogenes and target epigenetic regulators that contribute to drug resistance. AuNPs can also use for combining functionalization strategies to create multi-modal AuNPs capable of delivering ASOs, siRNA, TKIs, and immunomodulators simultaneously targeting different key players on CML pathogenesis: *BCR-ABL1*, *MDR1*, *c-MYC*, miRNAs.

Despite significant advances in targeted therapies, the emergence of resistance to TKIs like imatinib continues to challenge the long-term management of CML. This resistance is often due to point mutations in the *BCR-ABL1* gene, activation of alternative signaling pathways, or protective effects within the bone marrow microenvironment. The use of AuNPs in combination with imatinib and other kinase inhibitors represents a promising frontier in CML therapy, especially in overcoming drug resistance. Herein, we assessed the effect of combining IM (TKI) and other kinase inhibitors (Danu, Vola, and Adavo), which were then further combined with the silencing Au-nanoconjugates in sensitive and IM-resistant K562 cell models. We show that combining Au-nanoconjugates with IM increased the impact on CML cells when compared to IM alone. Moreover, the effect of the Au-nanoconjugate with Danu, Vola, and Adavo on IM-resistant cells was also analyzed and showed a synergistic effect.

Translation of these data to relevant in vivo model is still at large, mainly due to the cumbersome of developing suitable animal models of leukemia. In CML, usually spontaneously models are used whose molecular profiles need to be carefully ascertained to provide relevant information. Moreover, as described by *Kohnken* et al., [395], the liquid nature of these malignancies (spread all over the body) coupled to the complex microenvironment from which their arise and their multifaceted genetic basis has added to the difficulty in generating appropriate translational in vivo models to study CML, let alone models of TKI resistance.

REFERENCES

[1] Jibu RM, Veeraraghavan VP, Gayathri R, Kavitha S. Awareness on hematological malignancies among college students. J Adv Pharm Technol Res. 2022;13:S534-S538. doi:10.4103/japtr.japtr_175_22.

[2] Abdulmawjood B, Roma-Rodrigues C, Fernandes AR, Baptista PV. Liquid biopsies in myeloid malignancies. Cancer Drug Resist. 2019;2(4):1044-1061. doi:10.20517/cdr.2019.88.

[3] Hu D, Shilatifard A. Epigenetics of hematopoiesis and hematological malignancies. Genes Dev. 2016;30(18):2021-2041. doi:10.1101/gad.284109.116.

[4] Karunarathna I, De Alvis K, Gunasena P, Jayawardana A. Leukemia: Classification, risk factors, and diagnostic challenges. 2024.

[5] Arber DA, Orazi A, Hasserjian RP, et al. International Consensus Classification of Myeloid Neoplasms and Acute Leukemias: integrating morphologic, clinical, and genomic data. Blood. 2022;140(11):1200-1228. doi.org/10.1182/blood.2022015850.

[6] Chennamadhavuni A, Lyengar V, Mukkamalla SKR, Shimanovsky A. Leukemia. In: StatPearls. Treasure Island (FL): StatPearls Publishing; January 17, 2023.

[7] Rafiq S, Raza MH, Younas M, et al. Molecular Targets of Curcumin and Future Therapeutic Role in Leukemia. Journal of Biosciences and Medicines. 2018;06(04):33-50. doi.org/10.4236/jbm.2018.64003.

[8] Kantarjian HM, Kadia TM, DiNardo CD, Welch MA, Ravandi F. Acute myeloid leukemia: Treatment and research outlook for 2021 and the MD Anderson approach. Cancer. 2021;127(8):1186-1207. doi.org/10.1002/cncr.33477.

[9] Ekpa QL, Akahara PC, Anderson AM, et al. A Review of Acute Lymphocytic Leukemia (ALL) in the Pediatric Population: Evaluating Current Trends and Changes in Guidelines in the Past Decade. Cureus. 2023;15(12): e49930. doi:10.7759/cureus.49930.

[10] Patel K, Pagel JM. Current and future treatment strategies in chronic lymphocytic leukemia. Journal of Hematology & Oncology. 2021;14(1). doi.org/10.1186/s13045-021-01054-w.

[11] Lejman M, Chałupnik A, Chilimoniuk Z, Dobosz M. Genetic Biomarkers and Their Clinical Implications in B-Cell Acute Lymphoblastic Leukemia in Children. International Journal of Molecular Sciences. 2022;23(5):2755. doi.org/10.3390/ijms23052755.

[12] Blanco-Lopez J, Iguacel I, Pisanu S, et al. Role of Maternal Diet in the Risk of Childhood Acute Leukemia: A Systematic Review and Meta-Analysis. International Journal of Environmental Research and Public Health. 2023;20(7):5428. doi.org/10.3390/ijerph20075428.

[13] Hallek M, Al-Sawaf O. Chronic lymphocytic leukemia: 2022 update on diagnostic and therapeutic procedures. American Journal of Hematology. 2021;96(12):1679-1705. doi.org/10.1002/ajh.26367.

[14] Padmakumar D, Chandraprabha VR, Gopinath P, et al. A concise review on the molecular genetics of acute myeloid leukemia. Leukemia Research. 2021;111:106727. doi.org/10.1016/j.leukres.2021.106727.

[15] Gröschel S, Schlenk RF, Engelmann J, et al. Deregulated Expression of EVI1 Defines a Poor Prognostic Subset of MLL-Rearranged Acute Myeloid Leukemias: A Study of the German-Austrian Acute Myeloid Leukemia Study Group and the Dutch-Belgian-Swiss HOVON/SAKK Cooperative Group. Journal of Clinical Oncology. 2013;31(1):95-103. doi.org/10.1200/jco.2011.41.5505.

[16] Abdulmawjood B, Costa B, Roma-Rodrigues C, Baptista PV, Fernandes AR. Genetic Biomarkers in Chronic Myeloid Leukemia: What Have We Learned So Far?. International Journal of Molecular Sciences. 2021;22(22):12516. doi.org/10.3390/ijms222212516.

[17] Sampaio MM, Santos MLC, Marques HS, et al. Chronic myeloid leukemia-from the Philadelphia chromosome to specific target drugs: A literature review. World Journal of Clinical Oncology. 2021;12(2):69-94. doi.org/10.5306/wjco.v12.i2.69.

[18] Gonon-Demoulian R, Goldman JM, Nicolini FE. Historique de la leucémie myéloïde chronique : un paradigme de traitement du cancer. Bulletin du Cancer. 2015;101(1):56-67. doi.org/10.1684/bdc.2013.1876.

[19] Goldman JM. Chronic Myeloid Leukemia: A Historical Perspective. Seminars in Hematology. 2010;47(4):302-311. doi.org/10.1053/j.seminhematol.2010.07.001.

[20] Nowell C. The minute chromosome (Ph1) in chronic granulocytic leukemia. Blut Zeitschrift für die Gesamte Blutforschung. 1962;8(2):65-66. doi.org/10.1007/bf01630378.

[21] Minciacchi VR, Kumar R, Krause DS. Chronic Myeloid Leukemia: A Model Disease of the Past, Present and Future. Cells. 2021;10(1):117. doi.org/10.3390/cells10010117.

[22] Rowley JD. A New Consistent Chromosomal Abnormality in Chronic Myelogenous Leukaemia identified by Quinacrine Fluorescence and Giemsa Staining. Nature. 1973;243(5405):290-293. doi.org/10.1038/243290a0.

[23] Shah NP, Bhatia R, Altman JK, et al. Chronic Myeloid Leukemia, Version 2.2024, NCCN Clinical Practice Guidelines in Oncology. Journal of The National Comprehensive Cancer Network. 2024;22(1):43-69. doi.org/10.6004/jnccn.2024.0007.

[24] Daskalakis M, Feller A, Noetzli J, Bonadies N, Arndt V, Baerlocher GM. Potential to Improve Therapy of Chronic Myeloid Leukemia (CML), Especially for Patients with Older Age: Incidence, Mortality, and Survival Rates of Patients with CML in Switzerland from 1995 to 2017. Cancers. 2021;13(24):6269. doi.org/10.3390/cancers13246269.

[25] Anwer AA, Khaleel KJ, Abbas FA, Laftaah Al-Rubaii BA. Chronic Myeloid Leukemia: A retrospective study of clinical and pathological features. Bionatura. 2022;7(3):1-3. doi.org/10.21931/rb/2022.07.03.41.

[26] Kabat GC, Wu JW, Moore SC, et al. Lifestyle and Dietary Factors in Relation to Risk of Chronic Myeloid Leukemia in the NIH-AARP Diet and Health Study. Cancer Epidemiology Biomarkers & Prevention. 2013;22(5):848-854. doi.org/10.1158/1055-9965.epi-13-0093.

[27] Van Maele-Fabry G, Duhayon S, Lison D. A systematic review of myeloid leukemias and occupational pesticide exposure. Cancer Causes & Control. 2007;18(5):457-478. doi.org/10.1007/s10552-007-0122-2.

[28]Apperley JF. Chronic myeloid leukaemia. Lancet (London, England). 2015;385(9976):1447-1459. doi.org/10.1016/S0140-6736(13)62120-0.

[29] Jabbour E, Kantarjian H. Chronic myeloid leukemia: 2020 update on diagnosis, therapy and monitoring. American Journal of Hematology. 2020;95(6). doi.org/10.1002/ajh.25792.

[30] Cross NCP, Ernst T, Branford S, et al. European LeukemiaNet laboratory recommendations for the diagnosis and management of chronic myeloid leukemia. Leukemia. 2023;37(11):2150-2167. doi.org/10.1038/s41375-023-02048-y.

[31] Groffen J, Stephenson J, Heisterkamp N, Deklein A, Bartram C, Grosveld G. Philadelphia chromosomal breakpoints are clustered within a limited region, bcr, on chromosome 22. Cell. 1984;36(1):93-99. doi.org/10.1016/0092-8674(84)90077-1.

[32] Marzocchi G, Castagnetti F, Luatti S, Baldazzi C, Stacchini M, Gugliotta G, Amabile M, Specchia G, Sessarego M, Giussani U, et al. Variant Philadelphia translocations: Molecular-cytogenetic characterization and prognostic influence on frontline imatinib therapy, a GIMEMA working party on CML analysis. Blood. 2011;117:6793–6800. doi: 10.1182/blood-2011-01-328294.

[33] Huret JL. Complex translocations, simple variant translocations and Ph-negative cases in chronic myelogenous leukaemia. Hum. Genet. 1990;85:565–568. doi: 10.1007/BF00193575.

[34] Koshiyama DB, Capra ME, Paskulin GA, et al. Cytogenetic response to imatinib treatment in Southern Brazilian patients with chronic myelogenous leukemia and variant Philadelphia chromosome. Ann Hematol. 2013;92(2):185-189. doi:10.1007/s00277-012-1598-8.

[35] El-Zimaity MM, Kantarjian H, Talpaz M, et al. Results of imatinib mesylate therapy in chronic myelogenous leukaemia with variant Philadelphia chromosome. Br J Haematol. 2004;125(2):187-195. doi:10.1111/j.1365-2141.2004.04899.x.

[36] Valencia A, Cervera J, Such E, et al. Complex Variant t(9;22) Chromosome Translocations in Five Cases of Chronic Myeloid Leukemia. Adv Hematol. 2009;2009:187125. doi:10.1155/2009/187125.

[37] Fabarius A, Leitner A, Hochhaus A, et al. Impact of additional cytogenetic aberrations at diagnosis on prognosis of CML: long-term observation of 1151 patients from the randomized CML Study IV. Blood. 2011;118(26):6760-6768. doi:10.1182/blood-2011-08-373902.

[38] Hsiao HH, Liu YC, Tsai HJ, et al. Additional chromosome abnormalities in chronic myeloid leukemia. Kaohsiung J Med Sci. 2011;27(2):49-54. doi:10.1016/j.kjms.2010.09.001.

[39] Stagno F, Vigneri P, Del Fabro V, et al. Influence of complex variant chromosomal translocations in chronic myeloid leukemia patients treated with tyrosine kinase inhibitors. Acta Oncol. 2010;49(4):506-508. doi:10.3109/02841861003660031.

[40] Gorusu M, Benn P, Li Z, Fang M. On the genesis and prognosis of variant translocations in chronic myeloid leukemia. Cancer Genet Cytogenet. 2007;173(2):97-106. doi:10.1016/j.cancergencyto.2006.10.006.

[41] Lee SE, Choi SY, Bang JH, et al. The long-term clinical implications of clonal chromosomal abnormalities in newly diagnosed chronic phase chronic myeloid leukemia patients treated with imatinib mesylate. Cancer Genetics. 2012;205(11):563-571. doi:https://doi.org/10.1016/j.cancergen.2012.09.003.

[42] Vinhas R, Lourenço A, Santos S, et al. A double Philadelphia chromosome-positive chronic myeloid leukemia patient, co-expressing P210BCR-ABL1 and P195BCR-ABL1 isoforms. Haematologica. 2018;103(11):e549-e552. doi:10.3324/haematol.2018.192534.

[43] Arana-Trejo RM, Ruíz Sánchez E, Ignacio-Ibarra G, et al. BCR/ABL p210, p190 and p230 fusion genes in 250 Mexican patients with chronic myeloid leukaemia (CML). Clin Lab Haematol. 2002;24(3):145-150. doi:10.1046/j.1365-2257.2002.00413.x.

[44] Clarke CJ, Holyoake TL. Preclinical approaches in chronic myeloid leukemia: from cells to systems. Exp Hematol. 2017;47:13-23. doi:10.1016/j.exphem.2016.11.005.

[45] Skorski T. BCR/ABL, DNA damage and DNA repair: Implications for new treatment concepts. Leukemia & Lymphoma. 2008;49(4):610-614. doi.org/10.1080/03093640701859089.

[46] Giustacchini A, Thongjuea S, Barkas N, et al. Single-cell transcriptomics uncovers distinct molecular signatures of stem cells in chronic myeloid leukemia. Nat Med. 2017;23(6):692-702. doi:10.1038/nm.4336.

[47] Lakkireddy S, Aula S, Kapley A, et al. Association of Vascular Endothelial Growth Factor A (VEGFA) and its Receptor (VEGFR2) Gene Polymorphisms with Risk of Chronic Myeloid Leukemia and Influence on Clinical Outcome. Mol Diagn Ther. 2016;20(1):33-44. doi:10.1007/s40291-015-0173-0.

[48] Deregowska A, Pepek M, Pruszczyk K, Machnicki MM, Wnuk M, Stoklosa T. Differential Regulation of Telomeric Complex by BCR-ABL1 Kinase in Human Cellular Models of

Chronic Myeloid Leukemia-From Single Cell Analysis to Next-Generation Sequencing. Genes (Basel). 2020;11(10):1145. doi:10.3390/genes11101145.

[49] Zheng Y, Wang YP, Cao H, Chen Q, Zhang X. Integrated computational biology analysis to evaluate target genes for chronic myelogenous leukemia. Mol Med Rep. 2018;18(2):1766-1772. doi:10.3892/mmr.2018.9125.

[50] Bergamaschi G, Merante S, Orlandi E, Galli A, Bernasconi P, Cazzola M. TP53 codon 72 polymorphism in patients with chronic myeloid leukemia. Haematologica. 2004;89(7):868-869.

[51] Camelo-Santos J, do Prado Barbosa A, de Paula Silveira-Lacerda E, Guillo LA. Arginine homozygosity in codon 72 of p53 correlates with failure to imatinib response in chronic myeloid leukemia. Biomed Pharmacother. 2013;67(2):103-107. doi:10.1016/j.biopha.2012.11.004.

[52] Weich N, Ferri C, Moiraghi B, et al. TP53 codon 72 polymorphism predicts chronic myeloid leukemia susceptibility and treatment outcome. Blood Cells Mol Dis. 2016;59:129-133. doi:10.1016/j.bcmd.2016.05.007.

[53] Koschmieder S, Vetrie D. Epigenetic dysregulation in chronic myeloid leukaemia: A myriad of mechanisms and therapeutic options. Semin Cancer Biol. 2018;51:180-197. doi:10.1016/j.semcancer.2017.07.006.

[54] Machova Polakova K, Koblihova J, Stopka T. Role of epigenetics in chronic myeloid leukemia. Curr Hematol Malig Rep. 2013;8(1):28-36. doi:10.1007/s11899-012-0152-z.

[55] Amir M, Javed S. A Review on the Therapeutic Role of TKIs in Case of CML in Combination With Epigenetic Drugs. Front Genet. 2021;12:742802. doi:10.3389/fgene.2021.742802.

[56] Popp HD, Kohl V, Naumann N, et al. DNA Damage and DNA Damage Response in Chronic Myeloid Leukemia. Int J Mol Sci. 2020;21(4):1177. doi:10.3390/ijms21041177.

[57] Jamieson CH, Weissman IL, Passegué E. Chronic versus acute myelogenous leukemia: a question of self-renewal. Cancer Cell. 2004;6(6):531-533. doi:10.1016/j.ccr.2004.12.005.

[58] Ohyashiki K, Iwama H, Tauchi T, et al. Telomere dynamics and genetic instability in disease progression of chronic myeloid leukemia. Leuk Lymphoma. 2000;40(1-2):49-56. doi:10.3109/10428190009054880.

[59] Loscocco F, Visani G, Galimberti S, Curti A, Isidori A. BCR-ABL Independent Mechanisms of Resistance in Chronic Myeloid Leukemia. Front Oncol. 2019;9:939. doi:10.3389/fonc.2019.00939.

[60] Saikia T. The Cure of Chronic Myeloid Leukemia: Are We There Yet?. Curr Oncol Rep. 2018;20(2):12. Published 2018 Feb 28. doi:10.1007/s11912-018-0665-2.

[61] Skorski T. Chronic myeloid leukemia cells refractory/resistant to tyrosine kinase inhibitors are genetically unstable and may cause relapse and malignant progression to the terminal disease state. Leuk Lymphoma. 2011;52 Suppl 1(0 1):23-29. doi:10.3109/10428194.2010.546912.

[62] Pawlowska E, Blasiak J. DNA Repair--A Double-Edged Sword in the Genomic Stability of Cancer Cells--The Case of Chronic Myeloid Leukemia. Int J Mol Sci. 2015;16(11):27535-27549. doi:10.3390/ijms161126049.

[63] Nieborowska-Skorska M, Kopinski PK, Ray R, et al. Rac2-MRC-cIII-generated ROS cause genomic instability in chronic myeloid leukemia stem cells and primitive progenitors. Blood. 2012;119(18):4253-4263. doi:10.1182/blood-2011-10-385658.

[64] Nowicki MO, Falinski R, Koptyra M, et al. BCR/ABL oncogenic kinase promotes unfaithful repair of the reactive oxygen species-dependent DNA double-strand breaks. Blood. 2004;104(12):3746-3753. doi:10.1182/blood-2004-05-1941.

[65] Koptyra M, Falinski R, Nowicki MO, et al. BCR/ABL kinase induces self-mutagenesis via reactive oxygen species to encode imatinib resistance. Blood. 2006;108(1):319-327. doi:10.1182/blood-2005-07-2815.

[66] Raynaud CM, Sabatier L, Philipot O, Olaussen KA, Soria JC. Telomere length, telomeric proteins and genomic instability during the multistep carcinogenic process. Crit Rev Oncol Hematol. 2008;66(2):99-117. doi:10.1016/j.critrevonc.2007.11.006.

[67] Samassekou O, Hébert J, Mai S, Yan J. Nuclear remodeling of telomeres in chronic myeloid leukemia. Genes Chromosomes Cancer. 2013;52(5):495-502. doi:10.1002/gcc.22046.

[68] Bennour A, Saad A, Sennana H. Chronic myeloid leukemia: Relevance of cytogenetic and molecular assays. Crit Rev Oncol Hematol. 2016;97:263-274. doi:10.1016/j.critrevonc.2015.08.020.

[69] Cannella L, Loglisci G, Nanni M, et al. Trisomy 8 in Philadelphia chromosome negative cell preceding the evolution of a Philadelphia chromosome positive clone with the same additional change during imatinib treatment: revisiting the role of genetic instability in chronic myeloid leukemia. Leuk Lymphoma. 2012;53(3):497-498. doi:10.3109/10428194.2011.615425.

[70] Ochi Y. Genetic landscape of chronic myeloid leukemia. Int J Hematol. 2023;117(1):30-36. doi:10.1007/s12185-022-03510-w.

[71] Alkhatabi H, Aldahlawi S, Hazzazi MS, et al. Gene expression profiling on CML patients with Philadelphia translocation. Eur Rev Med Pharmacol Sci. 2024;28(4):1340-1355. doi:10.26355/eurrev_202402_35455.

[72] Villuendas R, Steegmann JL, Pollán M, et al. Identification of genes involved in imatinib resistance in CML: a gene-expression profiling approach. Leukemia. 2006;20(6):1047-1054. doi:10.1038/sj.leu.2404197.

[73] Deregowska A, Pepek M, Pruszczyk K, Machnicki MM, Wnuk M, Stoklosa T. Differential Regulation of Telomeric Complex by BCR-ABL1 Kinase in Human Cellular Models of Chronic Myeloid Leukemia-From Single Cell Analysis to Next-Generation Sequencing. Genes (Basel). 2020;11(10):1145. doi:10.3390/genes11101145.

[74] Sankar M, Tanaka K, Kumaravel TS, et al. Identification of a commonly deleted region at 17p13.3 in leukemia and lymphoma associated with 17p abnormality. Leukemia. 1998;12(4):510-516. doi:10.1038/sj.leu.2400973.

[75] Peller S, Yona R, Kopilova Y, et al. Molecular alterations in the TP53 gene of peripheral blood cells of patients with chronic myeloid leukemia. Genes Chromosomes Cancer. 1998;21(1):2-7. doi:10.1002/(sici)1098-2264(199801)21:1<2::aid-gcc2>3.0.co;2-5.

[76] Elkhouly EA, Khalifa KA, Radwan WM, Younis YA. 17PTumor suppressor P53 gene codon 72 polymorphism and imatinib cytogenetic response in chronic myeloid leukemia. Ann. Oncol. 2018; 29: vi6.

[77] Kokate P, Dalvi R, Mandava S. A complex three-way translocation with deletion of the TP53 gene in a blast crisis chronic myeloid leukemia patient. J Cancer Res Ther. 2015;11(4):1037. doi:10.4103/0973-1482.144372.

[78] Sill H, Goldman JM, Cross NC. Homozygous deletions of the p16 tumor-suppressor gene are associated with lymphoid transformation of chronic myeloid leukemia. Blood. 1995;85(8):2013-2016.

[79] Dierov J, Dierova R, Carroll M. BCR/ABL translocates to the nucleus and disrupts an ATR-dependent intra-S phase checkpoint. Cancer Cell. 2004;5(3):275-285. doi:10.1016/s1535-6108(04)00056-x.

[80] Rumpold H, Webersinke G. Molecular pathogenesis of Philadelphia-positive chronic myeloid leukemia - is it all BCR-ABL?. Curr Cancer Drug Targets. 2011;11(1):3-19. doi:10.2174/156800911793743619.

[81] Tobin LA, Robert C, Rapoport AP, et al. Targeting abnormal DNA double-strand break repair in tyrosine kinase inhibitor-resistant chronic myeloid leukemias. Oncogene. 2013;32(14):1784-1793. doi:10.1038/onc.2012.203.

[82] Sallmyr A, Fan J, Rassool FV. Genomic instability in myeloid malignancies: increased reactive oxygen species (ROS), DNA double strand breaks (DSBs) and error-prone repair. Cancer Lett. 2008;270(1):1-9. doi:10.1016/j.canlet.2008.03.036.

[83] Dinis J, Silva V, Gromicho M, et al. DNA damage response in imatinib resistant chronic myeloid leukemia K562 cells. Leuk Lymphoma. 2012;53(10):2004-2014. doi:10.3109/10428194.2012.681654.

[84] Tipping AJ, Deininger MW, Goldman JM, Melo JV. Comparative gene expression profile of chronic myeloid leukemia cells innately resistant to imatinib mesylate. Exp Hematol. 2003;31(11):1073-1080.

[85] Alves R, Gonçalves AC, Rutella S, et al. Resistance to Tyrosine Kinase Inhibitors in Chronic Myeloid Leukemia-From Molecular Mechanisms to Clinical Relevance. Cancers (Basel). 2021;13(19):4820. doi:10.3390/cancers13194820.

[86] Yaghmaie M, Yeung CC. Molecular Mechanisms of Resistance to Tyrosine Kinase Inhibitors. Curr Hematol Malig Rep. 2019;14(5):395-404. doi:10.1007/s11899-019-00543-7.

[87] Zhang LQ, Fan GL, Liu JJ, Liu L, Li QZ, Lin H. Identification of Key Histone Modifications and Their Regulatory Regions on Gene Expression Level Changes in Chronic Myelogenous Leukemia. Front Cell Dev Biol. 2021;8:621578. Published 2021 Jan 12. doi:10.3389/fcell.2020.621578.

[88] Zhang LQ, Li QZ. Estimating the effects of transcription factors binding and histone modifications on gene expression levels in human cells. Oncotarget. 2017;8(25):40090-40103. doi:10.18632/oncotarget.16988.

[89] Zhang X, Yang L, Liu X, et al. Research on the epigenetic regulation mechanism of the PTPN6 gene in advanced chronic myeloid leukaemia. Br J Haematol. 2017;178(5):728-738. doi:10.1111/bjh.14739.

[90] Zhang LQ, Li QZ, Jin W, Zuo Y, Guo SC. Genome-wide analysis of H3K36me3 and its regulations to cancer-related genes expression in human cell lines. Biosystems. 2018;171:59-65. doi:10.1016/j.biosystems.2018.07.004.

[91] Ma J, Wang JD, Zhang WJ, et al. Promoter hypermethylation and histone hypoacetylation contribute to pancreatic-duodenal homeobox 1 silencing in gastric cancer. Carcinogenesis. 2010;31(9):1552-1560. doi:10.1093/carcin/bgq140.

[92] Nimmanapalli R, Fuino L, Stobaugh C, Richon V, Bhalla K. Cotreatment with the histone deacetylase inhibitor suberoylanilide hydroxamic acid (SAHA) enhances imatinib-induced apoptosis of Bcr-Abl-positive human acute leukemia cells. Blood. 2003;101(8):3236-3239. doi:10.1182/blood-2002-08-2675.

[93] Schemionek M, Herrmann O, Reher MM, et al. Mtss1 is a critical epigenetically regulated tumor suppressor in CML. Leukemia. 2016;30(4):823-832. doi:10.1038/leu.2015.329.

[94] Bonifer C, Cockerill PN. Chromatin mechanisms regulating gene expression in health and disease. Adv Exp Med Biol. 2011;711:12-25. doi:10.1007/978-1-4419-8216-2_2.

[95] Chen WY, Wang DH, Yen RC, Luo J, Gu W, Baylin SB. Tumor suppressor HIC1 directly regulates SIRT1 to modulate p53-dependent DNA-damage responses. Cell. 2005;123(3):437-448. doi:10.1016/j.cell.2005.08.011

[96] Issa JP, Zehnbauer BA, Kaufmann SH, Biel MA, Baylin SB. HIC1 hypermethylation is a late event in hematopoietic neoplasms. Cancer Res. 1997;57(9):1678-1681.

[97] Riether C, Schürch CM, Flury C, et al. Tyrosine kinase inhibitor-induced CD70 expression mediates drug resistance in leukemia stem cells by activating Wnt signaling. Sci Transl Med. 2015;7(298):298ra119. doi:10.1126/scitranslmed.aab1740.

[98] Wang FY, Gu ZY, Gao CJ. Emerging role of long non-coding RNAs in normal and malignant hematopoiesis. Chin Med J (Engl). 2020;133(4):462-473. doi:10.1097/CM9.0000000000000624.

[99] Wang X, Chen K, Guo G, Chen JL. Noncoding RNAs and their functional involvement in regulation of chronic myeloid leukemia. Brief Funct Genomics. 2016;15(3):239-248. doi:10.1093/bfgp/elv059.

[100] Mercer TR, Dinger ME, Mattick JS. Long non-coding RNAs: insights into functions. Nat Rev Genet. 2009;10(3):155-159. doi:10.1038/nrg2521.

[101] Wilusz JE, Sunwoo H, Spector DL. Long noncoding RNAs: functional surprises from the RNA world. Genes Dev. 2009;23(13):1494-1504. doi:10.1101/gad.1800909.

[102] Bonasio R, Shiekhattar R. Regulation of transcription by long noncoding RNAs. Annu Rev Genet. 2014;48:433-455. doi:10.1146/annurev-genet-120213-092323.

[103] Yang Y, Cai Y, Wu G, et al. Plasma long non-coding RNA, CoroMarker, a novel biomarker for diagnosis of coronary artery disease. Clin Sci (Lond). 2015;129(8):675-685. doi:10.1042/CS20150121.

[104] Rinn JL, Chang HY. Genome regulation by long noncoding RNAs. Annu Rev Biochem. 2012;81:145-166. doi:10.1146/annurev-biochem-051410-092902.

[105] Wapinski O, Chang HY. Long noncoding RNAs and human disease. Trends Cell Biol. 2011;21(6):354-361. doi:10.1016/j.tcb.2011.04.001.

[106] Martens-Uzunova ES, Böttcher R, Croce CM, Jenster G, Visakorpi T, Calin GA. Long noncoding RNA in prostate, bladder, and kidney cancer. Eur Urol. 2014;65(6):1140-1151. doi:10.1016/j.eururo.2013.12.003.

[107] Takahashi K, Yan I, Haga H, Patel T. Long noncoding RNA in liver diseases. Hepatology. 2014;60(2):744-753. doi:10.1002/hep.27043.

[108] Spizzo R, Almeida MI, Colombatti A, Calin GA. Long non-coding RNAs and cancer: a new frontier of translational research?. Oncogene. 2012;31(43):4577-4587. doi:10.1038/onc.2011.621.

[109] Martelli AM, Evangelisti C, Chappell W, et al. Targeting the translational apparatus to improve leukemia therapy: roles of the PI3K/PTEN/Akt/mTOR pathway. Leukemia. 2011;25(7):1064-1079. doi:10.1038/leu.2011.46.

[110] Guo G, Kang Q, Zhu X, et al. A long noncoding RNA critically regulates Bcr-Abl-mediated cellular transformation by acting as a competitive endogenous RNA. Oncogene. 2015;34(14):1768-1779. doi:10.1038/onc.2014.131.

[111] Dutta S, Akhade VS, Choudhury SR, Roa MRS. Long non-coding RNAs: emerging functional players in the pathobiology and progression of myeloid leukemia. Frontiers in RNA Research. 2024;2. doi.org/10.3389/frnar.2024.1334464.

[112] Rudich A, Garzon R, Dorrance A. Non-Coding RNAs Are Implicit in Chronic Myeloid Leukemia Therapy Resistance. Int J Mol Sci. 2022;23(20):12271. doi:10.3390/ijms232012271.

[113] Friedman RC, Farh KK, Burge CB, Bartel DP. Most mammalian mRNAs are conserved targets of microRNAs. Genome Res. 2009;19(1):92-105. doi:10.1101/gr.082701.108.

[114] Alves R, Gonçalves AC, Jorge J, et al. MicroRNA signature refine response prediction in CML. Sci Rep. 2019;9(1):9666. doi:10.1038/s41598-019-46132-9.

[115] Yeh CH, Moles R, Nicot C. Clinical significance of microRNAs in chronic and acute human leukemia. Mol Cancer. 2016;15(1):37. doi:10.1186/s12943-016-0518-2.

[116] Chen ZX, Riggs AD. DNA methylation and demethylation in mammals. J Biol Chem. 2011;286(21):18347-18353. doi:10.1074/jbc.R110.205286.

[117] Feng YH, Tsao CJ. Emerging role of microRNA-21 in cancer. Biomed Rep. 2016;5(4):395-402. doi:10.3892/br.2016.747.

[118] Mirza MAB, Guru SA, Abdullah SM, Rizvi A, Saxena A. microRNA-21 Expression as Prognostic and Therapeutic Response Marker in Chronic Myeloid Leukaemia Patients. Asian Pac J Cancer Prev. 2019;20(8):2379-2383. doi:10.31557/APJCP.2019.20.8.2379.

[119] Seca H, Lima RT, Lopes-Rodrigues V, Guimaraes JE, Almeida GM, Vasconcelos MH. Targeting miR-21 induces autophagy and chemosensitivity of leukemia cells. Curr Drug Targets. 2013;14(10):1135-1143. doi:10.2174/13894501113149990185.

[120] Li Y, Wang H, Tao K, et al. miR-29b suppresses CML cell proliferation and induces apoptosis via regulation of BCR/ABL1 protein. Exp Cell Res. 2013;319(8):1094-1101. doi:10.1016/j.yexcr.2013.02.002.

[121] Yu Y, Yang L, Zhao M, et al. Targeting microRNA-30a-mediated autophagy enhances imatinib activity against human chronic myeloid leukemia cells. Leukemia. 2012;26(8):1752-1760. doi:10.1038/leu.2012.65.

[122] Khalil NA, Desouky MN, Diab IH, Hamed NAM, Mannaa HF. MicroRNA 30a Mediated Autophagy and Imatinib Response in Egyptian Chronic Myeloid Leukemia Patients. Indian J Hematol Blood Transfus. 2020;36(3):491-497. doi:10.1007/s12288-019-01241-3.

[123] Xu C, Fu H, Gao L, et al. BCR-ABL/GATA1/miR-138 mini circuitry contributes to the leukemogenesis of chronic myeloid leukemia. Oncogene. 2014;33(1):44-54. doi:10.1038/onc.2012.557.

[124] Bueno MJ, Pérez de Castro I, Gómez de Cedrón M, et al. Genetic and epigenetic silencing of microRNA-203 enhances ABL1 and BCR-ABL1 oncogene expression. Cancer Cell. 2008;13(6):496-506. doi:10.1016/j.ccr.2008.04.018.

[125] Shibuta T, Honda E, Shiotsu H, et al. Imatinib induces demethylation of miR-203 gene: an epigenetic mechanism of anti-tumor effect of imatinib. Leuk Res. 2013;37(10):1278-1286. doi:10.1016/j.leukres.2013.07.019.

[126] Zhang J, Jiang Y, Han X, et al. Differential expression profiles and functional analysis of plasma miRNAs associated with chronic myeloid leukemia phases. Future Oncol. 2019;15(7):763-776. doi:10.2217/fon-2018-0741.

[127] Lopotová T, Záčková M, Klamová H, Moravcová J. MicroRNA-451 in chronic myeloid leukemia: miR-451-BCR-ABL regulatory loop?. Leuk Res. 2011;35(7):974-977. doi:10.1016/j.leukres.2011.03.029.

[128] Khalifa K, Abbas O, Abdlfattah R, Alhassanin S, Shehata A, Esawy S. Decreased Expression of microRNA-451 is Associated with Imatinib Mesylate Resistance in Chronic Myeloid Leukemia Patients. Clinical Lymphoma Myeloma & Leukemia. 2019;19:S293-S293. doi:10.1016/j.clml.2019.07.240.

[129] Scholl V, Hassan R, Zalcberg IR. miRNA-451: A putative predictor marker of Imatinib therapy response in chronic myeloid leukemia. Leuk Res. 2012;36(1):119-121. doi:10.1016/j.leukres.2011.08.023.

[130] Liu L, Wang S, Chen R, et al. Myc induced miR-144/451 contributes to the acquired imatinib resistance in chronic myelogenous leukemia cell K562. Biochem Biophys Res Commun. 2012;425(2):368-373. doi:10.1016/j.bbrc.2012.07.098.

[131] Ninawe A, Guru SA, Yadav P, et al. miR-486-5p: A Prognostic Biomarker for Chronic Myeloid Leukemia. ACS Omega. 2021;6(11):7711-7718. doi:10.1021/acsomega.1c00035.

[132] Jabbour E, Kantarjian H. Chronic myeloid leukemia: 2012 update on diagnosis, monitoring, and management. Am J Hematol. 2012;87(11):1037-1045. doi:10.1002/ajh.23282.

[133] Jabbour E, Kantarjian H. Chronic myeloid leukemia: 2022 update on diagnosis, therapy, and monitoring. Am J Hematol. 2022;97(9):1236-1256. doi:10.1002/ajh.26642.

[134] Quintás-Cardama A, Cortes JE. Chronic myeloid leukemia: diagnosis and treatment. Mayo Clin Proc. 2006;81(7):973-988. doi:10.4065/81.7.973.

[135] Massimino M, Stella S, Tirrò E, et al. ABL1-Directed Inhibitors for CML: Efficacy, Resistance and Future Perspectives. Anticancer Res. 2020;40(5):2457-2465. doi:10.21873/anticanres.14215.

[136] Pophali PA, Patnaik MM. The Role of New Tyrosine Kinase Inhibitors in Chronic Myeloid Leukemia. Cancer J. 2016;22(1):40-50. doi:10.1097/PPO.0000000000000165.

[137] Höglund M, Sandin F, Simonsson B. Epidemiology of chronic myeloid leukaemia: an update. Ann Hematol. 2015;94 Suppl 2:S241-S247. doi:10.1007/s00277-015-2314-2.

[138] Jabbour E, Kantarjian H. Chronic myeloid leukemia: 2018 update on diagnosis, therapy and monitoring. Am J Hematol. 2018;93(3):442-459. doi:10.1002/ajh.25011.

[139] Deininger MW, Goldman JM, Melo JV. The molecular biology of chronic myeloid leukemia. Blood. 2000;96(10):3343-3356.

[140] Lugo TG, Pendergast AM, Muller AJ, Witte ON. Tyrosine kinase activity and transformation potency of bcr-abl oncogene products. Science. 1990;247(4946):1079-1082. doi:10.1126/science.2408149.

[141] Faderl S, Talpaz M, Estrov Z, O'Brien S, Kurzrock R, Kantarjian HM. The biology of chronic myeloid leukemia. N Engl J Med. 1999;341(3):164-172. doi:10.1056/NEJM199907153410306.

[142] Hochhaus A, O'Brien SG, Guilhot F, et al. Six-year follow-up of patients receiving imatinib for the first-line treatment of chronic myeloid leukemia [published correction appears in Leukemia. 2010 May;24(5):1102]. Leukemia. 2009;23(6):1054-1061. doi:10.1038/leu.2009.38.

[143] Bavaro L, Martelli M, Cavo M, Soverini S. Mechanisms of Disease Progression and Resistance to Tyrosine Kinase Inhibitor Therapy in Chronic Myeloid Leukemia: An Update. Int J Mol Sci. 2019;20(24):6141. doi:10.3390/ijms20246141.

[144] Özgür Yurttaş N, Eşkazan AE. Novel therapeutic approaches in chronic myeloid leukemia. Leuk Res. 2020;91:106337. doi:10.1016/j.leukres.2020.106337.

[145] Mancini M, De Santis S, Monaldi C, et al. Polo-like kinase-1, Aurora kinase A and WEE1 kinase are promising druggable targets in CML cells displaying BCR::ABL1-independent resistance to tyrosine kinase inhibitors. Front Oncol. 2022;12:901132. doi:10.3389/fonc.2022.901132.

[146] Machado CB, DA Silva EL, Dias Nogueira BM, et al. The Relevance of Aurora Kinase Inhibition in Hematological Malignancies. Cancer Diagn Progn. 2021;1(3):111-126. doi:10.21873/cdp.10016.

[147] Massimino M, Stella S, Tirrò E, et al. Non ABL-directed inhibitors as alternative treatment strategies for chronic myeloid leukemia. Molecular Cancer. 2018;17:56. doi:10.1186/s12943-018-0805-1.

[148] Alvarado Y, Cortés JE. Emerging Role of Aurora Kinase Inhibitors in Chronic Myeloid Leukemia. Clinical Leukemia. 2007;1(6):325-330. doi: 10.3816/clk.2007.n.025.

[149] Meulenbeld HJ, Mathijssen RH, Verweij J, de Wit R, de Jonge MJ. Danusertib, an aurora kinase inhibitor. Expert Opin Investig Drugs. 2012;21(3):383-393. doi:10.1517/13543784.2012.652303.

[150] Gontarewicz A, Balabanov S, Keller G, et al. Simultaneous targeting of Aurora kinases and Bcr-Abl kinase by the small molecule inhibitor PHA-739358 is effective against imatinib-resistant BCR-ABL mutations including T315I. Blood. 2008;111(8):4355-4364. doi:10.1182/blood-2007-09-113175.

[151] Borthakur G, Dombret H, Schafhausen P, et al. A phase I study of danusertib (PHA-739358) in adult patients with accelerated or blastic phase chronic myeloid leukemia and Philadelphia chromosome-positive acute lymphoblastic leukemia resistant or intolerant to imatinib and/or other second generation c-ABL therapy. Haematologica. 2015;100(7):898-904. doi:10.3324/haematol.2014.115279

[152] Dill V, Kauschinger J, Hauch RT, et al. Inhibition of PLK1 by capped-dose volasertib exerts substantial efficacy in MDS and sAML while sparing healthy haematopoiesis. Eur J Haematol. 2020;104(2):125-137. doi:10.1111/ejh.13354.

[153] Okabe S, Tauchi T, Tanaka Y, Sakuta J, Ohyashiki K. Efficacy of the polo-like kinase inhibitor rigosertib, alone or in combination with Abelson tyrosine kinase inhibitors, against break point cluster region-c-Abelson-positive leukemia cells. Oncotarget. 2015;6(24):20231-20240. doi:10.18632/oncotarget.4047.

[154] Gleixner KV, Ferenc V, Peter B, et al. Polo-like kinase 1 (Plk1) as a novel drug target in chronic myeloid leukemia: overriding imatinib resistance with the Plk1 inhibitor BI 2536. Cancer Res. 2010;70(4):1513-1523. doi:10.1158/0008-5472.CAN-09-2181.

[155] Do K, Doroshow JH, Kummar S. Wee1 kinase as a target for cancer therapy. Cell Cycle. 2013;12(19):3159-3164. doi:10.4161/cc.26062.

[156] Kastan MB, Bartek J. Cell-cycle checkpoints and cancer. Nature. 2004;432(7015):316-323. doi:10.1038/nature03097.

[157] Zeng F, Peng Y, Qin Y, et al. Wee1 promotes cell proliferation and imatinib resistance in chronic myeloid leukemia via regulating DNA damage repair dependent on ATM-γH2AX-MDC1. Cell Commun Signal. 2022;20(1):199. doi:10.1186/s12964-022-01021-z.

[158] Boutros R, Lobjois V, Ducommun B. CDC25 phosphatases in cancer cells: key players? Good targets?. Nat Rev Cancer. 2007;7(7):495-507. doi:10.1038/nrc2169.

[159] Jazayeri A, Falck J, Lukas C, et al. ATM- and cell cycle-dependent regulation of ATR in response to DNA double-strand breaks. Nat Cell Biol. 2006;8(1):37-45. doi:10.1038/ncb1337.

[160] Johnson N, Cai D, Kennedy RD, et al. Cdk1 participates in BRCA1-dependent S phase checkpoint control in response to DNA damage. Mol Cell. 2009;35(3):327-339. doi:10.1016/j.molcel.2009.06.036.

[161] Masaki T, Shiratori Y, Rengifo W, et al. Cyclins and cyclin-dependent kinases: comparative study of hepatocellular carcinoma versus cirrhosis. Hepatology. 2003;37(3):534-543. doi:10.1053/jhep.2003.50112.

[162] Iorns E, Lord CJ, Grigoriadis A, et al. Integrated functional, gene expression and genomic analysis for the identification of cancer targets. PLoS One. 2009;4(4):e5120. doi:10.1371/journal.pone.0005120.

[163] Tibes R, Bogenberger JM, Chaudhuri L, et al. RNAi screening of the kinome with cytarabine in leukemias. Blood. 2012;119(12):2863-2872. doi:10.1182/blood-2011-07-367557.

[164] Porter CC, Kim J, Fosmire S, et al. Integrated genomic analyses identify WEE1 as a critical mediator of cell fate and a novel therapeutic target in acute myeloid leukemia. Leukemia. 2012;26(6):1266-1276. doi:10.1038/leu.2011.392.

[165] Magnussen GI, Hellesylt E, Nesland JM, Trope CG, Flørenes VA, Holm R. High expression of wee1 is associated with malignancy in vulvar squamous cell carcinoma patients. BMC Cancer. 2013;13:288. doi:10.1186/1471-2407-13-288.

[166] Music D, Dahlrot RH, Hermansen SK, et al. Expression and prognostic value of the WEE1 kinase in gliomas. J Neurooncol. 2016;127(2):381-389. doi:10.1007/s11060-015-2050-4.

[167] Magnussen GI, Holm R, Emilsen E, Rosnes AK, Slipicevic A, Flørenes VA. High expression of Wee1 is associated with poor disease-free survival in malignant melanoma: potential for targeted therapy. PLoS One. 2012;7(6):e38254. doi:10.1371/journal.pone.0038254.

[168] Lal S, Burkhart RA, Beeharry N, et al. HuR posttranscriptionally regulates WEE1: implications for the DNA damage response in pancreatic cancer cells. Cancer Res. 2014;74(4):1128-1140. doi:10.1158/0008-5472.CAN-13-1915.

[169] Ghelli Luserna di Rorà A, Cerchione C, Martinelli G, Simonetti G. A WEE1 family business: regulation of mitosis, cancer progression, and therapeutic target. J Hematol Oncol. 2020;13(1):126. Published 2020 Sep 21. doi:10.1186/s13045-020-00959-2.

[170] Falchook GS, Sachdev J, Imedio ER, et al. A phase Ib study of adavosertib, a selective Wee1 inhibitor, in patients with locally advanced or metastatic solid tumors. Invest New Drugs. 2023;41(3):493-502. doi:10.1007/s10637-023-01371-6.

[171] Castedo M, Perfettini JL, Roumier T, Andreau K, Medema R, Kroemer G. Cell death by mitotic catastrophe: a molecular definition. Oncogene. 2004;23(16):2825-2837. doi:10.1038/sj.onc.1207528.

[172] Patel MR, Falchook GS, Wang JS, et al. Open-Label, Multicenter, Phase I Study to Assess Safety and Tolerability of Adavosertib Plus Durvalumab in Patients with Advanced Solid Tumors. Target Oncol. 2025;20(1):127-138. doi:10.1007/s11523-024-01110-8.

[173] Leijen S, van Geel RM, Pavlick AC, et al. Phase I Study Evaluating WEE1 Inhibitor AZD1775 As Monotherapy and in Combination With Gemcitabine, Cisplatin, or Carboplatin in Patients With Advanced Solid Tumors. J Clin Oncol. 2016;34(36):4371-4380. doi:10.1200/JCO.2016.67.5991.

[174] Hamilton EP, Falchook GS, Wang JS, et al. Adavosertib in Combination with Olaparib in Patients with Refractory Solid Tumors: An Open-Label, Dose-Finding, and Dose-Expansion Phase Ib Trial. Target Oncol. 2024;19(6):879-892. doi:10.1007/s11523-024-01102-8.

[175] Barbosa RSS, Dantonio PM, Guimarães T, et al. Sequential combination of bortezomib and WEE1 inhibitor, MK-1775, induced apoptosis in multiple myeloma cell lines. Biochem Biophys Res Commun. 2019;519(3):597-604. doi:10.1016/j.bbrc.2019.08.163.

[176] Rodríguez-Vázquez GO, Diaz-Quiñones AO, Chorna N, et al. Synergistic interactions of cytarabine-adavosertib in leukemic cell lines proliferation and metabolomic endpoints. Biomed Pharmacother. 2023;166:115352. doi:10.1016/j.biopha.2023.115352.

[177] Poudel G, Tolland MG, Hughes TP, Pagani IS. Mechanisms of Resistance and Implications for Treatment Strategies in Chronic Myeloid Leukaemia. Cancers (Basel). 2022;14(14):3300. doi:10.3390/cancers14143300.

[178] Bonifacio M, Stagno F, Scaffidi L, Krampera M, Di Raimondo F. Management of Chronic Myeloid Leukemia in Advanced Phase. Front Oncol. 2019;9:1132. doi:10.3389/fonc.2019.01132.

[179] Soverini S, Bassan R, Lion T. Treatment and monitoring of Philadelphia chromosome-positive leukemia patients: recent advances and remaining challenges. J Hematol Oncol. 2019;12(1):39. doi:10.1186/s13045-019-0729-2.

[180] Sun J, Hu R, Han M, et al. Mechanisms underlying therapeutic resistance of tyrosine kinase inhibitors in chronic myeloid leukemia. Int J Biol Sci. 2024;20(1):175-181. doi:10.7150/ijbs.86305.

[181] Braun TP, Eide CA, Druker BJ. Response and Resistance to BCR-ABL1-Targeted Therapies. Cancer Cell. 2020;37(4):530-542. doi:10.1016/j.ccell.2020.03.006.

[182] De Santis S, Monaldi C, Mancini M, Bruno S, Cavo M, Soverini S. Overcoming Resistance to Kinase Inhibitors: The Paradigm of Chronic Myeloid Leukemia. Onco Targets Ther. 2022;15:103-116. doi:10.2147/OTT.S289306.

[183] Wang R, Cong Y, Li C, Zhang C, Lin H. Predictive value of early molecular response for deep molecular response in chronic phase of chronic myeloid leukemia. Medicine (Baltimore). 2019;98(15):e15222. doi:10.1097/MD.0000000000015222.

[184] Zhan JY, Ma J, Zheng QC. Molecular dynamics investigation on the Asciminib resistance mechanism of I502L and V468F mutations in BCR-ABL. J Mol Graph Model. 2019;89:242-249. doi:10.1016/j.jmgm.2019.03.018.

[185] Qiang W, Antelope O, Zabriskie MS, et al. Mechanisms of resistance to the BCR-ABL1 allosteric inhibitor asciminib. Leukemia. 2017;31(12):2844-2847. doi:10.1038/leu.2017.264.

[186] Kaehler M, Cascorbi I. Molecular Mechanisms of Tyrosine Kinase Inhibitor Resistance in Chronic Myeloid Leukemia. Handb Exp Pharmacol. 2023;280:65-83. doi:10.1007/164_2023_639.

[187] Barnes DJ, Palaiologou D, Panousopoulou E, et al. Bcr-Abl expression levels determine the rate of development of resistance to imatinib mesylate in chronic myeloid leukemia. Cancer Res. 2005;65(19):8912-8919. doi:10.1158/0008-5472.CAN-05-0076.

[188] Mahon FX, Hayette S, Lagarde V, et al. Evidence that resistance to nilotinib may be due to BCR-ABL, Pgp, or Src kinase overexpression. Cancer Res. 2008;68(23):9809-9816. doi:10.1158/0008-5472.CAN-08-1008.

[189] Tang C, Schafranek L, Watkins DB, et al. Tyrosine kinase inhibitor resistance in chronic myeloid leukemia cell lines: investigating resistance pathways. Leuk Lymphoma. 2011;52(11):2139-2147. doi:10.3109/10428194.2011.591013.

[190] Bianchini M, De Brasi C, Gargallo P, Gonzalez M, Bengió R, Larripa I. Specific assessment of BCR-ABL transcript overexpression and imatinib resistance in chronic myeloid leukemia patients. Eur J Haematol. 2009;82(4):292-300. doi:10.1111/j.1600-0609.2008.01199.x.

[191] Shanmuganathan N, Branford S. The Hidden Pathogenesis of CML: Is BCR-ABL1 the First Event?. Curr Hematol Malig Rep. 2019;14(6):501-506. doi:10.1007/s11899-019-00549-1.

[192] Amarante-Mendes GP, Rana A, Datoguia TS, Hamerschlak N, Brumatti G. BCR-ABL1 Tyrosine Kinase Complex Signaling Transduction: Challenges to Overcome Resistance in Chronic Myeloid Leukemia. Pharmaceutics. 2022;14(1):215. Published 2022 Jan 17. doi:10.3390/pharmaceutics14010215.

[193] Ma L, Shan Y, Bai R, et al. A therapeutically targetable mechanism of BCR-ABL-independent imatinib resistance in chronic myeloid leukemia. Sci Transl Med. 2014;6(252):252ra121. doi:10.1126/scitranslmed.3009073.

[194] Suzuki M, Abe A, Imagama S, et al. BCR-ABL-independent and RAS / MAPK pathway-dependent form of imatinib resistance in Ph-positive acute lymphoblastic leukemia cell line with activation of EphB4. Eur J Haematol. 2010;84(3):229-238. doi:10.1111/j.1600-0609.2009.01387.x.

[195] Eiring AM, Kraft IL, Page BD, O'Hare T, Gunning PT, Deininger MW. STAT3 as a mediator of BCR-ABL1-independent resistance in chronic myeloid leukemia. Leuk Suppl. 2014;3(Suppl 1):S5-S6. doi:10.1038/leusup.2014.3.

[196] Zhang HP, Jiang RY, Zhu JY, et al. PI3K/AKT/mTOR signaling pathway: an important driver and therapeutic target in triple-negative breast cancer. Breast Cancer. 2024;31(4):539-551. doi:10.1007/s12282-024-01567-5.

[197] Burchert A, Wang Y, Cai D, et al. Compensatory PI3-kinase/Akt/mTor activation regulates imatinib resistance development. Leukemia. 2005;19(10):1774-1782. doi:10.1038/sj.leu.2403898.

[198] Mancini M, De Santis S, Monaldi C, et al. Hyper-activation of Aurora kinase a-polo-like kinase 1-FOXM1 axis promotes chronic myeloid leukemia resistance to tyrosine kinase inhibitors. J Exp Clin Cancer Res. 2019;38(1):216. Published 2019 May 23. doi:10.1186/s13046-019-1197-9.

[199] Zhao Q, Assimopoulou AN, Klauck SM, et al. Inhibition of c-MYC with involvement of ERK/JNK/MAPK and AKT pathways as a novel mechanism for shikonin and its derivatives in killing leukemia cells. Oncotarget. 2015;6(36):38934-38951. doi:10.18632/oncotarget.5380.

[200] Madden SK, de Araujo AD, Gerhardt M, Fairlie DP, Mason JM. Taking the Myc out of cancer: toward therapeutic strategies to directly inhibit c-Myc. Mol Cancer. 2021;20(1):3. doi:10.1186/s12943-020-01291-6.

[201] Abdulmawjood B, Roma-Rodrigues C, Baptista PV, Fernandes AR. Tackling Imatinib Resistance via Au-nanoconjugates using A Cml Resistant Cell Line. Particle & Particle Systems Characterization. 2024;41(1):2300090. doi:10.1002/ppsc.202300090.

[202] Pippa R, Odero MD. The Role of MYC and PP2A in the Initiation and Progression of Myeloid Leukemias. Cells. 2020;9(3):544. doi:10.3390/cells9030544.

[203] Sodaro G, Cesaro E, Montano G, et al. Role of ZNF224 in c-Myc repression and imatinib responsiveness in chronic myeloid leukemia. Oncotarget. 2017;9(3):3417-3431. doi:10.18632/oncotarget.23283.

[204] Bixby D, Talpaz M. Mechanisms of resistance to tyrosine kinase inhibitors in chronic myeloid leukemia and recent therapeutic strategies to overcome resistance. Hematology Am Soc Hematol Educ Program. 2009;461-476. doi:10.1182/asheducation-2009.1.461.

[205] Thomas J, Wang L, Clark RE, Pirmohamed M. Active transport of imatinib into and out of cells: implications for drug resistance. Blood. 2004;104(12):3739-3745. doi:10.1182/blood-2003-12-4276.

[206] Skoglund K, Moreno SB, Baytar M, Jönsson JI, Gréen H. ABCB1 haplotypes do not influence transport or efficacy of tyrosine kinase inhibitors in vitro. Pharmgenomics Pers Med. 2013;6:63-72. Published 2013 Aug 20. doi:10.2147/PGPM.S45522.

[207] Jeleń AM, Strehl B, Szmajda-Krygier D, Pązik M, Balcerczak E. Bioinformatics-Based Characterization of ATP-Binding Cassette Subfamily B Member 1 (ABCB1) Gene Expression in Non-Small-Cell Lung Cancer (NSCLC). Applied Sciences. 2023; 13(11):6576. doi 10.3390/app13116576.

[208] Ammar M, Louati N, Frikha I, et al. Overexpression of P-glycoprotein and resistance to Imatinib in chronic myeloid leukemia patients. J Clin Lab Anal. 2020;34(9):e23374. doi:10.1002/jcla.23374.

[209] Montaño-Samaniego M, Bravo-Estupiñan DM, Méndez-Guerrero O, Alarcón-Hernández E, Ibáñez-Hernández M. Strategies for Targeting Gene Therapy in Cancer Cells With Tumor-Specific Promoters. Front Oncol. 2020;10:605380. doi:10.3389/fonc.2020.605380.

[210] Kovecses O, Mercier FE, McKeague M. Nucleic acid therapeutics as differentiation agents for myeloid leukemias. Leukemia. 2024;38(7):1441-1454. doi:10.1038/s41375-024-02191-0.

[211] Singh P, Chaudhari V. Association of Early-Onset Sepsis and Vitamin D Deficiency in Term Neonates. Indian Pediatr. 2020;57(3):232-234.

[212] Rowley PT, Kosciolek BA, Kool ET. Circular antisense oligonucleotides inhibit growth of chronic myeloid leukemia cells. Mol Med. 1999;5(10):693-700.

[213] Tari Ashizawa A, Ohanian M, Cortes JE. BP1001, a Novel Therapeutic for Chronic Myelogenous Leukemia. Blood. 2016; 128 (22): 4239. doi: 10.1182/blood.V128.22.4239.4239.

[214] Hoshiko T, Kubota Y, Akisawa T, et al. Naked antisense double-stranded DNA oligonucleotide efficiently suppresses BCR-ABL positive leukemic cells. Invest New Drugs. 2020;38(4):1012-1019. doi:10.1007/s10637-019-00862-9.

[215] Gaj T, Gersbach CA, Barbas CF 3rd. ZFN, TALEN, and CRISPR/Cas-based methods for genome engineering. Trends Biotechnol. 2013;31(7):397-405. doi:10.1016/j.tibtech.2013.04.004.

[216] Kim S, Lee MJ, Kim H, Kang M, Kim JS. Preassembled zinc-finger arrays for rapid construction of ZFNs. Nat Methods. 2011;8(1):7. doi:10.1038/nmeth0111-7a.

[217] Gonzalez B, Schwimmer LJ, Fuller RP, Ye Y, Asawapornmongkol L, Barbas CF 3rd. Modular system for the construction of zinc-finger libraries and proteins. Nat Protoc. 2010;5(4):791-810. doi:10.1038/nprot.2010.34.

[218] Choo Y, Sánchez-García I, Klug A. In vivo repression by a site-specific DNA-binding protein designed against an oncogenic sequence. Nature. 1994;372(6507):642-645. doi:10.1038/372642a0.

[219] Huang N, Huang Z, Gao M, et al. Induction of apoptosis in imatinib sensitive and resistant chronic myeloid leukemia cells by efficient disruption of bcr-abl oncogene with zinc finger nucleases. J Exp Clin Cancer Res. 2018;37(1):62. doi:10.1186/s13046-018-0732-4.

[220] Rafii S, Tashkandi E, Bukhari N, Al-Shamsi HO. Current Status of CRISPR/Cas9 Application in Clinical Cancer Research: Opportunities and Challenges. Cancers (Basel). 2022;14(4):947. doi:10.3390/cancers14040947.

[221] Zhan T, Rindtorff N, Betge J, Ebert MP, Boutros M. CRISPR/Cas9 for cancer research and therapy. Semin Cancer Biol. 2019;55:106-119. doi:10.1016/j.semcancer.2018.04.001.

[222] Zhang S, Shen J, Li D, Cheng Y. Strategies in the delivery of Cas9 ribonucleoprotein for CRISPR/Cas9 genome editing. Theranostics. 2021;11(2):614-648. doi:10.7150/thno.47007.

[223] Younes S, Ismail MA, Al-Jurf R, et al. Management of chronic myeloid leukaemia: current treatment options, challenges, and future strategies. Hematology. 2023;28(1):2196866. doi:10.1080/16078454.2023.2196866.

[224] García-Tuñón I, Hernández-Sánchez M, Ordoñez JL, et al. The CRISPR/Cas9 system efficiently reverts the tumorigenic ability of BCR/ABL in vitro and in a xenograft model of chronic myeloid leukemia. Oncotarget. 2017;8(16):26027-26040. doi:10.18632/oncotarget.15215.

[225] Vuelta E, Ordoñez JL, Alonso-Pérez V, Méndez L, et al. CRISPR/Cas9 technology abolishes the BCR/ABL1 oncogene in chronic myeloid leukemia and restores normal hematopoiesis. bioRxiv. 2020: 2020-08. doi: 10.1101/2020.08.05.237610.

[226] Kaur J, Konar A, Halder S, Chakraborty S, Ghosh P. CRISPR-Cas9 to treat chronic myeloid leukaemia: A review. Int. J. Clin. Biol. Biochem. 2024;6(1):31-36. doi: 10.33545/26646188.2024.v6.i1a.56.

[227] Zhang J, Chen B, Gan C, Sun H, Zhang J, Feng L. A Comprehensive Review of Small Interfering RNAs (siRNAs): Mechanism, Therapeutic Targets, and Delivery Strategies for Cancer Therapy. Int J Nanomedicine. 2023;18:7605-7635.. doi:10.2147/IJN.S436038.

[228] Ranasinghe P, Addison ML, Dear JW, Webb DJ. Small interfering RNA: Discovery, pharmacology and clinical development-An introductory review. Br J Pharmacol. 2023;180(21):2697-2720. doi:10.1111/bph.15972.

[229] Landry B, Valencia-Serna J, Gul-Uludag H, et al. Progress in RNAi-mediated Molecular Therapy of Acute and Chronic Myeloid Leukemia. Mol Ther Nucleic Acids. 2015;4:e240. Published 2015 May 12. doi:10.1038/mtna.2015.13.

[230] Valencia-Serna J, Gul-Uludağ H, Mahdipoor P, Jiang X, Uludağ H. Investigating siRNA delivery to chronic myeloid leukemia K562 cells with lipophilic polymers for therapeutic BCR-ABL down-regulation. J Control Release. 2013;172(2):495-503. doi:10.1016/j.jconrel.2013.05.014.

[231] Valencia-Serna J, Chevallier P, Kc RB, Laroche G, Uludağ H. Fibronectin-modified surfaces for evaluating the influence of cell adhesion on sensitivity of leukemic cells to siRNA nanoparticles. Nanomedicine (Lond). 2016;11(9):1123-1138. doi:10.2217/nnm.16.32.

[232] Kc R, Thapa B, Ubeda A, Jiang X, Uludağ H. BCR-Abl Silencing by siRNA: A Potent Approach to Sensitize Chronic Myeloid Leukemia Cells to Tyrosine Kinase Inhibitor Therapy. Stem Cells Dev. 2019;28(11):734-744. doi:10.1089/scd.2018.0196.

[233] Valencia-Serna J, Aliabadi HM, Manfrin A, Mohseni M, Jiang X, Uludag H. siRNA/lipopolymer nanoparticles to arrest growth of chronic myeloid leukemia cells in vitro and in vivo. Eur J Pharm Biopharm. 2018;130:66-70. doi:10.1016/j.ejpb.2018.06.018.

[234] Vysochinskaya V, Dovbysh O, Gorshkov A, et al. Advancements and Future Prospects in Molecular Targeted and siRNA Therapies for Chronic Myeloid Leukemia. Biomolecules. 2024;14(6):644. Published 2024 May 30. doi:10.3390/biom14060644.

[235] Roma-Rodrigues C, Pombo I, Fernandes AR, Baptista PV. Hyperthermia Induced by Gold Nanoparticles and Visible Light Photothermy Combined with Chemotherapy to Tackle Doxorubicin Sensitive and Resistant Colorectal Tumor 3D Spheroids. Int J Mol Sci. 2020;21(21):8017. doi:10.3390/ijms21218017.

[236] Ferreira D, Fernandes AR, Baptista PV. Mild hyperthermia via gold nanoparticles and visible light irradiation for enhanced siRNA and ASO delivery in 2D and 3D tumour spheroids. Cancer Nanotechnology. 2024;15(1). doi:10.1186/s12645-024-00256-4.

[237] Oliveira BB, Fernandes AR, Baptista PV. Assessing the gene silencing potential of AuNP-based approaches on conventional 2D cell culture versus 3D tumor spheroid. Front Bioeng Biotechnol. 2024;12:1320729. doi:10.3389/fbioe.2024.1320729.

[238] Xu M, Han X, Xiong H, et al. Cancer Nanomedicine: Emerging Strategies and Therapeutic Potentials. Molecules. 2023;28(13):5145. doi:10.3390/molecules28135145.

[239] Saidi T, Fortuin J, Douglas TS. Nanomedicine for drug delivery in South Africa: a protocol for systematic review. Syst Rev. 2018;7(1):154. doi:10.1186/s13643-018-0823-5.

[240] Zhuo Y, Zhao YG, Zhang Y. Enhancing Drug Solubility, Bioavailability, and Targeted Therapeutic Applications through Magnetic Nanoparticles. Molecules. 2024;29(20):4854. doi:10.3390/molecules29204854.

[241] Singh M, Sharma V, Shrivastav A, Singh P, Verma N. Nanotechnology for Novel Drug Delivery: A Systematic Review of Classification, Preparation, Characterization, and Applications of Nanoparticles in Drug Delivery. Biotech Res Asia. 2023;20(4). doi:10.13005/bbra/3165.

[242] Beltrán-Gracia E, López-Camacho A, Higuera-Ciapara I, Velázquez-Fernández J, Vallejo-Cardona A. Nanomedicine review: clinical developments in liposomal applications. Cancer Nanotechnology. 2019;10(1). doi:10.1186/s12645-019-0055-y.

[243] Gabizon AA, Gabizon-Peretz S, Modaresahmadi S, La-Beck NM. Thirty years from FDA approval of pegylated liposomal doxorubicin (Doxil/Caelyx): an updated analysis and future perspective. BMJ Oncology. 2025;4(1). doi:10.1136/bmjonc-2024-000573.

[244] Patel P, Garala K, Singh S, Prajapati BG, Chittasupho C. Lipid-Based Nanoparticles in Delivering Bioactive Compounds for Improving Therapeutic Efficacy. Pharmaceuticals (Basel). 2024;17(3):329. doi:10.3390/ph17030329.

[245] Wang YS, Kumari M, Chen GH, Hong MH, Yuan JP, Tsai JL, Wu HC. mRNA-based vaccines and therapeutics: An in-depth survey of current and upcoming clinical applications. Journal of Biomedical Science. 2023;30(1):84. doi: 1186/s12929-023-00977-5.

[246] Li W, Peng A, Wu H, et al. Anti-Cancer Nanomedicines: A Revolution of Tumor Immunotherapy. Front Immunol. 2020;11:601497. doi:10.3389/fimmu.2020.601497.

[247] Toader C, Dumitru AV, Eva L, Serban M, Covache-Busuioc RA, Ciurea AV. Nanoparticle Strategies for Treating CNS Disorders: A Comprehensive Review of Drug Delivery and Theranostic Applications. Int J Mol Sci. 2024;25(24):13302. doi:10.3390/ijms252413302.

[248] Alshehri S, Imam SS, Rizwanullah M, et al. Progress of Cancer Nanotechnology as Diagnostics, Therapeutics, and Theranostics Nanomedicine: Preclinical Promise and Translational Challenges. Pharmaceutics. 2020;13(1):24. doi:10.3390/pharmaceutics13010024.

[249] Akhter MH, Rizwanullah M, Ahmad J, Ahsan MJ, Mujtaba MA, Amin S. Nanocarriers in advanced drug targeting: setting novel paradigm in cancer therapeutics. Artif Cells Nanomed Biotechnol. 2018;46(5):873-884. doi:10.1080/21691401.2017.1366333.

[250] Fan D, Cao Y, Cao M, Wang Y, Cao Y, Gong T. Nanomedicine in cancer therapy. Signal Transduct Target Ther. 2023;8(1):293. doi:10.1038/s41392-023-01536-y.

[251] Prajapati A, Rangra S, Patil R, Desai N, Jyothi VGSS, Salave S, Amate P, Benival D, Kommineni N. Receptor-Targeted Nanomedicine for Cancer Therapy. Receptors. 2024;3(3):323-361. doi:10.3390/receptors3030016.

[252] Haripriyaa M, Suthindhiran K. Pharmacokinetics of nanoparticles: current knowledge, future directions and its implications in drug delivery. Future Journal of Pharmaceutical Sciences. 2023;9(1):113. doi:10.1186/s43094-023-00569-y.

[253] Albanese A, Tang PS, Chan WC. The effect of nanoparticle size, shape, and surface chemistry on biological systems. Annu Rev Biomed Eng. 2012;14:1-16. doi:10.1146/annurev-bioeng-071811-150124.

[254] Tewabe A, Abate A, Tamrie M, Seyfu A, Abdela Siraj E. Targeted Drug Delivery - From Magic Bullet to Nanomedicine: Principles, Challenges, and Future Perspectives. J Multidiscip Healthc. 2021;14:1711-1724. doi:10.2147/JMDH.S313968.

[255] Mukwaya G, Forssen EA, Schmidt P, Ross M. DaunoXome®(Liposomal Daunorubicin) for first-line treatment of advanced, HIV-related Kaposi's Sarcoma. Long Circ. Liposomes Old Drugs New Ther. 1998;147–163. doi: 10.1007/978-3-662-22115-0_10.

[256] Gavas S, Quazi S, Karpiński TM. Nanoparticles for Cancer Therapy: Current Progress and Challenges. Nanoscale Res Lett. 2021;16(1):173. doi:10.1186/s11671-021-03628-6.

[257] Tian H, Zhang T, Qin S, et al. Enhancing the therapeutic efficacy of nanoparticles for cancer treatment using versatile targeted strategies. J Hematol Oncol. 2022;15(1):132. doi:10.1186/s13045-022-01320-5.

[258] Fiandra L, Mazzucchelli S, De Palma C, et al. Assessing the in vivo targeting efficiency of multifunctional nanoconstructs bearing antibody-derived ligands. ACS Nano. 2013;7(7):6092-6102. doi:10.1021/nn4018922.

[259] Sarbadhikary P, George BP, Abrahamse H. Recent Advances in Photosensitizers as Multifunctional Theranostic Agents for Imaging-Guided Photodynamic Therapy of Cancer. Theranostics. 2021;11(18):9054-9088. Published 2021 Aug 26. doi:10.7150/thno.62479

[260] Hong L, Li J, Luo Y, et al. Recent Advances in Strategies for Addressing Hypoxia in Tumor Photodynamic Therapy. Biomolecules. 2022;12(1):81. doi:10.3390/biom12010081.

[261] Liang R, Liu L, He H, et al. Oxygen-boosted immunogenic photodynamic therapy with gold nanocages@manganese dioxide to inhibit tumor growth and metastases. Biomaterials. 2018;177:149-160. doi:10.1016/j.biomaterials.2018.05.051.

[262] Li L , Nurunnabi M , Nafiujjaman M , Jeong YY , Lee YK , Huh KM . A photosensitizer-conjugated magnetic iron oxide/gold hybrid nanoparticle as an activatable platform for photodynamic cancer therapy. J Mater Chem B. 2014;2(19):2929-2937. doi:10.1039/c4tb00181h.

[263] Yoo SW, Oh G, Ahn JC, Chung E. Non-Oncologic Applications of Nanomedicine-Based Phototherapy. Biomedicines. 2021;9(2):113. doi:10.3390/biomedicines9020113.

[264] Kuo SH, Wu PT, Huang JY, Chiu CP, Yu J, Liao MY. Fabrication of Anisotropic Cu Ferrite-Polymer Core-Shell Nanoparticles for Photodynamic Ablation of Cervical Cancer Cells. Nanomaterials (Basel). 2020;10(12):2429. doi:10.3390/nano10122429.

[265] Zhou R, Zhang M, Xi J, et al. Gold Nanorods-Based Photothermal Therapy: Interactions Between Biostructure, Nanomaterial, and Near-Infrared Irradiation. Nanoscale Res Lett. 2022;17(1):68. doi:10.1186/s11671-022-03706-3.

[266] Han HS, Choi KY. Advances in Nanomaterial-Mediated Photothermal Cancer Therapies: Toward Clinical Applications. Biomedicines. 2021;9(3):305. doi:10.3390/biomedicines9030305.

[267] Chen W, Bardhan R, Bartels M, et al. A molecularly targeted theranostic probe for ovarian cancer. Mol Cancer Ther. 2010;9(4):1028-1038. doi:10.1158/1535-7163.MCT-09-0829.

[268] McGrath AJ, Chien YH, Cheong S, et al. Gold over Branched Palladium Nanostructures for Photothermal Cancer Therapy. ACS Nano. 2015;9(12):12283-12291. doi:10.1021/acsnano.5b05563.

[269] Siddique S, Chow JCL. Application of Nanomaterials in Biomedical Imaging and Cancer Therapy. Nanomaterials (Basel). 2020;10(9):1700. doi:10.3390/nano10091700.

[270] Lother D, Robert M, Elwood E, et al. Imaging in metastatic breast cancer, CT, PET/CT, MRI, WB-DWI, CCA: review and new perspectives. Cancer Imaging. 2023;23(1):53. doi:10.1186/s40644-023-00557-8.

[271] Wickline SA, Lanza GM. Nanotechnology for molecular imaging and targeted therapy. Circulation. 2003;107(8):1092-1095. doi:10.1161/01.cir.0000059651.17045.77.

[272] Sim S, Wong NK. Nanotechnology and its use in imaging and drug delivery (Review). Biomed Rep. 2021;14(5):42. doi:10.3892/br.2021.1418.

[273] Li X, Zhang XN, Li XD, Chang J. Multimodality imaging in nanomedicine and nanotheranostics. Cancer Biol Med. 2016;13(3):339-348. doi:10.20892/j.issn.2095-3941.2016.0055.

[274] Lee N, Choi SH, Hyeon T. Nano-sized CT contrast agents. Adv Mater. 2013;25(19):2641-2660. doi:10.1002/adma.201300081.

[275] Mojarrad P, Zamani S, Seyedhamzeh M, et al. Novel radiopharmaceutical (Technetium-99m)-(DOTA-NHS-ester)-Methionine as a SPECT-CT tumor imaging agent. Eur J Pharm Sci. 2020;141:105112. doi:10.1016/j.ejps.2019.105112.

[276] Giovinazzo H, Kumar P, Sheikh A, et al. Technetium Tc 99m sulfur colloid phenotypic probe for the pharmacokinetics and pharmacodynamics of PEGylated liposomal doxorubicin in women with ovarian cancer. Cancer Chemother Pharmacol. 2016;77(3):565-573. doi:10.1007/s00280-015-2945-y.

[277] Man F, Lammers T, T M de Rosales R. Imaging Nanomedicine-Based Drug Delivery: a Review of Clinical Studies. Mol Imaging Biol. 2018;20(5):683-695. doi:10.1007/s11307-018-1255-2.

[278] d'Angelo M, Castelli V, Benedetti E, et al. Theranostic Nanomedicine for Malignant Gliomas [published correction appears in Front Bioeng Biotechnol. 2020 Jan 30;7:468. doi: 10.3389/fbioe.2019.00468]. Front Bioeng Biotechnol. 2019;7:325. doi:10.3389/fbioe.2019.00325.

[279] Muthu MS, Leong DT, Mei L, Feng SS. Nanotheranostics - application and further development of nanomedicine strategies for advanced theranostics. Theranostics. 2014;4(6):660-677. doi:10.7150/thno.8698.

[280] Choi KY, Liu G, Lee S, Chen X. Theranostic nanoplatforms for simultaneous cancer imaging and therapy: current approaches and future perspectives. Nanoscale. 2012;4(2):330-342. doi:10.1039/c1nr11277e.

[281] Quiroz V, Devier J, Doloff J. Therapeutic Polymer Conjugates and Their Characterization. AAPS introductions in the pharmaceutical sciences. 2023:197-234. doi:10.1007/978-3-031-36135-7_10.

[282] Arora V, Bhandari DD, Puri R, Khatri N, HD. Synthesis, Self-Assembly, and Functional Chemistry of Amphiphilic Block Copolymers. 2023:1-25. doi:10.1007/978-981-99-0361-0_1.

[283] Li C , Tho CC , Galaktionova D , Chen X , Král P , Mirsaidov U . Dynamics of amphiphilic block copolymers in an aqueous solution: direct imaging of micelle formation and nanoparticle encapsulation. Nanoscale. 2019;11(5):2299-2305. doi:10.1039/c8nr08922a.

[284] Kuperkar K, Patel D, Atanase LI, Bahadur P. Amphiphilic Block Copolymers: Their Structures, and Self-Assembly to Polymeric Micelles and Polymersomes as Drug Delivery Vehicles. Polymers. 2022; 14(21):4702. doi:10.3390/polym14214702.

[285] Wakaskar RR. Polymeric Micelles and their Properties. Journal of Nanomedicine & Nanotechnology. 2017;08(02). doi: 10.4172/2157-7439.1000433.

[286] Yang H, Bao J, Mo L, et al. Bioreducible amphiphilic block copolymers based on PCL and glycopolypeptide as multifunctional theranostic nanocarriers for drug delivery and MR imaging. RSC Advances. 2017;7(34):21093-21106. doi:10.1039/c7ra01440f.

[287] Ji W, Zhang Y, Shao W, Kankala RK, Chen A. β-Cyclodextrin-based nanoassemblies for the treatment of atherosclerosis. Regen Biomater. 2024;11:rbae071. doi:10.1093/rb/rbae071.

[288] Guo B, Zhao J, Zhang Z, An X, Huang M, Wang S. Intelligent nanoenzyme for T1-weighted MRI guided theranostic applications. Chemical Engineering Journal. 2020;391:123609. doi:10.1016/j.cej.2019.123609.

[289] Vimbela GV, Ngo SM, Fraze C, Yang L, Stout DA. Antibacterial properties and toxicity from metallic nanomaterials [published correction appears in Int J Nanomedicine. 2018 Oct

16;13:6497. doi:10.2147/IJN.S183907.]. Int J Nanomedicine. 2017;12:3941-3965. doi:10.2147/IJN.S134526.

[290] Kulkarni S, Kumar S, Acharya S. Gold Nanoparticles in Cancer Therapeutics and Diagnostics. Cureus. 2022;14(10):e30096. doi:10.7759/cureus.30096.

[291] Xie M, Jiang J, Chao J. DNA-Based Gold Nanoparticle Assemblies: From Structure Constructions to Sensing Applications. Sensors (Basel). 2023;23(22):9229. Published 2023 Nov 16. doi:10.3390/s23229229.

[292] Sotnikov DV, Berlina AN, Ivanov VS, Zherdev AV, Dzantiev BB. Adsorption of proteins on gold nanoparticles: One or more layers?. Colloids Surf B Biointerfaces. 2019;173:557-563. doi:10.1016/j.colsurfb.2018.10.025.

[293] Chew AK, Dallin BC, Van Lehn RC. The Interplay of Ligand Properties and Core Size Dictates the Hydrophobicity of Monolayer-Protected Gold Nanoparticles. ACS Nano. 2021;15(3):4534-4545. doi:10.1021/acsnano.0c08623.

[294] Li C, Wang C, Ji Z, Jiang N, Lin W, Li D. Synthesis of thiol-terminated thermoresponsive polymers and their enhancement effect on optical limiting property of gold nanoparticles. European Polymer Journal. 2019;113:404-410. doi:10.1016/j.eurpolymj.2019.02.009.

[295] Fang W, Wang J, Lu S, et al. Encoding Morphogenesis of Quasi-Triangular Gold Nanoprisms with DNA. Angew Chem Int Ed Engl. 2022;61(39):e202208688. doi:10.1002/anie.202208688.

[296] Almeida JP, Chen AL, Foster A, Drezek R. In vivo biodistribution of nanoparticles. Nanomedicine (Lond). 2011;6(5):815-835. doi:10.2217/nnm.11.79.

[297] Lopez-Chaves C, Soto-Alvaredo J, Montes-Bayon M, Bettmer J, Llopis J, Sanchez-Gonzalez C. Gold nanoparticles: Distribution, bioaccumulation and toxicity. In vitro and in vivo studies. Nanomedicine. 2018;14(1):1-12. doi:10.1016/j.nano.2017.08.011.

[298] Boisselier E, Astruc D. Gold nanoparticles in nanomedicine: preparations, imaging, diagnostics, therapies and toxicity. Chem Soc Rev. 2009;38(6):1759-1782. doi:10.1039/b806051g.

[299] Milan J, Niemczyk K, Kus-Liśkiewicz M. Treasure on the Earth-Gold Nanoparticles and Their Biomedical Applications. Materials (Basel). 2022;15(9):3355. doi:10.3390/ma15093355.

[300] Iancu SD, Albu C, Chiriac L, et al. Assessment of Gold-Coated Iron Oxide Nanoparticles as Negative T2 Contrast Agent in Small Animal MRI Studies. Int J Nanomedicine. 2020;15:4811-4824. doi:10.2147/IJN.S253184.

[301] Rehan F, Zhang M, Fang J, Greish K. Therapeutic Applications of Nanomedicine: Recent Developments and Future Perspectives. Molecules. 2024;29(9):2073. doi:10.3390/molecules29092073.

[302] Mendes R, Fernandes AR, Baptista PV. Gold Nanoparticle Approach to the Selective Delivery of Gene Silencing in Cancer-The Case for Combined Delivery?. Genes (Basel). 2017;8(3):94. doi:10.3390/genes8030094.

[303] Patil T, Gambhir R, Vibhute A, Tiwari AP. Gold Nanoparticles: Synthesis Methods, Functionalization and Biological Applications. Journal of Cluster Science. 2022;34. doi:10.1007/s10876-022-02287-6.

[304] Nejati K, Dadashpour M, Gharibi T, Mellatyar H, Akbarzadeh A. Biomedical Applications of Functionalized Gold Nanoparticles: a Review. Journal of Cluster Science. 2021;33. doi:10.1007/s10876-020-01955-9.

[305] Ferreira D, Fontinha D, Martins C, Pires D, Fernandes AR, Baptista PV. Gold Nanoparticles for Vectorization of Nucleic Acids for Cancer Therapeutics. Molecules. 2020;25(15):3489. doi:10.3390/molecules25153489.

[306] Mahato K, Nagpal S, Shah MA, et al. Gold nanoparticle surface engineering strategies and their applications in biomedicine and diagnostics. 3 Biotech. 2019;9(2):57. doi:10.1007/s13205-019-1577-z.

[307] Fernandes AR, Baptista PV. Gene Silencing Using Multifunctionalized Gold Nanoparticles for Cancer Therapy. Methods Mol Biol. 2017;1530:319-336. doi:10.1007/978-1-4939-6646-2_19.

[308] Roma-Rodrigues C, Rivas-García L, Baptista PV, Fernandes AR. Gene Therapy in Cancer Treatment: Why Go Nano?. Pharmaceutics. 2020;12(3):233. doi:10.3390/pharmaceutics12030233.

[309] Baptista PV. Gold nanobeacons: a potential nanotheranostics platform. Nanomedicine (Lond). 2014;9(15):2247-2250. doi:10.2217/nnm.14.143.

[310] Kong L, Wu Y, Alves CS, Shi X. Efficient delivery of therapeutic siRNA into glioblastoma cells using multifunctional dendrimer-entrapped gold nanoparticles. Nanomedicine (Lond). 2016;11(23):3103-3115. doi:10.2217/nnm-2016-0240.

[311] Kong L, Wu Y, Alves CS, Shi X. Efficient delivery of therapeutic siRNA into glioblastoma cells using multifunctional dendrimer-entrapped gold nanoparticles. Nanomedicine. 2016;11(23):3103-3115. doi:10.2217/nnm-2016-0240.

[312] Adeyemi OS, Otuechere CA, Adewuyi A, Adeyanju AA, Awakan OJ, Otohinoyi DA. Gold nanoparticles in delivery applications. Elsevier eBooks. 2020:329-345. doi:10.1016/b978-0-08-102985-5.00014-0.

[313] Darmadi J, Anwar A. Current Progress on Gold Nanoparticle-Mediated Gene Delivery for Human Cancer Treatment. E3S Web of Conferences. 2024;488:03020-03020. doi:10.1051/e3sconf/202448803020.

[314] Raes L, Pille M, Harizaj A, et al. Cas9 RNP transfection by vapor nanobubble photoporation for ex vivo cell engineering. Molecular Therapy - Nucleic Acids. 2021;25:696-707. doi:10.1016/j.omtn.2021.08.014.

[315] Salama MM, Aborehab NM, El M, Zayed A, Ezzat SM. Nanotechnology in leukemia: diagnosis, efficient-targeted drug delivery, and clinical trials. European Journal of Medical Research. 2023;28(1). doi: 10.1186/s40001-023-01539-z.

[316] Janani G, Girigoswami A, Girigoswami K. Supremacy of nanoparticles in the therapy of chronic myelogenous leukemia. ADMET DMPK. 2023;11(4):499-511. doi:10.5599/admet.2013.

[317] Liu Y , Zhao G , Xu CF , Luo YL , Lu ZD , Wang J . Systemic delivery of CRISPR/Cas9 with PEG-PLGA nanoparticles for chronic myeloid leukemia targeted therapy. Biomater Sci. 2018;6(6):1592-1603. doi:10.1039/c8bm00263k.

[318] Vinhas R, Fernandes AR, Baptista PV. Gold Nanoparticles for BCR-ABL1 Gene Silencing: Improving Tyrosine Kinase Inhibitor Efficacy in Chronic Myeloid Leukemia. Mol Ther Nucleic Acids. 2017;7:408-416. doi:10.1016/j.omtn.2017.05.003.

[319] Fan L, Liu C, Hu A, et al. Dual oligopeptides modification mediates arsenic trioxide containing nanoparticles to eliminate primitive chronic myeloid leukemia cells inside bone marrow niches. Int J Pharm. 2020;579:119179. doi:10.1016/j.ijpharm.2020.119179.

[320] Min QH, Wang XZ, Zhang J, et al. Exosomes derived from imatinib-resistant chronic myeloid leukemia cells mediate a horizontal transfer of drug-resistant trait by delivering miR-365. Exp Cell Res. 2018;362(2):386-393. doi:10.1016/j.yexcr.2017.12.001.

[321] Liu D, Xing J, Xiong F, Yang F, Gu N. Preparation and in vivo safety evaluations of antileukemic homoharringtonine-loaded PEGylated liposomes. Drug Dev Ind Pharm. 2017;43(4):652-660. doi:10.1080/03639045.2016.1275670.

[322] Elderdery AY, Alzahrani B, Hamza SMA, Mostafa-Hedeab G, Mok PL, Subbiah SK. CuO-TiO2-Chitosan-Berbamine Nanocomposites Induce Apoptosis through the Mitochondrial Pathway with the Expression of P53, BAX, and BCL-2 in the Human K562 Cancer Cell Line [retracted in: Bioinorg Chem Appl. 2023 Dec 13;2023:9856534. doi: 10.1155/2023/9856534.]. Bioinorg Chem Appl. 2022;2022:9602725. doi:10.1155/2022/9602725.

[323] Jiang G, Huang Z, Yuan Y, Tao K, Feng W. Intracellular delivery of anti-BCR/ABL antibody by PLGA nanoparticles suppresses the oncogenesis of chronic myeloid leukemia cells. J Hematol Oncol. 2021;14(1):139. doi:10.1186/s13045-021-01150-x.

[324] Amerigos Daddy J C K, Chen M, Raza F, Xiao Y, Su Z, Ping Q. Co-Encapsulation of Mitoxantrone and β-Elemene in Solid Lipid Nanoparticles to Overcome Multidrug Resistance in Leukemia. Pharmaceutics. 2020;12(2):191. doi:10.3390/pharmaceutics12020191.

[325] Libutti SK, Paciotti GF, Byrnes AA, et al. Phase I and pharmacokinetic studies of CYT-6091, a novel PEGylated colloidal gold-rhTNF nanomedicine. Clin Cancer Res. 2010;16(24):6139-6149. doi:10.1158/1078-0432.CCR-10-0978.

[326] Khoobchandani M, Katti KK, Karikachery AR, et al. New Approaches in Breast Cancer Therapy Through Green Nanotechnology and Nano-Ayurvedic Medicine - Pre-Clinical and Pilot Human Clinical Investigations. Int J Nanomedicine. 2020;15:181-197. doi:10.2147/IJN.S219042.

[327] Kumthekar P, Ko CH, Paunesku T, et al. A first-in-human phase 0 clinical study of RNA interference-based spherical nucleic acids in patients with recurrent glioblastoma. Sci Transl Med. 2021;13(584):eabb3945. doi:10.1126/scitranslmed.abb3945.

[328] Cross NCP, White HE, Evans PAS, et al. Consensus on BCR-ABL1 reporting in chronic myeloid leukaemia in the UK. Br J Haematol. 2018;182(6):777-788. doi:10.1111/bjh.15542.

[329] Abdelmagid MG, Litzow MR, McCullough KB, et al. Chronic phase CML with sole P190 (e1a2) BCR::ABL1: long-term outcome among ten consecutive cases. Blood Cancer J. 2022;12(7):103. doi:10.1038/s41408-022-00696-4.

[330] Zenebe B, Nigussie H, Belay G, Seboka N. A review on characterization of BCR – ABL transcript variants for molecular monitoring of chronic myeloid leukemia phenotypes. Hematology. 2023;28(1). doi: 10.1080/16078454.2023.2284038.

[331] de Lavallade H, Kizilors A. The Importance of Mutational Analysis in Chronic Myeloid Leukaemia for Treatment Choice. EMJ Oncology. 2016;4[1]:86-95. doi:10.33590/emjoncol/10311536.

[332] Vinhas R, Cordeiro M, Pedrosa P, Fernandes AR, Baptista PV. Current trends in molecular diagnostics of chronic myeloid leukemia. Leuk Lymphoma. 2017;58(8):1791-1804. doi:10.1080/10428194.2016.1265116.

[333] van Dongen JJ, Macintyre EA, Gabert JA, et al. Standardized RT-PCR analysis of fusion gene transcripts from chromosome aberrations in acute leukemia for detection of minimal residual disease. Report of the BIOMED-1 Concerted Action: investigation of minimal residual disease in acute leukemia. Leukemia. 1999;13(12):1901-1928. doi:10.1038/sj.leu.2401592.

[334] Kagita S, Mamidi TK, Digumarti L, Gundeti S, Digumarti R. Assessment of BCR-ABL1 Fusion Transcripts and Their Association with Response to Imatinib Treatment in Chronic Myeloid Leukemia Patients. Indian Journal of Medical and Paediatric Oncology. 2018;39(02):165-171. doi:10.4103/ijmpo.ijmpo_80_17.

[335] Arun AK, Senthamizhselvi A, Mani S, et al. Frequency of rare BCR-ABL1 fusion transcripts in chronic myeloid leukemia patients. Int J Lab Hematol. 2017;39(3):235-242. doi:10.1111/ijlh.12616.

[336] Hanfstein B, Lauseker M, Hehlmann R, et al. Distinct characteristics of e13a2 versus e14a2 BCR-ABL1 driven chronic myeloid leukemia under first-line therapy with imatinib. Haematologica. 2014;99(9):1441-1447. doi:10.3324/haematol.2013.096537.

[337] Deb P, Chakrabarti P, Chakrabarty S, et al. Incidence of BCR-ABL transcript variants in patients with chronic myeloid leukemia: Their correlation with presenting features, risk scores and response to treatment with imatinib mesylate. Indian J Med Paediatr Oncol. 2014;35(1):26-30. doi:10.4103/0971-5851.133707.

[338] Osman EA, Hamad K, Elmula IM, Ibrahim ME. Frequencies of BCR-ABL1 fusion transcripts among Sudanese chronic myeloid leukaemia patients. Genet Mol Biol. 2010;33(2):229-231. doi:10.1590/S1415-47572010005000037.

[339] Yaghmaie M, Ghaffari SH, Ghavamzadeh A, et al. Frequency of BCR-ABL fusion transcripts in Iranian patients with chronic myeloid leukemia. Arch Iran Med. 2008;11(3):247-251.

[340] Quintás-Cardama A, Kantarjian H, Cortes J. Imatinib and beyond--exploring the full potential of targeted therapy for CML. Nat Rev Clin Oncol. 2009;6(9):535-543. doi:10.1038/nrclinonc.2009.112.

[341] Seman ZA, Ahid F, Kamaluddin NR, et al. Mutation analysis of BCR-ABL1 kinase domain in chronic myeloid leukemia patients with tyrosine kinase inhibitors resistance: a Malaysian cohort study. BMC Res Notes. 2024;17(1):111. doi:10.1186/s13104-024-06772-1.

[342] Poláková KM, Polívková V, Rulcová J, et al. Constant BCR-ABL transcript level >or=0.1% (IS) in patients with CML responding to imatinib with complete cytogenetic remission may indicate mutation analysis. Exp Hematol. 2010;38(1):20-26. doi:10.1016/j.exphem.2009.10.003.

[343] American Type Culture Collection. K562 (ATCC® CCL-243™) [Cell line]. Manassas, VA: ATCC; [2025]. Available from: https://www.atcc.org.

[344] Pedrosa P, Mendes R, Cabral R, Martins LMDRS, Baptista PV, Fernandes AR. Combination of chemotherapy and Au-nanoparticle photothermy in the visible light to tackle doxorubicin resistance in cancer cells. Sci Rep. 2018;8(1):11429. doi:10.1038/s41598-018-29870-0.

[345] Balatzenko G, Vundinti BR, Margarita G. Correlation between the type of bcr-abl transcripts and blood cell counts in chronic myeloid leukemia - a possible influence of mdr1 gene expression. Hematol Rep. 2011;3(1):e3. doi:10.4081/hr.2011.e3.

[346] Kang ZJ, Liu YF, Xu LZ, et al. The Philadelphia chromosome in leukemogenesis. Chin J Cancer. 2016;35:48. doi:10.1186/s40880-016-0108-0.

[347] Tiribelli M, Eskazan AE. Tyrosine Kinase Inhibitor Sequencing in Patients with Chronic Myeloid Leukemia. Oncology and Therapy. 2019;95:100. doi: 10.1007/s40487-019-00098-w.

[348] Massimino M, Vigneri P, Stella S, et al. Combined Inhibition of Bcl2 and Bcr-Abl1 Exercises Anti-Leukemia Activity but Does Not Eradicate the Primitive Leukemic Cells. J Clin Med. 2021;10(23):5606. doi:10.3390/jcm10235606.

[349] Mojtahedi H, Yazdanpanah N, Rezaei N. Chronic myeloid leukemia stem cells: targeting therapeutic implications. Stem Cell Res Ther. 2021;12(1):603. doi:10.1186/s13287-021-02659-1.

[350] Elbadawy M, Usui T, Yamawaki H, Sasaki K. Emerging Roles of C-Myc in Cancer Stem Cell-Related Signaling and Resistance to Cancer Chemotherapy: A Potential Therapeutic Target Against Colorectal Cancer. Int J Mol Sci. 2019;20(9):2340. doi:10.3390/ijms20092340.

[351] Sorolla A, Wang E, Golden E, et al. Precision medicine by designer interference peptides: applications in oncology and molecular therapeutics. Oncogene. 2019; 39:1167-1184. doi:https://doi.org/10.1038/s41388-019-1056-3.

[352] Wang T, Cai B, Ding M, Su Z, Liu Y, Shen L. c-Myc Overexpression Promotes Oral Cancer Cell Proliferation and Migration by Enhancing Glutaminase and Glutamine Synthetase Activity. Am J Med Sci. 2019;358(3):235-242. doi:10.1016/j.amjms.2019.05.014.

[353] Baluapuri A, Wolf E, Eilers M. Target gene-independent functions of MYC oncoproteins. Nat Rev Mol Cell Biol. 2020;21(5):255-267. doi:10.1038/s41580-020-0215-2.

[354] Liu N, Li P, Zang S, et al. Novel agent nitidine chloride induces erythroid differentiation and apoptosis in CML cells through c-Myc-miRNAs axis. PLoS One. 2015;10(2):e0116880. doi:10.1371/journal.pone.0116880.

[355] Roskoski R Jr. Targeting BCR-Abl in the treatment of Philadelphia-chromosome positive chronic myelogenous leukemia. Pharmacol Res. 2022;178:106156. doi:10.1016/j.phrs.2022.106156.

[356] Remant KC, Thapa B, Ubeda A, Jiang X, Uludag H. BCR-Abl Silencing by siRNA: A Potent Approach to Sensitize Chronic Myeloid Leukemia Cells to Tyrosine Kinase Inhibitor Therapy. STEM CELLS AND DEVELOPMENT. 2019;28(11):734-744. doi:10.1089/scd.2018.019.

[357] Crooke ST, Liang XH, Baker BF, Crooke RM. Antisense technology: A review. J Biol Chem. 2021;296:100416. doi:10.1016/j.jbc.2021.100416.

[358] Krishnan AV, Mishra D. Antisense Oligonucleotides: A Unique Treatment Approach. Indian Pediatrics. 2020;57(2):165-171. doi:.1007/s13312-020-1736-7.

[359] Le BT, Raguraman P, Kosbar TR, Fletcher S, Wilton SD, Veedu RN. Antisense Oligonucleotides Targeting Angiogenic Factors as Potential Cancer Therapeutics. Mol Ther Nucleic Acids. 2019;14:142-157. doi:10.1016/j.omtn.2018.11.007.

[360] Lee PC, Meisel D. Adsorption and surface-enhanced Raman of dyes on silver and gold sols. The Journal of Physical Chemistry. 1982;86(17):3391-3395. doi: 10.1021/j100214a025.

[361] Liu X, Atwater M, Wang J, Huo Q. Extinction coefficient of gold nanoparticles with different sizes and different capping ligands. Colloids Surf B Biointerfaces. 2007;58(1):3-7. doi:10.1016/j.colsurfb.2006.08.005.

[362] Livak KJ, Schmittgen TD. Analysis of relative gene expression data using real-time quantitative PCR and the 2(-Delta Delta C(T)) Method. Methods. 2001;25(4):402-408. doi:10.1006/meth.2001.1262.

[363] Conde J, Dias JT, GrazÃo V, Moros M, Baptista PV, de la Fuente JM. Revisiting 30 years of biofunctionalization and surface chemistry of inorganic nanoparticles for nanomedicine. Frontiers in Chemistry. 2014;2;48. doi: 10.3389/fchem.2014.00048.

[364] Jokerst JV, Lobovkina T, Zare RN, Gambhir SS. Nanoparticle PEGylation for imaging and therapy. Nanomedicine (Lond). 2011;6(4):715-728. doi:10.2217/nnm.11.19.

[365] Conde J, Doria G, Baptista P. Noble metal nanoparticles applications in cancer. J Drug Deliv. 2012;2012:751075. doi:10.1155/2012/751075.

[366] Baptista P, Conde J, Rosa J, Baptista P. Gold-Nanobeacons as a theranostic system for the detection and inhibition of specific genes. 2013. doi: 10.1038/protex.2013.088.

[367] Khlebtsov NG. Optics and biophotonics of nanoparticles with a plasmon resonance. Quantum Electronics. 2008;38(6):504-529. doi: 10.1070/qe2008v038n06abeh013829.

[368] Susnik E, Bazzoni A, Taladriz-Blanco P, et al. Epidermal growth factor alters silica nanoparticle uptake and improves gold-nanoparticle-mediated gene silencing in A549 cells. Front Nanotechnol. 2023;5:1220514. doi:10.3389/fnano.2023.1220514.

[369] Srijampa S, Buddhisa S, Ngernpimai S, et al. Influence of Gold Nanoparticles with Different Surface Charges on Localization and Monocyte Behavior. Bioconjug Chem. 2020;31(4):1133-1143. doi:10.1021/acs.bioconjchem.9b00847.

[370] Wang P, Wang X, Wang L, Hou X, Liu W, Chen C. Interaction of gold nanoparticles with proteins and cells. Science and Technology of Advanced Materials. 2015;16(3):034610. doi: 10.1088/1468-6996/16/3/034610.

[371] Kus-Liśkiewicz M, Fickers P, Ben Tahar I. Biocompatibility and Cytotoxicity of Gold Nanoparticles: Recent Advances in Methodologies and Regulations. Int J Mol Sci. 2021;22(20):10952. doi:10.3390/ijms222010952.

[372] Li Z, Lei Z, Zhang J, Liu D, Wang Z. Effects of Size, Shape, Surface Charge and Functionalization on Cytotoxicity of Gold Nanoparticles. Nano LIFE. 2015;05(01):1540003. doi:10.1142/s1793984415400036.

[373] Sharma N, Magistroni V, Piazza R, et al. BCR/ABL1 and BCR are under the transcriptional control of the MYC oncogene. Molecular Cancer. 2015;14(1). doi: 10.1186/s12943-015-0407-0.

[374] Perrotti D, Jamieson C, Goldman J, Skorski T. Chronic myeloid leukemia: mechanisms of blastic transformation. J Clin Invest. 2010;120(7):2254-2264. doi:10.1172/JCI41246.

[375] Albajar M, Gómez-Casares MT, Llorca J, et al. MYC in chronic myeloid leukemia: induction of aberrant DNA synthesis and association with poor response to imatinib. Mol Cancer Res. 2011;9(5):564-576. doi:10.1158/1541-7786.MCR-10-0356.

[376] Kari S, Subramanian K, Altomonte IA, Murugesan A, Yli-Harja O, Kandhavelu M. Programmed cell death detection methods: a systematic review and a categorical comparison. Apoptosis. 2022;27(7-8):482-508. doi:10.1007/s10495-022-01735-y.

[377] Haririan M, Kaviani S, Soleimani M, Ghaemi SR, Delalat B, Atashi A. Morpholino Oligo Antisense efficiently suppresses BCR/ABL and cell proliferation in CML: specific inhibition of BCR-ABL gene expression by Morpholino Oligo Antisense in BCR-ABL(+) cells. Hematology. 2012;17(1):28-34. doi:10.1179/102453311X13127324303470.

[378] Jacquel A, Herrant M, Legros L, et al. Imatinib induces mitochondria-dependent apoptosis of the Bcr-Abl-positive K562 cell line and its differentiation toward the erythroid lineage [published correction appears in FASEB J. 2003 Dec;17(15):2347]. FASEB J. 2003;17(14):2160-2162. doi:10.1096/fj.03-0322.

[379] Jacquel A, Colosetti P, Grosso S, et al. Apoptosis and erythroid differentiation triggered by Bcr-Abl inhibitors in CML cell lines are fully distinguishable processes that exhibit differ-

ent sensitivity to caspase inhibition. Oncogene. 2007;26(17):2445-2458. doi:10.1038/sj.onc.1210034.

[380] Notari M, Neviani P, Santhanam R, et al. A MAPK/HNRPK pathway controls BCR/ABL oncogenic potential by regulating MYC mRNA translation. Blood. 2006;107(6):2507-2516. doi:10.1182/blood-2005-09-3732

[381] Skorski T, Bellacosa A, Nieborowska-Skorska M, et al. Transformation of hematopoietic cells by BCR/ABL requires activation of a PI-3k/Akt-dependent pathway. EMBO J. 1997;16(20):6151-6161. doi:10.1093/emboj/16.20.6151.

[382] Birchenall-Roberts MC, Yoo YD, Bertolette DC 3rd, et al. The p120-v-Abl protein interacts with E2F-1 and regulates E2F-1 transcriptional activity. J Biol Chem. 1997;272(14):8905-8911. doi:10.1074/jbc.272.14.8905.

[383] Xie S, Lin H, Sun T, Arlinghaus RB. Jak2 is involved in c-Myc induction by Bcr-Abl. Oncogene. 2002;21(47):7137-7146. doi:10.1038/sj.onc.1205942.

[384] Sawyers CL, Callahan W, Witte ON. Dominant negative MYC blocks transformation by ABL oncogenes. Cell. 1992;70(6):901-910. doi:10.1016/0092-8674(92)90241-4.

[385] Gómez-Casares MT, García-Alegria E, López-Jorge CE, et al. MYC antagonizes the differentiation induced by imatinib in chronic myeloid leukemia cells through downregulation of p27(KIP1.). Oncogene. 2013;32(17):2239-2246. doi:10.1038/onc.2012.246.

[386] Kawano T, Horiguchi-Yamada J, Iwase S, et al. Depsipeptide enhances imatinib mesylate-induced apoptosis of Bcr-Abl-positive cells and ectopic expression of cyclin D1, c-Myc or active MEK abrogates this effect. Anticancer Res. 2004;24(5A):2705-2712.

[387] Jabbour E, Kantarjian H, Jones D, et al. Frequency and clinical significance of BCR-ABL mutations in patients with chronic myeloid leukemia treated with imatinib mesylate. Leukemia. 2006;20(10):1767-1773. doi:10.1038/sj.leu.2404318.

[388] Shah NP, Nicoll JM, Nagar B, et al. Multiple BCR-ABL kinase domain mutations confer polyclonal resistance to the tyrosine kinase inhibitor imatinib (STI571) in chronic phase and blast crisis chronic myeloid leukemia. Cancer Cell. 2002;2(2):117-125. doi:10.1016/s1535-6108(02)00096-x.

[389] Weisberg E, Manley PW, Cowan-Jacob SW, Hochhaus A, Griffin JD. Second generation inhibitors of BCR-ABL for the treatment of imatinib-resistant chronic myeloid leukaemia. Nat Rev Cancer. 2007;7(5):345-356. doi:10.1038/nrc2126.

[390] Donato NJ, Wu JY, Stapley J, et al. Imatinib mesylate resistance through BCR-ABL independence in chronic myelogenous leukemia [published correction appears in Cancer Res. 2004 Mar 15;64(6):2306. Shishodin, Shishir [corrected to Shishodia, Shishir]]. Cancer Res. 2004;64(2):672-677. doi:10.1158/0008-5472.can-03-1484.

[391] Khorashad JS, Anand M, Marin D, et al. The presence of a BCR-ABL mutant allele in CML does not always explain clinical resistance to imatinib. Leukemia. 2006;20(4):658-663. doi:10.1038/sj.leu.2404137.

[392] Xie S, Wang Y, Liu J, et al. Involvement of Jak2 tyrosine phosphorylation in Bcr-Abl transformation. Oncogene. 2001;20(43):6188-6195. doi:10.1038/sj.onc.1204834.

[393] Samanta AK, Lin H, Sun T, Kantarjian H, Arlinghaus RB. Janus kinase 2: a critical target in chronic myelogenous leukemia. Cancer Res. 2006;66(13):6468-6472. doi:10.1158/0008-5472.CAN-06-0025.

[394] Conde J, Rosa J, de la Fuente JM, Baptista PV. Gold-nanobeacons for simultaneous gene specific silencing and intracellular tracking of the silencing events. Biomaterials. 2013;34(10):2516-2523. doi:10.1016/j.biomaterials.2012.12.015.

[395] Kohnken R, Porcu P, Mishra A. Overview of the Use of Murine Models in Leukemia and Lymphoma Research. Front Oncol. doi:10.3389/fonc.2017.00022.

[396] Bayat Mokhtari R, Homayouni TS, Baluch N, et al. Combination therapy in combating cancer. Oncotarget. 2017;8(23):38022-38043. doi:10.18632/oncotarget.16723.

[397] Frei E 3rd, Karon M, Levin RH, et al. The effectiveness of combinations of antileukemic agents in inducing and maintaining remission in children with acute leukemia. Blood. 1965;26(5):642-656.

[398] Ayoub NM. Editorial: Novel Combination Therapies for the Treatment of Solid Cancers. Front Oncol. 2021;11:708943. Published 2021 Jun 18. doi:10.3389/fonc.2021.708943.

[399] Plana D, Palmer AC, Sorger PK. Independent Drug Action in Combination Therapy: Implications for Precision Oncology. Cancer Discov. 2022;12(3):606-624. doi:10.1158/2159-8290.CD-21-0212.

[400] Blagosklonny MV. Overcoming limitations of natural anticancer drugs by combining with artificial agents. Trends in Pharmacological Sciences. 2005;26(2):77-81. doi:10.1016/j.tips.2004.12.002.

[401] Shrestha B, Wang L, Zhang H, Hung CY, Tang L. Gold Nanoparticles Mediated Drug-Gene Combinational Therapy for Breast Cancer Treatment. Int J Nanomedicine. 2020;15:8109-8119. doi:10.2147/IJN.S258625.

[402] Amreddy N, Babu A, Panneerselvam J, et al. Chemo-biologic combinatorial drug delivery using folate receptor-targeted dendrimer nanoparticles for lung cancer treatment. Nanomedicine. 2018;14(2):373-384. doi:10.1016/j.nano.2017.11.010.

[403] Xie Z, Guo W, Guo N, et al. Targeting tumor hypoxia with stimulus-responsive nanocarriers in overcoming drug resistance and monitoring anticancer efficacy. Acta Biomater. 2018;71:351-362. doi:10.1016/j.actbio.2018.03.013.

[404] Han X, Li Y, Xu Y, et al. Reversal of pancreatic desmoplasia by re-educating stellate cells with a tumour microenvironment-activated nanosystem. Nat Commun. 2018;9(1):3390. doi:10.1038/s41467-018-05906-x.

[405] Hameed H, Sarwar HS, Younas K, et al. Exploring the potential of nanomedicine for gene therapy across the physicochemical and cellular barriers. Funct Integr Genomics. 2024;24(5):177. doi:10.1007/s10142-024-01459-z.

[406] Bhargava C, Sharma PK, Sachdeva A. The Era of Nanotechnology. CRC Press; 2021.

[407] Beik J, Khateri M, Khosravi Z, et al. Gold nanoparticles in combinatorial cancer therapy strategies. Coordination Chemistry Reviews. 2019;387:299-324. doi: 10.1016/j.ccr.2019.02.025.

[408] Westerweel PE, Te Boekhorst PAW, Levin MD, Cornelissen JJ. New Approaches and Treatment Combinations for the Management of Chronic Myeloid Leukemia. Front Oncol. 2019;9:665. doi:10.3389/fonc.2019.00665.

[409] Giles FJ, Cortes J, Jones D, Bergstrom D, Kantarjian H, Freedman SJ. MK-0457, a novel kinase inhibitor, is active in patients with chronic myeloid leukemia or acute lymphocytic leukemia with the T315I BCR-ABL mutation. Blood. 2007;109(2):500-502. doi:10.1182/blood-2006-05-025049.

[410] Hyun SY, Hwang HI, Jang YJ. Polo-like kinase-1 in DNA damage response [published correction appears in BMB Rep. 2014 Jun;47(6):360. Hwan Hyo-In [corrected to Hwang Hyo-In]]. BMB Rep. 2014;47(5):249-255. doi:10.5483/bmbrep.2014.47.5.061.

[411] Edwards DM, Speers C, Wahl DR. Targeting Noncanonical Regulators of the DNA Damage Response to Selectively Overcome Cancer Radiation Resistance. Semin Radiat Oncol. 2022;32(1):64-75. doi:10.1016/j.semradonc.2021.09.006.

[412] Do K, Wilsker D, Ji J, et al. Phase I Study of Single-Agent AZD1775 (MK-1775), a Wee1 Kinase Inhibitor, in Patients With Refractory Solid Tumors. J Clin Oncol. 2015;33(30):3409-3415. doi:10.1200/JCO.2014.60.4009.

[413] Leijen S, van Geel RM, Sonke GS, et al. Phase II Study of WEE1 Inhibitor AZD1775 Plus Carboplatin in Patients With TP53-Mutated Ovarian Cancer Refractory or Resistant to First-Line Therapy Within 3 Months. J Clin Oncol. 2016;34(36):4354-4361. doi:10.1200/JCO.2016.67.5942.

[414] De Santis S, Monaldi C, Mancini M, Bruno S, Cavo M, Soverini S. Overcoming Resistance to Kinase Inhibitors: The Paradigm of Chronic Myeloid Leukemia. Onco Targets Ther. 2022;15:103-116. Published 2022 Jan 25. doi:10.2147/OTT.S289306.

[415] Otto T, Sicinski P. Cell cycle proteins as promising targets in cancer therapy. Nat Rev Cancer. 2017;17(2):93-115. doi:10.1038/nrc.2016.138.

[416] Rossari F, Minutolo F, Orciuolo E. Past, present, and future of Bcr-Abl inhibitors: from chemical development to clinical efficacy. J Hematol Oncol. 2018;11(1):84. doi:10.1186/s13045-018-0624-2.

[417] Balabanov S, Gontarewicz A, Keller G, et al. Abcg2 overexpression represents a novel mechanism for acquired resistance to the multi-kinase inhibitor Danusertib in BCR-ABL-positive cells in vitro. PLoS One. 2011;6(4):e19164. doi:10.1371/journal.pone.0019164.

[418] Awad S A, Dufva O, Klievink J, et al. Integrated drug profiling and CRISPR screening identify BCR::ABL1-independent vulnerabilities in chronic myeloid leukemia. Cell Rep Med. 2024;5(5):101521. doi:10.1016/j.xcrm.2024.101521.

A

An Appendix

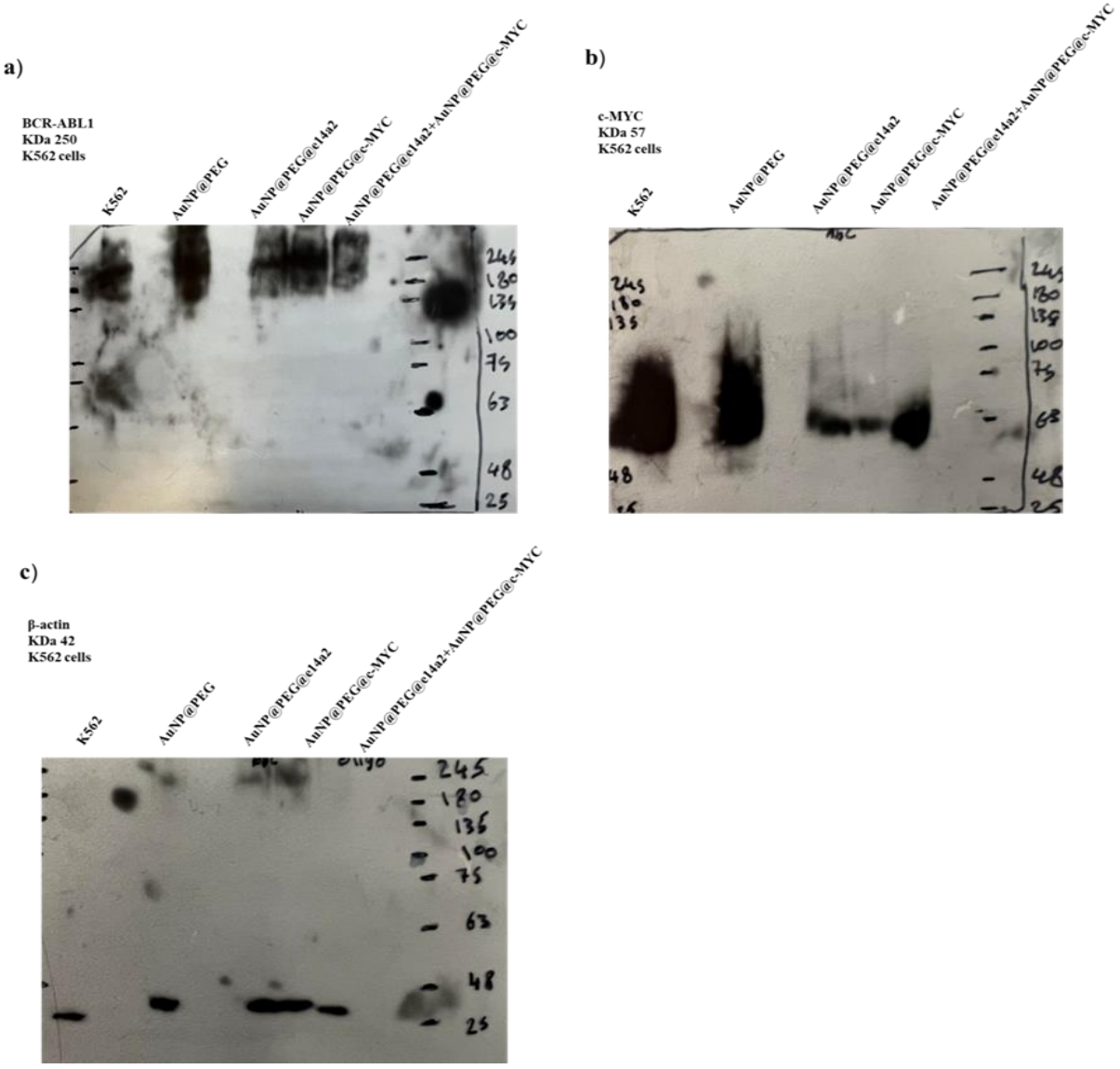

Figure A.1 — Western blot images for BCR-ABL, c-MYC and β-actin protein expression levels in K562 cell line after exposure cells to Au-nanoconjugates (old lysis buffer). (a) protein expression levels of BCR-ABL1 (250 KDa) after challenged cells with Au-nanoconjugates for 24h; (b) protein expression levels of c-MYC (57 KDa) after challenged cells with Au-nanoconjugates for 24h; (c) protein expression levels of β-actin (42 KDa) after challenged cells with Au-nanoconjugates for 24h.

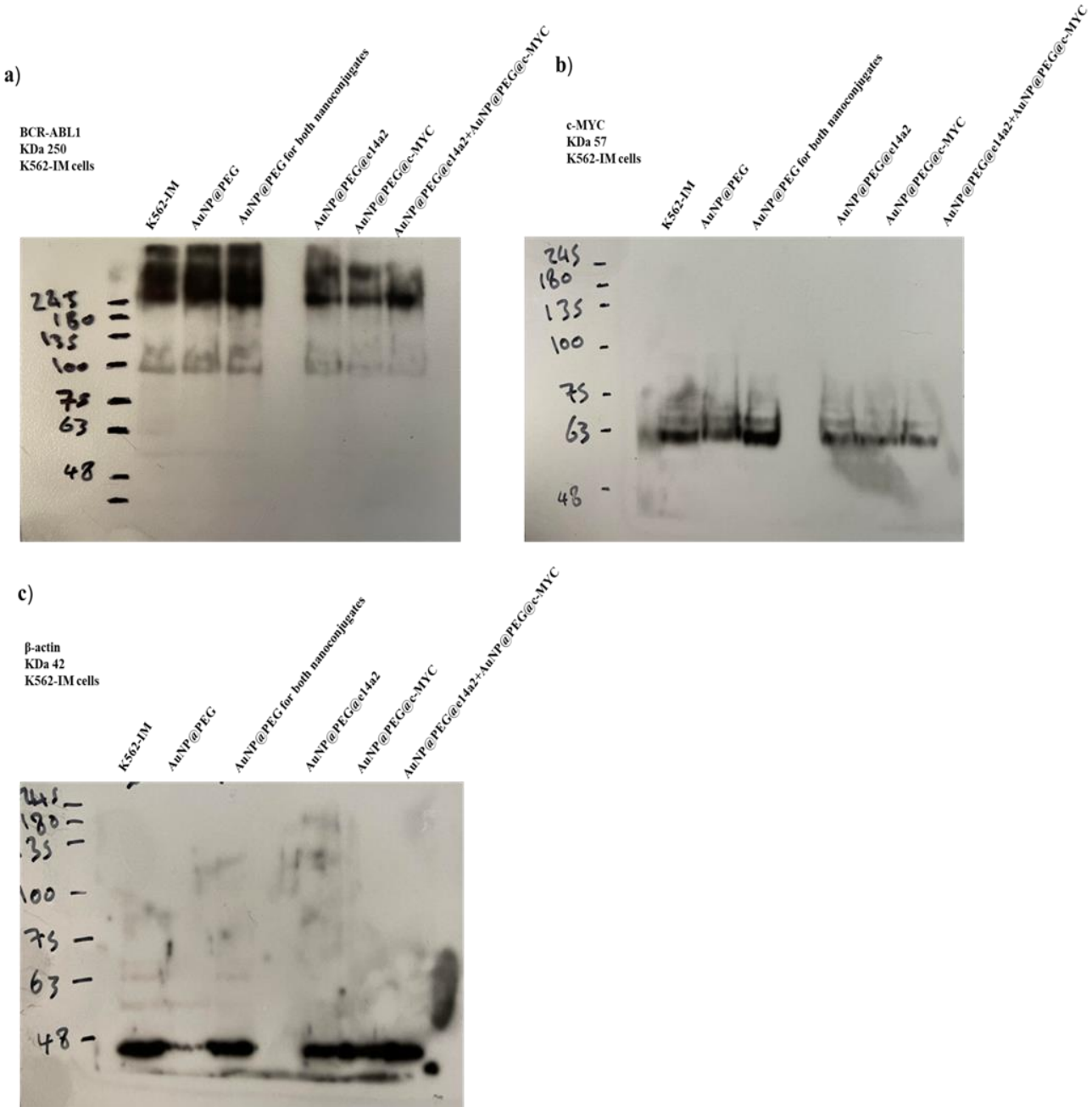

Figure A.2 — Western blot images for BCR-ABL, c-MYC and β-actin protein expression levels in K562-IM cell line after exposure cells to Au-nanoconjugates (old lysis buffer). (a) protein expression levels of BCR-ABL1 (250 KDa) after challenged cells with Au-nanoconjugates for 24h; (b) protein expression lev-

els of c-MYC (57 KDa) after challenged cells with Au-nanoconjugates for 24h; (c) protein expression levels of β-actin (42 KDa) after challenged cells with Au-nanoconjugates for 24h.

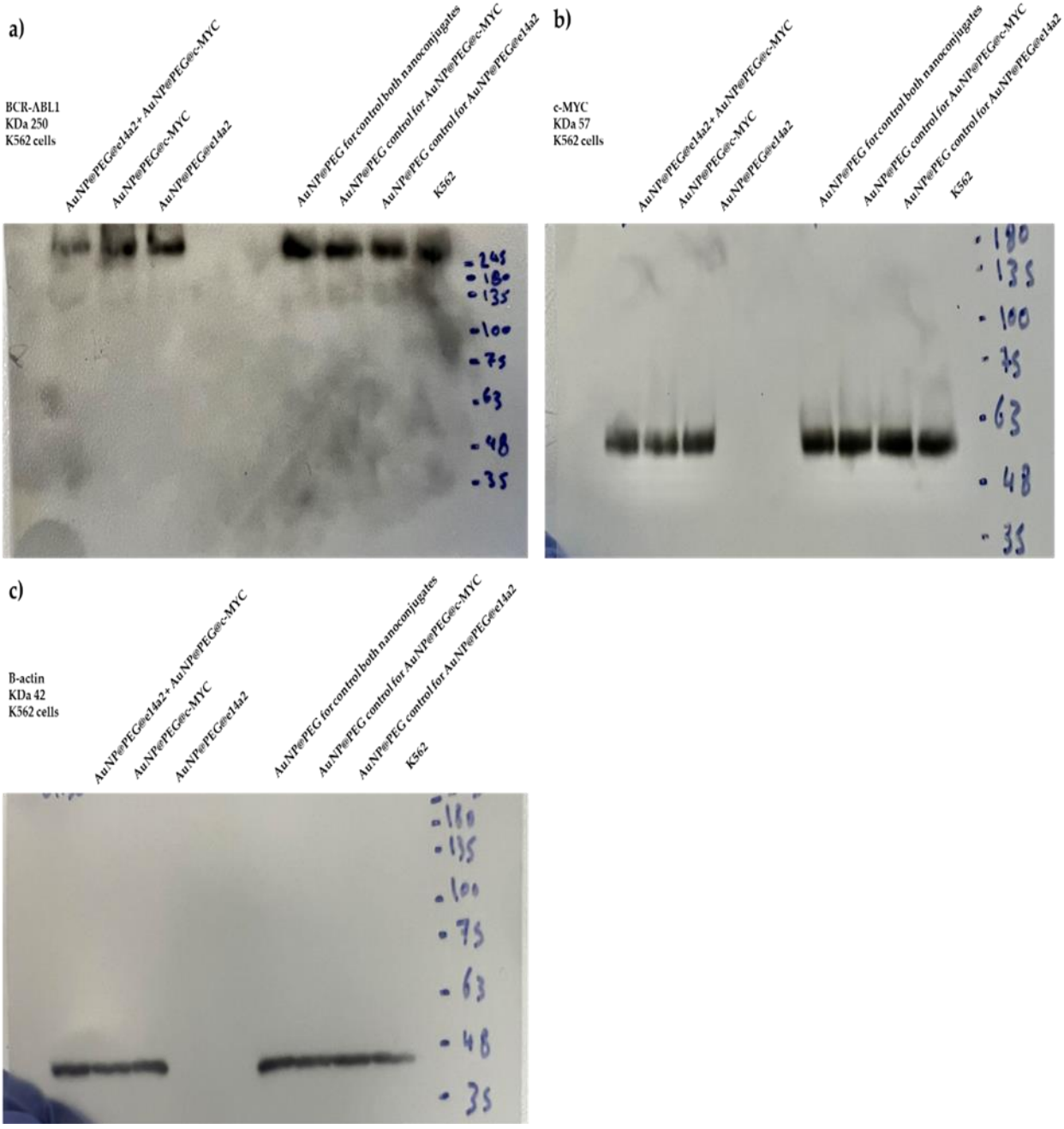

Figure A.3 — Western blot images for BCR-ABL, c-MYC and β-actin protein expression levels in K562 cell line after exposure cells to Au-nanoconjugates (replaced lysis buffer). (a) protein expression levels of BCR-ABL1 (250 KDa) after challenged cells with Au-nanoconjugates for 24h; (b) protein expression levels of c-MYC (57 KDa) after challenged cells with Au-nanoconjugates for 24h; (c) protein expression levels of β-actin (42 KDa) after challenged cells with Au-nanoconjugates for 24h.

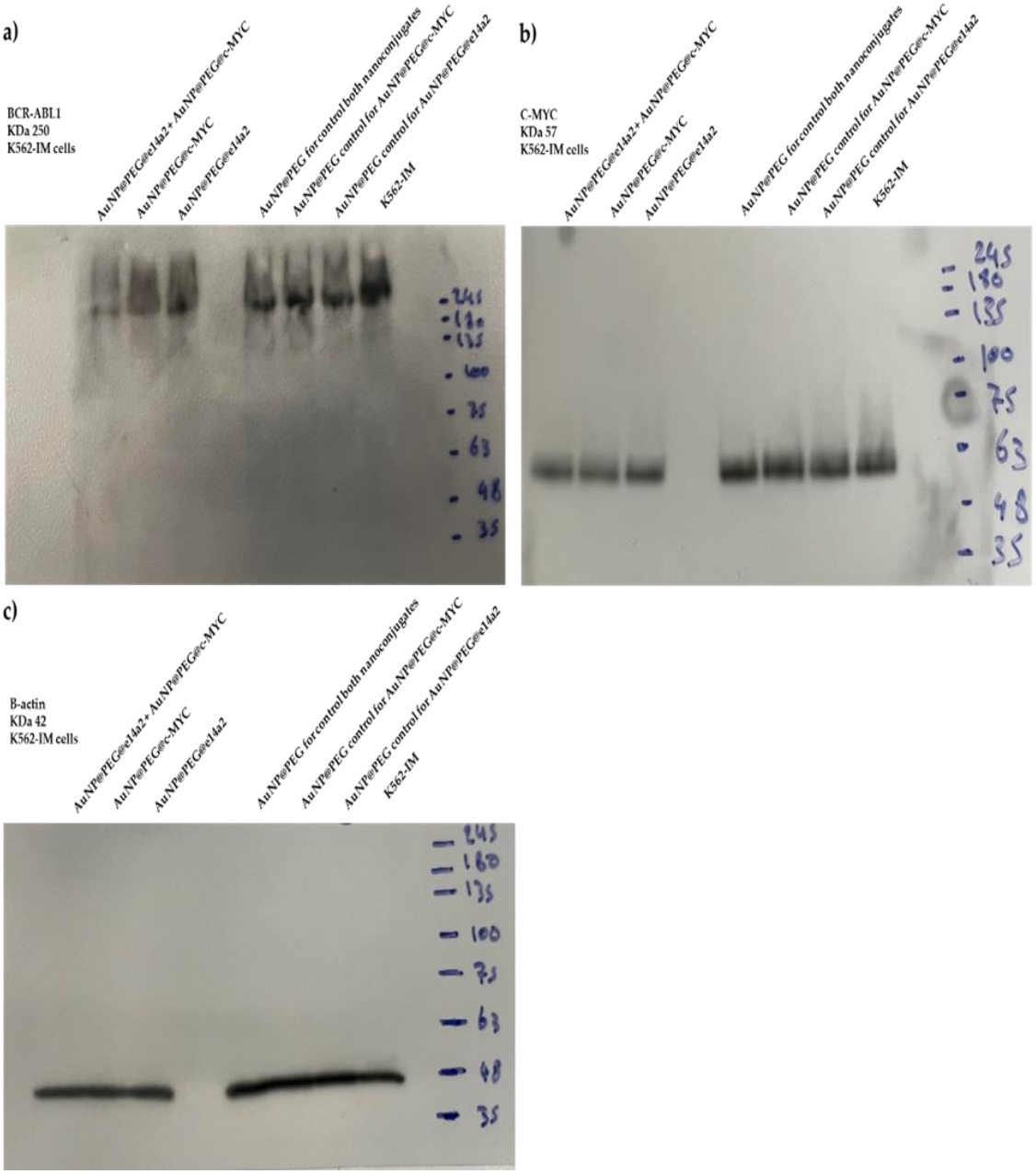

Figure A.4 — Western blot images for BCR-ABL, c-MYC and β-actin protein expression levels in K562-IM cell line after exposure cells to Au-nanoconjugates (replaced lysis buffer). (a) protein expression levels of BCR-ABL1 (250 KDa) after challenged cells with Au-nanoconjugates for 24h; (b) protein expression levels of c-MYC (57 KDa) after challenged cells with Au-nanoconjugates for 24h; (c) protein expression levels of β-actin (42 KDa) after challenged cells with Au-nanoconjugates for 24h.

2025

BILAL RABAH QASIM ABDULMAWJOOD

Managing of Chronic Myeloid Leukemia via Au-nanoconjugates In TKIs Sensitive/Resistance CML Cells